International Atomic Energy Agency

INDC(NDS)-135/GA

INDC INTERNATIONAL NUCLEAR DATA COMMITTEE

CHARGE EXCHANGE BETWEEN HIGHLY CHARGED IONS AND ATOMIC HYDROGEN: A CRITICAL REVIEW OF THEORETICAL DATA

R.K. Janev and B.H. Bransden

Joint Institute for Laboratory Astrophysics
University of Colorado and National Bureau of Standards
Boulder, Colorado 80309, USA

Submitted within the framework of the
IAEA Coordinated Research Programme on
Atomic Collision Data for Diagnostics of Magnetic Fusion Plasmas

July 1982

Reproduced by the IAEA in Austria
July 1982
82-4047

INDC(NDS)-135/GA

CHARGE EXCHANGE BETWEEN HIGHLY CHARGED IONS AND ATOMIC HYDROGEN: A CRITICAL REVIEW OF THEORETICAL DATA

R. K. Janev* and B. H. Bransden†

Joint Institute for Laboratory Astrophysics
University of Colorado and National Bureau of Standards
Boulder, Colorado 80309 U.S.A.

---

*JILA Visiting Fellow, 1981-82, on leave of absence from the Institute of Physics, Belgrade, Yugoslavia.

†JILA Visiting Fellow, 1981-82, on leave of absence from the University of Durham, Durham, Great Britain.

TABLE OF CONTENTS

1. INTRODUCTION

The investigation of charge exchange processes between highly charged ions and neutral atoms has been strongly stimulated during the past decade by the recognition of the extremely important role of these reactions in high-temperature plasmas. Particular impetus for these studies has come from the requirements of thermonuclear fusion research for cross section data [1]. In the last ten years, a better understanding of the collision dynamics has led to the development of important new theoretical and experimental methods which has allowed the accumulation of a significant amount of charge exchange cross section data, and a critical analysis of this information is now required. This review attempts to provide such an analysis of the theoretically produced data and of the theoretical models employed, for charge exchange between positive ions and atomic hydrogen.

Our analysis has two main objectives. First, to define as closely as possible the ranges of physical parameters (energy, charge state, etc.) in which each currently used theoretical model for charge exchange between charged ions and atomic hydrogen is expected to attain a specified accuracy; and second, to review the theoretical data that have been produced. This review will be from a mainly theoretical standpoint, although the experimental cross sections have been included in the accompanying diagrams for comparison. The overall objective is to provide a selection of the most reliable theoretical data and of the most reliable models for producing new data, keeping in mind the priorities that have been established in the current thermonuclear fusion research programs [2].

The cross sections of interest are both the total cross section and the partial cross sections leading to electron capture into a given final state. Specifically we have:

$$A^{Z+} + H(1s) \rightarrow A^{(Z-1)+} + H^{+} \qquad (1)$$

where A^{Z+} may be a fully or partially stripped ion. If A^{Z+} is a fully stripped ion, the ion $A^{(Z-1)+}$ contains one electron and the final state is then characterized by the usual hydrogenic quantum number ($n\ell m$). Since the relative velocity of the colliding ions is the relevant parameter, energies will be quoted in the form of the laboratory energy of an ion in eV (or keV) incident on a stationary target divided by the mass of the incident ion in atomic mass units. In these terms the range of energies of interest [2] extends from 10 eV/amu to a few MeV/amu. In theoretical expressions atomic units are used ($a_o = m_e = \hbar = 1$), except where otherwise specified, while in graphical representations of data, cross sections are given in units of cm^2.

2. THEORETICAL METHODS

In this section we briefly discuss the intrinsic strengths and limitations of the theoretical models that have been used to produce cross sections for charge exchange between charged ions and hydrogen atoms. We do not go into technical details but rather outline the essential features and character of the approximations involved. A detailed account of the current theoretical models can be found in several recent reviews [3-6].

2.1. Classification of Methods

The theoretical methods employed can be most naturally classified according to the parameter (v/v_o) where v is the relative collision velocity and v_o is the Bohr velocity of the electron in the target hydrogen atom (v_o = 1 a.u. = 2.18×10^8 cm/sec). We shall distinguish three broad regions in which the collision

dynamics and associated theoretical models are different, although of course there is no hard and fast division between these regions. These are: (a) $(v/v_o) \ll 1$ — the adiabatic region; (b) $(v/v_o) \sim 1$ — the intermediate velocity region, and (c) $(v/v_o) \gg 1$ — the high velocity region.

The collision dynamics also depend qualitatively on the number of electrons in the projectile A^{+Z}. If this number is large, there are very many interaction paths and, in the adiabatic region, this fact allows the introduction of some simple pictures of the electron transfer mechanism. To take the other extreme, in the one-electron system in which the incident ion is fully stripped, the number of interaction paths is comparatively small because of the high degree of symmetry of the system. The one-electron system is of particular theoretical simplicity because the electronic structure of the system can be considered known, since in the limit of large internuclear distances the wave function reduces to that of a hydrogen-like atom, while at finite distances the adiabatic eigenvalue problem can be solved exactly by well-known numerical procedures. For this reason, theoretical cross sections for the one-electron system differ only in the method used to solve the scattering equations and this system provides an excellent test of the accuracy of different scattering approximations in a given energy region.

2.2. Low Energy Charge Transfer

From a dynamical point of view the collision system $A^{Z+} + H$ at low energies ($v \ll Z^{1/4}$, $E \ll 25\ Z^{1/2}$ keV/amu) is best described within a molecular framework. The transitions between the molecular electronic states are either caused by the nuclear motion (which in the energy interval considered can be treated semi-classically), or by any interactions excluded from the molecular Hamiltonian. The number of interacting discrete molecular states is extremely

large (infinite for the one-electron case), but usually only a restricted number is effectively involved in the dynamics of charge transfer. In extreme cases, the main couplings are highly localized, each being separated from the others, or, in contrast, the couplings can be densely distributed. In both these extremes simple, physically transparent, models for charge transfer have been devised. Quite generally, the system $(A^{Z+} + H)$ can be described by a set of coupled equations for the state amplitudes, obtained by expanding the full Schrödinger equation in terms of the molecular orbitals. These equations can be solved approximately in three ways: (a) If only a limited number of states is of importance, a directed solution of the truncated set of equations is possible, either numerically or through some analytical approximation; (b) the Landau-Zener nonadiabatic theory can be generalized to the multichannel solution, and (c) the concept can be introduced that the initial electronic state decays because of the interaction with the effective continuum of final ionic states. Each approach emphasizes some particular aspects of the physics of the process, and we should now analyze each in turn to assess the accuracy to be expected from the computed cross sections.

2.2.1. Multi-state close coupling models

If a truncated molecular orbital expansion is combined with a semi-classical approximation for the nuclear motion, the collision problem consists of solving a set of first-order differential equations for the state amplitudes, the size of the set depending on the number of terms retained in the expansion. Provided only a finite number of terms is important in the expansion, the results will converge as the size of the basis is increased. This general approach is referred to as the CC-MO (close coupling of molecular orbital method). In practice, the calculations can be divided into two steps. In the

first, electronic structure calculations are carried out to provide molecular orbitals and energies, which in turn are used to calculate the potential motion coupling the channels; in the second step the coupled equations themselves must be solved. The accuracy of the computed cross section depends on the success with which both these steps can be carried out. As we have already noted, for the case of a fully stripped ion incident on atomic hydrogen (Z + H), the electronic structure calculations can be performed to any required degree of accuracy without difficulty, but on the other hand, for several- or many-electron systems the standard of accuracy that can be achieved in practice is sometimes poor. The molecular structure calculations can either be performed using a basis which diagonalizes the electronic Hamiltonian — an adiabatic basis — or with a basis chosen in some other way, for example to minimize some particular coupling terms — a diabatic basis. Although with sufficiently large basis sets the final cross sections obtained should be the same, the form of the scattering equations is different in each case, and with small unconverged basis sets the final cross sections obtained will be different. Usually an adiabatic basis is more appropriate for the lower part of the adiabatic energy region, and a diabatic basis is more appropriate in the upper part. The CC-MO method employing an adiabatic basis and neglecting the momentum transfer of the captured electron constitutes the original form of the perturbed stationary state (PSS) approximation introduced in the 1930s.

a. The PSS approximation. Using an adiabatic basis, two different types of coupling induce transitions: radial coupling (depending on the rate of change of the internuclear distance) and rotational coupling (depending on the rate of change of the orientation of the internuclear axis). The size of the expansion basis must be sufficient to include all the important couplings at a

given energy. The radial couplings are usually peaked at internuclear distances for which a pseudocrossing of the potential energy curves occurs for molecular states of the same symmetry. The rotational coupling connects states of different symmetry and is effective at smaller internuclear distances and these distances are only accessible, for the excited states of the $H + A^{Z+}$ system, at energies above ~10 eV. (Below this energy, a semi-classical treatment becomes inadequate and the full quantal formulation of the PSS approximation should be used [7].)

In the PSS method the origin of coordinates is chosen to be some point in the internuclear line. Asymptotically the electron shares the translational motion, relative to the origin, of the nucleus to which it is attached. This translational motion is neglected in the PSS method and the method is not Galilean invariant [8]. This has the consequence that the individual terms in the PSS expansion do not satisfy the Schrödinger equation in the asymptotic limit of large separations, so that the couplings between channels do not vanish in this limit. Further the results obtained using a finite basis set can be altered significantly with the choice of origin. To remedy these defects suitable translational phase factors can be associated with the basis functions, which describe the asymptotic translational motion of the electron. Two difficulties arise in the use of translational factors: first, the form of these factors in the interaction region is not defined; and second, a considerable increase in numerical complexity may result. The former difficulty can in principle be overcome by optimizing the translational factors at finite internuclear separations using the variational method, but this again may result in formidable computational problems.

If only a total cross section is required, the origin of coordinates can be placed on the target nucleus, in which case the initial asymptotic conditions

are satisfied trivially, and the translational factor for the final rearranged state can be omitted. Although the spurious long-range interactions remain, the total charge exchange probability summed over all the final states converges and can be calculated correctly [9]. However, in order to calculate cross sections for capture into individual levels, the translational factor associated with the final translational motion must be included [8,10,11].

When the translational factors are ignored completely, the results of total cross section calculations using different origins differ by as much as 20% at $v = 0.2$ and 100% at $v = 1$ even if a fairly large number of terms have been used in the basis set [12].

A study of the very many PSS total cross sections (see Section 3), performed with straight line trajectories for the nuclear motion leads to the following conclusions (for the case of H + fully stripped ions):

1) If no translational factors are included the uncertainty in the computed total cross sections may be of the order 100% at $v \approx 1$ a.u., 20% at $v \approx 0.2$ a.u., and less than 10% for $v \lesssim 0.1$ a.u., where it is assumed the number of basis states is $N \approx Z$.

2) With simple translational factors, the PSS method can produce cross sections within a 20% accuracy for v up to ~1 a.u., provided a basis is used which includes all the important channels.

3) With elaborate, optimized, translation factors cross sections can be obtained with an expected accuracy of less than 10% for v up to ~1 a.u.

4) The size of the basis required for total cross section calculations depends on Z, the charge on the ion, and v. For small Z, the number of important radial couplings r_o is restricted, but this number increases with Z. An estimate of r_o is given by the formula [13]:

$$r_o = (Z^{1/2} - 1)\left[Z^{1/2} + 1 - (1 + 2\,Z^{1/2})^{1/2}\right] \quad .$$

Thus for large Z and for an accuracy of $\lesssim$20%, the minimum number of states included in a total cross section calculation should be of the order of Z. Within the same accuracy the effects of rotational coupling can be neglected at low velocities $v \lesssim 0.05$.

5) The calculation of partial cross sections, particularly when both the distributions in n, the principal quantum number, and ℓ, the angular momentum quantum number, are required, necessitates the use of much larger basis sets. For example, to determine the (n,ℓ) distributions in the $H + C^{+6}$ system, just for the n = 3, 4, 5, 6 and 7 levels requires in principle about 80 terms in the basis. Recently [10], it has been found that of these only 33 are important, if 10% accuracy is sufficient.

It should be noted that the PSS method gives rise to additional problems when applied to the interaction of partially stripped ions with atomic hydrogen. The required molecular structure calculations are much more elaborate; furthermore, the number of interacting states becomes much larger.

b. An analytic approximation to the CC-MO model. The coupled differential equations of the CC-MO model in the diabatic representation can be solved exactly, under the following assumptions [14]:

(1) The n and ℓ dependences of the coupling matrix elements can be factored;

(2) the energy differences between the ionic diabatic potentials do not depend on the orbital quantum number ℓ; and

(3) the rotational coupling of the molecular states can be neglected.

All these assumptions are compatible and are reasonably well satisfied for the H + Z system provided $Z \gg 1$ and the velocity is low so that the important

internuclear distances are restricted to the region $(2Z)^{1/2} \lesssim R \lesssim 2Z$. This model (denoted by CC-MO-An), predicts strong oscillations of the total cross section as a function of Z for $Z \lesssim 30$. This feature has not been confirmed experimentally because of the paucity of data. Another feature of the model is that the distribution in ℓ of the captured electron is:

$$W_\ell = \frac{(2\ell+1)}{Z} \exp\left[-\frac{\ell(\ell+1)}{Z}\right] \quad , \quad Z \gg 1 \quad , \qquad (2)$$

a result which is independent of the dynamical equations. The validity of the CC-MO-An model is restricted to $Z \gtrsim 10$ and $v \lesssim 0.2$-0.5 a.u.

2.2.2. Multichannel Landau-Zener model

The multichannel Landau-Zener model for the $H + A^{Z+}$ system [15] assumes that the pseudo-crossings of the potential energy curves are well separated so that each pseudo-crossing can be treated in isolation by the two-state Landau-Zener model. This model, denoted by M-LZ, can be applied to the H + Z system if Z is not too small ($Z \gtrsim 5$); it is usually not applicable to the collision of H with a partially stripped ion, since in this case the crossing regions usually overlap. Rotational coupling between the degenerate ionic levels is important and this can be included in the model [16] (M-LZ-RC). When this is done much better agreement with experiment is obtained [17]. Since the M-LZ-RC is an approximation to the CC-MO model, its domain of validity is restricted both by that of the CC-MO model and by the additional approximations. Since translational effects are ignored, for a required accuracy of ~30%, the velocity must satisfy $v \lesssim 0.5$ a.u. A particular limitation of the M-LZ-RC model is that transitions to states with $n \gtrsim Z$ are not allowed, because there are no curve crossings from these states to the initial Z + H(1s) state. It is also clear that captures to states with $n \lesssim Z$ are underestimated. These

limitations are reduced as Z increases since for large Z captures are predominately into the levels close to $n = Z/2$. The cross section calculations of the M-LZ-RC model are much more rapid than those of the PSS method, and this advantage is particularly marked for large Z for which the PSS method requires an impractically large basis.

Within the M-LZ-RC model the n-distributions are accurate to better than ~50% for $v \lesssim 0.5$ at $Z \gtrsim 10$ (except for $n \gtrsim Z$). In the region $v \lesssim 0.2$ to 0.3 a.u., the relative ℓ distributions are given by [17]:

$$W_{n\ell} = (2\ell+1) \frac{[(n-1)!]^2}{(n-\ell)!(n-1-\ell)!} \quad . \tag{3}$$

For large v, the model predicts a statistical distribution in ℓ of the capture electrons.

2.2.3. Decay models (DM)

Decay models [18-20] are based on the concept that the number or open charge exchange channels in the $(H + A^{Z+})$ system is very large and that the open channels are densely distributed in energy. In the simplest model of this kind, the absorbing sphere model (ASM) [18], electron capture takes place with unit probability once R reaches a critical value R_c. In the electron tunneling models (ETT) [19,20], the transition probability is determined by the decay rate of the initial state due to its interaction with the quasi-continuum of final ionic states. The assumptions of the decay models are best satisfied for many electron systems and for $0.2 \lesssim v \lesssim 0.5$ a.u. The concept of a quasi-continuum requires large values of Z, higher than ~14 for the H + Z system and higher than 8 for $H + A^{Z+}$. Even in this region, these models appear to overestimate the cross section, sometimes by a factor of up to 2.

The most likely value of n in the final state is

$$n_m \approx 2^{1/4} Z^{3/4} \quad , \quad Z \gg 1 \qquad (4)$$

but the n and ℓ distributions cannot be predicted.

2.3. Intermediate Energy Charge Transfer

In general, the charge exchange problem at intermediate velocities ($v \sim 1$ a.u.) is difficult because no suitable small expansion parameter exists. Often many states are coupled together and the electron momentum transfer cannot be ignored. Although an expansion in molecular orbits, which form a complete set, could in principle be employed, a practical alternative is to employ an atomic orbital expansion based on both centres, supplemented by pseudostates to represent the continuum (CC-AO method). In contrast, methods based on purely classical mechanics have been also devised for this region.

2.3.1. CC-AO model-numerical treatment

In applications, care must be taken when using a two-centre atomic orbital basis to avoid obtaining impractically larger sets of differential equations. For example, if all atomic orbitals with $n \leq 4$ were placed on each centre for the (H + Z) system, the basis would contain 30 terms. However, for a system such as (H + Z) where the interaction is strong, the basis can be reduced to a 1s orbital about the proton together with the orbitals representing the most important final states about the nucleus Z. For $v \gtrsim 1$, there is little difference between the results of such a calculation and the sum of the cross sections from two-state calculations taking each final state in turn. However for $v < 1$ at least, the degenerate levels for a given n of the final ionic state should be coupled together. The contribution to the total cross section

from states with $n \gtrsim Z$ can be estimated from the Oppenheimer n^{-3} rule. For the $H + A^{Z+}$ system, extensive calculations using the full CC-AO method have only been performed at intermediate velocities for He^{2+} and Li^{3+} ions [21], and at low energies for the C^{6+} ion [22], but calculations for $Z < 10$ should certainly be feasible.

The lower limit in velocity for the CC-AO method is not known. It is certainly valid down to $v = 0.2$ a.u., and good agreement between MO and AO calculations has been reported for C^{6+} for velocities down to $v = 0.03$ a.u. At high velocities, it is known that continuum intermediate states become increasingly important, which requires the introduction of pseudostates into the basis for a proper description and thus may restrict the use of the CC-AO method without pseudostates to $v \lesssim 3$-4 a.u. The one-and-one-half centre expansion of Reading and coworkers [23] which employs a large basis set on the ionic centre, with a simplified description of H(1s) channel appears to give a good account of both ionization and charge exchange and promises to provide a practical method of calculating without any definite upper velocity limit. It should be noted that as with the MO method, the calculation of partial $(n\ell)$ cross sections always requires a much larger basis than is needed for single total cross section calculations, and that the practical information now available is insufficient.

2.3.2. Approximate treatments of the CC-AO equations

For the H-Z system, with $Z > 1$, a sufficient basis is obtained by including only the H(1s) orbital together with a complete set of orbitals representing the final (ionic) states [5]. For convenience, the discrete ionic orbitals can be orthogonalized to the H(1s) orbital, for all values of R. The set of equations formed from this basis can be approximated in either

of two ways: 1) by the unitarized distorted wave approximation (UDW) [24], in which the couplings between the final ionic states are ignored, and 2) by making an approximate analytical solution of the infinite set of coupled equations in which the second and higher-order transition effects are ignored [25], and in which the potential matrix is calculated within the Vainshtein-Presnyakov-Sobel'man (VPS) approximation (this method will be denoted as M-VPS). Neither the UDW nor the M-VPS methods take into account coupling with the continuum and so can only be used for velocities v less than $v_{max} \approx 3$-4 a.u. Because at lower velocities the omitted second-order terms become important, the UDW approximation is accurate only for $v_{min} \gtrsim 0.8$ a.u. and for the M-VPS method the lower limit can be estimated as 0.2-0.3 a.u., however in this case additional approximations restrict Z to $Z \gtrsim 10$.

Both these methods tend to overestimate the cross section, and when used outside the specified regions, the computed cross section can exceed the true cross section by a factor of up to 2. The UDW method should be used with caution in the prediction of the ℓ distribution because this will be sensitive to the omitted second-order terms. The M-VPS method is capable of systematic improvement but this has not been done to date.

In the two-state version, the M-VPS method has been applied to the interaction of partially stripped ions and atomic hydrogen [26], and to account for the omitted effects an empirical factor of 1/3 has been introduced. We shall refer to this as VPS-emp method.

2.3.3. Classical methods

By representing the hydrogen atom with a classical microcanonical distribution in momentum space, classical dynamics can be used to calculate charge exchange cross sections for the H + Z system in the intermediate energy

region. Having done this, the classical three-body problem can be solved numerically by making a random selection of initial conditions [27]. Within this classical trajectory Monte Carlo method (CTMC) both total and partial capture cross sections can be calculated.

A second classical model [28] relies on the fact that the transition of the electron from the atomic to the ionic well is classically allowed when $R \lesssim R_o$, where $R_o = 2(2Z-1)^{1/2}$. This is the classical analogue of the absorbing sphere model and can be treated analytically (Cℓ M-An).

Partly because of the difficulty of obtaining statistically meaningful results, the upper velocity limit of the CTMC model is about $v_{max} \approx 3$ a.u., while below $v_{min} \approx 1$ a.u., molecular effects may become important. The approximation will be more accurate for higher Z because capture takes place to states with large values of n, for which a classical description is more appropriate. The Cℓ M-An model assumes the motion of the nuclei can be treated adiabatically, which gives an upper limit of $v_{max} = 1$ a.u., while below $v_{min} = 0.5$ a.u., quantum barrier penetration effects are large. High values of Z are required ($Z \gtrsim 15$). The accuracy obtained by the CTMC method is surprisingly high, and this method can also be applied to partially stripped ions if these are represented by an effective charge. The Cℓ M-An model is less successful and tends to overestimate the cross section by a factor of $\lesssim 1.5$.

2.4. High Energy Methods

In the energy region under consideration (<5 MeV/amu), the first-order perturbation approximation is completely inaccurate (sometimes by an order of magnitude) and second Born approximation (which ultimately dominates the cross section as $v \to \infty$) is worse. It follows that methods that take into account the

important higher-order effects must be used. These include those based on the eikonal (Glauber) approximation and the continuum distorted wave method (CDW).

2.4.1. The Brinkman-Kramers and Eikonal Methods

The first-order term in the perturbation series for charge exchange, omitting the internuclear potential, provides the Brinkman-Kramers (BK) approximation. Although an inadequate approximation in itself, it appears to provide moderately accurate cross-section ratios. At a given velocity, this ratio is

$$\frac{\sigma(n)}{\sigma(n_o)} = \left(\frac{n_o}{n}\right)^3 \tag{5}$$

and thus becomes more accurate for large n_o, with $n > n_o$. This expression is often used to extrapolate the results obtained by some other method to obtain a large n correction.

By representing the total wave function by an eikonal (Glauber) approximation and using this function in the exact T-matrix element for the transition, all higher-order terms in the Born series are allowed for approximately. For the H(1s) + Z system the cross section in this approximation (BK-Eik) for capture into the n^{th} shell [29] is

$$\sigma^{BK}_{Eik}(n) = \alpha(n,Z,v)\ \sigma^{BK}(n) \tag{6}$$

where

$$\sigma^{BK}(n) = \frac{2^8\,\pi Z^5}{5n^3v^2\left[\left(\frac{v}{2}+\frac{\omega_n}{2}\right)^2+\frac{Z^2}{n^2}\right]^5} \quad , \quad \omega_n = \left(\frac{Z^2}{2n^2}-\frac{1}{2}\right) \quad . \tag{7}$$

and $\alpha(n,Z,v)$ is a scaling function, weakly dependent on n and Z, but relatively

strongly on v. The cross section for capture into individual (nℓ) levels can also be obtained.

The BK-Eik method appears to provide reasonably accurate cross sections for $2 \lesssim v \lesssim 7$ and like other methods it can be applied to a partially stripped ion by introducing an effective charge.

2.4.2. The continuum distorted wave and related models

In the continuum distorted wave (CDW) approximation [30], the interaction in the initial state, between the incident nucleus and the bound electron, is represented by a Coulomb function; a similar approximation is made in the wave function representing the final state. The approximate transition matrix element includes contributions to all higher-order terms of the perturbation series and, in particular, an important part of the second-order term. It provides very accurate results for the (H + Z) system for $v > 2.5$ a.u., and in the limit $v \to \infty$, it is practically equivalent to the second Born approximation. Although applications can be made in the case of partially stripped ions, most work to date has been for (H + Z) with low values of Z. Each partial cross section is calculated separately and summed to provide the total cross section. Although the $1/n^3$ rule is often used in conjunction with the CDW method, it has not been deduced from the method, but it has been justified within the second-Born approximation for $n \gg 1$ [31]. The impulse approximation has also been applied in the high-energy region, but in general is less satisfactory than the CDW model.

2.5. Resumé of the Regions of Validity of Models for Charge Exchange

As we have seen, the accuracy of theoretical charge exchange models for A^{Z+} + H(1s) can be specified with respect to ranges of two parameters: the

velocity v, and charge on the incident in Z. In some theories (for example, methods based on perturbation theory) these parameters are connected, but in others the collision dynamics depends on v and Z separately. It is convenient to combine v and Z in a reduced velocity $\tilde{v} = v/Z^{1/4}$ and to classify domains of validity in terms of $\tilde{v}$ and Z. The parameter $\tilde{v}$ appears naturally both in the adiabatic region and at high energies [32]. At intermediate velocities, where the cross section behaves like Z^3/v^7 (for $v \approx 2$-3 [33]) the combination $v/Z^{1/2}$ is, perhaps, a more appropriate parameter.

With these remarks in mind, the domains of validity of the various models we have discussed are illustrated in Fig. 1, while in Table 1 a summary appears of the various points raised in our discussion together with specific comments on the methods and assessed accuracy. It will, of course, be realized that the boundaries of the domain of validity of the various models are not hard and fast, but are intended to serve as a guide. In order to specify the degree of accuracy provided by different methods, we have introduced the following categories (last column in Table 1):

Category	Accuracy
(a)	Better than ±20%
(b)	±20% - ±50%
(c)	±50% - ±100%
(d)	Worse than 100%

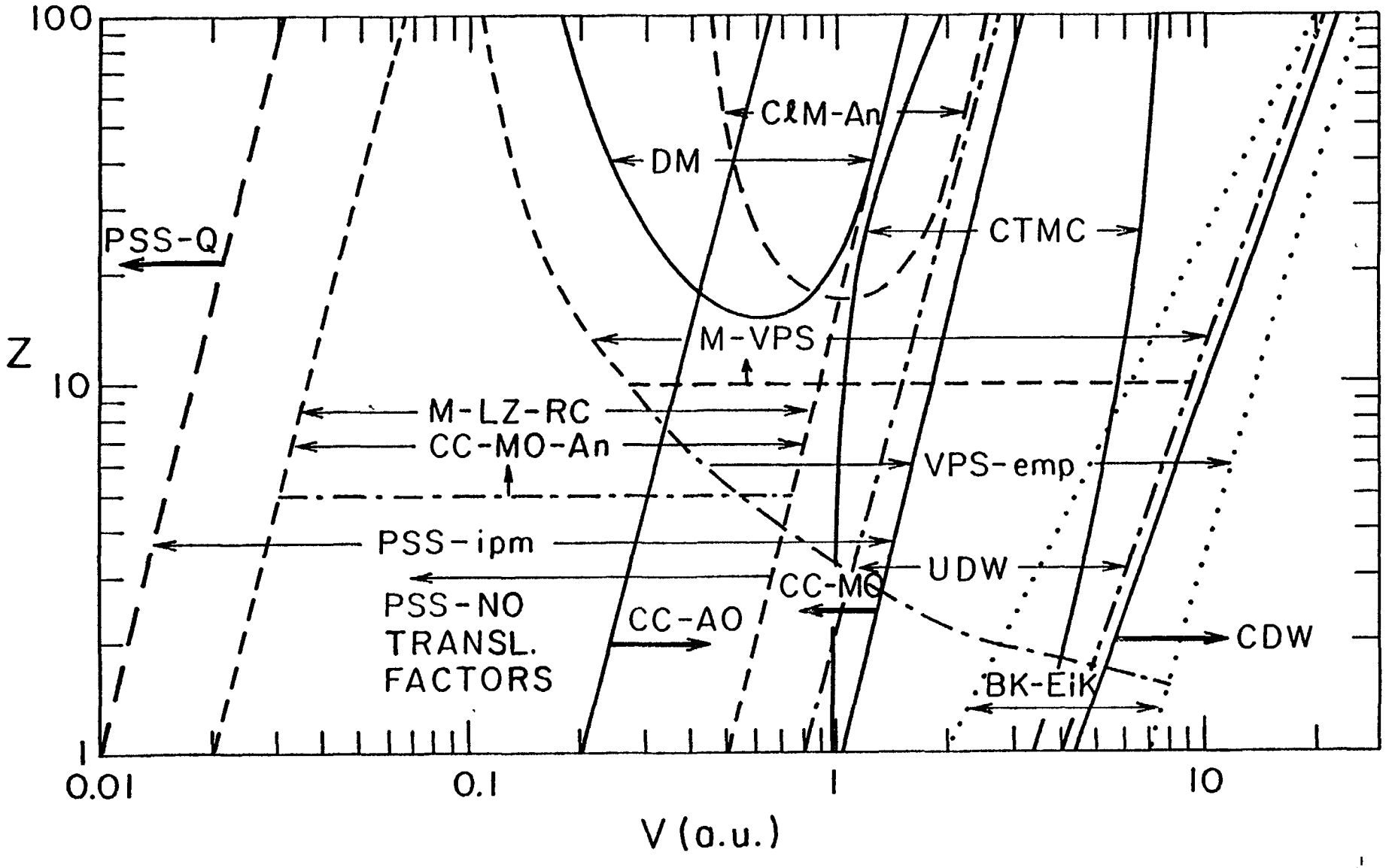
100
10
1
Z
0.01
0.1
1
10
V (a.u.)
ClM-An
DM
CTMC
PSS-Q
M-VPS
M-LZ-RC
CC-MO-An
VPS-emp
PSS-ipm
UDW
CC-MO
PSS-NO
TRANSL.
FACTORS
CC-AO
CDW
BK-EIK

Figure 1

TABLE 1. Validity Regions and Accuracy of Different Theoretical Methods for Charge Exchange

Method	Velocity Range (a.u.)	Z-region	Comments	Accuracy
			A. Low-energy methods	
1) CC-MO				
a) PSS-Quant.	$\lesssim 0.01$	all	- quantum-mechanical treatment of nuclear motion - translational factors unnecessary	depends on number of states coupled
b) PSS-ipm	0.01-0.5	all	- classical treatment of of nuclear motion - translational factors optional	same as above
	0.5-1	all	- classical treatment of nuclear motion - translational factors necessary	same as above
2) CC-MO-An	0.02-0.5	$\gtrsim 10$	- analytic model - all states included - radial coupling only - no translational factors - applicable only to H + Z	(b) or (c)
3) M-LZ	0.02-0.5	$\gtrsim 5$	- radial coupling only - no translational factors	(c) or (d), $v \lesssim 0.3$ (b) or (c), $v \gtrsim 0.3$
4) M-LZ-RC	0.02-0.5	$\gtrsim 5$	- rotational coupling within given n included - no translational factors - applicable only for H + Z system	(b), $v \gtrsim 0.1$, $Z \gtrsim 10$ (b) or (c), $v \gtrsim 0.1$, $Z \lesssim 10$ (c) or (d), $v \lesssim 0.1$
5) ASM	0.2-0.6	$\gtrsim 14$ (H+Z) $\gtrsim 8$ ($H+A^{q+}$)	- no rotational coupling - no translational factors	overestimates σ; (b)(c), smaller v, $Z \gtrsim 14$ (c)(d), higher v, $Z < 14$
6) DM	0.2-0.6	same	same	same

TABLE 1. (cont'd.)

Method	Velocity Range (a.u.)	Z-region	Comments	Accuracy
			B. Intermediate-energy methods	
1) CC-AO	0.2—3-4	all	- plane wave or Coulomb translational factors necessary	depends on number of close coupled states
2) M-VPS	0.3—3-4	≳10	- unitarity preserved	(b) or (c), $v \lesssim 2$ (d), $v > 2$
3) UDW	0.7—3-4	all	- unitarity preserved - effective charge for incompletely stripped ions	same
4) CTMC	1—3-4	all	- effective charge for incompletely stripped ions	(a), (b), $Z > 6$ (c), $Z \lesssim 6$
5) Cℓ M-An	0.5-1	≳10	- applicable only for H + Z system	(b), (c)
6) VPS-emp	0.3—6	all	- 2-state VPS for each final state - empirical factor 1/3 introduced	(b), (c)
			C. High-energy methods	
1) BK	>2	all	- nucleus-nucleus interaction excluded - incorrect asymptotic v-behavior of σ	(d), overestimates σ by a factor of 3 to 10
2) B1 JS, Coul-B	>2	all	- all interactions included - incorrect asymptotics	unspecified
3) DW	1—3-4	all	- unitarity not preserved	(b) or (c), $v \lesssim 2$ (d), $v > 2.5$
4) BK-Eik	2-7	all		(b), (c)
5) CDW	≳4	all		(a), (b)

3. REVIEW OF THEORETICAL CROSS SECTION DATA

3.1. General Remarks

In this section we critically review the theoretical charge exchange data for hydrogen atom-highly charged ion collisions in the energy region above 10 eV/amu. We restrict ourselves to those ionic species that are of major interest to magnetic fusion research. In Table 2, we group the ions that, according to the IAEA data [2], have the highest priority with respect to obtaining charge exchange data in collisions with hydrogen atoms.

TABLE 2. Groups of Ionic Species with Highest Priority for Fusion Research

Group	Ions, A^{z+}	Priority*
1	C, O, Ti, Fe	1.1
2	He, Aℓ, Cr, Ni	1.3
3	Ne, Ar, Kr	1.8
4	B, N, F, Si, Cℓ, Xe	2.0
5	Cu, Zr, Mo, W	2.1

*The priority number is determined also with respect to other processes of these ions by an averaging procedure. The highest priority is 1 and the lowest is 3.

The evaluation of the data was based on the following:

a) use of criteria established in Section 2 for the validity regions of the theoretical methods and the accuracy they provide in the calculations;

b) comparisons with the most accurate experimental data.

From the point of view of the accuracy of theoretical calculations, it is convenient to analyze the data for completely and partially stripped ions separately. For the first category, the quality of the data mainly depends on the model, whereas for the second category the results depend also on the electronic structure calculations.

The data are presented in two ways: 1) in the form of tables, in which all the cross section information is presented, and 2) selected cross section data (with the highest accuracy in a given energy region obtained by using a particular method) is presented graphically. Some of the most accurate experimental data are also presented on the figures, for comparison purposes.

3.2. Total and Partial Cross Sections for Completely Stripped Ions

A compilation of the available theoretical charge exchange cross section data for completely stripped ions of the elements listed in Table 2, is presented in Table 3 (given at the end of the paper). For each ion, this table contains the references in which the original data can be found, the energy ranges in which the cross sections have been performed, the applied method (with some comments on it, when necessary), and the character of the information contained (total/partial cross section, or both). The accuracy of the data can be judged by using Table 1. The references mentioned in Table 3 are given separately at the end of this review (see Appendix A). By comparing the energy ranges in Tables 1 and 3, it can be seen that some of the cross section calculations are carried out well beyond the limits of validity of the

applied method. If such data are selected to be included in the recommended list of cross section data (which are represented graphically, see below), then only the part of them that conforms with the validity region of the corresponding method is taken.

When selecting the cross section data for a graphical presentation, the following criteria have been adopted:

- to cover as much as possible the energy range considered in this review ($0.01-10^3$ keV/amu);
- from all the available calculations using the same method, only those with highest accuracy are graphically presented;
- in some cases, when the results of two or more methods are available in the same energy region, only those with highest accuracy are included in the graphical presentation.

These criteria enabled us to give information about the cross section in a wide energy range, preserving the clarity of the presentation.

The graphically represented total cross section data are collected in the GRAPH.SET No. 1, given at the end of the review. As a source for the experimental data we have used Ref. 34. The original experimental references, mentioned on the figures of Graph.Set No. 1, are given at the end of Appendix A.

The presentation of the partial cross section σ_n (capture into a particular final principal shell n) and $\sigma_{n\ell}$ (capture into a particular final n,ℓ-substate) is given either in tabular form (for low Z-values) or graphically (for high Z-values). The set of tables for σ_n and $\sigma_{n\ell}$ are given in the TABLE SET No. 1 at the end of the review, and the graphical presentations of σ_n and $\sigma_{n\ell}$ are given in GRAPH.SET No. 2. The accuracy of σ_n and $\sigma_{n\ell}$ provided by some methods (e.g. M-LZ-CR, UDW, CTMC) is generally lower than the accuracy of the total cross sections. The expansion methods (CC-MO and CC-AO) with a large basis and the

CDW method produce the most accurate partial cross section data for charge exchange.

3.3. Total Cross Sections for Partially Stripped Ions

A classification of the references containing charge exchange cross section data for hydrogen atoms with incompletely stripped ions, is presented in Table 4 (given at the end). The presentation is similar to that for completely stripped ions (Table 3). The list of references associated with Table 4 is given in Appendix B. The evaluation of the data has been performed by using the same criteria that were applied in the completely stripped ion case. The accuracy of the cross section data for the incompletely stripped ion case is, generally speaking, lower than for the case of fully stripped ions. It is noticeable that the close-coupling cross section calculations are not as numerous for the case of incompletely stripped ion-hydrogen atom charge exchange collisions, due to the necessity of performing complex electronic structure calculations. Selected cross section data are presented graphically in the GRAPH.SET No. 3. The selection was performed using the same criteria as in the case of completely stripped ions. The solid curves in some of the figures of GRAPH.SET No. 3 represent experimental data. Again, as the main source for the experimental data we have used the recent IPP Nagoya compilation [34]. The experimental references which were the sources of data are presented in the figures of GRAPH.SET No. 3, are given at the end of Appendix B.

3.4. Summary on the Available Theoretical Cross Section Data and Recommendations for the Future Calculations

Although the amount of charge exchange cross section data presented in Tables 3 and 4 and on the GRAPH.SETS Nos. 1-3 may look impressive, the general

situation of data basis is still far from adequate to meet the needs of fusion research programs. The accuracy of the existing data is still insufficient (with a few exceptions) and for an overwhelming number of incompletely stripped ions no data exist at all.

The situation is particularly unsatisfactory regarding the status of partial cross section data. For example, no partial cross section calculations have as yet been performed for incompletely stripped ions.

The main conclusions of our analysis of the available theoretical data are summarized below.

3.4.1. Total and partial cross sections of completely stripped ions

The most reliable (with an accuracy better than ±50%) total cross section data for completely stripped ions are summarized in Table 5. For only a restricted number of ions (He^{2+}, B^{5+}, C^{6+}, O^{8+} and F^{9+}) and in limited energy intervals, do some of the calculations provide an accuracy better than ±20%. Most of the reliable data lie in the range from ~0.5 to 200 keV/amu. The absence of experimental data (except for He^{2+}, B^{5+}, C^{6+} in very restricted energy regions, and for N^{7+}, O^{8+} at only one energy) forced us to assess the accuracy of the cross section data mainly on pure theoretical arguments (see Table 1 and discussions in Section 2). Where the comparison with experimental data is possible, the best agreement is achieved with the results of the large basis close-coupling calculations (in the low and medium energy region) and with the results of CTMC (in the region 30-200 keV/amu). Above ≈300-400 keV/amu the most accurate results can be obtained by the CDW method.

TABLE 5. Reliable Total Charge Exchange Cross Section Data for Completely Stripped Ions

Ion	Energy Range (keV/amu)	Accuracy	References*
He^{2+}	0.25-500	(a) or (b)	3, 36, 24, 38, 44, 35, 48, 9
B^{5+}	0.05-25	(a) or (b)	12, 25 (PSS - data of Salop and Olson)
	0.8-200	(a) or (b)	25, 13
C^{6+}	0.013-27	(a)	41, 15
	0.5-50	(b)	43, 46, 17
	25-200	(b)	13, 43
N^{7+}	0.5-80	(b)	47
	37-150	(b)	13
O^{8+}	0.25-1	(a) or (b)	28
	0.5-50	(b)	21, 46
	37-150	(b)	13, 15
F^{9+}	1-50	(b)	47
	500-5,000	(a) or (b)	39
Ne^{10+}	1-50	(b)	26, 47
	30-200	(b)	13, 26
Al^{13+}	0.8-50	(b)	47
Si^{14+}	0.8-50	(b)	43, 47
	35-200	(b)	13, 47
Cl^{17+}	0.8-60	(b)	47
Ar^{18+}	0.5-70	(b)	33, 47
	37-200	(b)	13
Ti^{22+}, Cr^{24+}	0.5-80	(b)	47
Fe^{26+}	0.5-80	(b)	47
	37-200	(b)	13
Ni^{28+}, Cu^{29+}	0.5-80	(b)	47
Kr^{36+}	0.5-90	(b)	33, 47
	37-200	(b)	13
Zr^{40+}, Mo^{42+}, Xe^{54+}, W^{74+}	0.5-100	(b) or (c)	47

*References from Appendix A.

Thus, to reach an accuracy of ~20% or better in the total charge exchange cross section data, the following methods are recommended:

1) Energy region below 25 keV/amu:

   PSS with a large MO-basis ($N \approx 2Z$) and appropriate translational factors

2) Energy range ~10—~400 keV/amu:

   CC-AO with a large ($N \approx 5Z$) basis (centered around both the proton and highly charged ion) and plane wave translational factors

3) Energy region above 400 keV/amu:

   CDW method, applied to a large number of final states (this number increases with increasing Z).

Such calculations are usually very lengthy and time consuming, even on the biggest existing computer facilities.

The charge exchange partial cross section data are much more scarce than those for the total cross sections. This is a result of the fact that capture to specific final states has only recently become experimentally measurable (and is still restricted to low charged ions and/or high energies). In most of the theoretical methods, the calculation of the partial cross sections σ_n, $\sigma_{n\ell}$ and $\sigma_{n\ell m}$ is a necessary step for obtaining the total cross section. (To this group of methods belong all AO- or MO-expansion methods, UDW, CDW, VPS, etc.) In M-LZ-RC and CC-MO-An, only σ_n is obtained directly from the calculations, and for calculating $\sigma_{n\ell}$ or $\sigma_{n\ell m}$ additional assumptions have to be made. An additional procedure is also needed to obtain σ_n and $\sigma_{n\ell}$ within the CTMC method. The partial cross sections cannot be obtained at all within the decay models and Cℓ M-An.

The most accurate data for the partial cross sections can be obtained again using CC-MO, CC-AO and CDW methods in the region of their validity.

However, due to the coupling of sub-states, in order to obtain a distribution of the captured electrons over the final state quantum numbers n or ℓ, one must use an extremely large basis, whose size increases dramatically with increasing Z.

3.4.2. Cross sections for partially stripped ions

The theoretical charge exchange cross section data for incompletely stripped ions are rather scarce due to the following circumstances:

a) not all of the methods discussed in Section 2 (see also Table 1) are applicable to this case (e.g. M-LZ-RC, Cℓ M-An, CC-MO-An);

b) in any of the CC methods, the basis set increases dramatically as the number of electrons in the colliding system increases;

c) in some of the methods (e.g. CTMC, BK-Eik, UDW) the presence of electrons in the ionic core can be taken into account by introducing the concept of "effective charge," but this procedure may produce an uncontrollable error in the result.

The last two circumstances inhibit extensive and systematic charge exchange cross section calculations for incompletely stripped ions.

The application of the CC methods with a restricted basis or the introduction of effective charge for the ion necessarily implies a reduced accuracy of the obtained results. At very high collision energies, the structure of incompletely stripped ions more directly influences the dynamics of the collision event. At these energies, the ion-core electrons may also make transitions either in the discrete or into the continuous spectrum. In this situation, the methods of Section 2 become inadequate to describe the collision dynamics. Their formal application to calculate the charge exchange cross section may include uncontrollable errors.

All of the above discussion illustrates that charge exchange cross section calculations for partially stripped ions involve considerable conceptional and technical difficulties. Extensive CC calculations seem to be unavoidable for obtaining cross section data of high accuracy in the low and intermediate velocity region. In the high energy region (but below the energies when inner-shell processes dominate) the concept of effective charge, combined with the usual high-energy models, may be sufficient for obtaining cross section data of modest ((b) or (c)) accuracy.

4. SCALING LAWS FOR THE CHARGE EXCHANGE CROSS SECTIONS

Another approach to meet the needs for cross section data in a wide region of dynamical parameters v and Z, is to try to establish firmly some scaling relationships which will provide an easy estimate of the cross section with a given accuracy. It should be immediately said, however, that the very existence of a scaling law with respect to a given collision parameter (say Z) is connected with the predominance of a single physical mechanism that governs the charge exchange process. As discussed in Section 2, the mechanisms responsible for the charge exchange process are different in different velocity regions, and one should expect that the corresponding scaling laws are also different. It is thus necessary to employ a semiempirical matching procedure to connect the scaling relations valid in different velocity regions.

The most important, from a practical point of view, is the scaling of the total charge exchange cross section with respect to the ionic charge Z. This has recently been discussed in detail elsewhere [32]. We would like to mention at once that the close-coupling methods (CC-MO or CC-AO), both because of their conceptual and practical aspects, cannot provide scaling relationships in a

physically transparent way. Yet, under the condition that a large number of close-coupling cross sections are performed (for different Z and with accordingly sized basis sets), one may expect that some suitable analytical formulae, generalizing such results, can be established (as in the case of the UDW results, for example; see below). At present, very limited numbers of CC calculations are performed, mostly for the H + Z system with low values of Z and using different basis sets, translational factors, etc.

Simplification of the collision dynamics in certain velocity regions with reference to a particular model is the easiest way to obtain a cross section scaling law for the process. However, the accuracy of the models is in most cases within a factor of two, and this accuracy is transferred also in the scaling. For the H + Z system, the following scaling laws, within the models discussed in Section 2, have been established [5,32,35]:

$$\sigma_{ASM} = 1.1 \times 10^{-17}\ Z\ \ell n^2 \left[\frac{690}{zv}\ \ell n^2\ \frac{690}{zv}\right]\ (cm^2) \qquad (8)$$

$$\sigma_{DM} = 1.5 \times 10^{-16}\ Z\ \ell n \left(\frac{314}{v}\right)\ (cm^2) \qquad (9)$$

$$\sigma_{Cl\ M\text{-}An} \simeq 7 \times 10^{-16}\ Z\ (cm^2)\ ,\quad Z \gtrsim 10,\ v \lesssim 1 \qquad (10)$$

$$\sigma_{CTMC} \simeq 4.6 \times 10^{-16}\ Z\ (cm^2)\ ,\quad v \approx 1\ . \qquad (11)$$

The validity region of the scaling laws σ_{ASM} and σ_{DM} is determined by the validity regions of the ASM and DM themselves.

The results of the M-LZ-RC can be analytically represented by the formula [36]

$$\sigma_{M\text{-}LZ\text{-}RC} = 2.25 \times 10^{-16}\ Z\ \ell n \left(\frac{15}{v}\right)\ cm^2 \qquad (12)$$

$$16 \lesssim Z \lesssim 74\ ,\quad 0.04 \lesssim v \lesssim 2$$

with an accuracy of $\lesssim$5%.

In all the above formulae, (8)-(12), the velocity v is expressed in atomic units. These formulae are valid in the region below v ~ 1-2. A semi-empirical formula for the cross section in a wide energy region ($\sim 10^{-3}$-10^{3} keV/amu) has recently been proposed [34] on the basis of the UDW calculations and existing experimental data. By introducing scaled (or reduced) quantities

$$\tilde{\sigma} = \frac{\sigma}{Z^{1.07}} \quad , \quad \tilde{E} = \frac{E}{Z^{0.465}} \tag{13}$$

and expressing $\tilde{E}$ in units of eV/amu/charge, the "universal" cross section formula reads:

a) $1 \leq \log_{10}\tilde{E} \leq 4$

$$\log_{10}\tilde{\sigma} = -15.0706 - 0.0224531\ \xi_1 - 0.0144073\ \xi_1^2 \tag{14a}$$

$$\xi_1 = \log_{10}\tilde{E} - 1$$

b) $4 \leq \log_{10}\tilde{E} \leq 5$

$$\log_{10}\tilde{\sigma} = -15.2676 - 0.474885\ \xi_2 - 1.04186\ \xi_2^2 - 0.301838\ \xi_2^3 \tag{14b}$$

$$\xi_2 = \log_{10}\tilde{E} - 4$$

c) $5 \leq \log_{10}\tilde{E} \leq 6$

$$\log_{10}\tilde{\sigma} = -17.0862 - 4.39144\ \xi_3 - 0.221343\ \xi_3^2 \tag{14c}$$

$$\xi_3 = \log_{10}\tilde{E} - 5$$

where $\tilde{\sigma}$ is expressed in cm^2.

The expression (14) for $\tilde{\sigma}$ is compatible within a factor of two with almost all existing theoretical and experimental data for $10 \lesssim Z \lesssim 50$.

The BK-Eikonal model has also provided a scaling formula for the H + Z charge exchange cross sections in the region $2 \leq v \leq 5$. That formula is given

by Eqs. (6) and (7) in which the correction function $\alpha(n,Z,v)$ is given by [29]

$$\alpha(n,Z,v) = \frac{(\pi/v)}{\mathrm{sh}(\pi/v)} \exp\left[-\frac{2}{v}\arctan\left(\frac{v}{2}+\frac{\omega_n}{v}\right)\right] \times$$

$$\times \left[\frac{23}{48} + \left(\frac{1}{6} - \frac{5\omega_n}{6}\right)\frac{1}{v^2} + \frac{5}{12}\frac{\omega_n^2}{v^4}\right] \qquad (15)$$

where $\omega_n = [(Z^2/2n^2) - (1/2)]$. For $v \gg Z/n$, the function $\alpha(n,Z,v)$ very weakly depends on n and Z, and it increases smoothly between the values 0.15 and 0.4 when v increases from v = 2 to v = 5.

Starting with an integral representation of the Brinkman-Kramers cross section, one can derive the following Z-dependences of the electron capture cross section at medium and high collision velocities [37,38]

$$\sigma \sim Z^3 \quad , \quad Z^{1/2} \gtrsim v \qquad (16a)$$

$$\sigma \sim Z^5 \quad , \quad v \gg Z^{1/2} \qquad (16b)$$

The Z^3-dependence of σ in the region of $v \approx 2$-5 is consistent both with the CDW results and the experimental data [33]. The Z^5-dependence of σ can be reached only at very high collision velocities and experimentally has been proven [39] for $Z \lesssim 20$ and $v \sim 100$.

In order to summarize our discussion on the Z scaling of the charge exchange cross section, let us represent σ in the form

$$\sigma = \sigma_o(\tilde{v})\, Z^{\alpha(\tilde{v})} \quad , \quad \tilde{v} = v/Z^{1/4} \quad . \qquad (17)$$

In the interval $0.1 \lesssim \tilde{v} \lesssim 100$, the function $\alpha(\tilde{v})$ behaves as shown in Fig. 2. In the region $\tilde{v} \lesssim 1$, α takes a value of ≈ 1.1. The two-state coupled channel calculations [37] have predicted an increase of α from the values $\alpha \approx 2$ to $\alpha \approx 5$ in the region between $\tilde{v} \approx 1$ and $\tilde{v} \approx 25$. However, the correct scaling

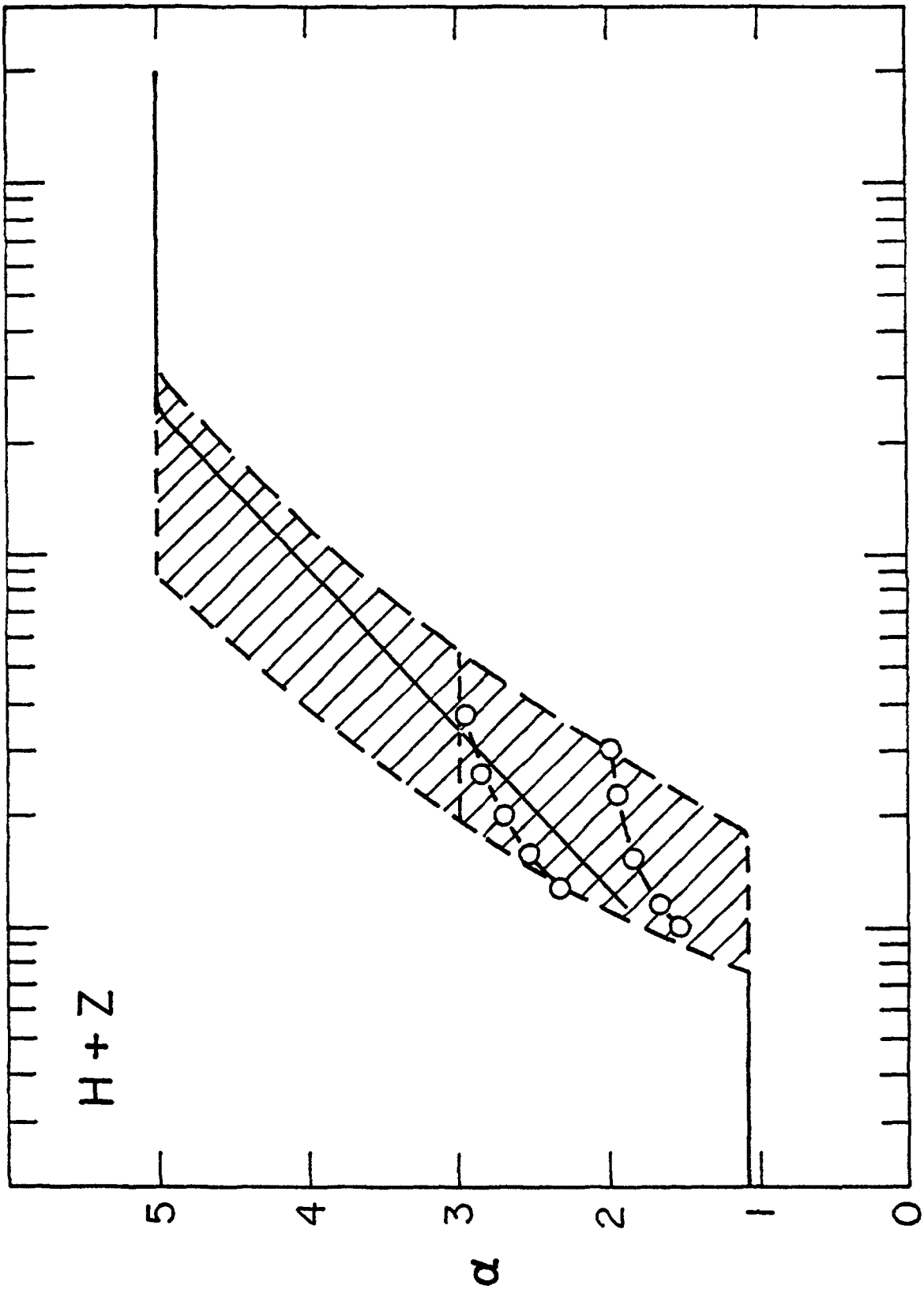

Figure 2

law in this region cannot be considered as well established. The experimental data (obtained mostly for many-electron targets and/or with incompletely stripped ions) are fairly scattered and cannot provide a conclusive answer for the scaling law in the velocity region $\tilde{v} \sim 1\text{-}20$ (see the open symbols in Fig. 2). For many-electron colliding systems, the cross section in the region of $\tilde{v}$ between $\approx 3\text{-}20$ strongly depends on the structure of the colliding particles. For such systems it is difficult to expect a simple Z-scaling.

5. CONCLUDING REMARKS

In the past decade, theoretical investigations of the charge exchange process between multiply charged ions and atomic hydrogen have been characterized by developing and testing different methods for describing the process. The cross section calculations were primarily illustrative in character and, with a few exceptions, neither their accuracy nor systematic cross section data production was their ultimate goal. This situation changed only very recently when suitable improvements in some of the methods made them adequate for high accuracy cross section calculations. Still, the current rate of production of charge exchange cross section data for the multiply charged ions is far short of meeting the needs for such data in the controlled fusion programs. The methods capable of providing high accuracy data (such as CC-MO, CC-AO and CDW), require a hugh amount of computer time, especially for the cross sections of high-Z ions. Nevertheless, it seems at present that such extensive calculations are necessary to perform, at least for a reasonably large number of ions with charge states covering a wide range, in order to obtain rigorous results which could serve as benchmarks and criteria for clarifying or checking some of the uncertainties still present in some of the

theoretical methods. Such rigorous results could be especially useful in setting up the Z-scaling laws, the n- and ℓ-distributions of captured electrons (and their velocity and charge state dependences), as well as for establishing sufficiently accurate semi-empirical formulae for the cross sections. In order to support such an approach in reducing the task for a straightforward accumulation of all charge transfer cross section data needed for fusion, it would be desirable to have also accurate experimental data for the corresponding colliding pairs, for which the detailed calculations are done. At present, such a program has been accomplished only for the low charge completely stripped ions He^{2+}, Li^{3+} and C^{6+} (partly).

Acknowledgment

This work has been performed during our stays at the Joint Institute for Laboratory Astrophysics of the University of Colorado and National Bureau of Standards, Boulder. It gives us great pleasure to express our gratitude to J. Gallagher and to the other staff of the JILA Information Center for their devoted assistance in the course of this work and in particular for the help in technical presentation of the material. We are also deeply indepted to L. Volsky and the staff of the JILA Publications Office for exceptional editorial assistance.

References

1. M. C. R. McDowell and A. Ferendeci, eds. Atomic and Molecular Processes in Thermonuclear Fusion Research (Plenum, New York, 1980).
2. See, e.g., Phys. Rep. 37 (1978); Physica Scripta 23 (No. 2) (1981).
3. R. E. Olson, in Electronic and Atomic Collisions, Eds. N. Oda and K. Takayanagi (North-Holland, Amsterdam, 1980), p. 391.
4. B. H. Bransden, see Ref. 1, p. xxx.
5. R. K. Janev and L. P. Presnyakov, Phys. Rev. 70, 1 (1981).
6. P. T. Greenland, Phys. Rep. 81, 131 (1982).
7. N. F. Mott and H. S. W. Massey, The Theory of Atomic Collisions, 3rd ed. (Oxford University Press, Oxford, 1971).
8. D. R. Bates and R. McCarroll, Proc. R. Soc. (London) Ser. A 245, 175 (1958).
9. R. D. Piacentini and A. Salin, J. Phys. B 7, 1666 (1974).
10. T. A. Green, E. J. Shipsey and J. C. Browne, Phys. Rev. 23, 546 (1981); ibid., 25, 1364 (1982).
11. C. Har el and A. Salin, J. Phys. B 10, 3511 (1977).
12. A. Salop and R. E. Olson, Phys. Rev. 19, 1921 (1979).
13. L. I. Ponomarev, Zh. Eksp. Teor. Fiz. 55, 1836 (1968).
14. L. P. Presnyakov, D. B. Uskov and R. K. Janev, Phys. Lett. 84A, 243 (1981); Zh. Eksp. Teor. Fiz. (1982, in press).
15. A. Salop and R. E. Olson, Phys. Rev. A 13, 1312 (1976).
16. V. A. Abramov, F. F. Baryshnikov and V. S. Lisitsa, Sov. Phys.-JETP 47, 469 (1979).
17. R. K. Janev and D. S. Belić, Phys. Rev. (submitted).
18. R. E. Olson and A. Salop, Phys. Rev. A 14, 576 (1976).
19. M. I. Chibisov, JETP Lett. 24, 46 (1976).
20. T. P. Grozdanov and R. K. Janev, Phys. Rev. A 17, 880 (1978).

21. B. H. Bransden, C. W. Newby and C. J. Noble, J. Phys. B 13, 4245 (1980); B. H. Bransden and C. J. Noble, J. Phys. B 14, L297 (1981); ibid., 15, 451 (1982).

22. N. Fritsch, J. Phys. B 15 (in press).

23. J. F. Reading, A. L. Ford and R. L. Becker, J. Phys. B 14, 1995 (1981); ibid., 15 (in press).

24. H. Ryufuku and T. Watanabe, Phys. Rev. A 18, 2005 (1978); ibid., 19, 1538 (1979); ibid., 20, 1828 (1979).

25. L. P. Presnyakov and A. D. Ulantsev, Sov. J. Quant. Electronics 4, 1320 (1975).

26. V. P. Shevel'ko, Z. Phys. A 287, 19 (1978).

27. R. E. Olson and A. Salop, Phys. Rev. A 16, 531 (1977).

28. T. P. Grozdanov, J. Phys. B 13, 3835 (1980).

29. F. T. Chan and J. Eichler, Phys. Rev. Lett. 42, 58 (1979); Phys. Rev. A 20, 104 (1979); ibid., 20, 1841 (1979).

30. See, e.g. Dz. Belkić, R. Gayet and A. Salin, Phys. Rep. 56, 279 (1979).

31. R. Shakeshaft, Phys. Rev. A 10, 1096 (1974).

32. R. K. Janev and P. Hvelplund, Comments Atom. Molec. Phys. 11, 75 (1981).

33. See, e.g., H. B. Gilbody, Physica Scripta 23, 143 (1981).

34. Y. Kaneko et al., IPP J-AM-15, Inst. Plasma Phys. Nagoya Univ. (1980).

35. V. A. Abramov, F. F. Baryshnikov and V. S. Lisitsa, Physica Scripta 23, 125 (1981).

36. D. S. Belić, B. H. Bransden and R. K. Janev, Phys. Rev. (submitted).

37. A. Müller and V. P. Shevelko, Zh. Tech. Fiz. 50, 985 (1980).

38. D. S. F. Crothers and N. R. Todd, J. Phys. B 13, 2277 (1980).

39. G. M. Raisbeck, H. J. Crawford, P. J. Lindstrom, D. E. Greiner, F. S. Beiser and H. H. Keckman, X ICPEAC, Paris, 1977, abstract of papers, eds. M. Barat and J. Reinchardt (North-Holland, Amsterdam, 1977), p. 854.

Table 3. Theoretical Data for Charge Transfer Between Atomic Hydrogen and Totally Stripped Ions

Reference*	Energy Range (keV/amu)	Energy Region	Method[a]	Comments	Data
			H-He^{2+}		
24	0.25-17	L†	CC-MO	10-state including plane wave functions	$\sigma_t, \sigma_{n\ell}$
36	0.75-5	L	CC-MO		$\sigma_t, \sigma_{n\ell}$
38	0.25-5	L	CC-MO	12-state	$\sigma_t, \sigma_{n\ell}$
1	1.5-250	(L)M	CC-AO	5-state	$\sigma_t, \sigma_{n\ell}$
3	1.5-4000	M(H)	CC-AO	8-state	$\sigma_t, \sigma_{n\ell}$
4	0.25-150	(L)M	CC-AO	8- and 11-state	$\sigma_t, \sigma_n, \sigma_{n\ell}$
11	1-50	(L)M	CC-AO	No translational factors	σ_t
30	5-200	M	CC-AO	$n \leq 4$: 2-state $n > 4$: n^{-3} low	$\sigma_t, \sigma_{n\ell}$
35	2.5-250	M	CC-AO	8-state basis $n \geq 3$ by n^{-3}	$\sigma_t, \sigma_{n\ell}$
37	1.5-100	(L)M	CC-AO		$\sigma_t, \sigma_{n\ell}$
42	25-110	M	CC-AO		$\sigma_t, \sigma_{n\ell}$
44	1-50	(L)M	CC-AO	Plane wave factors (a) 8-state atomic (b) 19-24 Sturmian	σ_t
48	3.5-220	M	CC-AO	20-state basis for $n \leq 3$	$\sigma_t, \sigma_{n\ell}$
49	3.5-220	M	CC-AO	2-state for $n = 4$ n^{-3} rule for $n \geq 5$	$\sigma_t, \sigma_{n\ell}$
21	0.025-200	(L)M	UDW		σ_t
14	20-180	M	CTMC		σ_t
19	100	(M)H	BK		$\sigma_{n\ell}$
19	100	(M)H	B1		$\sigma_{n\ell}$
32	25-2000	(M)H	B1	5-state with variational translational factor	$\sigma_t, \sigma_{n\ell}$
34	6-200	(M)H	DW		$\sigma_{n\ell}$
2	6-750	(M)H	CDW		$\sigma_t, \sigma_{n\ell}$
9	25-500	(M)H	CDW		$\sigma_t, \sigma_{n\ell}$
10	625	H	CDW		$\sigma_{n\ell}$
34	132	H	CDW	Capture into $1 \leq n \leq 15$ to illustrate departure from n^{-3} rule	σ_n
			H-B^{5+}		
12	0.25-25	L	PSS	3-states	σ_t
25	0.05-8	L	PSS		σ_t
40	0.5,1	L	CC-MO-An	n,ℓ separable interaction model	σ_t
46	0.49,1,10,25	L	M-LZ-RC	Rotational coupling included	$\sigma_t, \sigma_{n\ell}$
7	2.58	L	ASM		σ_t
18	1-100	L(M)	DM		σ_t

*The references in this table are given in Appendix A.

†L, M, H stand for Low-, Medium- and High-energy region.

Table 3. (cont'd.)

Reference	Energy Range (keV/amu)	Energy Region	Method[a]	Comments	Data
			H-B^{5+}		
20	2.58,47.3	L(M)	DM		σ_t
11	1-170	M	CC-AO	Sequence of two-state CC	σ_t
30	5-200	M	CC-AO	$n \lesssim 5$, 2-state CC $n > n^{-3}$ low	$\sigma_t,\sigma_n,\sigma_{nl}$
25	0.02-200	(L)M	UDW		σ_t
43	0.01-5000	(L)M(H)	UDW		σ_t
13	37.5-150	M	CTMC		σ_t
27	25,32,55,73	M	CTMC		$\sigma_t,\sigma_n,\sigma_{nl}$
39	50	M	CTMC		$\sigma_t,\sigma_n,\sigma_{nl}$
10	625	H	CDW		σ_{nl}
			H-C^{6+}		
31	0.0625-25	L	CC-MO		σ_t
41	0.013-27.4	L	CC-MO	Translational factors nonlinear trajectories below 1.3 keV/amu	$\sigma_t,\sigma_n,\sigma_{nl}$
15	0.05-20	L	PSS	6 molecular states coord. origin on H^+ rotational coupling included	σ_t
16	0.0625-6.25	L	PSS	11 states (adiabatic molecular) Rotational coupling included Coulomb trajectories for nuclei R-adjustable translational factors	σ_t
40	0.5,1	L	CC-MO-An	Separable interactions model	σ_t
8	0.04-2.8	L	M-LZ	Rotational coupling of degenerated states not taken into account	σ_t
17	0.01-25	L	M-LZ-RC	Rotational coupling included	σ_t
46	0.04-50	L	M-LZ-RC	Rotational coupling included	$\sigma_t,\sigma_n,\sigma_{nl}$
47	0.1,1,10	L	M-LZ-RC	Rotational coupling included	σ_t,σ_n
7	2.58	L	ASM		σ_t
18	1-100	L(M)	DM		σ_t
20	2.58,47.3	L(M)	DM		σ_t
11	1-180	M	CC-AO	Sequence of two-state coupling	σ_t
25	0.02-2000	(L)M(H)	UDW		σ_t
43	0.01-5000	(L)M(H)	UDW	Includes ionization and excitation channels	σ_t
13	37.5-150	M	CTMC		σ_t
15	20-200	M	CTMC		σ_t
27	25,33,55,76	M	CTMC		$\sigma_t,\sigma_n,\sigma_{nl}$
39	25,50,75,100	M	CTMC		$\sigma_t,\sigma_n,\sigma_{nl}$
23	50,500,5000	(M)H	BK-Eik		σ_n
10	500-5000	H	CDW		σ_{nl}

Table 3. (cont'd.)

Reference	Energy Range (keV/amu)	Energy Region	Method[a]	Comments	Data
			$H-N^{7+}$		
40	0.5-1	L	CC-MO-An	n,ℓ - separable model	σ_t
8	0.028-2.8	L	M-LZ	Rotational coupling excluded	σ_t
46	0.49,1,10,25	L	M-LZ-RC	Rotational coupling included	σ_t,σ_n
47	0.01-100	L(M)	M-LZ-RC	Rotational coupling included	σ_t
7	2.58	L	ASM		σ_t
18	1-1000	L(M)	DM		σ_t
20	2.58,47.3	L(M)	DM		σ_t
11	1-200	M	CC-AO	Sequence of 2-state coupling	σ_t
13	37.5-150	M	CTMC		σ_t
39	50	M	CTMC		$\sigma_t,\sigma_n,\sigma_{n\ell}$
10	625	H	CDW		$\sigma_{n\ell}$
			$H-O^{8+}$		
40	0.5,1	L	CC-MO	n,ℓ - separable coupling interaction	σ_t
12	0.25-25	L	PSS	3-molecular states + rotational coupling Origin on O^{8+}	σ_t
28	0.025-7.56	L	PSS	8-molecular states + rotational coupling Origin on O^{8+} Origin on H^+	σ_t
7	0.028-2.8	L	M-LZ	No rotational coupling	σ_t
17	0.01-25	L	M-LZ-RC	Rotational coupling included	σ_t
46	0.01-50	L	M-LZ-RC	Rotational coupling included	$\sigma_t,\sigma_n,\sigma_{n\ell}$
47	0.1,1,10	L(M)	M-LZ-RC	Rotational coupling included	σ_t,σ_n
7	2.58	L	ASM		σ_t
18	1-100	L(M)	DM		σ_t
20	2.58,47.3	L(M)	DM		σ_t
11	1-180	M	CC-AO	Sequence of 2-state CC	σ_t
21	0.02-200	(L)M	UDW		σ_t
13	37.5-150	M	CTMC		σ_t
27	25,32,55,76	M	CTMC		$\sigma_t,\sigma_n,\sigma_{n\ell}$
28	25-900	M(H)	CTMC		σ_t
39	50-100	M	CTMC		$\sigma_t,\sigma_n,\sigma_{n\ell}$
33	0.5-100	M	C1M-An		σ_t
22	100	(M)H	BK-Eik		$\sigma_{n\ell}$
10	625	H	CDW		$\sigma_{n\ell}$

Table 3. (cont'd.)

Reference	Energy Range (keV/amu)	Energy Region	Method[a]	Comments	Data
			H-F^{9+}		
40	0.5,1	L	CC-MO-An		σ_t
46	0.49,1,10,25	L	M-LZ-RC	Rotational coupling included	σ_t,σ_n
47	0.01-100	L(M)	M-LZ-RC	Rotational coupling included	σ_t
7	2.58	L	ASM		σ_t
18	1-100	L(M)	DM		σ_t
20	2.58,47.3	L(M)	DM		σ_t
11	1-225	M	CC-AO	Sequence of 2-state CC	σ_t
39	50	M	CTMC		$\sigma_t,\sigma_n,\sigma_{n\ell}$
7	625	H	CDW		$\sigma_{n\ell}$
			H-Ne^{10+}		
40	0.5,1	L	CC-MO-An		σ_t
8	0.028-2.8	L	M-LZ	Rotational coupling excluded	σ_t
46	0.49,1,10,25	L	M-LZ-RC	Rotational coupling included	$\sigma_t,\sigma_n,\sigma_{n\ell}$
47	0.01-100	L(M)	M-LZ-RC	Rotational coupling included	σ_t,σ_n
7	2.58	L	ASM		σ_t
6	50	L(M)	DM		σ_t
18	1-100	L(M)	DM		σ_t
20	0.002-337	L(M)	DM		σ_t
5	0.01-1600	(L)M(H)	CC-AO	VPS approximation for 2-state amplitudes	σ_t
11	1-225	M	CC-AO		σ_t
26	5-2000	(L)M(H)	UDW		$\sigma_t,\sigma_n,\sigma_{n\ell}$
13	37.5-200	M	CTMC		σ_t
39	50,100	M	CTMC		$\sigma_t,\sigma_n,\sigma_{n\ell}$
33	0.5-100	(L)M	CℓM-An		σ_t
10	625	H	CDW		$\sigma_{n\ell}$
			H-$A\ell^{13+}$		
40	0.5,1	L	CC-MO-An		σ_t
46	0.5,1	L	M-LZ-RC	Rotational coupling included	σ_t,σ_n
47	0.01-100	L(M)	M-LZ-RC	Rotational coupling included	σ_t,σ_n
7	2.58	L	ASM		σ_t
18	1-100	L(M)	DM		σ_t
20	2.58,47.3	L(M)	DM		σ_t
10	625	H	CDW		$\sigma_{n\ell}$

Table 3. (cont'd.)

Reference	Energy Range (keV/amu)	Energy Region	Method[a]	Comments	Data
			H-Si^{14+}		
40	0.1-350	L(M)	CC-MO-An		σ_t
8	0.028-2.8	L	M-LZ	Rotational coupling excluded	σ_t
46	0.01-50	L	M-LZ-RC	Rotational coupling included	$\sigma_t,\sigma_n,\sigma_{nl}$
47	0.01-100	L(M)	M-LZ-RC	Rotational coupling included	σ_t
7	2.58	L	ASM		σ_t
18	1-100	L(M)	DM		σ_t
20	2.58,47.3	L(M)	DM		σ_t
11	1-225	M	CC-AO		σ_t
26	5-2000	(L)M(H)	UDW		σ_n
43	0.01-5000	(L)M(H)	UDW		σ_t
13	37.5-200	M	CTMC		σ_t
39	100	M	CTMC		σ_n,σ_{nl}
33	0.5-100	(L)M	CℓM-An		σ_t
10	625	H	CDW		σ_{nl}
			H-$C\ell^{17+}$		
40	I	L	CC-MO-An		σ_t
47	0.01-100	L	M-LZ-RC	Rotational coupling included	σ_t
7	2.58	L	ASM		σ_t
18	1-100	L(M)	DM		σ_t
20	2.58,47.3	L(M)	DM		σ_t
10	625	H	CDW		σ_{nl}
			H-Ar^{18+}		
40	I	L	CC-MO-An		σ_t
8	0.028-2.8	L	M-LZ		σ_t
46	0.5,1,10,25	L	M-LZ-RC	Rotational coupling included	σ_n
47	0.01-100	L(M)	M-LZ-RC	Rotational coupling included	σ_t
7	2.58	L	ASM		σ_t
18	1-100	L(M)	DM		σ_t
20	2.58,47.3	L(M)	DM		σ_t
11	1-225	M	CC-AO		σ_t
13	37.5-200	M	CTMC		σ_t
39	100	M	CTMC		$\sigma_t,\sigma_n,\sigma_{nl}$
33	0.5-100	(L)M	CℓM-An		σ_t
10	625	H	CDW		σ_{nl}

Table 3. (cont'd.)

Reference	Energy Range (keV/amu)	Energy Region	Method[a]	Comments	Data
			H-Ti^{22+}		
40	0.5,1	L	CC-MO-An		σ_t
47	0.01-100	L(M)	M-LZ-RC	Rotational coupling included	σ_t,σ_n
7	2.58	L	ASM		σ_t
18	1-100	L(M)	DM		σ_t
20	2.58,47.3	L(M)	DM		σ_t
10	625	H	CDW		$\sigma_{n\ell}$
			H-Cr^{24+}		
40	0.5,1	L	CC-MO-An		σ_t
46	0.4,100	L(M)	M-LZ-RC	Rotational coupling included	σ_t,σ_n
47	0.01-100	L(M)	M-LZ-RC	Rotational coupling included	σ_t,σ_n
7	2.58	L	ASM		σ_t
18	1-100	L(M)	DM		σ_t
20	2.58,47.3	L(M)	DM		σ_t
10	625	H	CDW		$\sigma_{n\ell}$
			H-Fe^{26+}		
29	0.21,1.3,5.3	L	PSS	17 molecular states	σ_t
40	0.5,1	L	CC-MO-An		σ_t
46	1,10,25	L	M-LZ-RC	Rotational coupling included	σ_n
47	0.01-100	L(M)	M-LZ-RC	Rotational coupling included	σ_t,σ_n
7	2.58	L	ASM		σ_t
18	1-100	L(M)	DM		σ_t
20	2.58,47.3	L(M)	DM		σ_t
33	0.5-100	L	C&M-An		σ_t
13	37.5-200	M	CTMC		σ_t
29	84-258	M	CTMC		σ_t
10	625	H	CDW		$\sigma_{n\ell}$
			H-Ni^{28+}		
40	0.5,1	L	CC-MO-An		σ_t
46	10,25	L	M-LZ-RC	Rotational coupling included	σ_n
47	0.01-100	L(M)	M-LZ-RC	Rotational coupling included	σ_t,σ_n
7	2.58	L	ASM		σ_t
18	1-100	L(M)	DM		σ_t
20	2.58,47.3	L(M)	DM		σ_t
10	625	H	CDW		$\sigma_{n\ell}$

Table 3. (cont'd.)

Reference	Energy Range (keV/amu)	Energy Region	Method[a]	Comments	Data
			H-Cu^{29+}		
40	0.5,1	L	CC-MO-An		σ_t
47	0.01-100	L(M)	M-LZ-RC	Rotational coupling included	σ_t
7	2.58	L	ASM		σ_t
18	1-100	L(M)	DM		σ_t
20	2.58,47.3	L(M)	DM		σ_t
10	625	H	CDW		$\sigma_{n\ell}$
			H-Kr^{36+}		
46	10,25	L	M-LZ-RC	Rotational coupling included	σ_n
47	0.01-100	L(M)	M-LZ-RC	Rotational coupling included	σ_t
7	2.58	L	ASM		σ_t
20	2.58,47.3	L(M)	DM		σ_t
13	37.5-200	M	CTMC	Numerical	σ_t
33	0.5-100	(L)M	CℓM-An	Analytical	σ_t
			H-Zr^{40+}		
47	0.01-100	L(M)	M-LZ-RC	Rotational coupling included	σ_t
7	2.58	L	ASM		σ_t
20	2.58,47.3	L(M)	DM		σ_t
			H-Mo^{42+}		
47	0.01-100	L(M)	M-LZ-RC	Rotational coupling included	σ_t,σ_n
7	2.58	L	ASM		σ_t
			H-Xe^{54+}		
47	0.01-100	L(M)	M-LZ-RC	Rotational coupling included	σ_t
			H-W^{74+}		
47	0.01-100	L(M)	M-LZ-RC	Rotational coupling included	σ_t

[a]Definition of abbreviations for methods used in Tables 3 and 4:

CC-MO	Close coupling - molecular orbital
PSS-Q	Perturbed stationary state - quantal version
PSS	Perturbed stationary state - impact parameter version
LZ	Landau-Zener
CC-MO-An	Close-coupling molecular orbital, analytic
M-LZ	Multichannel Landau-Zener
M-LZ-RC	Multichannel Landau-Zener with rotational coupling
ASM	Absorbing sphere model
DM	Decay model
CC-AO	Close coupling - atomic orbital
M-VPS	Multichannel Vainstein-Presnyakov-Sobelman
UDW	Unitarized distorted wave
CTMC	Classical trajectory Monte Carlo
Cl•M-An	Classical model, analytical
VPS-emp	Vainstein-Presnyakov-Sobelman, empirical
BK	Brinkmann-Kramers
Bl	First Born
BK-Eik	Brinkmann-Kramers - Eikonal
CDW	Continuum distorted wave

Table 4. Theoretical Data for Charge Exchange of Atomic Hydrogen with Partially Stripped Ions

Reference*	Energy Range	LMH	Method†	Comments	Data
			H-B^{2+}		
11	0.03-9 keV/amu	(L)M	CC-AO	2 states Exponential factor	σ_t
			H-B^{3+}		
5	0.053-5.3 keV/amu	L	PSS	8 molecular states	σ_t
4	37.5-130 keV/amu	M	CTMC	Effective charge	σ_t
			H-B^{4+}		
4	37.5-130 keV/amu	M	CTMC	Effective charge	σ_t
			H-C^{2+}		
10	0.5-5 eV	(T^1)L	PSS-Q	Full quantum treatment CI^+ - basis	k_T§
14	40-700 keV/amu	(M)H	Bk-Eik	Effective charge	σ_t
			H-C^{3+}		
1	0.1-1.75 eV	(T)L	PSS-Q	2 states	σ_t
8	0.001-4 eV	(T)L	PSS-Q	2 states	σ_t, k_T
10	0.5-5 eV	(T)L	PSS-Q	CI - large basis Full quantum treatment	k_T
16	0.27-8.1 eV	(T)L	PSS-Q	CI - large basis	σ_t
4	37.5-150 keV/amu	M	CTMC	Effective charge	σ_t
14	40-1000 keV/amu	(M)H	BK-Eik	Effective charge	σ_t
			H-C^{4+}		
15	0.01-100 eV	(T)L	PSS-Q	5 coupled states	σ_t, k_T
5	0.053-5.26 keV/amu	L	PSS	7 molecular states	σ_t
9	0.1-2.7 eV	(T)	LZ		k_T
3	2.58 keV/amu	L	ASM	Accuracy ~40%	σ_t
4	37.5-150 keV/amu	M	CTMC	Effective charge	σ_t
12	0.25-2.5 keV/amu	(L)M	VPS-emp	1/3 empirical factor introduced	σ_t
14	50;100;145;1000 keV/amu	(M)H	BK-Eik	Effective charge	σ_t

*The references in this table are given in Appendix B.

†Thermal energy region; L, M, H have same meaning as in Table 3.

§Reaction rate coefficient.

‡Configuration interaction method.

Table 4. (cont'd.)

Reference	Energy Range	LMH	Method[a]	Comments	Data
			H-C^{5+}		
17	0.0132-7.58 keV/amu	(T)L	PSS	5 molecular states	σ_t
3	2.58 keV/amu	L	ASM	Accuracy ~±40%	σ_t
4	37-150 keV/amu	M	CTMC	Effective charge	σ_t
14	50;100;145;1000 keV/amu	(M)H	BK-Eik	Effective charge	σ_t
			H-N^{2+}		
10	0.5-5 eV	(T)L	PSS-Q	CI - large basis	k_T
16	2.7×10^{-4} - 8.1	(T)L	PSS-Q	CI - large basis	σ_t
14	40-800 keV/amu	(M)H	BK-Eik	Effective charge	σ_t
			H-N^{3+}		
8	0.001-4 eV	(T)L	PSS-Q	2 states	σ_t, k_T
10	0.5-5 eV	(T)L	PSS-Q	CI - large basis	k_T
15	10^{-4}-100 eV	(T)L	PSS-Q	4 states	σ_t, σ_n, k_T
4	37.5-150 keV/amu	M	CTMC	Effective charge	σ_t
14	40-1000 keV/amu	(M)H	BK-Eik	Effective charge	σ_t
			H-N^{4+}		
9	0.1-2.7 eV	(T)L	LZ		k_T
3	2.58 keV/amu	L	ASM	Accuracy ~±40%	σ_t
4	37.5-150 keV/amu	M	CTMC	Effective charge	σ_t
12	0.25-2500 keV/amu	M(H)	VPS-emp	1/3 empirical factor for second order effects	σ_t
14	50;100;145;1000 keV/amu	(M)H	BK-Eik	Effective charge	σ_t
			H-N^{5+}		
17	0.0132-7.58 keV/amu	(T)L	PSS	5 molecular states	σ_t
3	2.58 keV/amu	L	ASM	Accuracy ~±40%	σ_t
4	37.5-150 keV/amu	M	CTMC	Effective charge	σ_t
14	50;100;145;1000 keV/amu	(M)H	BK-Eik	Effective charge	σ_t
			H-N^{6+}		
3	2.58 keV/amu	L	ASM	Accuracy ~±40%	σ_t
4	37.5-150	M	CTMC	Effective charge	σ_t
12	0.25-2500	M(H)	VPS-emp	1/3 empirical fator in σ_t	σ_t
14	50;100;145;1000 keV/amu	(M)H	BK-Eik	Effective charge	σ_t

Table 4. (cont'd.)

Reference	Energy Range	LMH	Method[a]	Comments	Data
			$H-O^{2+}$		
10	0.5-5 eV	(T)L	PSS-Q	Full quantal treatment	k_T
14	40-800 keV/amu	(M)H	BK-Eik	Effective charge	σ_t
			$H-O^{3+}$		
10	0.5-5 eV	(T)L	PSS-Q		k_T
13	0.5-5 eV	(T)L	PSS-Q	Production of $(O^{2+})^*$	k_T
4	37.5-100 keV/amu	M	CTMC	Effective charge	σ_t
14	40-1000 keV/amu	(M)H	BK-Eik	Effective charge	σ_t
			$H-O^{4+}$		
9	0.1-2.7 eV	(T)L	LZ		k_T
3	2.58 keV/amu	L	ASM	Accuracy ~±40%	σ_t
4	37.5-125 keV/amu	M	CTMC	Effective charge	σ_t
14	50;100;145;1000 keV/amu	(M)H	BK-Eik	Effective charge	σ_t
			$H-O^{5+}$		
3	2.58 keV/amu	L	ASM	Accuracy ~±40%	σ_t
4	37.5-125 keV/amu	M	CTMC	Effective charge	σ_t
14	50;100;145;1000 keV/amu	(M)H	BK-Eik	Effective charge	σ_t
			$H-O^{6+}$		
17	0.013-7.6 keV/amu	(T)L	PSS	8-state molecular CC	σ_t
3	2.58 keV/amu	L	ASM	Accuracy ~±40%	σ_t
4	37.5-125 keV/amu	M	CTMC	Effective charge	σ_t
14	50;100;145;1000 keV/amu	(M)H	BK-Eik	Effective charge	σ_t
			$H-O^{7+}$		
3	2.58 keV/amu	L	ASM	Accuracy ~±40%	σ_t
4	37.5-150 keV/amu	M	CTMC	Effective charge	σ_t
14	50;100;145;1000 keV/amu	(M)H	BK-Eik	Effective charge	σ_t
			$H-Ne^{2+}$		
10	0.5-5 eV	(T)L	PSS-Q		k_T

Table 4. (cont'd.)

Reference	Energy Range	LMH	Method[a]	Comments	Data
			H-Ne^{3+}		
10	0.5-5 eV	(T)L	PSS-Q		k_T
			H-Ne^{4+}		
9	0.1-2.7 eV	(T)L	LZ		k_T
12	0.25-2500 keV/amu	(L)M(H)	VPS-emp	1/3 empirical factor in σ_t	σ_t
			H-Ne^{6+}		
12	0.25-2500 keV/amu	(L)M(H)	VPS-emp	1/3 empirical factor in σ_t	σ_t
			H-Ne^{8+}		
12	0.25-2500 keV/amu	(L)M(H)	VPS-emp	1/3 empirical factor in σ_t	σ_t
			H-Al^{q+}; q = 4,6,8,10		
12	0.25-2500 keV/amu	(L)M(H)	VPS-emp	1/3 empirical factor in σ_t	σ_t
			H-Si^{2+}		
2	10^{-4} - 2.5 eV	(T)L	PSS-Q		σ_t, k_T
			H-Si^{3+}		
9	0.1-2.7 eV	(T)L	LZ		k_T
			H-Si^{4+}		
9	0.1-2.7 eV	(T)L	LZ		k_T
12	0.25-2500 keV/amu	(L)M(H)	VPS-emp	1/3 empirical factor in σ_t	σ_t
			H-Si^{q+}; q = 6,8,10		
12	0.25-2500 keV/amu	(L)M(H)	VPS-emp	1/3 empirical factor in σ_t	σ_t
			H-Ar^{q+}; q = 2,3		
9	0.1-2.7 eV	(T)L	LZ		k_T
			H-Ar^{4+}		
9	0.1-2.7 eV	(T)L	LZ		k_T
6	0.2-2000 keV/amu	(L)M	VPS-emp	1/3 empirical factor in σ_t	σ_t

Table 4. (cont'd.)

Reference	Energy Range	LMH	Method[a]	Comments	Data
			$H-Ar^{q+}$; q = 6,8,10		
6	0.2-2000 keV/amu	(L)M	VPS-emp	1/3 empirical factor in σ_t	σ_t
			$H-Ti^{q+}$; q = 4,6,8,10		
12	0.25-2500 keV/amu	(L)M(H)	VPS-emp	1/3 empirical factor in σ_t	σ_t
			$H-Fe^{q+}$; q = 4,6,8		
6	0.2-2000 keV/amu	(L)M(H)	VPS-emp	1/3 empirical factor in σ_t	σ_t
			$H-Fe^{10+}$		
7	47.3-340 keV/amu	M	CTMC		σ_t
6	0.2-2000 keV/amu	(L)M(H)	VPS-emp	1/3 empirical factor in σ_t	σ_t
			$H-Fe^{15+}$		
7	47.3-340 keV/amu	M	CTMC		σ_t
			$H-Kr^{q+}$; q = 4,6,8,10		
6	0.2-2000 keV/amu	(L)M(H)	VPS-emp	1/3 empirical factor in σ_t	σ_t
			$H-Mo^{q+}$; q = 4,6,8,10		
6	0.2-2000 keV/amu	(L)M(H)	VPS-emp	1/3 empirical factor in σ_t	σ_t
			$H-Mo^{14+}$		
7	47.3-340 keV/amu	M	CTMC		σ_t
			$H-Xe^{q+}$		
6	0.2-2000 keV/amu	(L)M(H)	VPS-emp	1/3 empirical factor in σ_t	σ_t
			$H-W^{q+}$; q = 4,6,8,10		
6	0.2-2000 keV/amu	(L)M(H)	VPS-emp	1/3 empirical factor in σ_t	σ_t

[a]Methods defined in footnote to Table 3 (see p. 44).

APPENDIX A

1) Theoretical References for Charge Transfer between Atomic Hydrogen and Fully Stripped Ions

1. Malaviya, V., J. Phys. B 2, 843-850 (1969).
2. Belkic, D. S., Janev, R. K., J. Phys. B 6, 1020-1027 (1973).
3. Msezane, A., Gallaher, D. F., J. Phys. B 6, 2334-2354 (1973).
4. Rapp, D., J. Chem. Phys. 61, 3777-3779 (1974).
5. Presnyakov, L. P., Ulantsev, A. D., [Kvant. Elektron. 1, 2377-2385 (1974)] Sov. J. Quant. Electron. 4, 1320-1324 (1975).
6. Chibisov, M. I., [Pisma Zh. Eksp. Teor. Fiz. 24, 56-60 (1976)] JETP Lett. 24, 46-49 (1976).
7. Olson, R. E., Salop, A., Phys. Rev. A 14, 579-585 (1976).
8. Salop, A., Olson, R. E., Phys. Rev. A 13, 1312-1320 (1976).
9. Belkic, D., Gayet, R., J. Phys. B 10, 1911-1921 (1977).
10. Belkic, D., McCarroll, R., J. Phys. B 10, 1933-1943 (1977).
11. Bottcher, C., J. Phys. B 10, L213-L217 (1977).
12. Harel, C., Salin, A., J. Phys. B 10, 3511-3522 (1977).
13. Olson, R. E., Salop, A., Phys. Rev. A 16, 531-541 (1977).
14. Olson, R. E., Salop, A., Phaneuf, R. A., Meyer, F. W., Phys. Rev. A 16, 1867-1872 (1977).
15. Salop, A., Olson, R. E., Phys. Rev. A 16, 1811-1816 (1977).
16. Vaaben, J., Briggs, J. S., J. Phys. B 10, L521-L526 (1977).
17. Abramov, V. A., Baryshnikov, F. F., Lisitsa, V. S., [Zh. Eksp. Teor. Fiz. 74, 897-910 (1978)] Sov. Phys. JETP 47, 469-476 (1978).
18. Duman, E. L., Smirnov, B. M., [Fiz. Plazmy 4, 1161-1166 (1978)] Sov. J. Plasma Phys. 4, 650-652 (1978).

19. Golden, J. E., McGuire, J. H., Omidvar, K., Phys. Rev. A 18, 2373-2376 (1978).

20. Grozdanov, T. P., Janev, R. K., Phys. Rev. A 17, 880-888 (1978).

21. Ryufuku, H., Watanabe, T., Phys. Rev. A 18, 2005-2015 (1978).

22. Chan, F. T., Eichler, J., Phys. Rev. A 20, 1841-1847 (1979).

23. Eichler, J., Chan, F. T., Phys. Rev. A 20, 104-112 (1979).

24. Hatton, G. J., Lane, N. F., Winter, T. G., J. Phys. B 12, L571-L577 (1979).

25. Ryufuku, H., Watanabe, T., Phys. Rev. A 19, 1538-1549 (1979).

26. Ryufuku, H., Watanabe, T., Phys. Rev. A 20, 1828-1837 (1979).

27. Salop, A., J. Phys. B 12, 919-928 (1979).

28. Salop, A., Olson, R. E., Phys. Rev. A 19, 1921-1929 (1979).

29. Salop, A., Olson, R. E., Phys. Lett. A 71, 407-410 (1979).

30. Bransden, B. H., Newby, C. W., Noble, C. J., J. Phys. B 13, 4245-4255 (1980).

31. Crothers, D. S. F., Todd, N. R., J. Phys. B 13, 547-563 (1980).

32. Datta, S., Mukherjee, S. C., J. Phys. B 13, 539-546 (1980).

33. Grozdanov, T. P., J. Phys. B 13, 3835-3847 (1980).

34. Saha, H. P., Maiti, N., Sil, N. C., J. Phys. B 13, 327-342 (1980).

35. Bransden, B. H., Noble, C. J., J. Phys. B 14, 1849-1856 (1981).

36. Crothers, D. S. F., Todd, N. R., J. Phys. B 14, 3251-3258 (1981).

37. Fujiwara, K., J. Phys. B 14, 3977-3986 (1981).

38. Kimura, M., Thorson, W. R., Phys. Rev. A 24, 3019-3031 (1981).

39. Olson, R. E., Phys. Rev. A 24, 1726-1733 (1981).

40. Presnyakov, L. P., Uskov, D. B., Janev, R. K., Phys. Lett. A 84, 243-246 (1981).

41. Green, T. A., Shipsey, E. J., Browne, J. C., Phys. Rev. A 25, 1364-1373 (1982).

42. Reading, J. F., Ford, A. L., Becker, R. L., J. Phys. B 15, 625-632 (1982).

43. Ryufuku, H., Phys. Rev. A 25, 720-736 (1982).

44. Winter, T. G., Phys. Rev. A 25, 697-712 (1982).

45. Fritsch, W., J. Phys. B (submitted), (1982).

46. Janev, R. K., Belic, D. S., Phys. Rev. A (submitted), (1982).

47. Belic, D. S., Bransden, B. H., Janev, R. K., Unpublished, (1982).

48. Bransden, B. H., Chandler, J., Noble, C. J., Unpublished, (1982).

49. Bransden, B. H., Newby, C. W., Noble, C. J., Unpublished, (1982).

2) Experimental References for Charge Transfer Cross Sections between Atomic Hydrogen and Fully Stripped Ions

1. Olson, R. E., Salop, A., Phaneuf, R. A., Meyer, F. W., Phys. Rev. A 16, 1867 (1977).
2. Nutt, W. L., McCullough, R. W., Brady, K., Shah, M. B., Gilbody, H. B., J. Phys. B 11, 1457 (1978).
3. Shah, M. B., Gilbody, H. B., J. Phys. B 11, 121 (1978).
4. Crandall, D. H., Phaneuf, R. A., Meyer, F. W., Phys. Rev. A 19, 504 (1979).
5. Goffe, T. V., Shah, M. B., Gilbody, H. B., J. Phys. B 12, 3763 (1979).
6. Meyer, F. W., Phaneuf, R. A., Kim, H. J., Hvelplund, P., Stelson, P. H., Phys. Rev. A 19, 515 (1979).
7. Phaneuf, R. A., Alvarez, I., Meyer, F. W., Crandall, D. H., Phys. Rev. A (submitted), (1982).
8. Bayfield, J. E., Khayrallah, G. A., Phys. Rev. A 12, 869 (1975).

APPENDIX B

1) Theoretical References for Charge Transfer Data between Atomic Hydrogen and Partially Stripped Ions

1. Blint, R. J., Watson, W. D., Christensen, R. B., Astrophys. J. 205, 634-637 (1976).
2. McCarroll, R., Valiron, P., Astron. Astrophys. 53, 83-88 (1976).
3. Olson, R. E., Salop, A., Phys. Rev. A 14, 579-585 (1976).
4. Olson, R. E., Salop, A., Phys. Rev. A 16, 531-541 (1977).
5. Olson, R. E., Shipsey, E. J., Browne, J. C., J. Phys. B 11, 699-708 (1978).
6. Shevelko, V. P., Z. Phys. A 287, 19-26 (1978).
7. Meyer, F. W., Phaneuf, R. A., Kim, H. J., Hvelplund, P., Stelson, P. H., Phys. Rev. A 19, 515-525 (1979).
8. Watson, W. D., Christensen, R. B., Astrophys. J. 231, 627-631 (1979).
9. Butler, S. E., Dalgarno, A., Astrophys. J. 241, 838-843 (1980).
10. Butler, S. E., Heil, T. G., Dalgarno, A., Astrophys. J. 241, 442-447 (1980).
11. Crothers, D. S. F., Todd, N. R., J. Phys. B 13, 547-563 (1980).
12. Shevelko, V. P., Proc. Lebedev. Phys. Inst. 119, 108 (1980).
13. Dalgarno, A., Heil, T. G., Butler, S. E., Astrophys. J. 245, 793-797 (1981).
14. Eichler, J. K. M., Tsuji, A., Ishihara, T., Phys. Rev. A 23, 2833-2840 (1981).
15. Gargaud, M., Hanssen, J., McCarroll, R., Valiron, P., J. Phys. B 14, 2259-2276 (1981).
16. Heil, T. G., Butler, S. E., Dalgarno, A., Phys. Rev. A 23, 1100-1109 (1981).

17. Shipsey, E. J., Browne, J. C., Olson, R. E., J. Phys. B 14, 869-880 (1981).

2) Experimental References for Charge Transfer Cross Sections between Atomic Hydrogen and Partially Stripped Ions

1. Gardner, L. D., Bayfield, J. E., Koch, P. M., Kim, H. J., Stelson, P. H., Phys. Rev. A 16, 1415-1418 (1977).
2. Kim, H. J., Phaneuf, R. A., Meyer, F. W., Stelson, P. H., Phys. Rev. A 17, 854-858 (1978).
3. Nutt, W. L., McCullough, R. W., Gilbody, H. B., J. Phys. B 11, L181-L184 (1978).
4. Phaneuf, R. A., Meyer, F. W., McKnight, R. H., Phys. Rev. A 17, 534-545 (1978).
5. Shah, M. B., Goffe, T. V., Gilbody, H. B., J. Phys. B 11, L233-L236 (1978).
6. Crandall, D. H., Phaneuf, R. A., Meyer, F. W., Phys. Rev. A 19, 504-514 (1979).
7. Goffe, T. V., Shah, M. B., Gilbody, H. B., J. Phys. B 12, 3763-3773 (1979).
8. McCullough, R. W., Nutt, W. L., Gilbody, H. B., J. Phys. B 12, 4159-4169 (1979).
9. Meyer, F. W., Phaneuf, R. A., Kim, H. J., Hvelplund, P., Stelson, P. H., Phys. Rev. A 19, 515-525 (1979).
10. Crandall, D. H., Phaneuf, R. A., Meyer, F. W., Phys. Rev. A 22, 379-387 (1980).
11. Gardner, L. D., Bayfield, J. E., Koch, P. M., Sellin, I. A., Pegg, D. J., Peterson, R. S., Crandall, D. H., Phys. Rev. A 21, 1397-1402 (1980).

12. Scim, W., Muller, A., Wirkner-Bott, I., Salzborn, E., J. Phys. B 14, 3475-3491 (1981).

13. Phaneuf, R. A., Alvarez, I., Meyer, F. W., Crandall, D. H., Phys. Rev. A (submitted), (1982).

GRAPH.SET No. 1

Evaluated total charge exchange cross section for hydrogen atom-fully stripped ion systems.

Note: References after the symbol in the Legend of each figure are given in Appendix A. The reference number accompanied by letter E denotes the reference from which the experimental data have been taken (Appendix A.2).

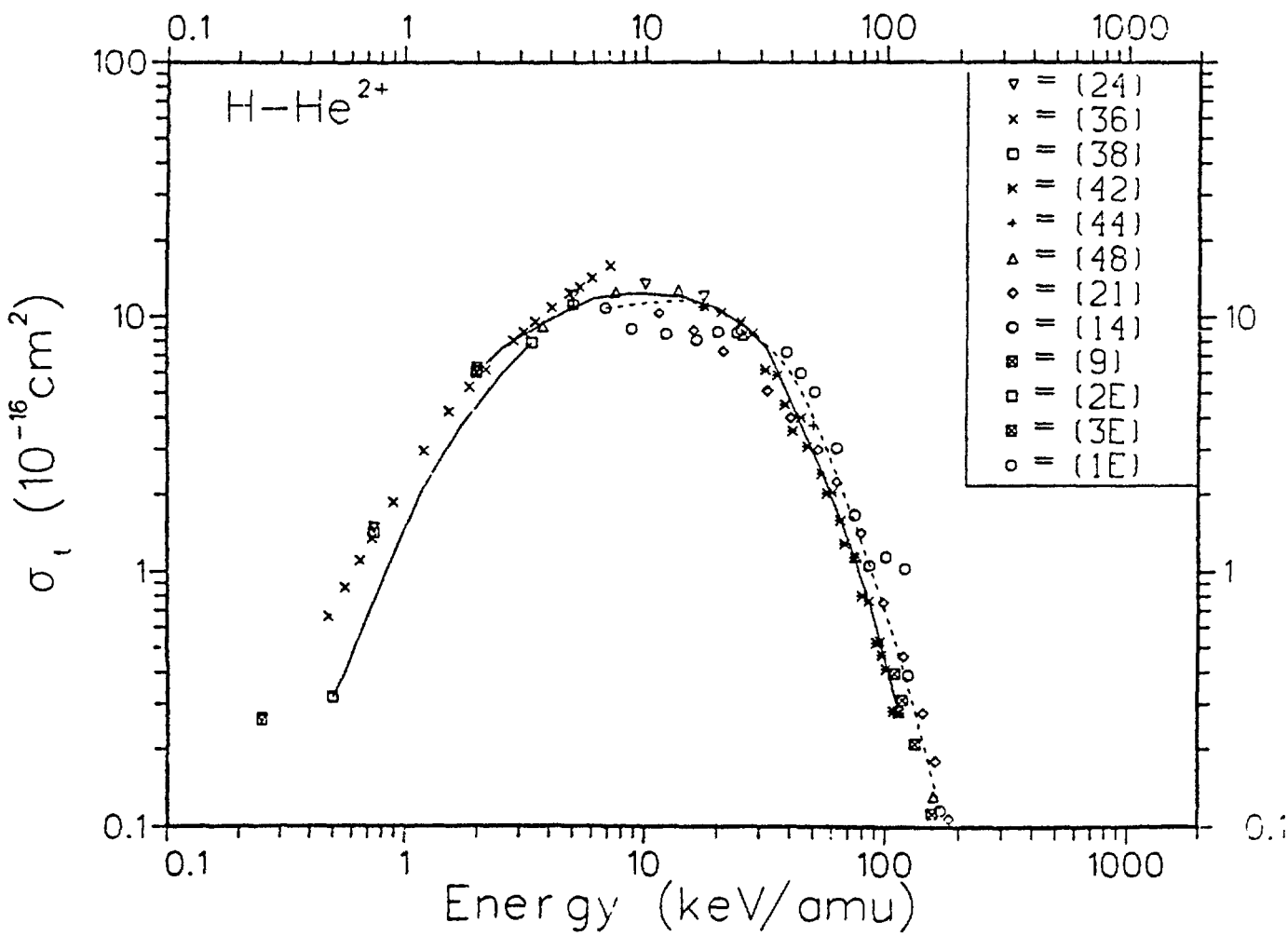
H−He2+
▽ = (24)
× = (36)
□ = (38)
× = (42)
+ = (44)
△ = (48)
◇ = (21)
○ = (14)
⊠ = (9)
□ = (2E)
⊠ = (3E)
○ = (1E)
σt (10−16cm2)
Energy (keV/amu)
0.1
1
10
100
1000

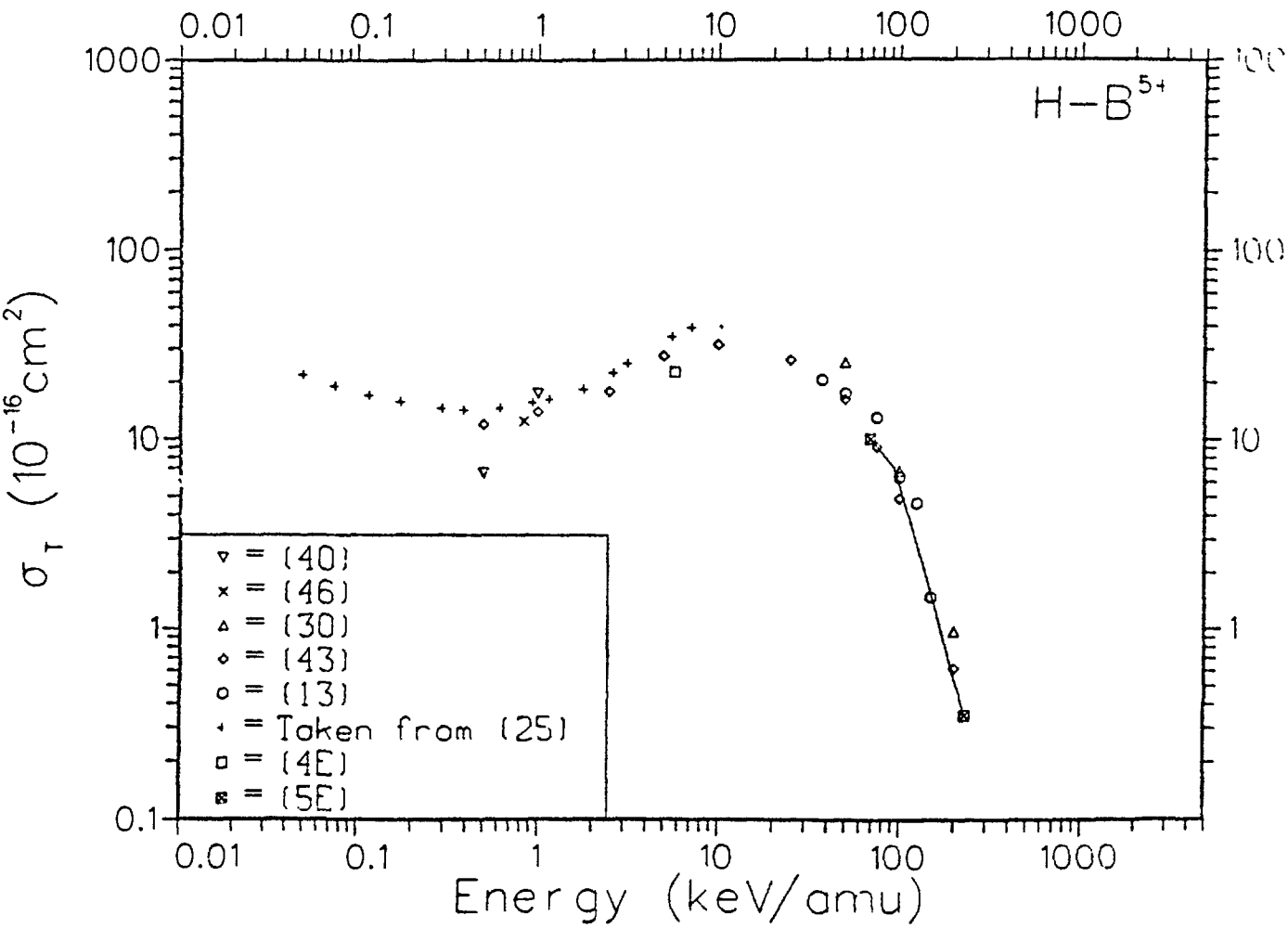
H−B5+
σT (10−16cm2)
Energy (keV/amu)
0.01
0.1
1
10
100
1000
0.1
1
10
100
1000
▽ = (40)
× = (46)
△ = (30)
◇ = (43)
○ = (13)
· = Taken from (25)
□ = (4E)
⊠ = (5E)

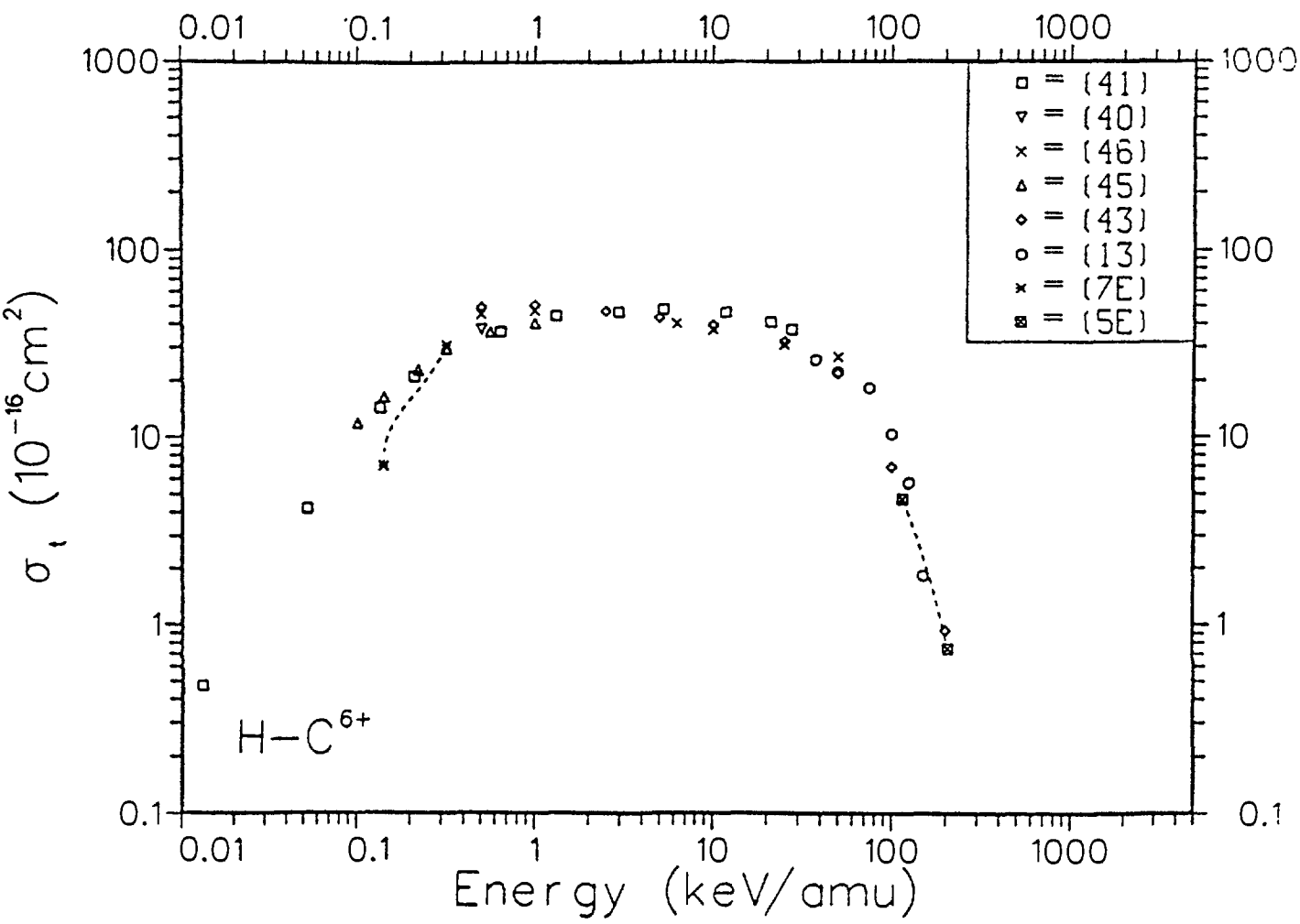
0.01
0.1
1
10
100
1000
1000
100
10
1
0.1
□ = (41)
▽ = (40)
× = (46)
△ = (45)
◇ = (43)
○ = (13)
* = (7E)
⊠ = (5E)
H−C6+
σt (10−16cm2)
Energy (keV/amu)

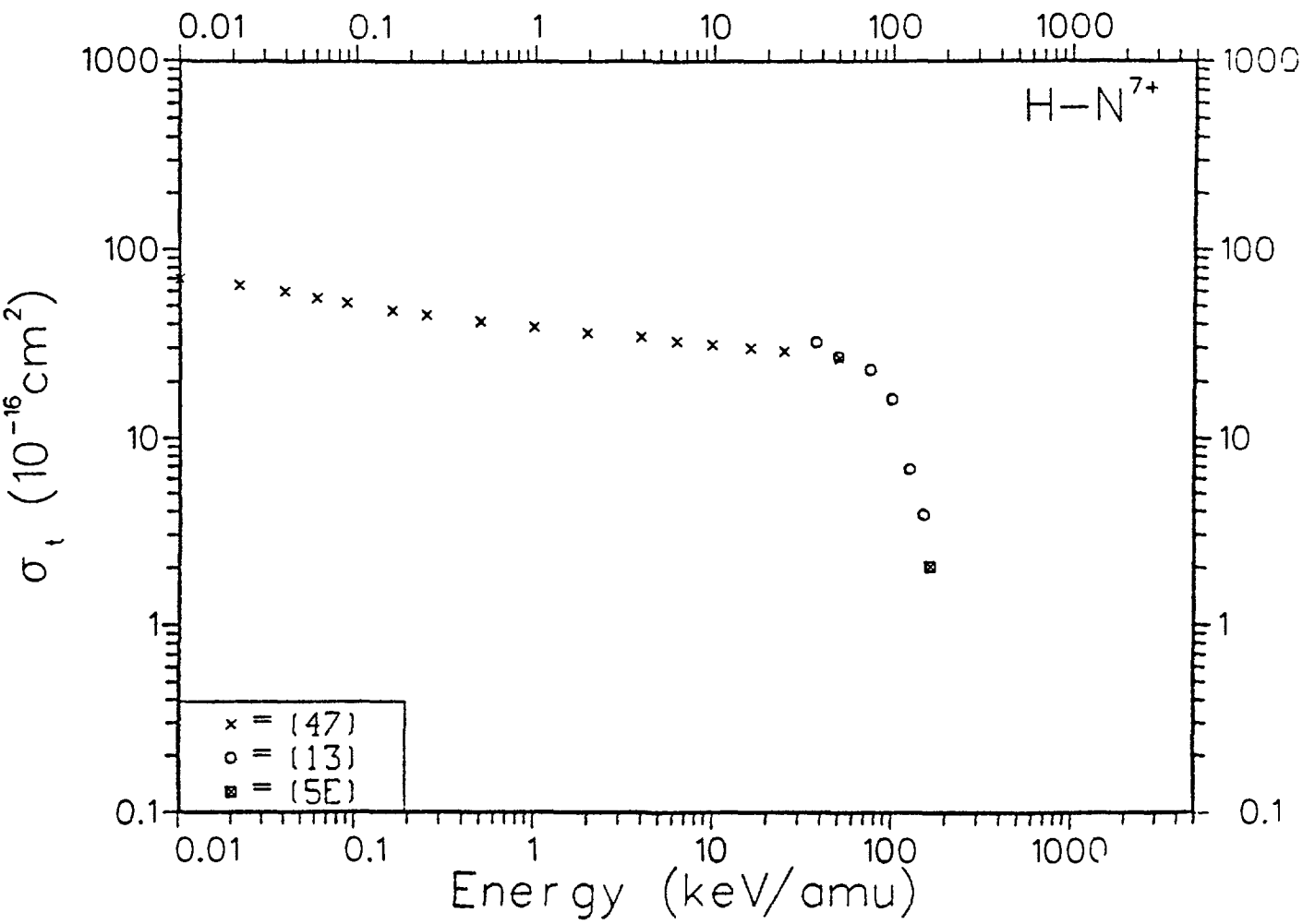
H−N7+
σt (10−16cm2)
Energy (keV/amu)
× = (47)
o = (13)
⊠ = (5E)
0.01
0.1
1
10
100
1000
0.1
1
10
100
1000

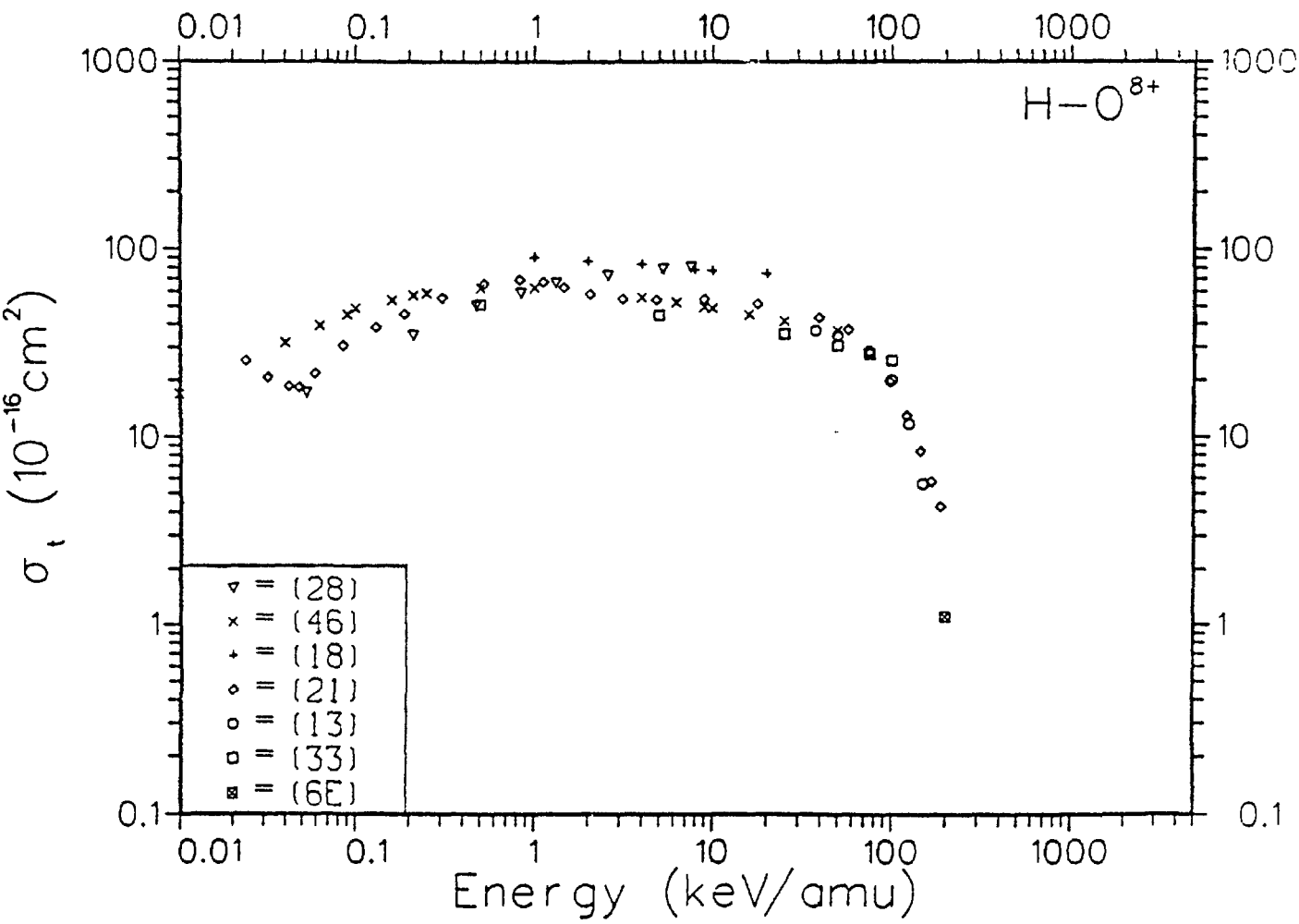
H−O8+
σt (10−16cm2)
Energy (keV/amu)
0.01
0.1
1
10
100
1000
0.1
1
10
100
1000
▽ = (28)
× = (46)
+ = (18)
◇ = (21)
○ = (13)
□ = (33)
⊠ = (6E)

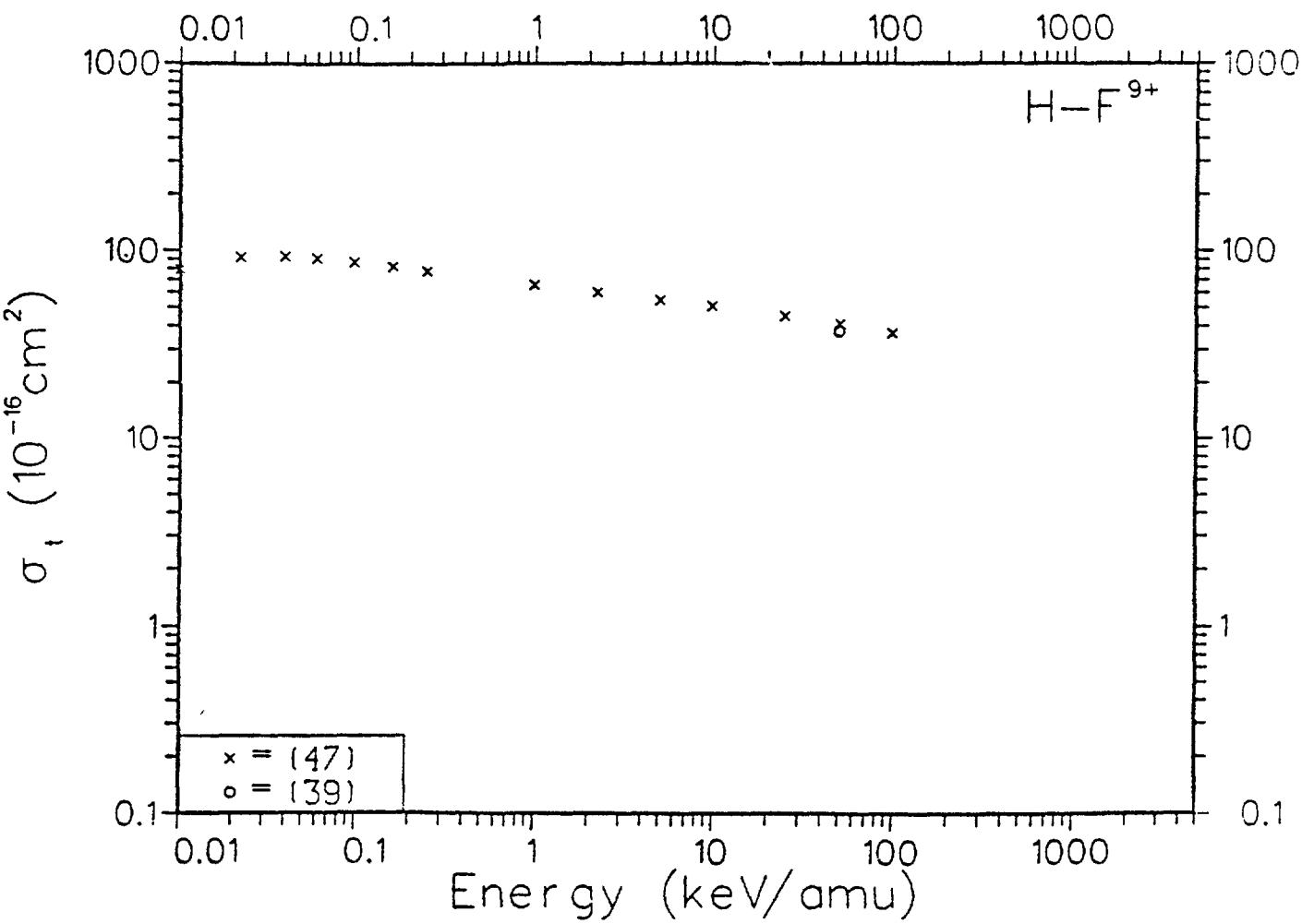
H—F 9+
× = (47)
o = (39)
0.01
0.1
1
10
100
1000
1000
100
10
1
0.1
σt (10-16cm2)
Energy (keV/amu)

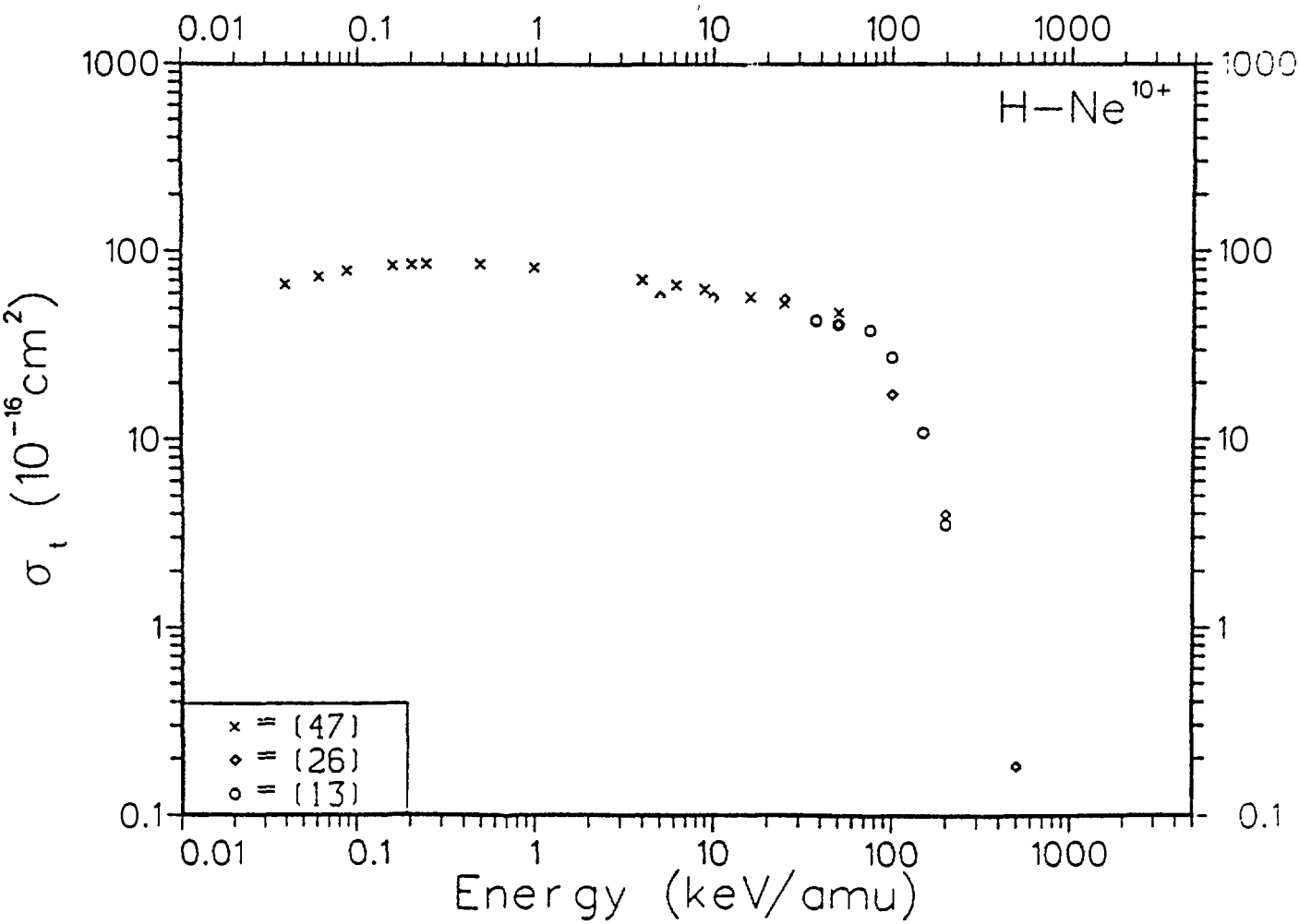
H–Ne10+
σt (10-16cm2)
Energy (keV/amu)
× = (47)
◇ = (26)
○ = (13)
0.01
0.1
1
10
100
1000
0.1
1
10
100
1000

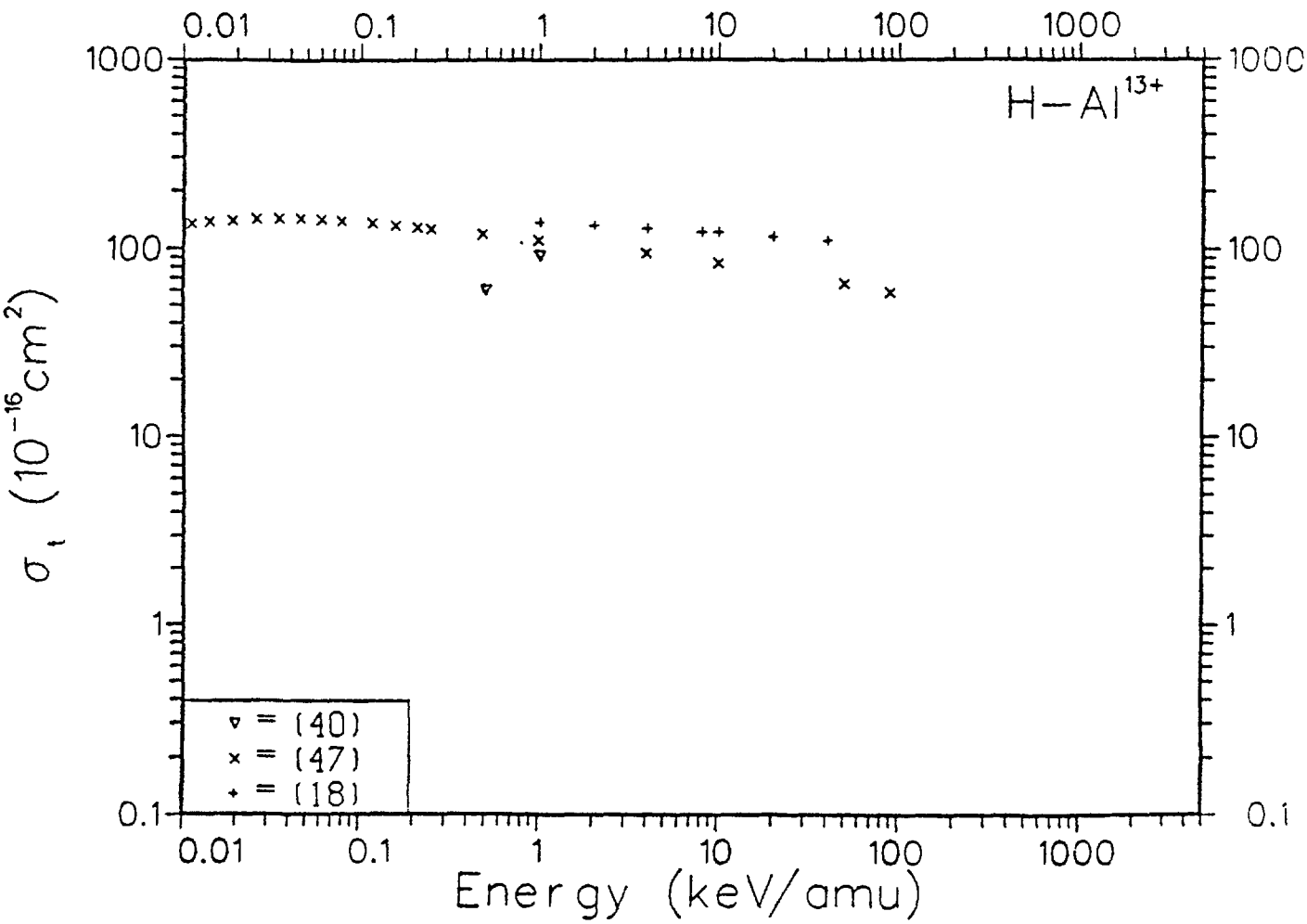
H—Al13+
σt (10-16cm2)
Energy (keV/amu)
0.01
0.1
1
10
100
1000
0.1
1
10
100
1000
▽ = (40)
× = (47)
+ = (18)

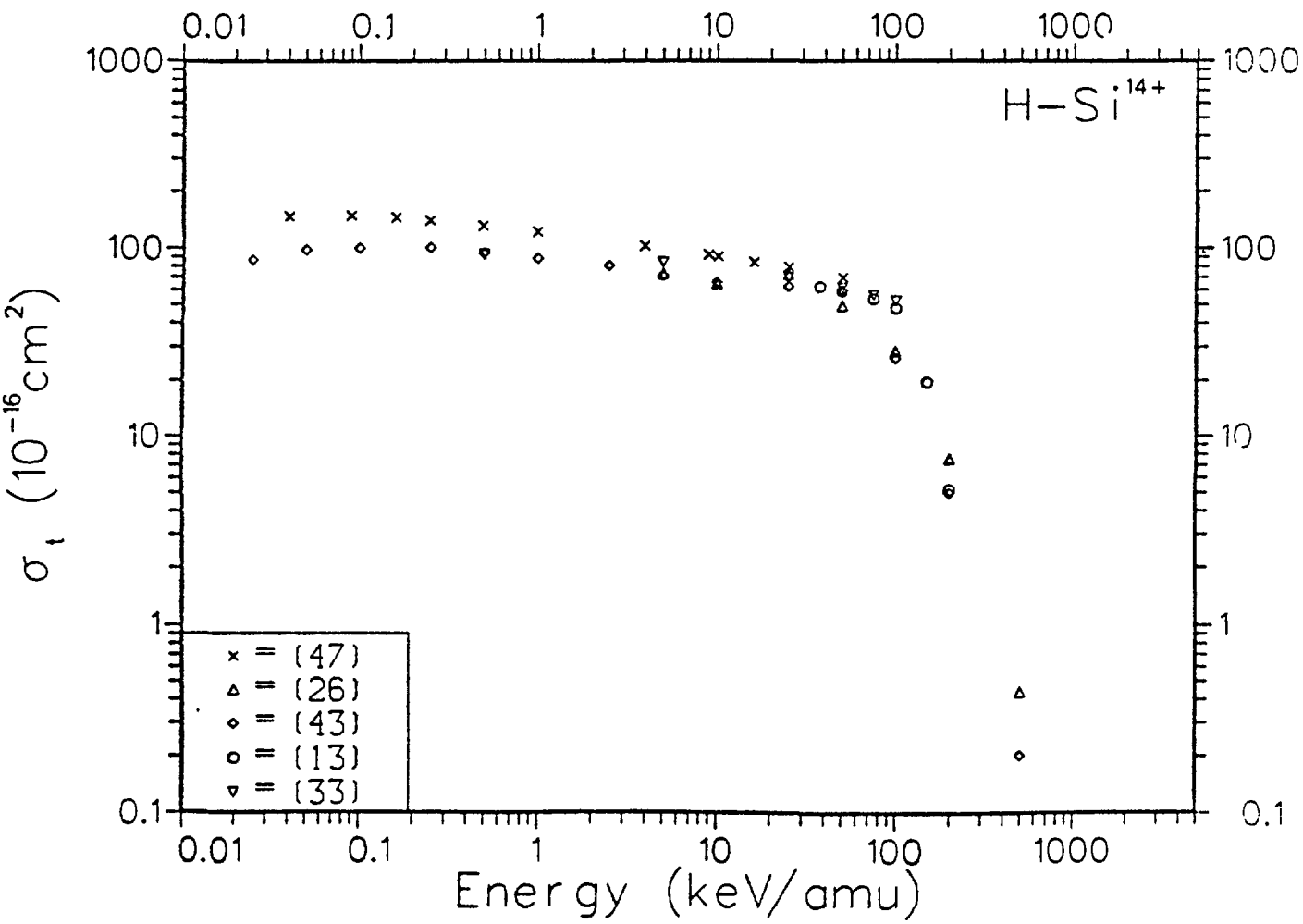
H–Si^{14+}
× = (47)
△ = (26)
◇ = (43)
○ = (13)
▽ = (33)
σ_t (10^{-16}cm^2)
Energy (keV/amu)
0.01
0.1
1
10
100
1000
0.1
1
10
100
1000

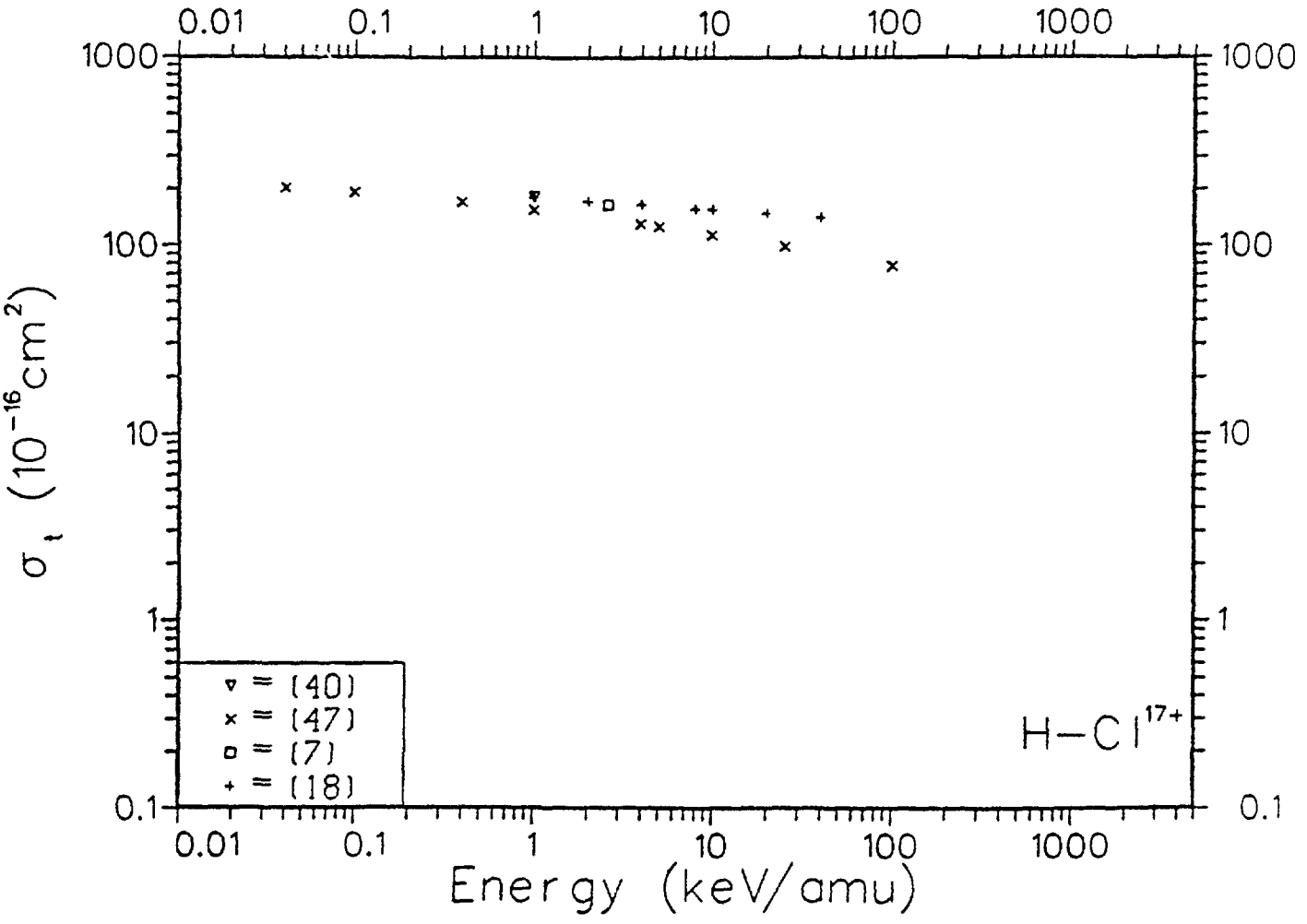
0.01
0.1
1
10
100
1000
1000
100
10
1
0.1
σ_t (10^{-16}cm^2)
▽ = (40)
× = (47)
□ = (7)
+ = (18)
H−Cl^{17+}
Energy (keV/amu)

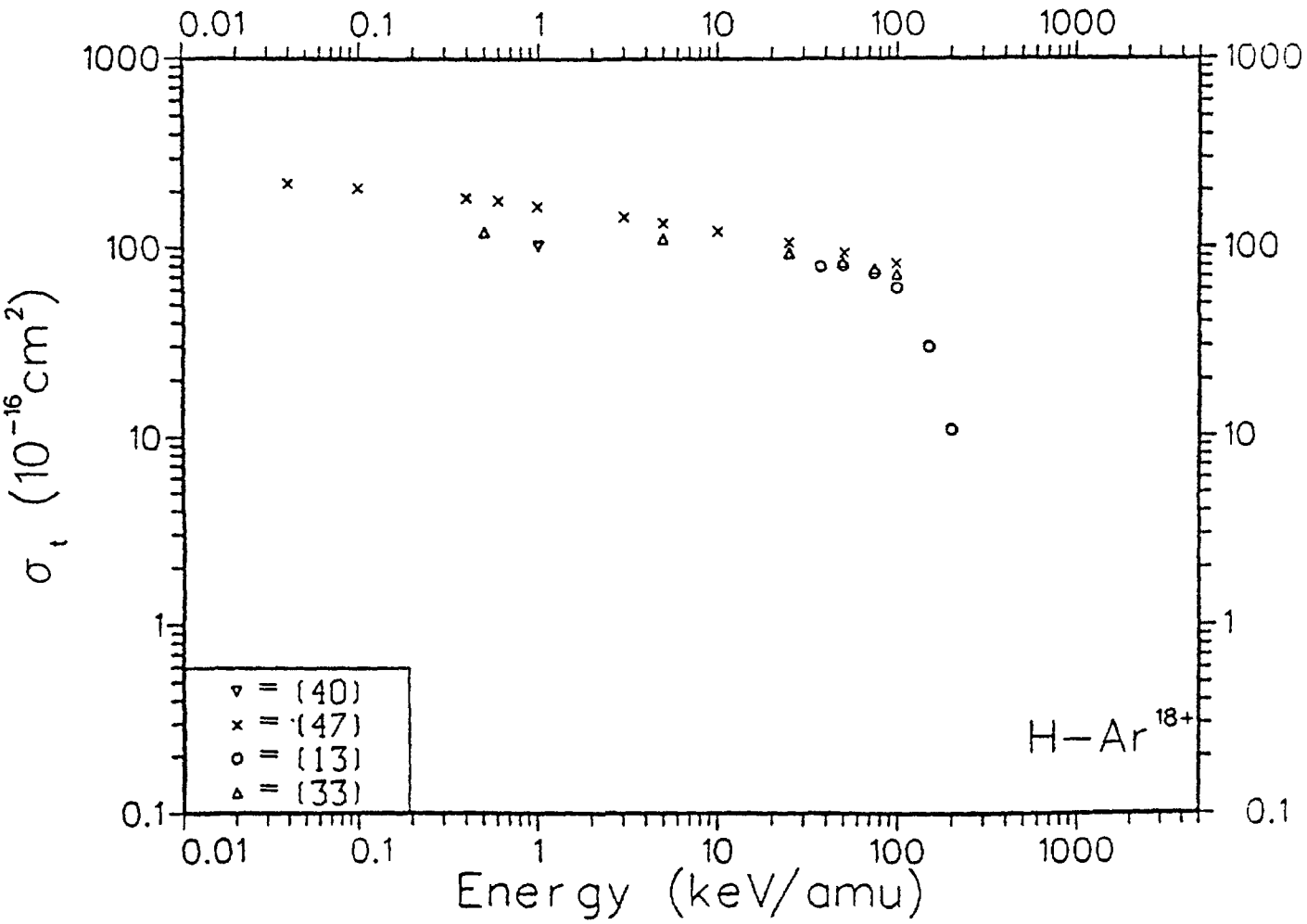
0.01
0.1
1
10
100
1000
1000
100
10
1
0.1
σ_t (10^{-16}cm^2)
▽ = (40)
× = (47)
○ = (13)
△ = (33)
H−Ar^{18+}
Energy (keV/amu)

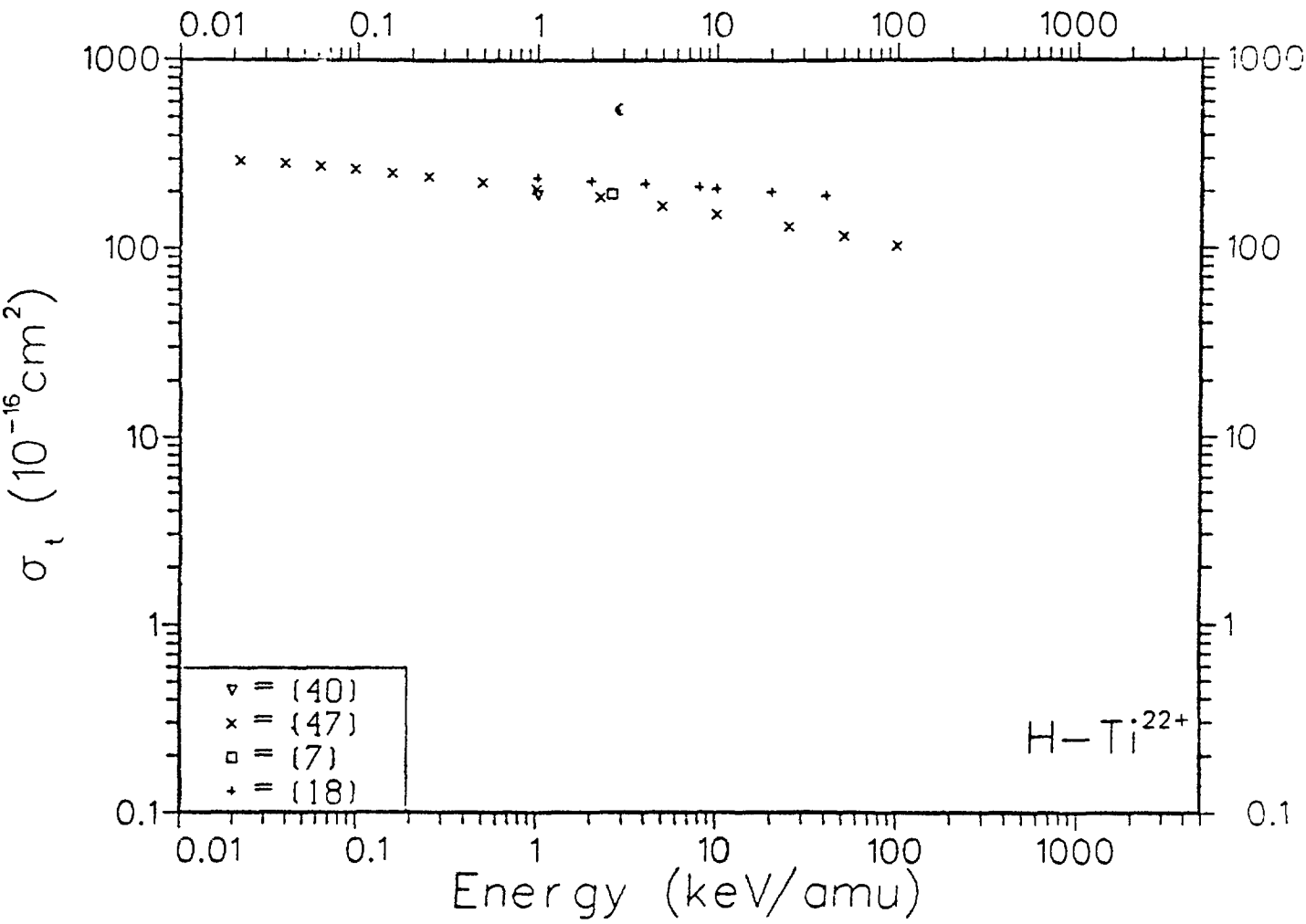
0.01
0.1
1
10
100
1000
1000
100
10
1
0.1
σ_t (10^{-16}cm^2)
▽ = (40)
× = (47)
□ = (7)
+ = (18)
H–Ti^{22+}
Energy (keV/amu)

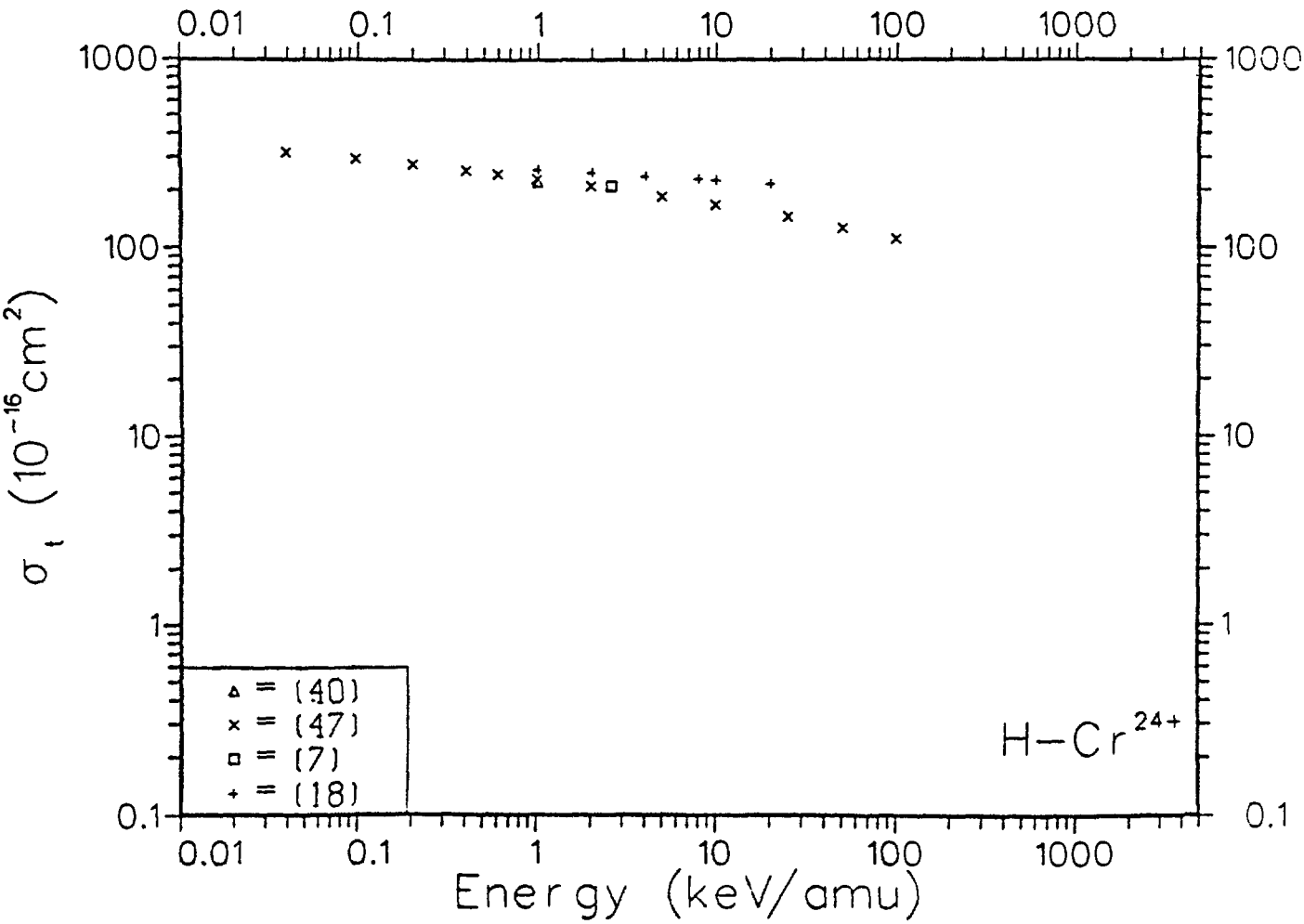
0.01
0.1
1
10
100
1000
1000
100
10
1
0.1
σ_t (10^{-16}cm^2)
Energy (keV/amu)
△ = (40)
× = (47)
□ = (7)
+ = (18)
H−Cr^{24+}

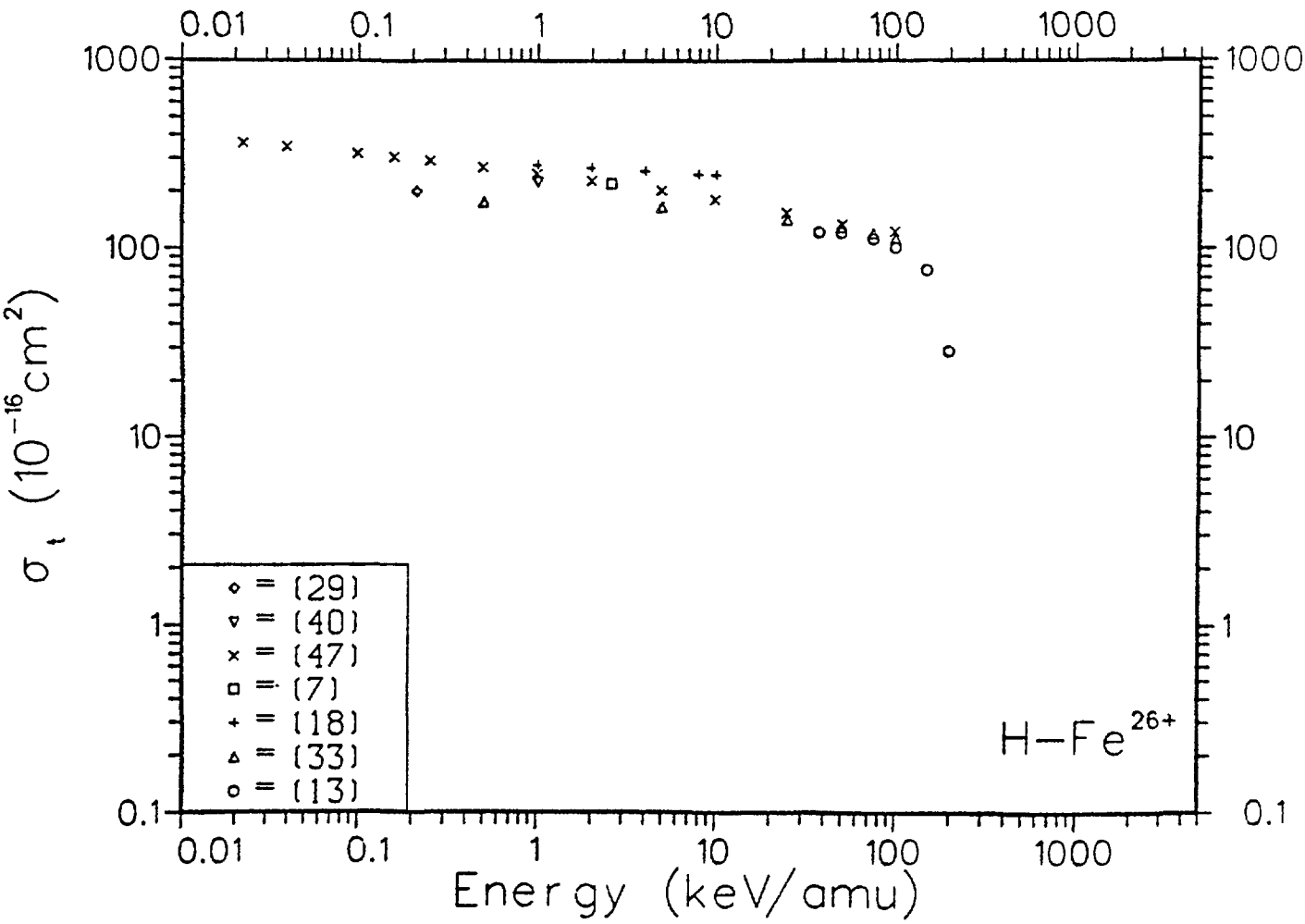
0.01
0.1
1
10
100
1000
1000
100
10
1
0.1
σ_t (10^{-16}cm^2)
◇ = (29)
▽ = (40)
× = (47)
□ = (7)
+ = (18)
△ = (33)
○ = (13)
H–Fe^{26+}
Energy (keV/amu)

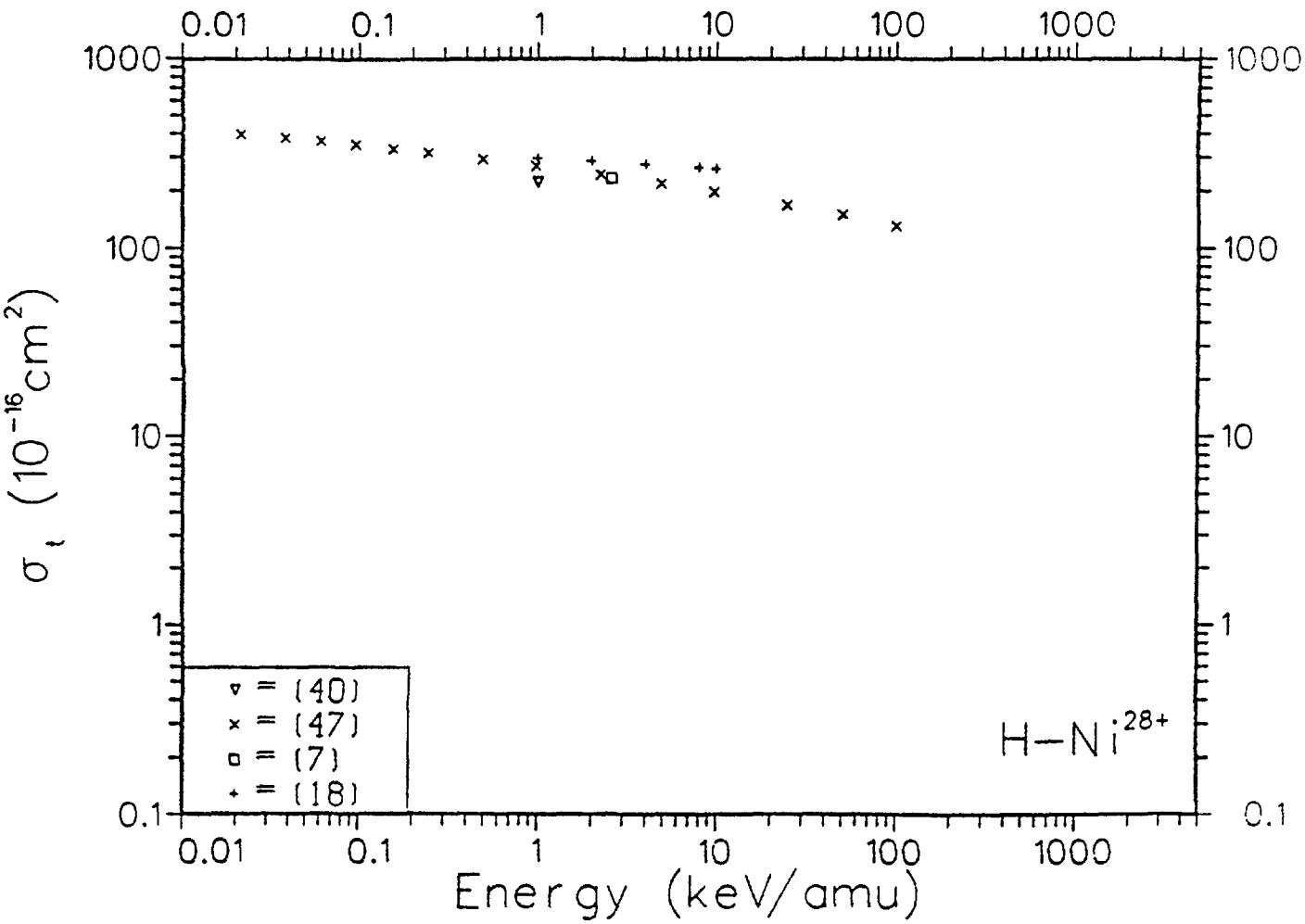
0.01
0.1
1
10
100
1000
1000
100
10
1
0.1
σ_t (10^{-16}cm^2)
▽ = (40)
× = (47)
□ = (7)
+ = (18)
H–Ni^{28+}
Energy (keV/amu)

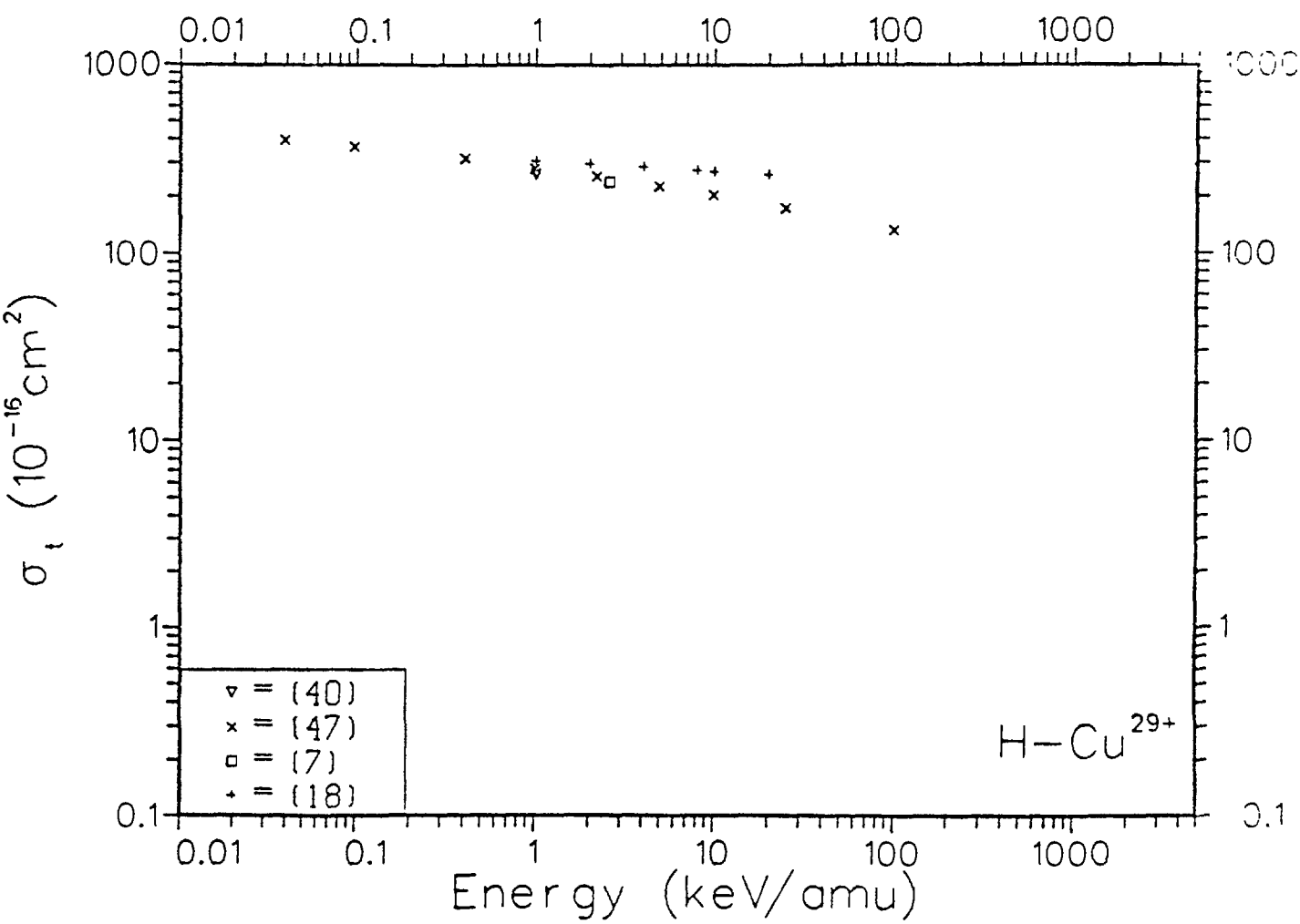
0.01
0.1
1
10
100
1000
1000
100
10
1
0.1
σ_t (10^{-16}cm^2)
▽ = (40)
× = (47)
□ = (7)
+ = (18)
H−Cu^{29+}
Energy (keV/amu)

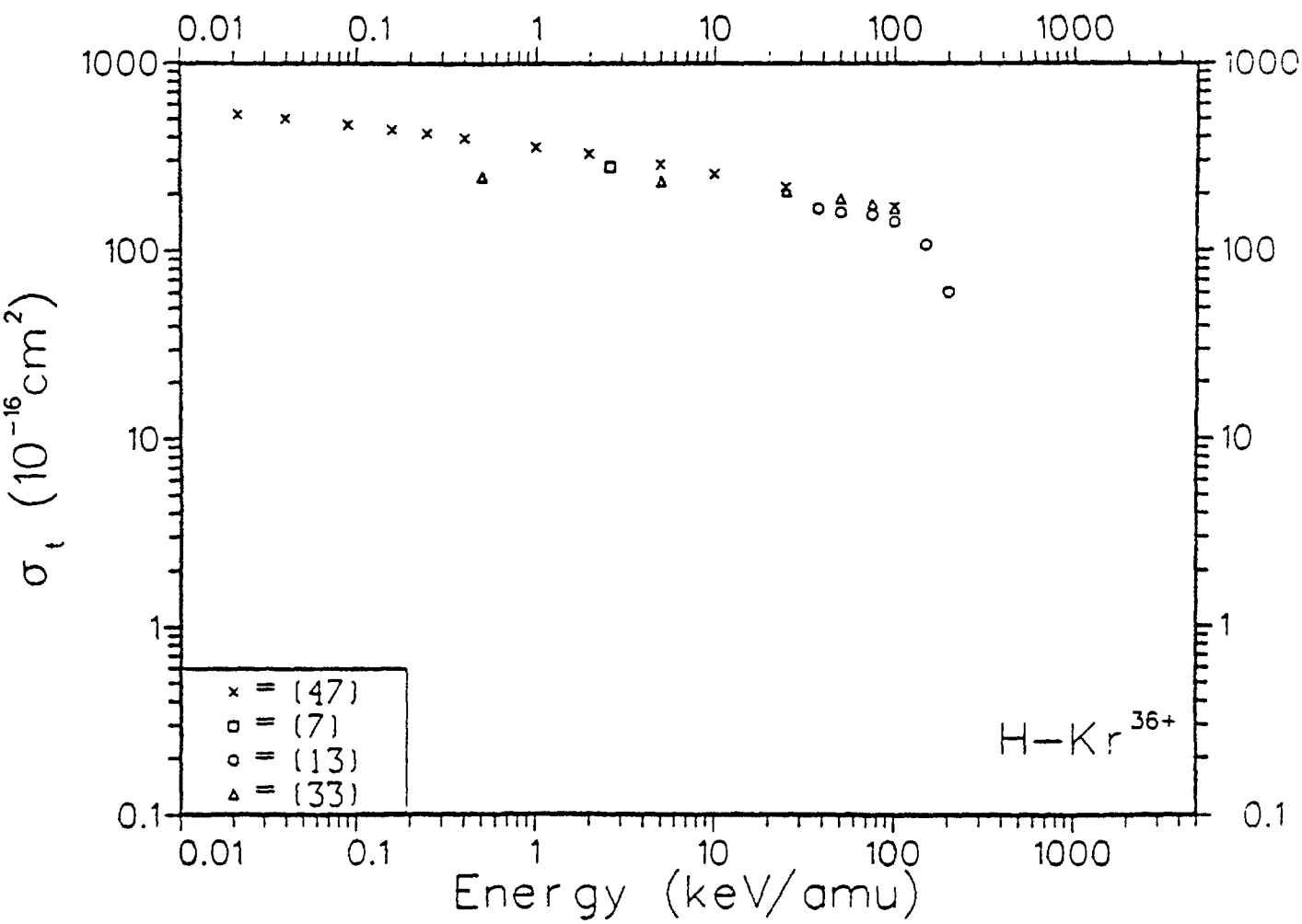
0.01
0.1
1
10
100
1000
1000
100
10
1
0.1
σ_t (10^{-16}cm^2)
× = (47)
□ = (7)
○ = (13)
△ = (33)
H—Kr^{36+}
Energy (keV/amu)

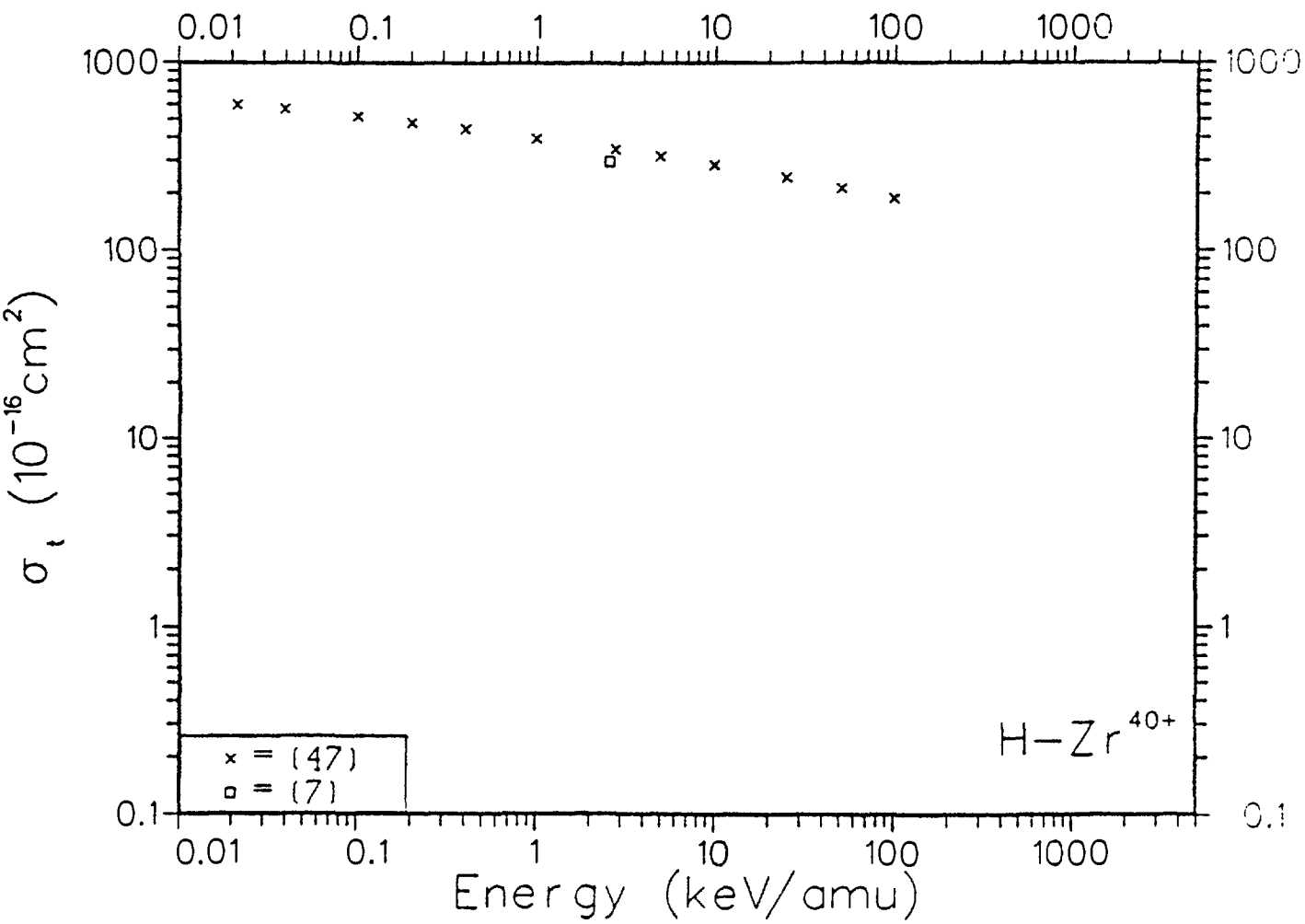
0.01
0.1
1
10
100
1000
1000
100
10
1
0.1
σ_t (10^{-16}cm^2)
× = (47)
□ = (7)
H−Zr^{40+}
Energy (keV/amu)

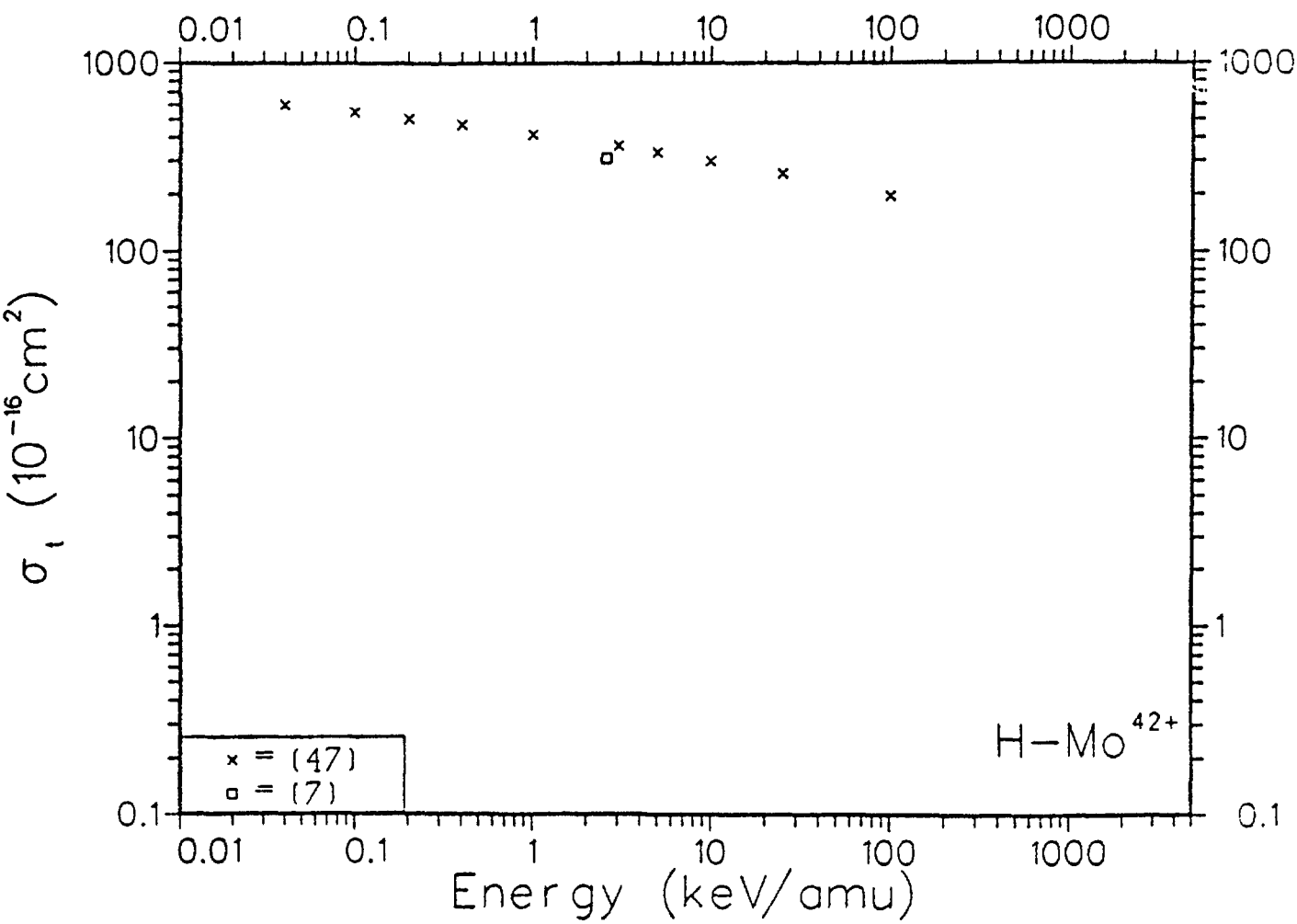
0.01
0.1
1
10
100
1000
1000
100
10
1
0.1
σ_t (10^{-16}cm^2)
× = (47)
□ = (7)
H−Mo^{42+}
Energy (keV/amu)

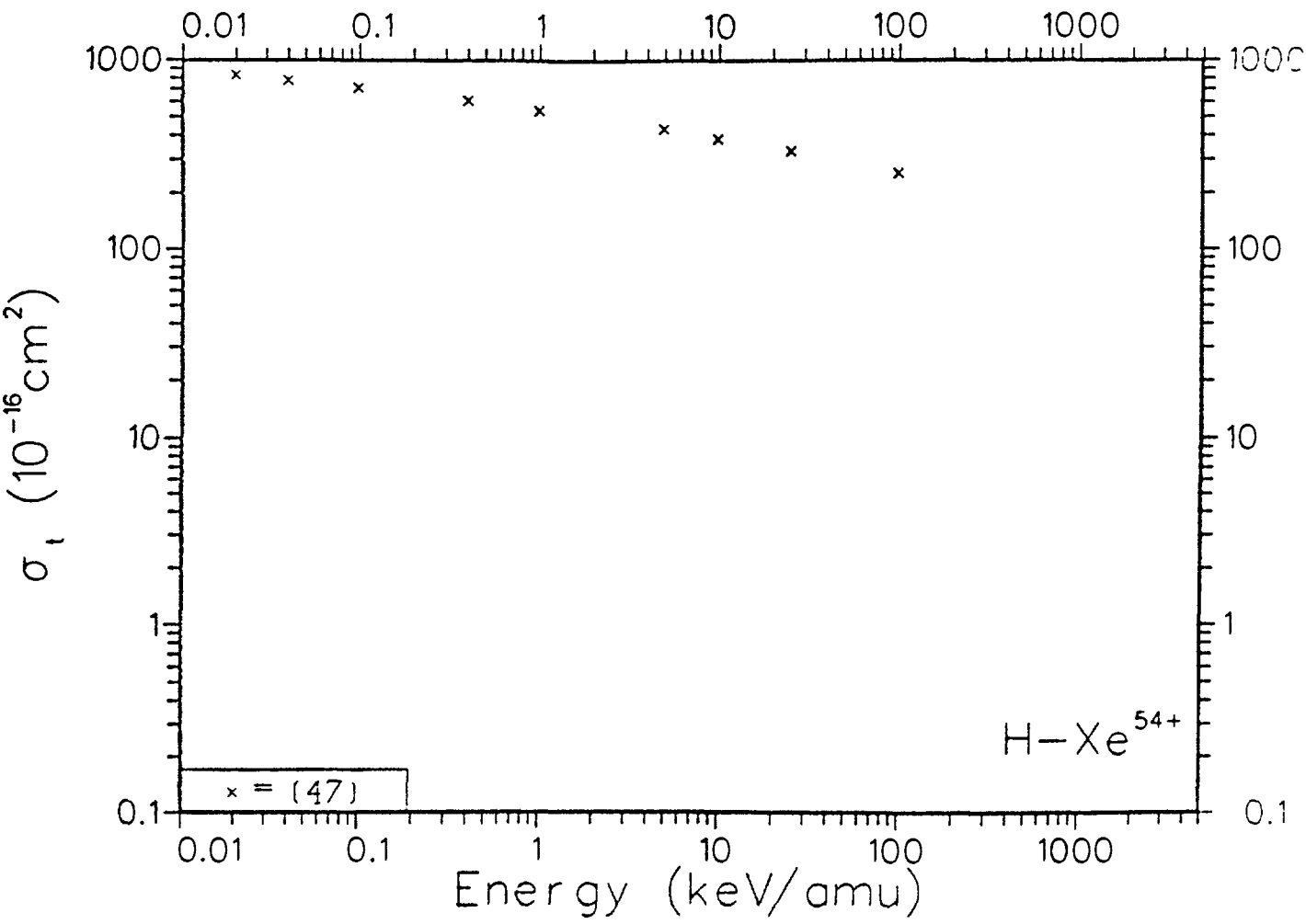
0.01
0.1
1
10
100
1000
1000
100
10
1
0.1
σ_t (10^{-16}cm^2)
H−Xe^{54+}
× = (47)
Energy (keV/amu)

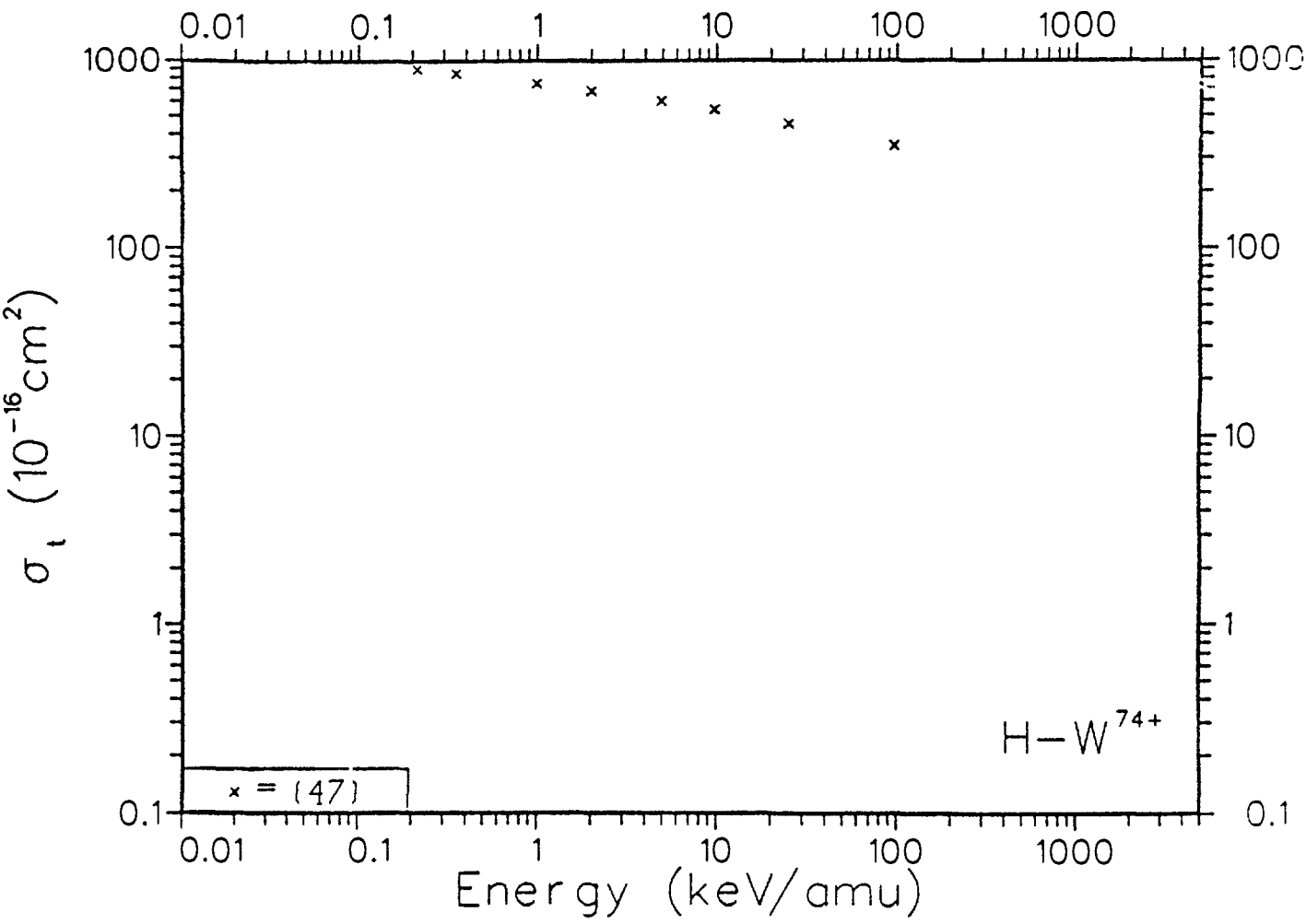
0.01
0.1
1
10
100
1000
1000
100
10
1
0.1
σ_t (10^{-16}cm^2)
H—W^{74+}
× = (47)
Energy (keV/amu)

TABLE SET No. 1

Partial cross sections σ_n and $\sigma_{n\ell}$ for $H + A^{Z+}$ (Z = 5-18)

Notes:

1) The partial cross sections $\sigma_{n\ell}$ for $H + He^{2+}$ and σ_n for $H + A^{Z+}$, with $Z \geq 13$ are given in GRAPH.SET No. 2, following this set of tables.

2) The references used in these tables are given in Appendix A.1.

H - B^{5+}

Reference 30, E = 5.0 keV/amu

n	2	3	4	5
$\sigma_n(10^{-16}cm^2)$	2.10	49.6	13.0	0.140

Reference 30, E = 10.0 keV/amu

n	2	3	4	5
$\sigma_n(10^{-16}cm^2)$	2.10	49.6	13.0	0.140

ℓ	$\sigma_{n\ell}(10^{-16}cm^2)$
0	0.0690
1	0.204
2	0.315
3	0.358
4	0.430

Reference 27, E = 25 keV/amu

n	2	3	4	5	6
$\sigma_n(10^{-16}cm^2)$	0.518	10.3	10.3	0.855	0.473

ℓ	$\sigma_{n\ell}(10^{-16}cm^2)$		
0	0.194	0.0878	0.113
1	1.18	0.846	0.126
2	5.94	2.97	0.180
3		6.19	0.475
4			0.0968

H - B^{5+}

Reference 46, E = 0.49 keV/amu

n	3	4
$\sigma_n(10^{-16}cm^2)$	8.95	1.26

Reference 46, E = 1.0 keV/amu

n	3	4
$\sigma_n(10^{-16}cm^2)$	11.6	0.886

Reference 46, E = 10.0 keV/amu

n	2	3	4
$\sigma_n(10^{-16}cm^2)$	0.0190	15.1	0.284

Reference 46, E = 25.0 keV/amu

n	2	3	4
$\sigma_n(10^{-16}cm^2)$	0.104	15.4	0.179

H - B^{5+}

Reference 27, E = 32 keV/amu

n	2	3	4	5	6	7
$\sigma_n(10^{-16}cm^2)$	0.329	8.41	9.96	1.58	0.879	0.307
	$\sigma_{n\ell}(10^{-16}cm^2)$					
0		0.215	0.0679			
1		1.35	1.30	0.182		
2		5.30	3.18	0.353		
3			4.88	0.545		
4				0.679		

Reference 39, E = 50 keV/amu

n	2	3	4	5	6	7	8	9	10
$\sigma_n(10^{-16}cm^2)$	0.397	4.92	6.13	3.26	1.65	1.11	0.512	0.322	0.214
	$\sigma_{n\ell}(10^{-16}cm^2)$								
0	0.532	0.110	0.0830	0.0890	0.0280	0.0220	0.0140	0.0440	
1	0.302	1.04	0.601	0.360	0.227	0.135	0.0840	0.0840	
2		3.38	1.61	0.727	0.365	0.186	0.129	0.102	
3			3.84	1.31	0.615	0.320	0.191	0.0550	
4				0.889	0.360	0.212	0.0650		
5					0.0100				

Reference 27, E = 73 keV/amu

n	2	3	4	5	6	7	8	9
$\sigma_n(10^{-16}cm^2)$	0.262	2.71	3.43	3.91	1.66	0.924	0.339	0.477
	$\sigma_{n\ell}(10^{-16}cm^2)$							
0		0.0647	0.149		0.0308			
1		0.588	0.257	0.363	0.194			
2		1.53	1.33	0.901	0.319			
3			1.62	1.33	0.671			
4				1.33	0.477			

Reference 46, E = 0.49 keV/amu

n	3	4
$\sigma_n(10^{-16}cm^2)$	1.00	44.3
	$\sigma_{n\ell}(10^{-16}cm^2)$	
0	0.324	10.9
1	0.508	19.4
2	0.157	10.9
3		2.17

Reference 46, E = 1.0 keV/amu

n	3	4
$\sigma_n(10^{-16}cm^2)$	2.10	45.1
	$\sigma_{n\ell}(10^{-16}cm^2)$	
0	0.691	11.4
1	1.08	19.7
2	0.343	11.1
3		2.21

Reference 46, E = 10.0 keV/amu

n	3	4
$\sigma_n(10^{-16}cm^2)$	5.95	31.2

Reference 46, E = 25.0 keV/amu

n	3	4
$\sigma_n(10^{-16}cm^2)$	6.91	24.0

H - C^{6+}

Reference 39, E = 25 keV/amu

n	2	3	4	5	6	7	8	9	10	11
$\sigma_n(10^{-16}cm^2)$	0.0695	5.49	16.8	3.76	0.842	0.376	0.141	0.0868	0.0497	0.0189

Reference 39, E = 50 keV/amu

n	2	3	4	5	6	7	8	9	10
$\sigma_n(10^{-16}cm^2)$	0.142	2.91	7.10	6.01	3.06	1.36	0.747	0.492	0.315

ℓ	$\sigma_{n\ell}(10^{-16}cm^2)$								
0	0.0380	0.113	0.0980	0.0678	0.0270				
1	0.0820	0.678	0.452	0.267	0.192	0.0940	0.0560	0.0260	0.0200
2		1.67	1.24	0.758	0.439	0.216	0.104	0.0880	0.0560
3			3.98	1.35	0.584	0.342	0.219	0.174	0.0904
4				2.15	1.01	0.463	0.309	0.185	0.133
5					0.404	0.263	0.171	0.119	0.0640

Reference 39, E = 50 keV/amu (continued)

n	11	12	13	14	15
$\sigma_n(10^{-16}cm^2)$	0.233	0.138	0.0945	0.0916	0.0549

H - C^{6+}

Reference 39, E = 75 keV/amu

n	2	3	4	5	6	7	8	9	10
$\sigma_n(10^{-16}cm^2)$	0.125	1.64	3.28	2.97	2.19	1.50	1.03	0.700	0.475

Reference 39, E = 75 keV/amu (continued)

n	11	12	13	14	15
$\sigma_n(10^{-16}cm^2)$	0.402	0.286	0.232	0.184	0.140

Reference 39, E = 100 keV/amu

n	2	3	4	5	6	7	8	9	10
$\sigma_n(10^{-16}cm^2)$	0.116	0.851	1.43	1.51	1.19	0.903	0.647	0.467	0.352

Reference 39, E = 100 keV/amu (continued)

n	11	12	13	14	15
$\sigma_n(10^{-16}cm^2)$	0.290	0.225	0.192	0.166	0.116

H - C^{6+}

Reference 41, E = 0.013 keV/amu

n	4
$\sigma_n(10^{-16}cm^2)$	0.470

ℓ	$\sigma_{n\ell}(10^{-16}cm^2)$
0	0.064
1	0.047
2	0.168
3	0.192
4	

Reference 41, E = 0.053 keV/amu

n	4	5
$\sigma_n(10^{-16}cm^2)$	3.82	0.390

ℓ	$\sigma_{n\ell}(10^{-16}cm^2)$	
0	0.432	0.0386
1	1.17	0.0628
2	1.24	0.101
3	0.982	0.132
4		0.0558

Reference 41, E = 0.135 keV/amu

n	4	5
$\sigma_n(10^{-16}cm^2)$	11.0	3.28

ℓ	$\sigma_{n\ell}(10^{-16}cm^2)$	
0	0.901	0.262
1	2.37	0.299
2	2.87	0.499
3	4.85	1.16
4		1.06

Reference 41, E = 0.21 keV/amu

n	4	5
$\sigma_n(10^{-16}cm^2)$	16.2	4.80

ℓ	$\sigma_{n\ell}(10^{-16}cm^2)$	
0	1.17	0.480
1	3.32	0.667
2	3.24	0.835
3	8.48	1.43
4		1.39

Reference 41, E = 0.64 keV/amu

n	4	5
$\sigma_n(10^{-16}cm^2)$	29.9	6.45

ℓ	$\sigma_{n\ell}(10^{-16}cm^2)$	
0	1.85	0.652
1	5.76	0.897
2	10.1	1.86
3	12.2	2.06
4		0.980

Reference 41, E = 1.32 keV/amu

n	2	3	4
$\sigma_n(10^{-16}cm^2)$	0.02	37.4	6.62

ℓ	$\sigma_{n\ell}(10^{-16}cm^2)$		
0	0.0046	2.40	0.947
1	0.0093	8.39	1.93
2	0.0062	13.3	1.91
3		13.3	1.29
4			0.536

H - C^{6+}

Reference 41, E = 2.96 keV/amu

n	4	5
$\sigma_n(10^{-16}cm^2)$	38.1	7.76

ℓ	$\sigma_{n\ell}(10^{-16}cm^2)$	
0	2.21	0.310
1	7.54	1.13
2	14.5	1.53
3	14.0	2.22
4		2.57

Reference 41, E = 5.26 keV/amu

n	3	4	5
$\sigma_n(10^{-16}cm^2)$	1.07	36.6	9.47

ℓ	$\sigma_{n\ell}(10^{-16}cm^2)$		
0	0.290	1.83	0.237
1	0.503	6.92	0.663
2	0.277	14.0	1.28
3		13.9	2.95
4			4.34

Reference 41, E = 11.8 keV/amu

n	3	4	5
$\sigma_n(10^{-16}cm^2)$	2.13	29.0	12.5

ℓ	$\sigma_{n\ell}(10^{-16}cm^2)$		
0	0.345	0.957	0.175
1	0.931	3.77	0.501
2	0.852	8.64	1.29
3		15.6	3.09
4			7.45

Reference 41, E = 21.0 keV/amu

n	3	4	5
$\sigma_n(10^{-16}cm^2)$	2.24	23.4	12.2

ℓ	$\sigma_{n\ell}(10^{-16}cm^2)$		
0	0.237	0.656	0.134
1	0.746	2.43	0.549
2	1.26	7.12	1.32
3		13.2	2.99
4			7.21

Reference 41, E = 27.4 keV/amu

n	3	4	5
$\sigma_n(10^{-16}cm^2)$	1.96	20.3	12.3

ℓ	$\sigma_{n\ell}(10^{-16}cm^2)$		
0	0.167	0.466	0.160
1	0.566	1.84	0.664
2	1.23	6.18	1.29
3		11.8	2.93
4			7.25

H - N^{7+}

Reference 46, E = 0.49 keV/amu

n	4	5
$\sigma_n(10^{-16}cm^2)$	20.0	21.6

Reference 46, E = 1.0 keV/amu

n	4	5
$\sigma_n(10^{-16}cm^2)$	22.9	15.8

Reference 39, E = 50 keV/amu

n	3	4	5	6	7	8	9	10	11
$\sigma_n(10^{-16}cm^2)$	1.41	6.89	7.55	5.24	2.51	1.15	0.740	0.413	0.285
ℓ	$\sigma_{n\ell}(10^{-16}cm^2)$								
0	0.0710	0.101	0.0380	0.0290	0.0250				
1	0.466	0.562	0.427	0.238	0.0990	0.0630	0.0260	0.0140	
2	0.859	2.04	1.19	0.592	0.231	0.128	0.0480	0.0380	
3		4.42	1.79	0.959	0.373	0.176	0.108	0.0760	
4			4.51	1.35	0.684	0.292	0.221	0.160	
5				1.88	0.895	0.334	0.251	0.112	
6					0.173	0.0750	0.0560	0.0290	

$H - O^{8+}$

Reference 46, E = 0.49 keV/amu

n	4	5	6
$\sigma_n(10^{-16}cm^2)$	3.51	57.5	1.08
ℓ	$\sigma_{n\ell}(10^{-16}cm^2)$		
0	0.862	11.5	0.177
1	1.59	22.8	0.328
2	0.877	16.0	0.300
3	0.171	5.61	0.144
4		0.814	0.0366
5			

Reference 46, E = 1.0 keV/amu

n	4	5	6
$\sigma_n(10^{-16}cm^2)$	5.99	55.5	0.760
ℓ	$\sigma_{n\ell}(10^{-16}cm^2)$		
0	1.50	10.8	0.120
1	2.68	21.7	0.265
2	1.48	15.5	0.208
3	0.291	5.28	0.101
4		0.765	0.258

Reference 46,E = 10 keV/amu

n	4	5	6
$\sigma_n(10^{-16}cm^2)$	12.9	35.4	0.245

Reference 46, E = 25 keV/amu

n	4	5	6
$\sigma_n(10^{-16}cm^2)$	14.4	26.7	0.156
ℓ	$\sigma_{n\ell}(10^{-16}cm^2)$		
0	0.914	1.10	0.0401
1	2.750	3.27	0.119
2	4.560	5.36	0.198
3	6.210	7.54	0.278
4		9.65	0.363
5			0.446

H - O^{8+}

Reference 39, E = 50 keV/amu

n	3	4	5	6	7	8	9	10	11
$\sigma_n(10^{-16}cm^2)$	0.548	5.09	10.00	7.89	4.33	1.95	0.989	0.604	0.321

ℓ	$\sigma_{n\ell}(10^{-16}cm^2)$							
0	0.0560	0.0730	0.0510	0.0230				
1	0.161	0.585	0.426	0.326	0.145	0.0710	0.0220	0.0130
2	0.339	1.53	1.20	0.736	0.417	0.133	0.0710	0.0390
3		2.69	2.10	1.13	0.484	0.261	0.194	0.0520
4			5.25	1.76	0.848	0.487	0.257	0.142
5				3.60	1.27	0.576	0.254	0.155
6					1.10	0.460	0.204	0.141
7							0.0130	

Reference 39, E = 100 keV/amu

n	3	4	5	6	7	8	9	10
$\sigma_n(10^{-16}cm^2)$	0.387	1.35	2.41	2.31	1.96	1.58	1.18	0.908

Reference 39, E = 100 keV/amu

n	11	12	13	14	15
$\sigma_n(10^{-16}cm^2)$	0.724	0.665	0.421	0.350	0.258

$H - F^{9+}$

Reference 46, E = 0.49 keV/amu

n	4	5	6	7
$\sigma_n(10^{-16}cm^2)$	0.0400	32.4	39.6	0.0250

Reference 46, E = 1.0 keV/amu

n	4	5	6	7
$\sigma_n(10^{-16}cm^2)$	0.239	35.8	29.5	0.0174

Reference 39, E = 50 keV/amu

n	3	4	5	6	7	8	9	10	11
$\sigma_n(10^{-16}cm^2)$	0.213	0.321	9.38	10.4	6.75	2.88	1.34	0.873	0.562
ℓ	$\sigma_{n\ell}(10^{-1-}cm^2)$								
0	0.0220	0.107	0.0800	0.0440					
1	0.0450	0.485	0.450	0.430	0.232	0.0800			
2	0.135	0.910	1.32	0.890	0.567	0.143	0.0270		
3		1.58	2.57	1.35	0.638	0.183	0.106		
4			4.67	2.08	0.998	0.500	0.123		
5				5.41	1.71	0.654	0.337	0.164	
6					2.86	0.930	0.492	0.289	
7						0.452	0.216	0.145	

H - Ne^{10+}

Reference 46, E = 0.49 keV/amu

n	5	6	7	8
$\sigma_n(10^{-16}cm^2)$	9.33	69.9	5.90	0.0800

Reference 46, E = 1.0 keV/amu

n	5	6	7	8
$\sigma_n(10^{-16}cm^2)$	13.6	64.0	4.18	0.0580

ℓ	$\sigma_{n\ell}(10^{-16}cm^2)$			
0	2.69	10.7	0.582	
1	5.30	21.3	1.34	0.0159
2	3.94	18.7	1.26	0.0159
3	1.39	8.98	0.680	0.0102
4	0.197	2.26	0.244	
5		0.255	0.0479	

Reference 46, E = 10.0 keV/amu

n	4	5	6	7	8
$\sigma_n(10^{-16}cm^2)$	0.700	23.0	36.5	1.38	0.0190

ℓ	$\sigma_{n\ell}(10^{-16}cm^2)$			
0	0.173	4.73	6.18	0.192
1	0.301	8.94	13.2	0.424
2	0.169	6.50	10.5	0.389
3	0.0337	2.32	5.18	0.222
4		0.319	1.32	0.0778
5			0.146	0.0155

$H - Ne^{+10}$

Reference 46, E = 25.0 keV/amu

n	4	5	6	7	8
$\sigma_n(10^{-16}cm^2)$	1.84	23.8	26.8	0.880	0.0120

ℓ	$\sigma_{n\ell}(10^{-16}cm^2)$		
0	0.118	0.962	0.759
1	0.345	2.89	2.23
2	0.580	4.75	3.66
3	0.812	6.60	5.11
4		8.49	6.61
5			7.94

Reference 26, E = 1.0 keV/amu

n	2	3	4	5	6
$\sigma_n(10^{-16}cm^2)$	0.0516	0.421	4.11	12.8	52.1

ℓ	$\sigma_{n\ell}(10^{-16}cm^2)$				
0	0.0456	0.220	0.0490	2.07	4.87
1	0.00603	0.150	1.32	4.10	13.9
2		0.0500	1.95	3.70	11.8
3			0.790	2.15	12.5
4				0.76	6.87
5					2.23

Reference 26, E = 5.0 keV/amu

n	2	3	4	5	6
$\sigma_n(10^{-16}cm^2)$	0.200	14.2	88.9	1430	4220

H - Ne^{10+}

Reference 26, E = 10.0 keV/amu

n	2	3	4	5	6	7	8
$\sigma_n(10^{-16}cm^2)$	0.00400	19.4	193	1590	2930	867	81.5

Reference 26, E = 25.0 keV amu

n	2	3	4	5	6	7	8	9
$\sigma_n(10^{-16}cm^2)$	0.0760	83.6	359	1270	1880	1230	557	192

ℓ	$\sigma_{n\ell}(10^{-16}cm^2)$							
0	0.000066	0.376	0.432	0.627	0.224	0.0709	0.0275	0.00780
1	0.000749	0.214	1.11	1.99	0.819	0.281	0.0898	0.0267
2		0.199	1.29	3.28	1.94	0.548	0.164	0.0446
3			0.844	3.97	3.69	0.990	0.261	0.0737
4				2.71	5.90	1.76	0.432	0.122
5					5.77	3.25	0.701	0.196
6						5.57	1.17	0.292
7							2.61	0.482
8								0.841

Reference 26, E = 50 keV/amu

n	2	3	4	5	6	7	8	6	10
$\sigma_n(10^{-16}cm^2)$	0.340	80.1	299	688	902	823	632	421	274

Reference 26, E = 100 keV/amu

n	2	3	4	5	6	7	8	9	10
$\sigma_n(10^{-16}cm^2)$	0.805	46.4	151	266	321	296	255	214	169

H - Ne^{10+}

Reference 26, E = 200 keV/amu

n	2	3	4	5	6	7	8	9	10
$\sigma_n(10^{-16}cm^2)$	1.01	20.1	47.2	65.4	69.2	62.5	52.7	43.5	35.4

Reference 26, E = 500 keV/amu

n	2	3	4	5	6	7	8	9	10
$\sigma_n(10^{-16}cm^2)$	0.421	2.33	3.14	3.16	2.76	2.16	1.77	1.43	1.11
ℓ	$\sigma_{n\ell}(10^{-16}cm^2)$								
0	0.204	0.363	0.163	0.132	0.102	0.0708	0.0539	0.0432	0.0337
1	0.215	0.293	0.231	0.179	0.134	0.0961	0.0739	0.0557	0.0418
2		1.67	0.890	0.563	0.396	0.274	0.209	0.157	0.114
3			2.02	1.51	1.12	0.772	0.612	0.438	0.334
4				0.901	0.845	0.696	0.569	0.432	0.333
5					0.261	0.278	0.269	0.227	0.177
6						0.0407	0.0639	0.0717	0.0565
7							0.00590	0.0102	0.0112
8									0.00112

Reference 26, E = 1000 keV/amu

n	2	3	4	5	6	7	8
$\sigma_n(10^{-16}cm^2)$	0.0870	0.205	0.195	0.150	0.107	0.0770	0.0560

Reference 26, E = 2000 keV/amu

n	2	3	4	5	6
$\sigma_n(10^{-16}cm^2)$	0.0100	0.0110	0.00700	0.00500	0.00300

H - Ne^{10+}

Reference 39, E = 50 keV/amu

n	4	5	6	7	8	9	10	11	12	13
$\sigma_n(10^{-16}cm^2)$	1.51	7.50	11.6	10.2	4.94	2.27	1.11	0.670	0.379	0.289

ℓ	$\sigma_{n\ell}(10^{-16}cm^2)$									
0	0.0860	0.0450	0.0350	0.0150						
1	0.213	0.484	0.366	0.271	0.0810					
2	0.459	1.39	0.956	0.747	0.237	0.0340				
3	0.729	2.41	1.48	0.993	0.330	0.0770	0.0200			
4		3.21	2.67	1.20	0.420	0.125	0.110	0.0690		
5			5.97	2.11	0.728	0.415	0.159	0.0890		
6				4.57	1.28	0.600	0.309	0.194		
7					1.58	0.811	0.365	0.204		
8						0.150	0.0920	0.0600		

Reference 39, E = 100 keV/amu

n	4	5	6	7
$\sigma_n(10^{-16}cm^2)$	0.801	1.99	2.87	3.07

Reference 39, E = 100 keV/amu (continued)

n	8	9	10	11	12	13	14	15	16
$\sigma_n(10^{-16}cm^2)$	2.68	2.42	1.85	1.54	1.25	0.965	0.758	0.630	0.525

ℓ	$\sigma_{n\ell}(10^{-16}cm^2)$			
0	0.0100			
1	0.0680		0.00200	0.0200
2	0.134		10.5	0.0400
3	0.221		0.0340	0.0670
4	0.398		0.00950	0.110
5	0.562			0.166
6	0.700			0.263
7	0.483			0.313
8				0.219
9				0.147

H - Si^{14+}

Reference 46, E = 1.0 keV/amu

n	6	7	8	9	10
$\sigma_n(10^{-16}cm^2)$					
ℓ	$\sigma_{n\ell}(10^{-16}cm^2)$				
0	0.214	5.88	8.40	1.24	0.0116
1	0.465	13.0	19.9	2.92	0.0292
2	0.393	12.0	20.1	3.17	0.0321
3	0.177	6.82	12.8	2.20	0.0243
4	0.0454	2.43	5.54	1.07	0.0132
5		0.486	1.56	0.383	
6		0.0431	0.259	0.0432	
7			0.0194		

Reference 46, E = 10.0 keV/amu

n	6	7	8	9	10
$\sigma_n(10^{-16}cm^2)$	10.9	43.5	33.1	3.80	0.0400
ℓ	$\sigma_{n\ell}(10^{-16}cm^2)$				
0	1.77	6.33	4.06	0.412	
1	3.75	13.8	9.44	1.03	0.00950
2	3.14	12.5	9.47	1.08	0.0104
3	1.46	7.15	6.13	0.746	
4	0.385	2.52	2.79	0.385	
5	0.0409	0.507	0.732	0.126	
6		0.0400	0.123	0.0297	
7			0.0100		

Reference 46, E = 25 keV/amu

n	6	7	8	9	10
$\sigma_n(10^{-16}cm^2)$	15.4	38.3	23.2	2.44	0.0250

H - Si^{14+}

Reference 46, E = 25 keV/amu

n	6	7	8	9	10
$\sigma_n(10^{-16}cm^2)$	17.8	33.3	17.6	1.75	0.0180

Reference 39, E = 100 keV/amu

n	5	6	7	8	9	10	11	12
$\sigma_n(10^{-16}cm^2)$	0.754	2.01	3.82	4.73	4.85	4.65	3.81	3.22

ℓ	$\sigma_{n\ell}(10^{-16}cm^2)$			
0			0.0130	
1			0.0770	0.0640	0.0450
2			0.192	0.219	0.0920
3			0.244	0.205	0.0960
4			0.365	0.257	0.180
5			0.620	0.352	0.239
6			0.914	0.592	0.291
7			2.27	0.740	0.328
8				1.03	0.546
9				1.11	0.767
10					0.642
11					0.0660

Reference 39, E = 100 keV/amu (continued)

n	13	14	15	16	17	18	19
$\sigma_n(10^{-16}cm^2)$	2.56	2.17	1.76	1.42	1.23	1.06	0.874

H - Si^{14+}

Reference 26, E = 5.0 keV/amu

n	2	3	4	5	6	7	8
$\sigma_n(10^{-16}cm^2)$	0.191	3.51	24.2	85.3	339	3160	3670

Reference 26, E = 10 keV/amu

n	2	3	4	5	6	7	8
$\sigma_n(10^{-16}cm^2)$	0.00200	1.06	8.00	61.7	609	2690	3080

Reference 26, E = 25 keV/amu

n	3	4	5	6	7	8	9	10
$\sigma_n(10^{-16}cm^2)$	5.89	74.3	292	902	1780	2050	1400	689

Reference 26, E = 50 keV/amu

n	3	4	5	6	7	8	9	10
$\sigma_n(10^{-16}cm^2)$	15.9	80.9	265	608	993	1140	1040	779

Reference 26, E = 100 keV/amu

n	2	3	4	5	6	7	8	9	10	11	12
$\sigma_n(10^{-16}cm^2)$	0.00800	8.14	68.7	175	311	417	453	435	400	332	262

H - Si^{14+}

Reference 26, E = 200 keV/amu

n	3	4	5	6	7	8	9	10	11	12
$\sigma_n(10^{-16}cm^2)$	6.97	32.7	68.3	95.8	106	106	102	91.3	80.1	69.9

Reference 26, E = 500 keV/amu

n	2	3	4	5	6	7	8	9	10	11
$\sigma_n(10^{-16}cm^2)$	0.0700	1.52	4.18	5.83	6.54	6.24	5.43	4.67	3.77	3.13

Reference 26, E = 1000 keV/amu

n	2	3	4	5	6	7	8	9	10	11
$\sigma_n(10^{-16}cm^2)$	0.0450	0.269	0.414	0.429	0.363	0.295	0.236	0.189	0.147	0.116

Reference 26, E = 2000 keV/amu

n	2	3	4	5	6	7	8	9	10	11
$\sigma_n(10^{-16}cm^2)$	0.0110	0.0220	0.0220	0.0170	0.0120	0.00800	0.00700	0.00600	0.00500	0.00400

H - Ar^{18+}

Reference 46, E = 0.49 keV/amu

n	7	8	9	10	11
$\sigma_n(10^{-16}cm^2)$	2.47	53.3	82.6	17.5	0.488

Reference 46, E = 1.0 keV/amu

n	6	7	8	9	10	11
$\sigma_n(10^{-16}cm^2)$	0.0109	5.88	58.0	67.4	12.7	0.344

Reference 39, E = 100 keV/amu

n	5	6	7	8	9	10	11	12
$\sigma_n(10^{-16}cm^2)$	0.287	1.19	2.81	4.83	5.70	5.95	5.59	4.44

ℓ	$\sigma_{n\ell}(10^{-16}cm^2)$			
0		0.0160		
1		0.0830	0.0780	
2		0.164	0.239	0.0850
3		0.317	0.249	0.198
4		0.297	0.327	0.255
5		0.442	0.537	0.324
6		0.982	0.542	0.422
7		1.33	0.940	0.626
8			1.25	0.765
9			2.67	0.767
10				1.48
11				1.68

Reference 39, E = 100 keV/amu (continued)

n	13	14	15	16	17	18	19	20
$\sigma_n(10^{-16}cm^2)$	3.79	3.05	2.31	2.38	1.79	1.43	1.33	1.06

GRAPH. SET No. 2

1) Partial cross sections $\sigma_{n\ell}$ for the H + He^{2+} system

2) Partial cross section σ_n for the H + A^{Z+} systems, with $Z \geq 13$

Note: The theoretical references are given in Appendix A.1; the experimental references (supplemented by E) are given in Appendix A.2.

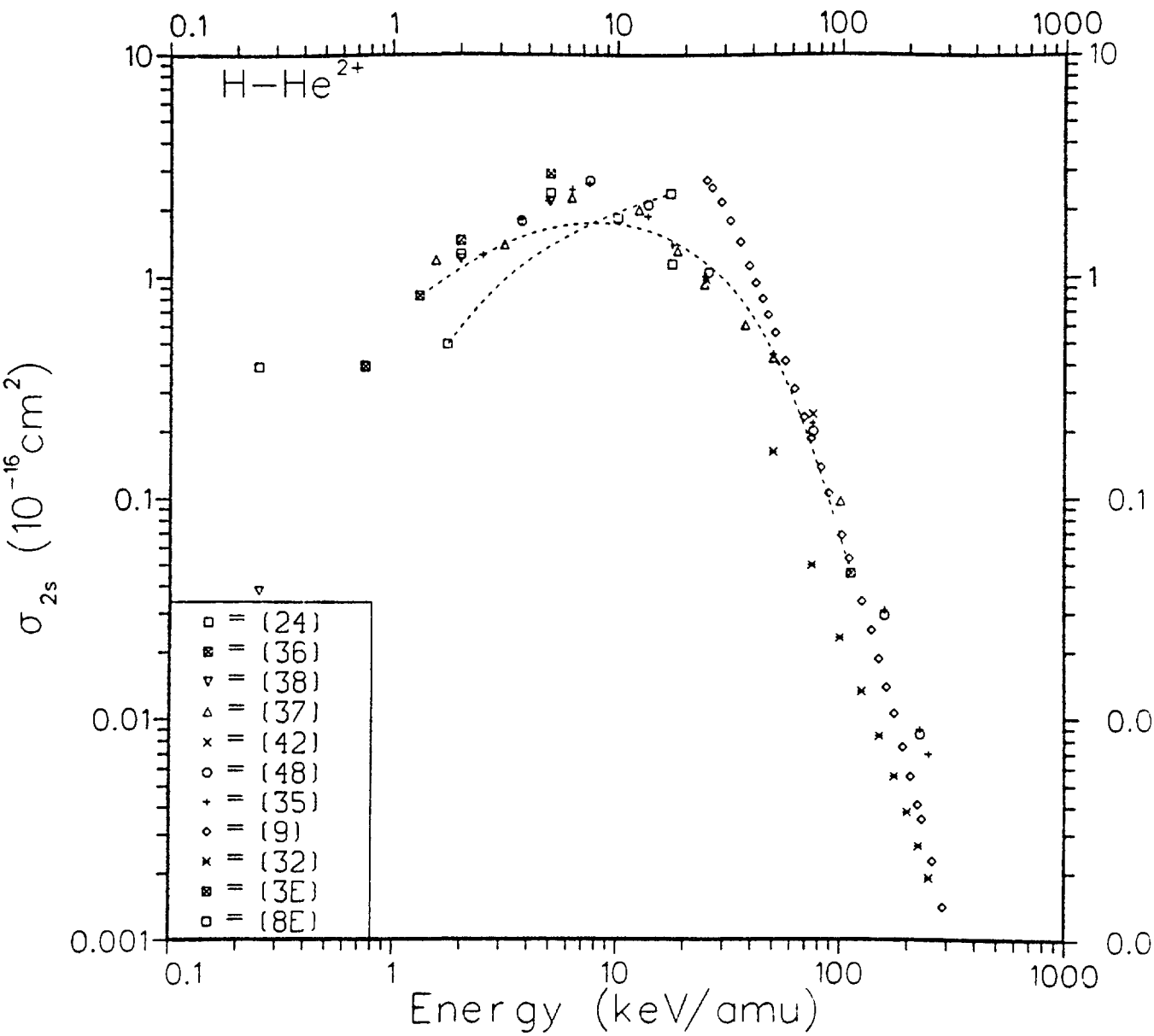
H−He2+
σ2s (10−16cm2)
Energy (keV/amu)
0.1
1
10
100
1000
0.001
0.01
0.1
1
10
0.0
□ = (24)
⊠ = (36)
▽ = (38)
△ = (37)
× = (42)
○ = (48)
+ = (35)
◇ = (9)
✕ = (32)
⊠ = (3E)
□ = (8E)

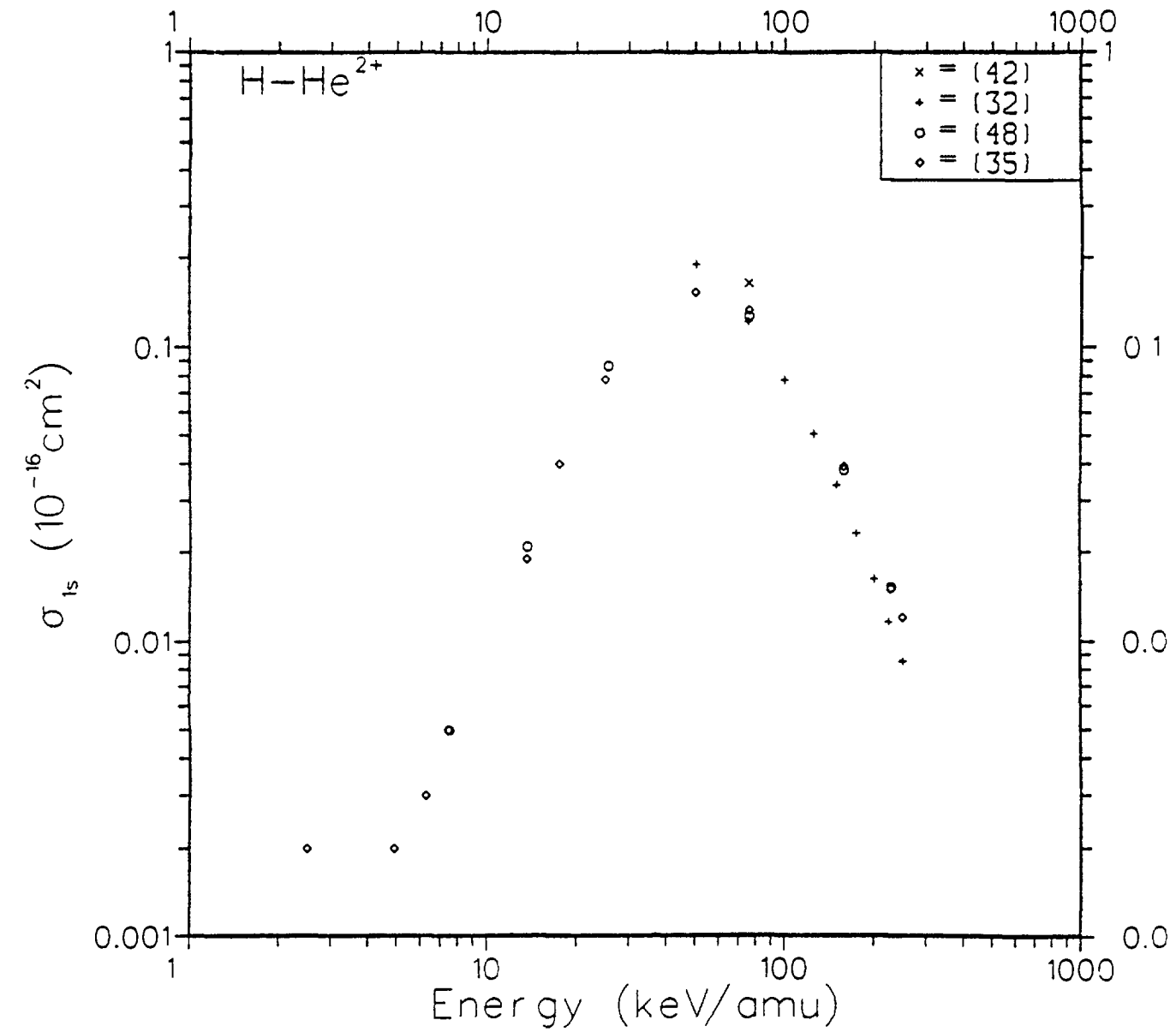
H−He2+
× = (42)
+ = (32)
o = (48)
◇ = (35)
σ1s (10−16cm2)
Energy (keV/amu)
1
10
100
1000
0.1
0.01
0.001
0.0

82/06/10 14.50 57. 3

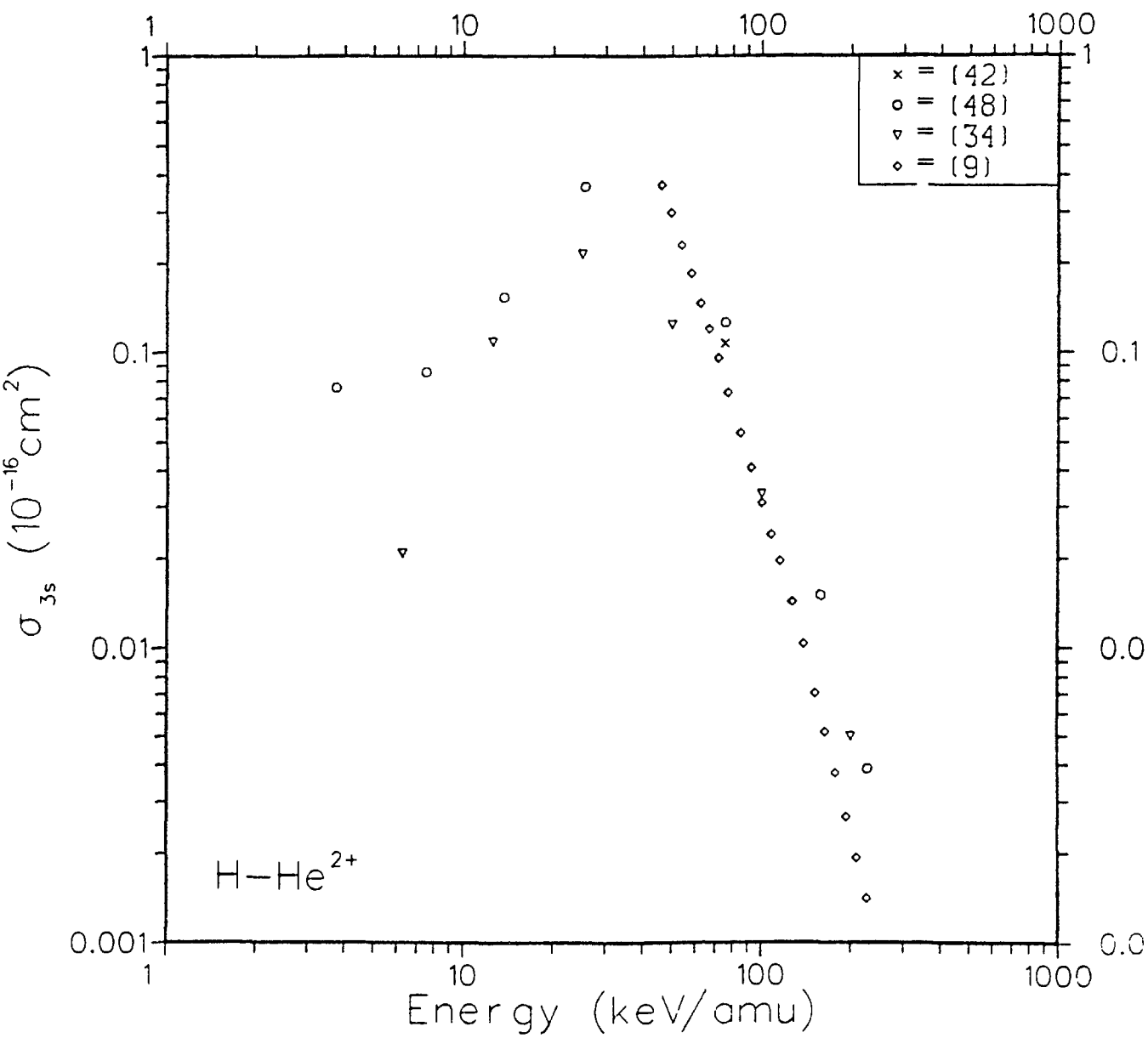

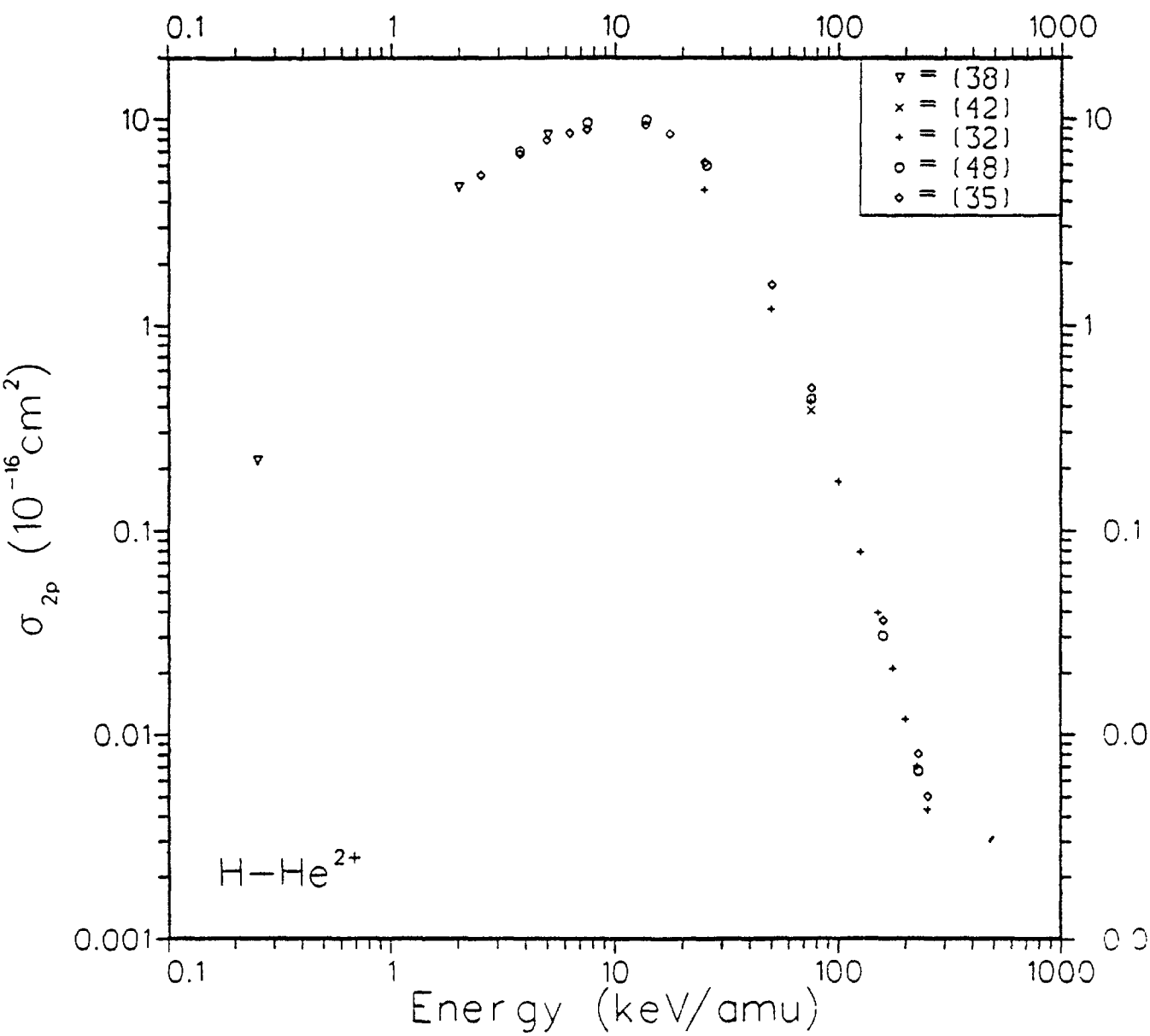
0.1
1
10
100
1000
▽ = (38)
× = (42)
+ = (32)
○ = (48)
◇ = (35)
10
1
0.1
0.01
0.001
σ_{2p} (10^{-16}cm^2)
H—He^{2+}
Energy (keV/amu)

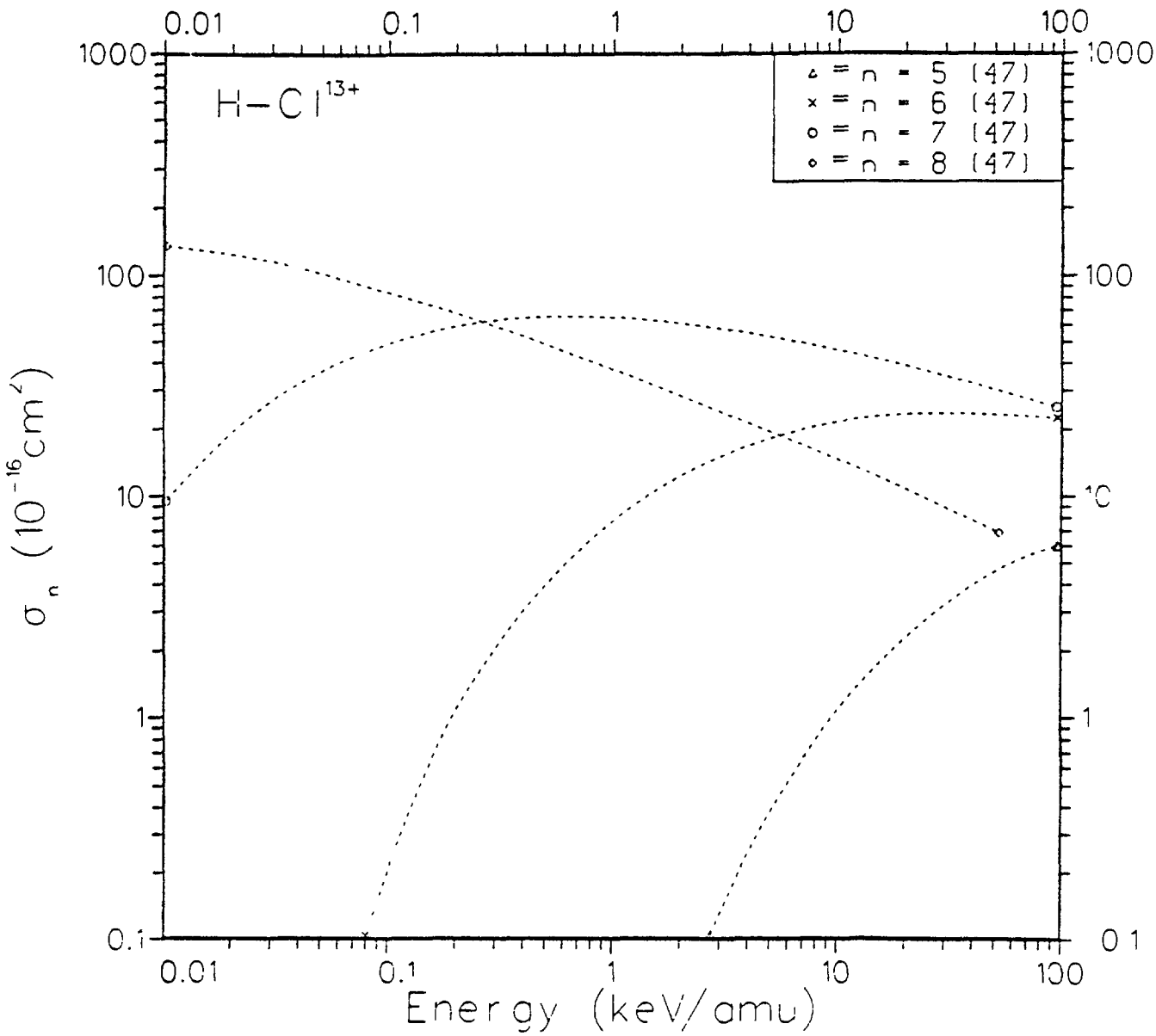
H−Cl13+
n = 5 (47)
n = 6 (47)
n = 7 (47)
n = 8 (47)
σn (10−16cm2)
Energy (keV/amu)
0.01
0.1
1
10
100
1000

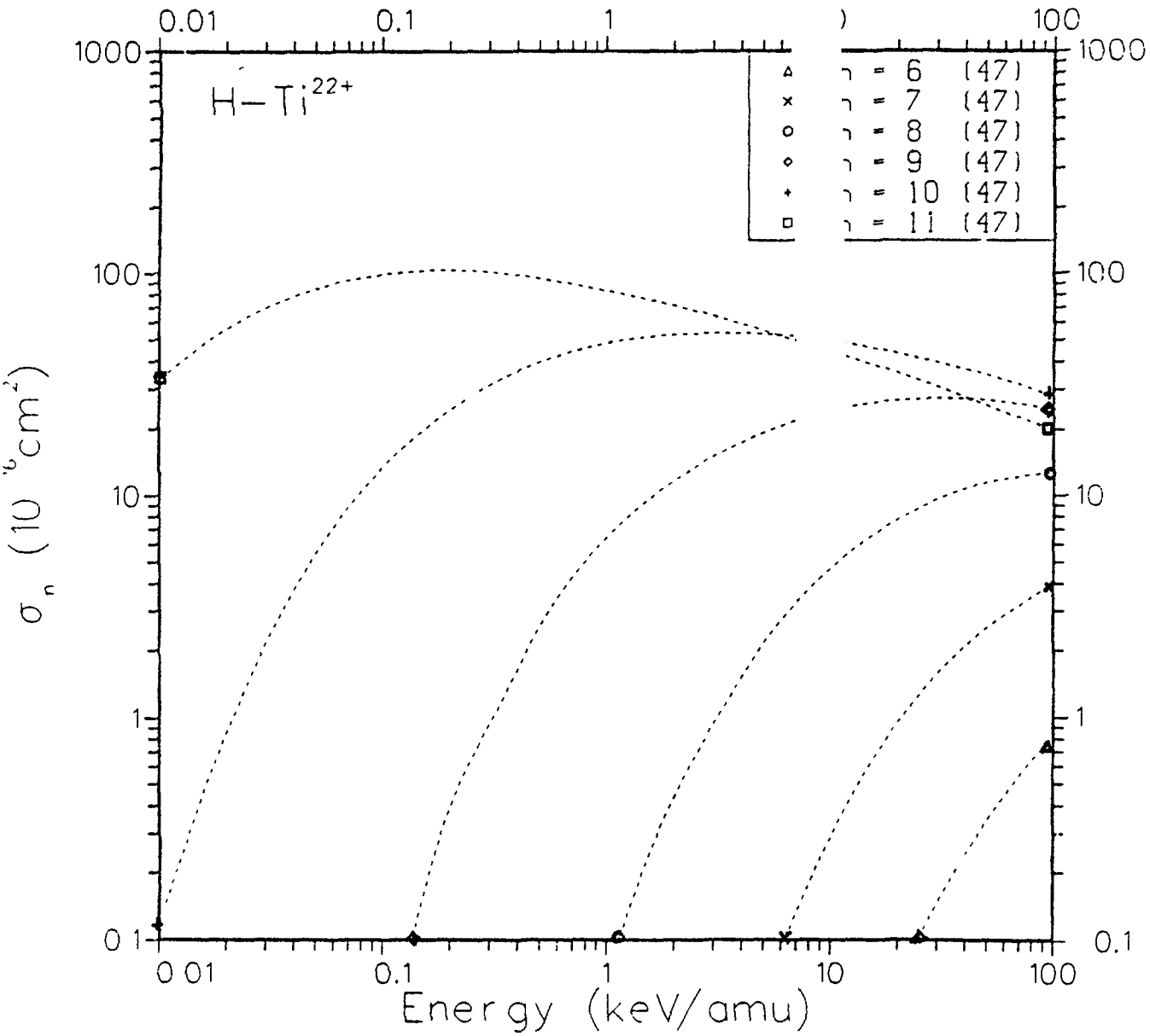
H–Ti^{22+}
n = 6 (47)
n = 7 (47)
n = 8 (47)
n = 9 (47)
n = 10 (47)
n = 11 (47)
σ_n (10^{-16} cm^2)
Energy (keV/amu)
0.01
0.1
1
10
100
1000

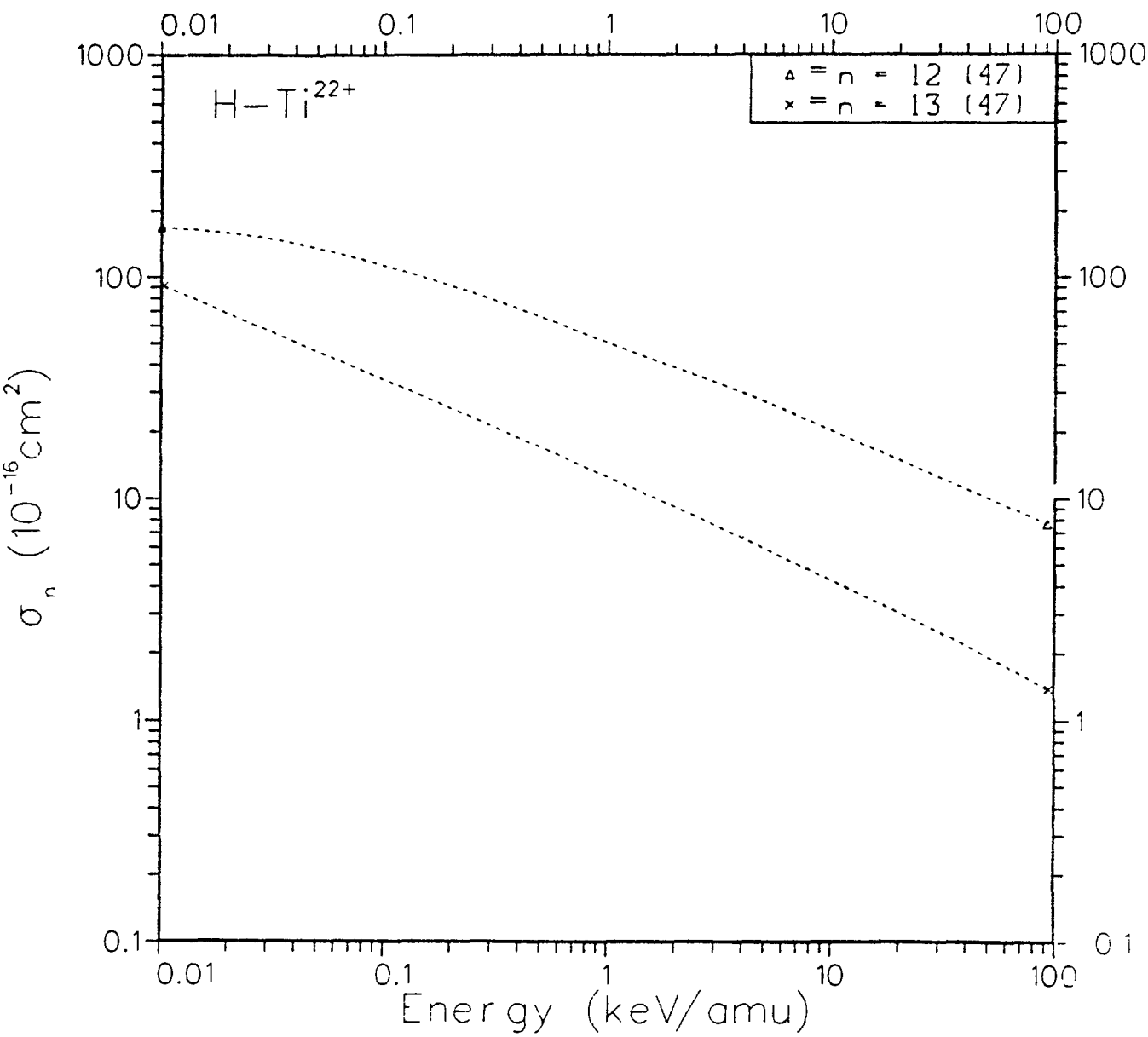
H—Ti^{22+}
Δ = n = 12 (47)
× = n = 13 (47)
σ_n (10^{-16}cm^2)
Energy (keV/amu)
0.01
0.1
1
10
100
1000

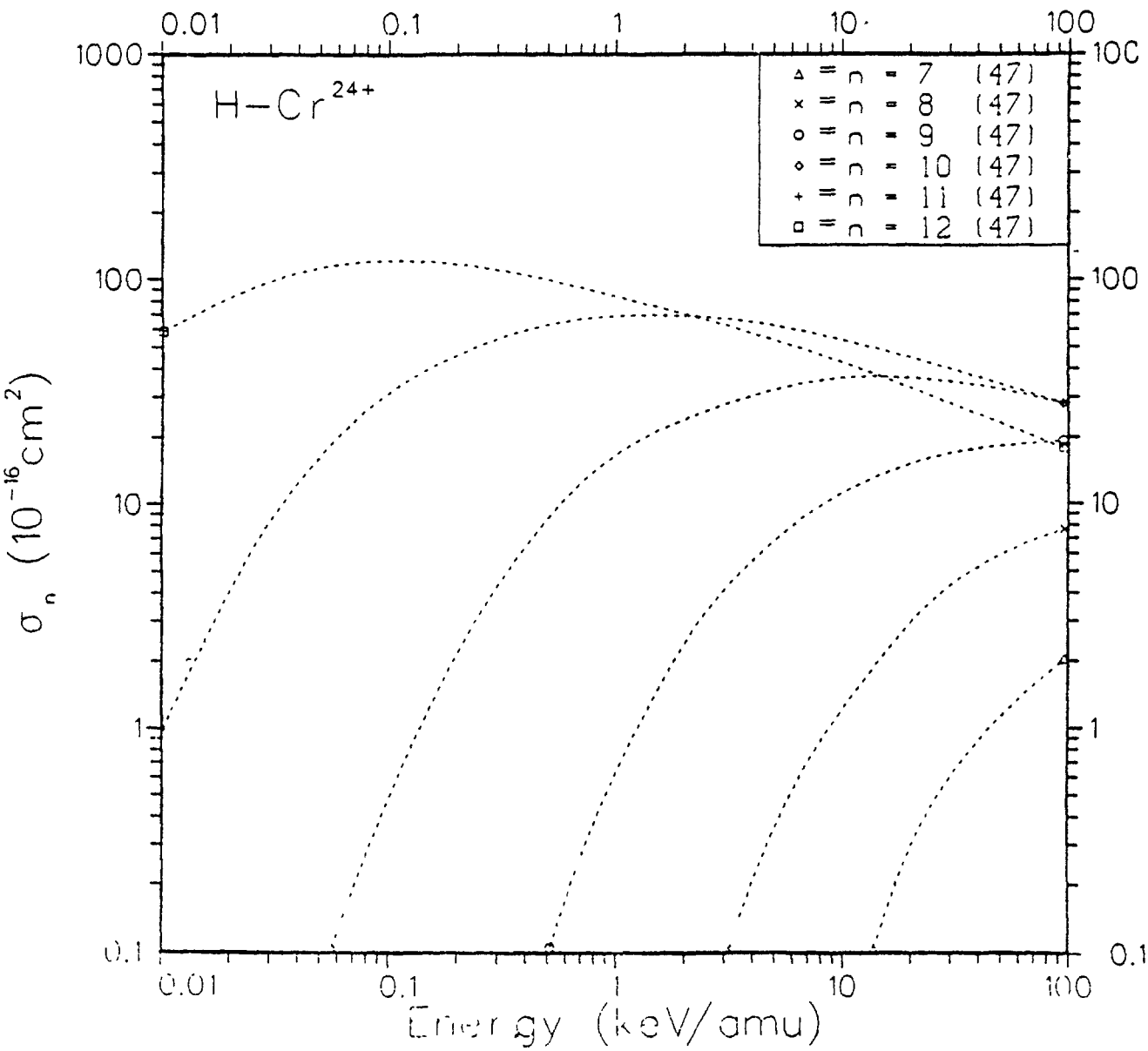

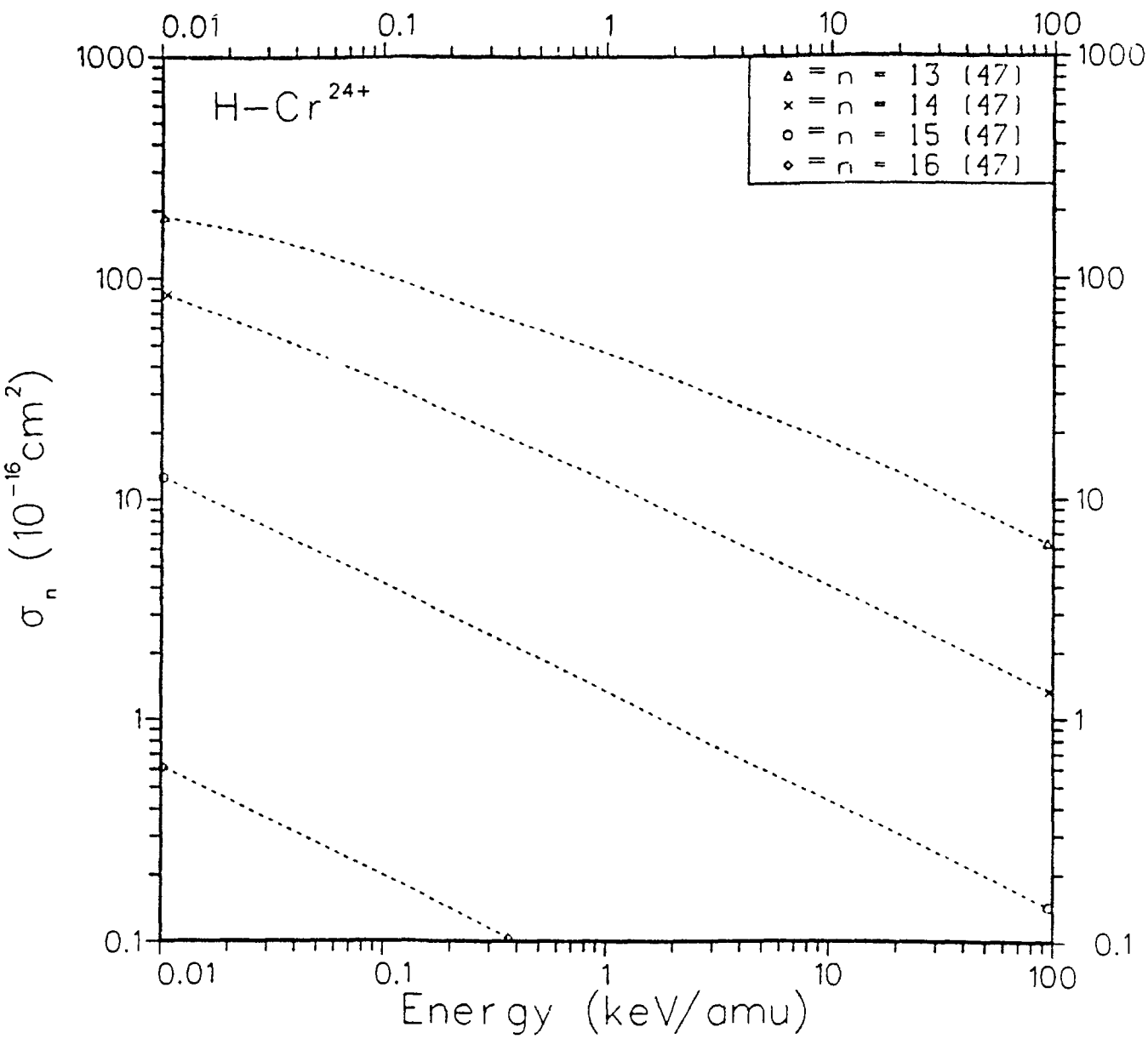
H−Cr 24+
Δ = n = 13 (47)
× = n = 14 (47)
o = n = 15 (47)
◇ = n = 16 (47)
σn (10−16cm2)
Energy (keV/amu)
0.01
0.1
1
10
100
1000

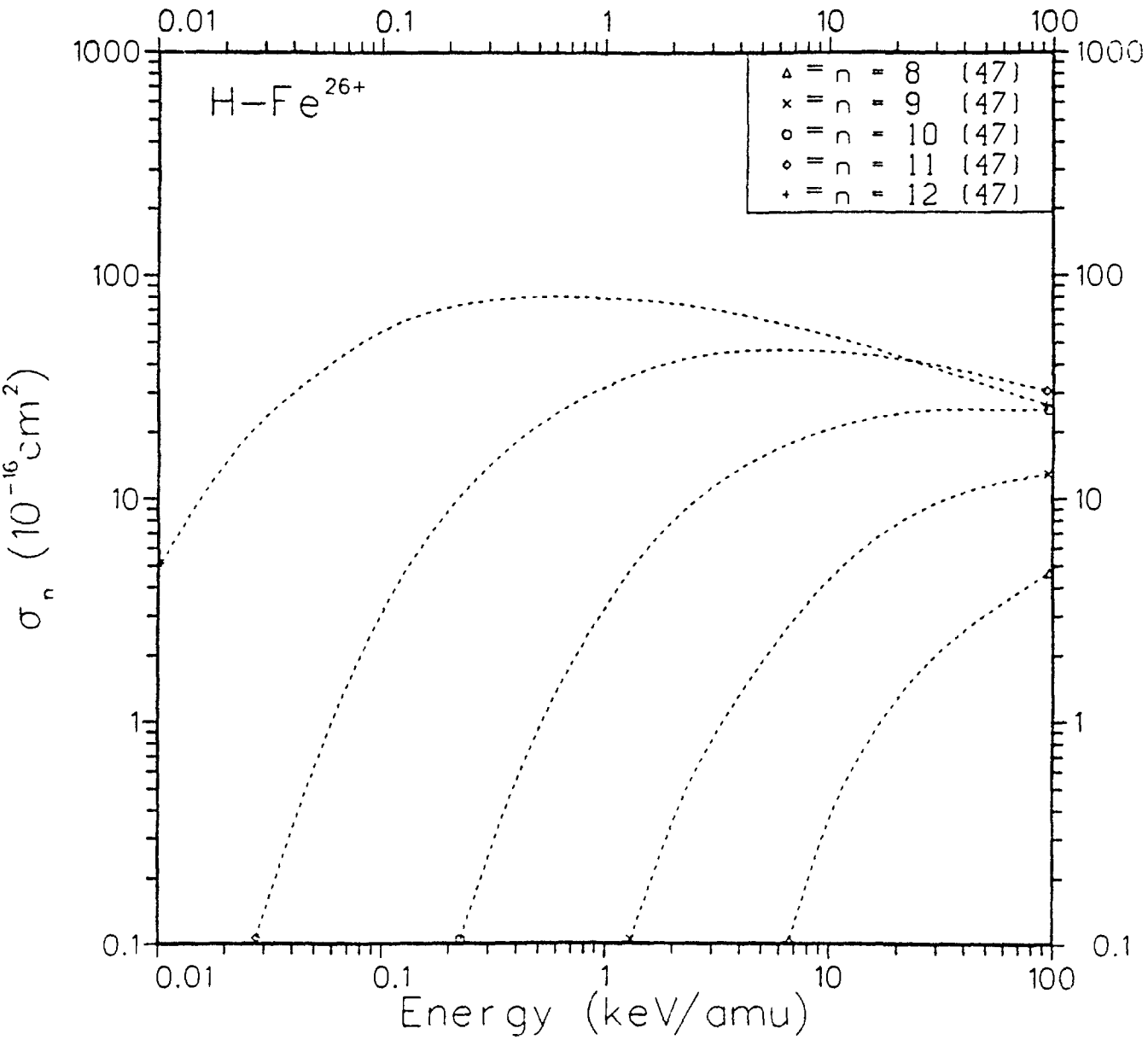
H–Fe^{26+}
Δ = n = 8 (47)
× = n = 9 (47)
o = n = 10 (47)
◇ = n = 11 (47)
+ = n = 12 (47)
σ_n (10^{-16}cm^2)
Energy (keV/amu)
0.01
0.1
1
10
100
1000

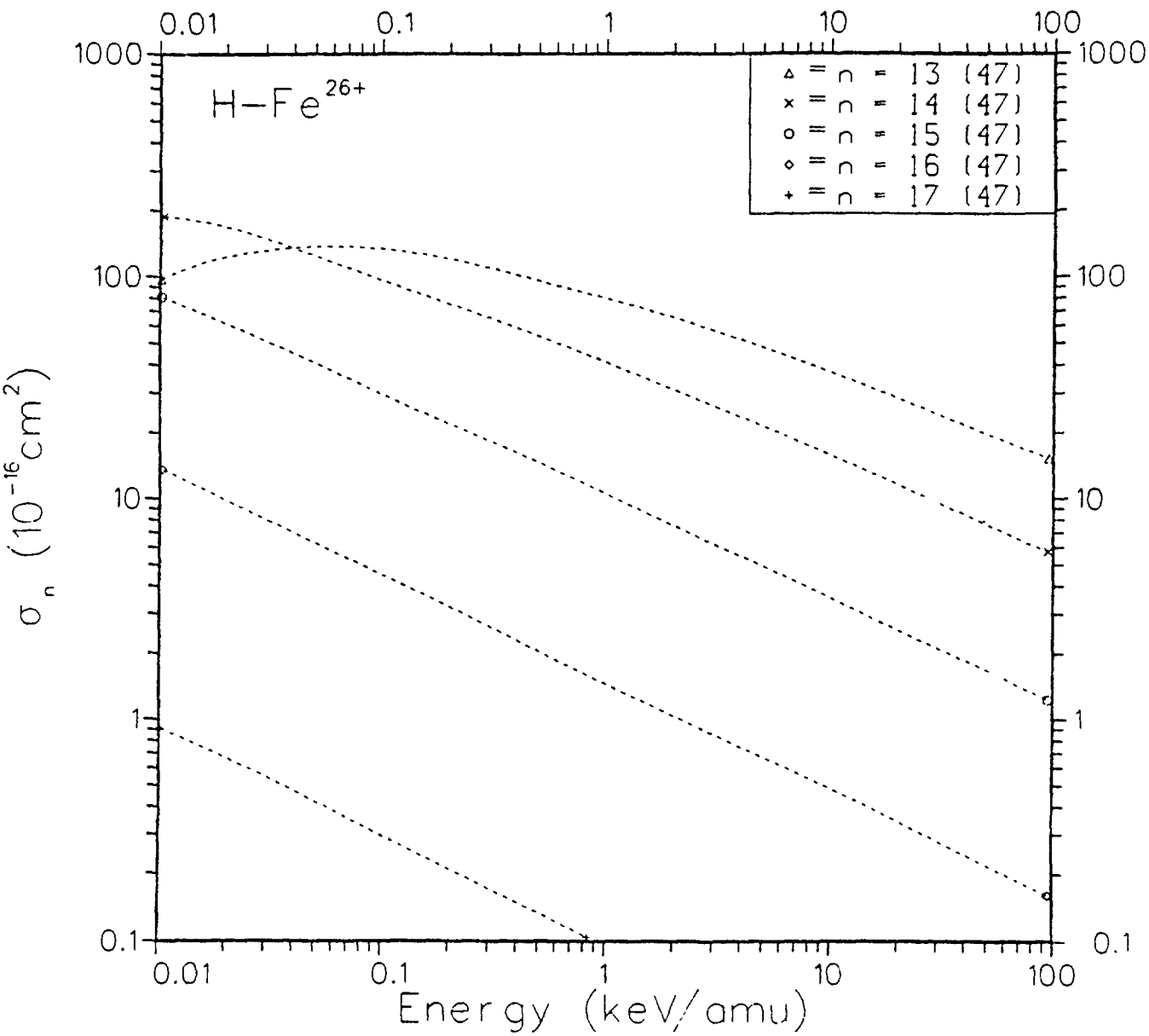
H−Fe26+
△ = n = 13 (47)
× = n = 14 (47)
○ = n = 15 (47)
◇ = n = 16 (47)
+ = n = 17 (47)
σn (10−16cm2)
Energy (keV/amu)
0.01
0.1
1
10
100
1000

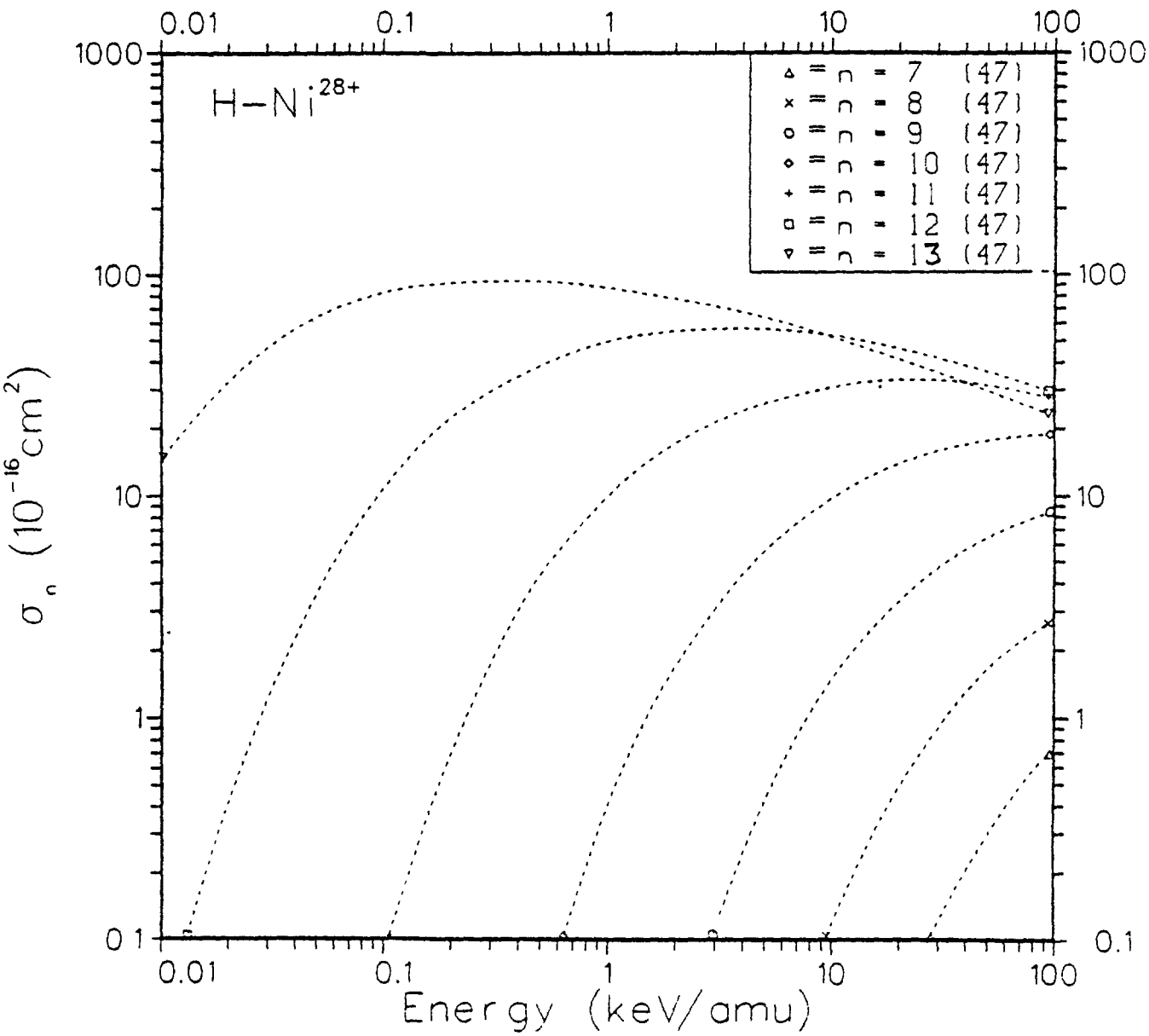

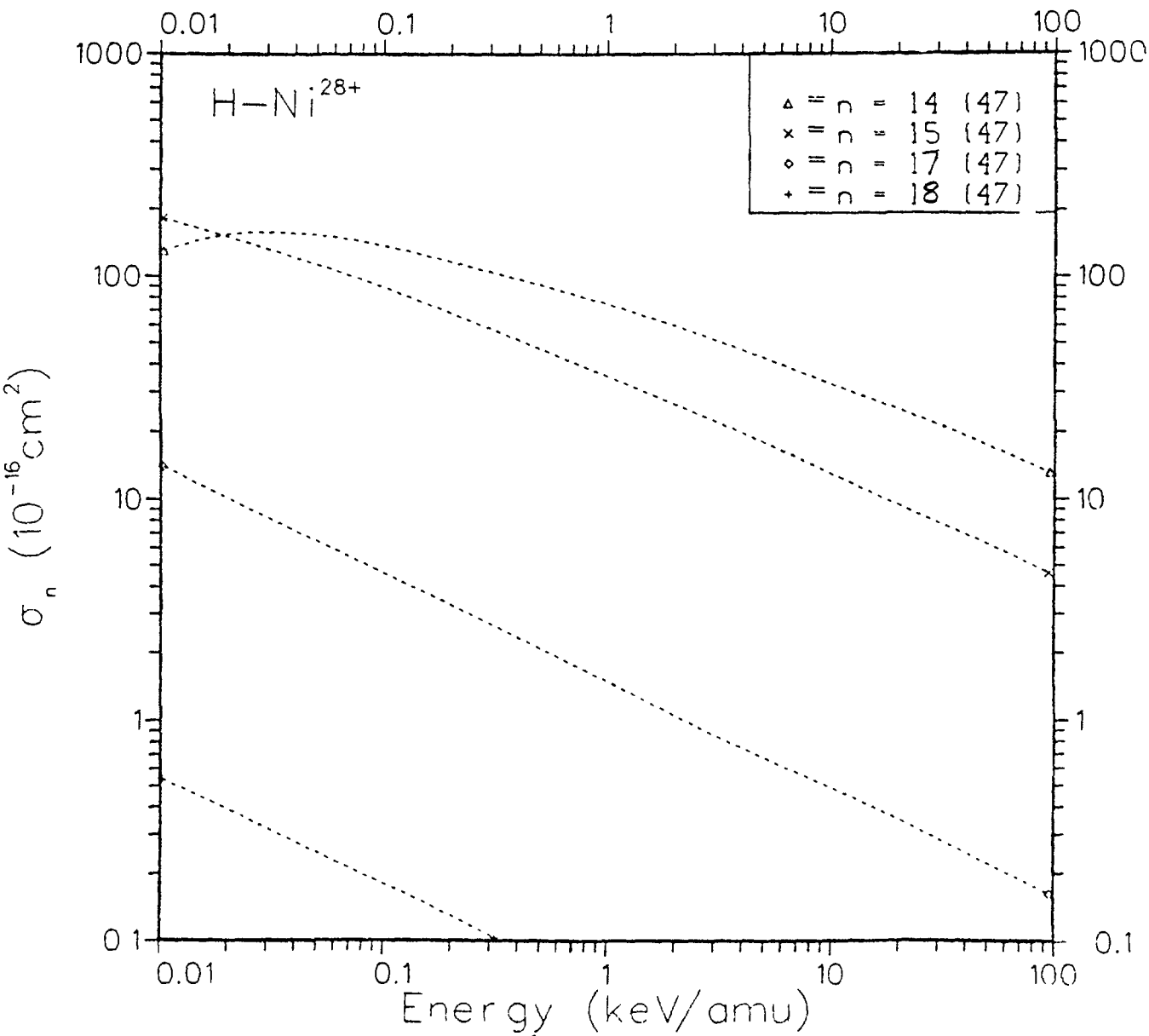

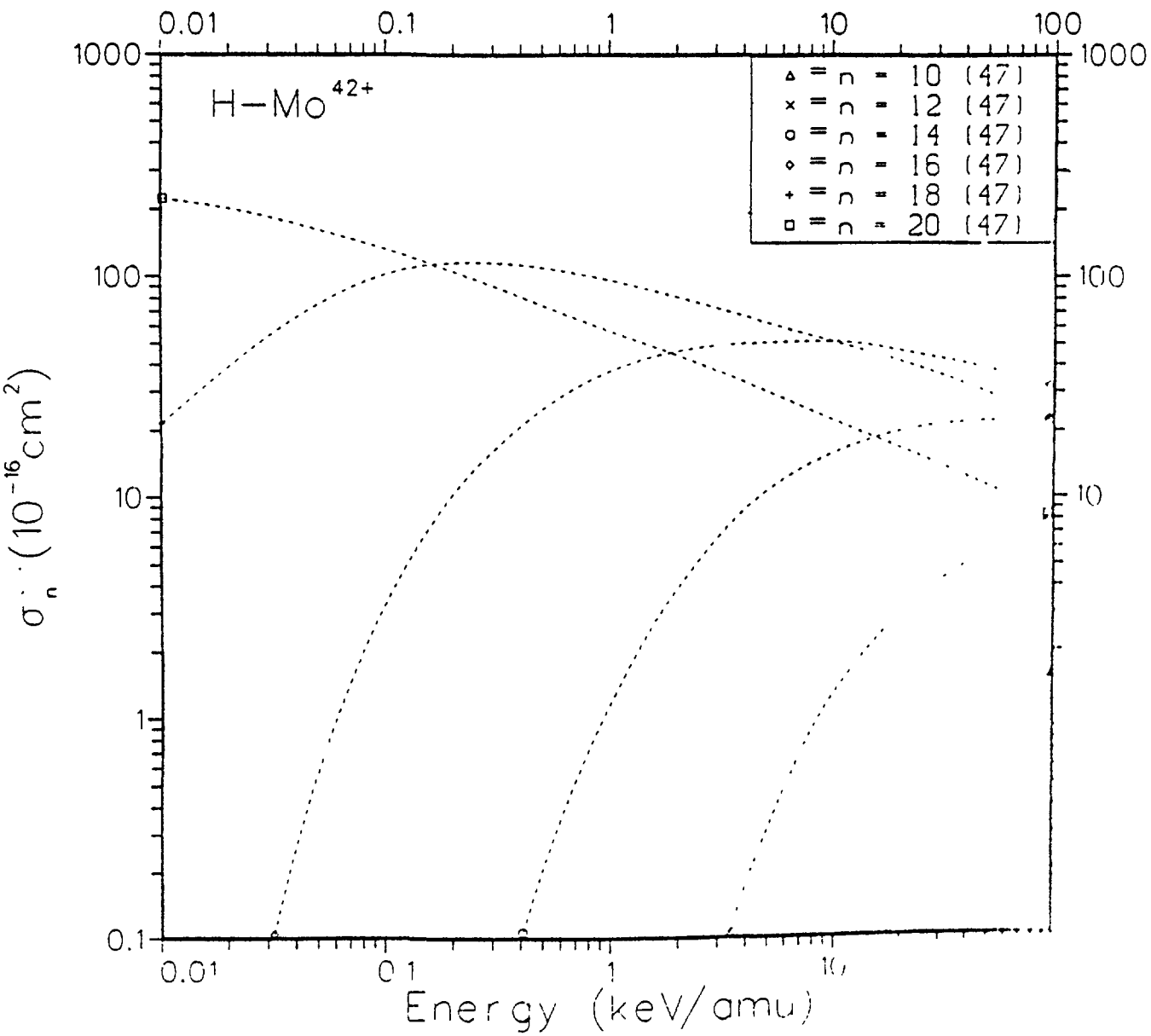

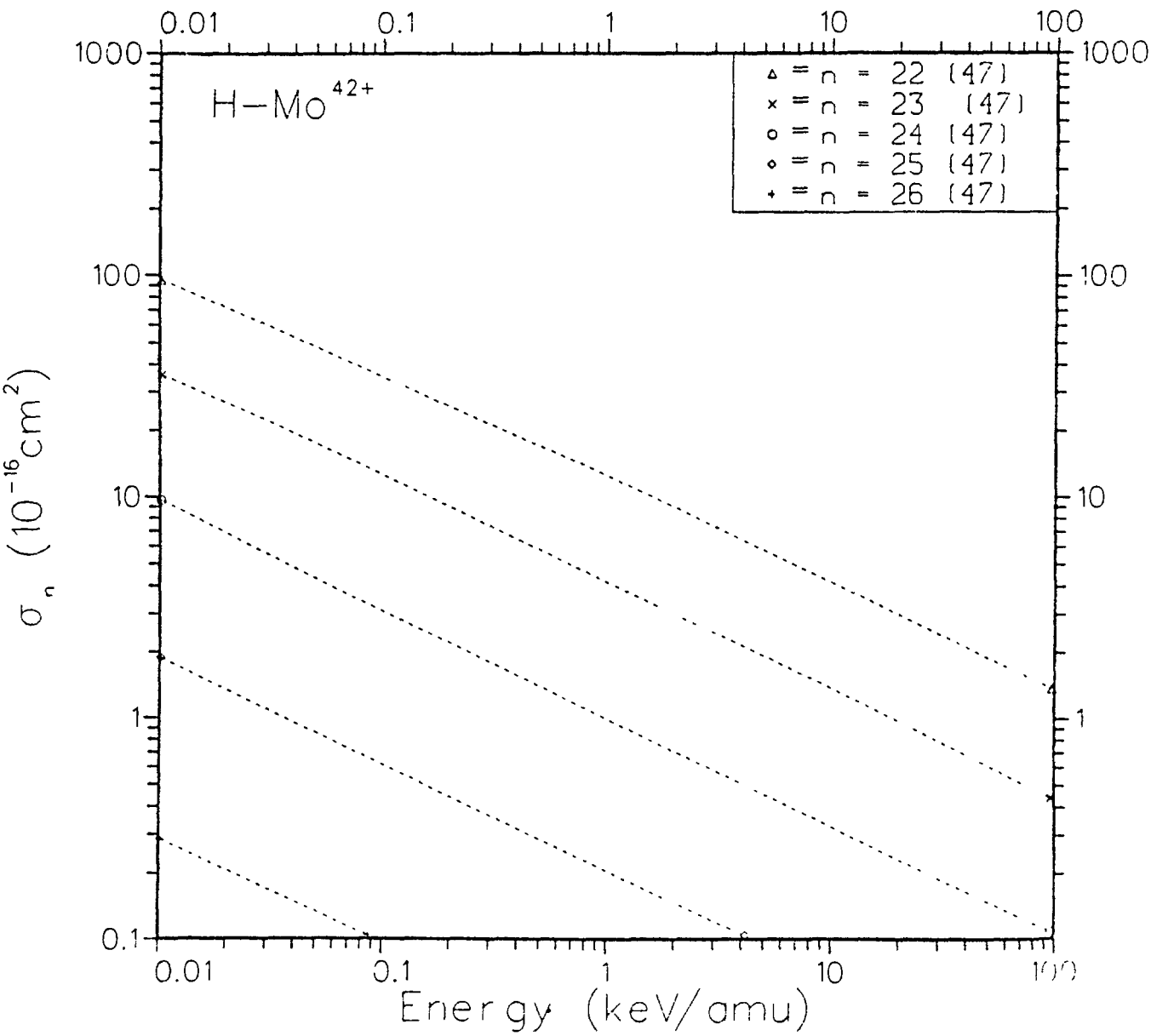

GRAPH SET No. 3

Evaluated total charge exchange cross sections for the hydrogen atom-incompletely stripped ions

Note: References after the symbol in the Legend are given in Appendix B. The reference number, supplemented by a letter E, denotes the reference from which the experimental data have been taken (Appendix B.2).

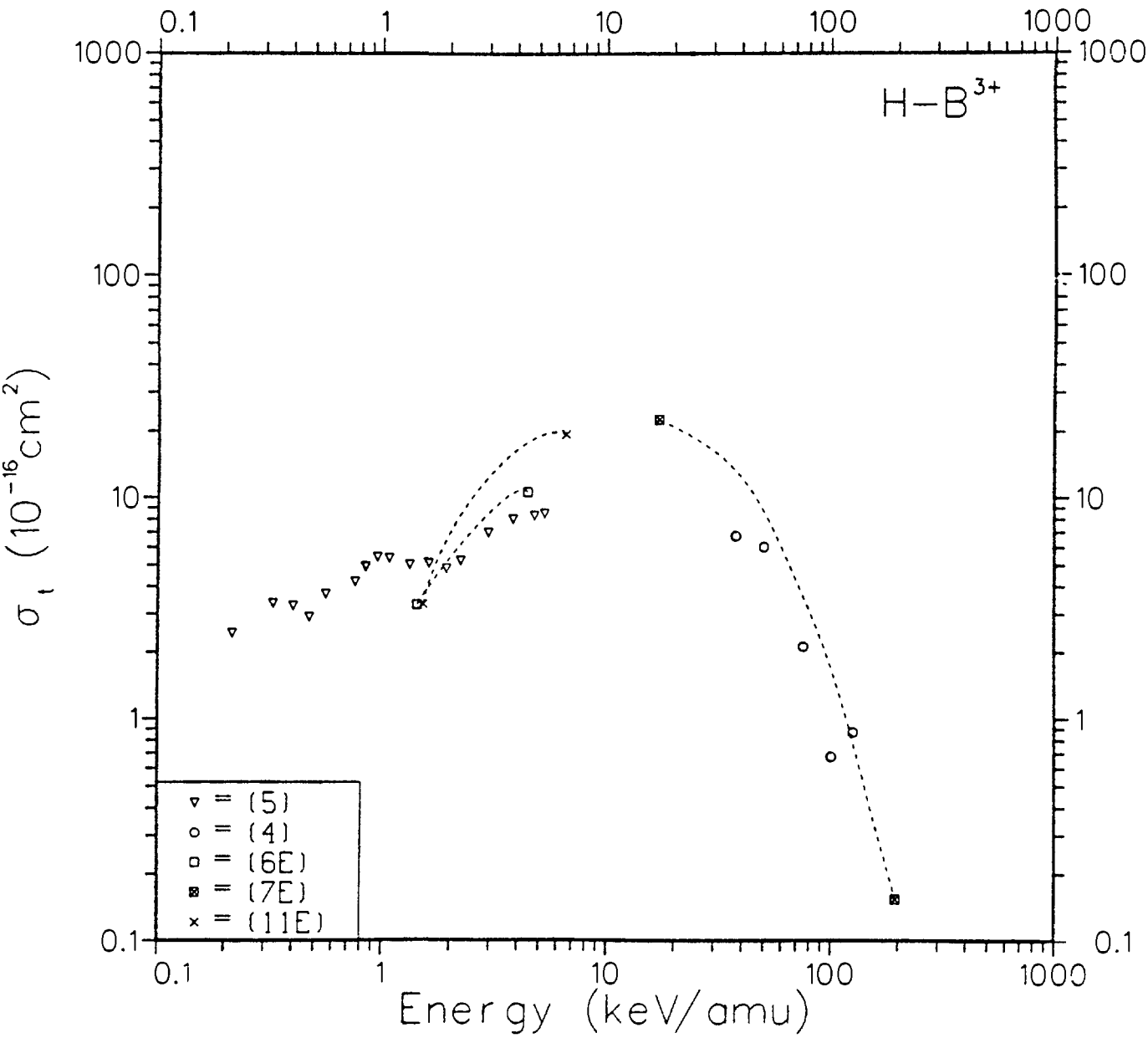
H−B3+
σt (10−16cm2)
Energy (keV/amu)
▽ = (5)
○ = (4)
□ = (6E)
⊠ = (7E)
× = (11E)
0.1
1
10
100
1000

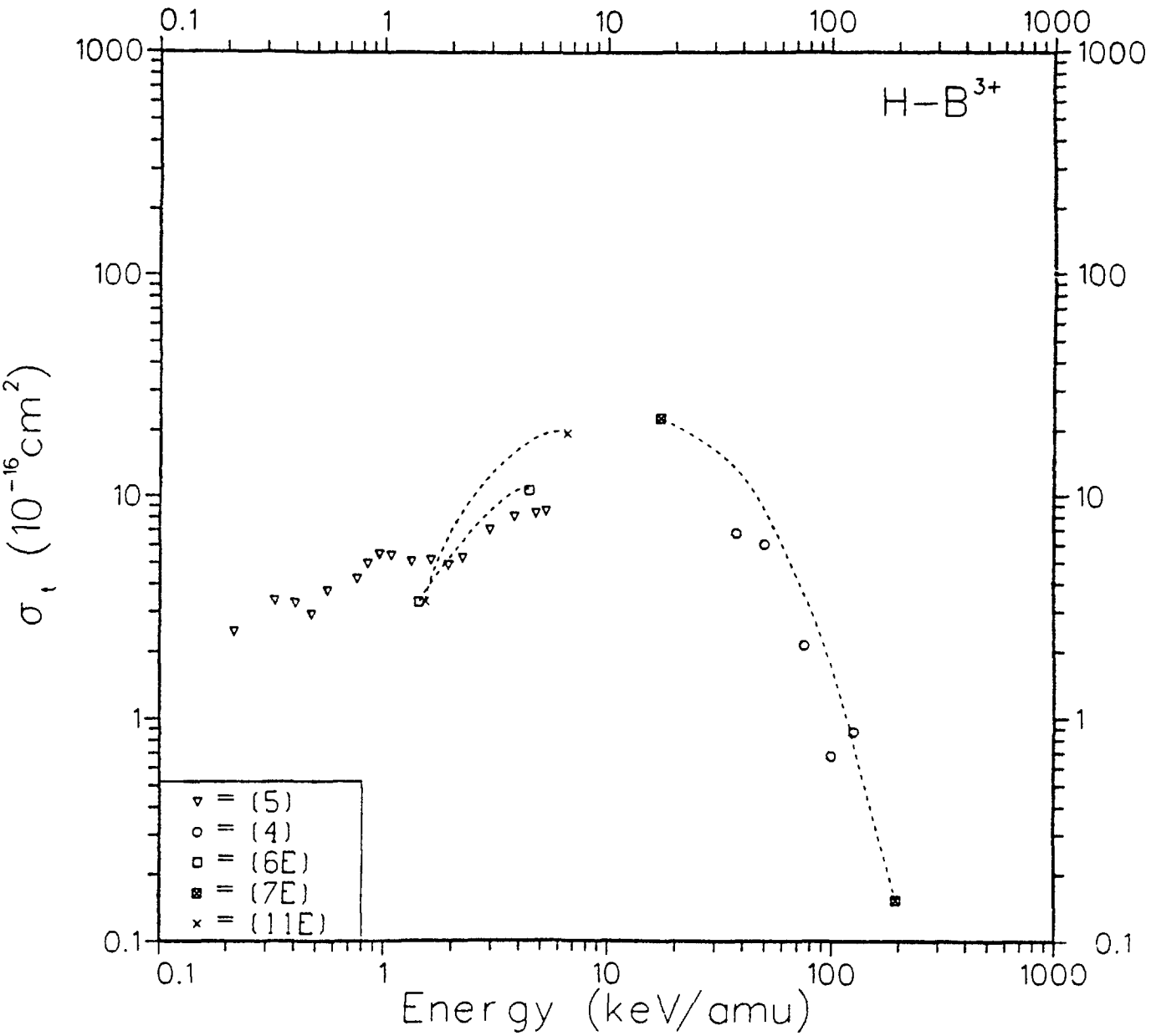
H−B3+
σt (10−16cm2)
Energy (keV/amu)
▽ = (5)
○ = (4)
□ = (6E)
▣ = (7E)
× = (11E)
0.1
1
10
100
1000

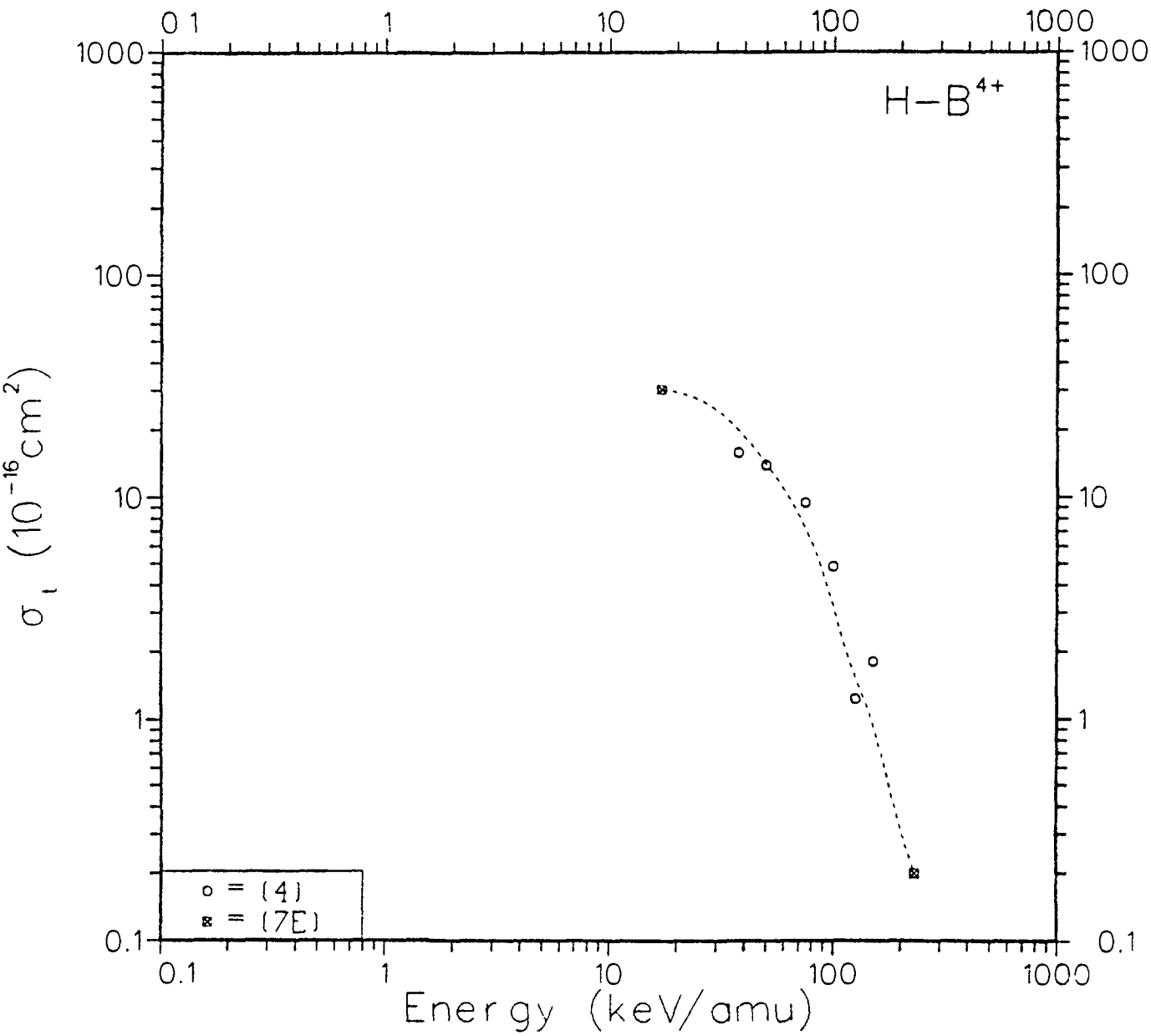
0.1
1
10
100
1000
H−B4+
σt (10−16cm2)
o = (4)
⊠ = (7E)
Energy (keV/amu)

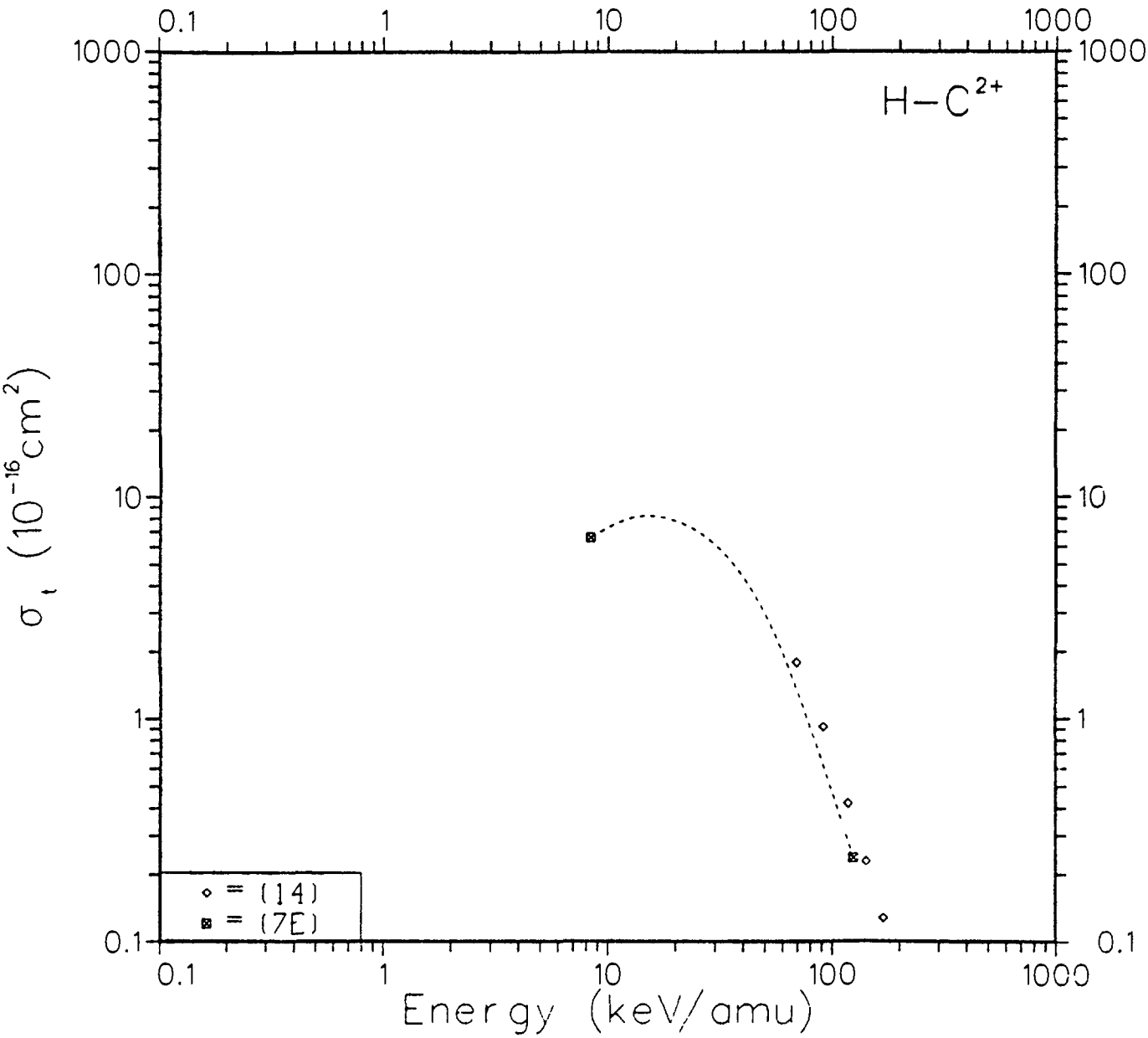
H−C2+
σt (10−16cm2)
Energy (keV/amu)
◇ = (14)
⊠ = (7E)
0.1
1
10
100
1000

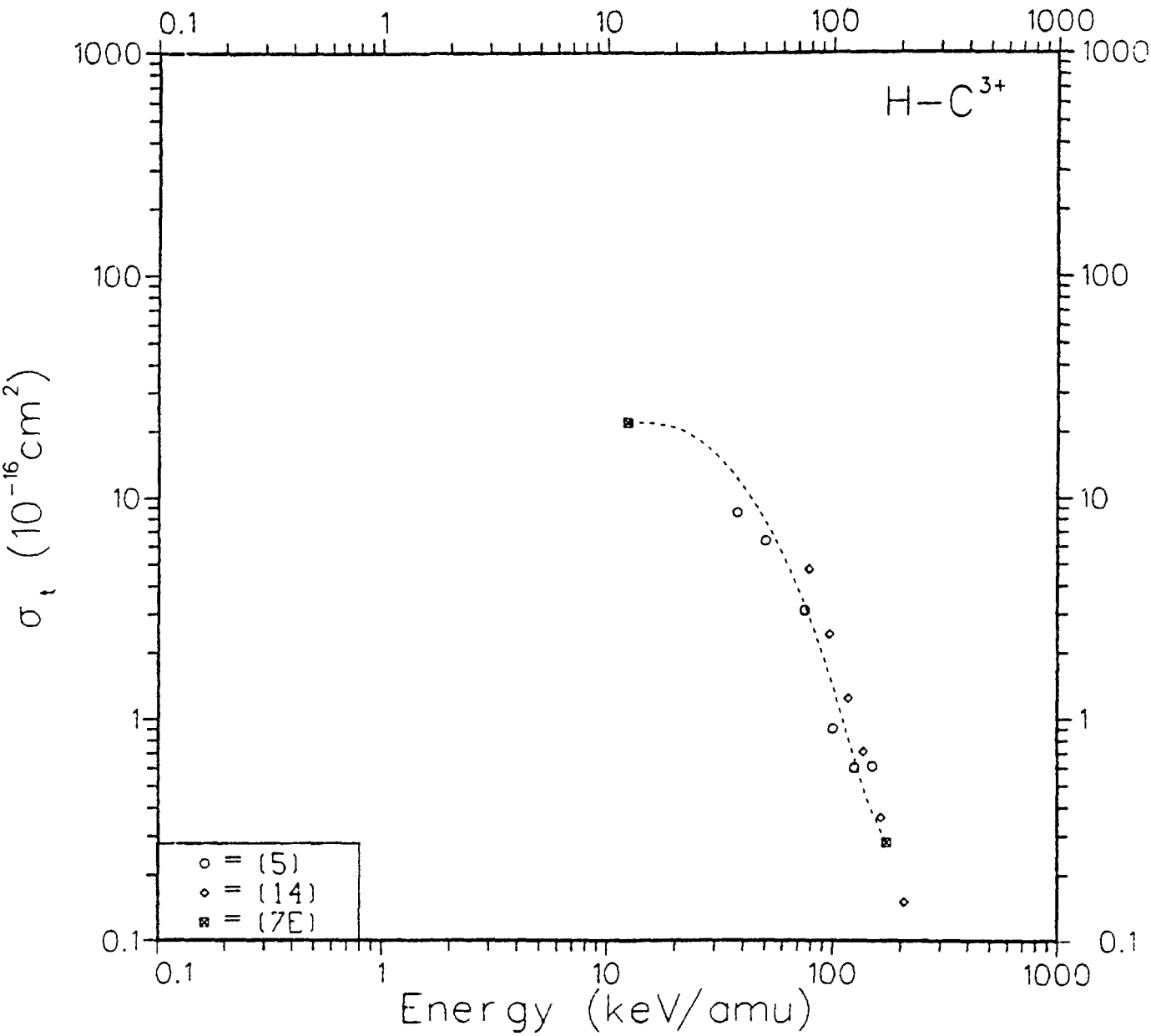
H−C3+
σt (10−16cm2)
Energy (keV/amu)
0.1
1
10
100
1000
○ = (5)
◇ = (14)
⊠ = (7E)

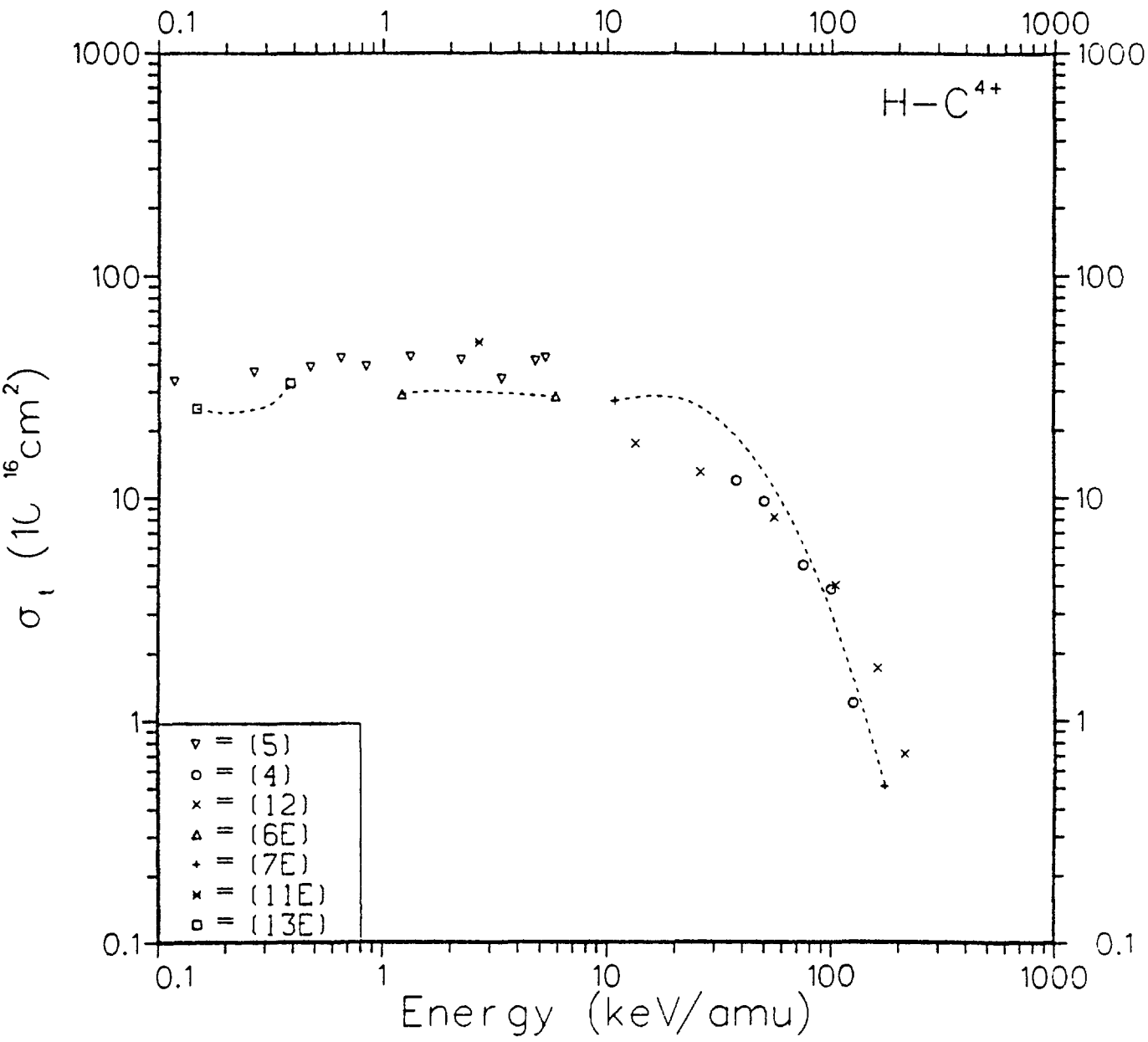
H−C4+
σt (10 16cm2)
Energy (keV/amu)
0.1
1
10
100
1000
▽ = (5)
○ = (4)
× = (12)
△ = (6E)
+ = (7E)
✕ = (11E)
□ = (13E)

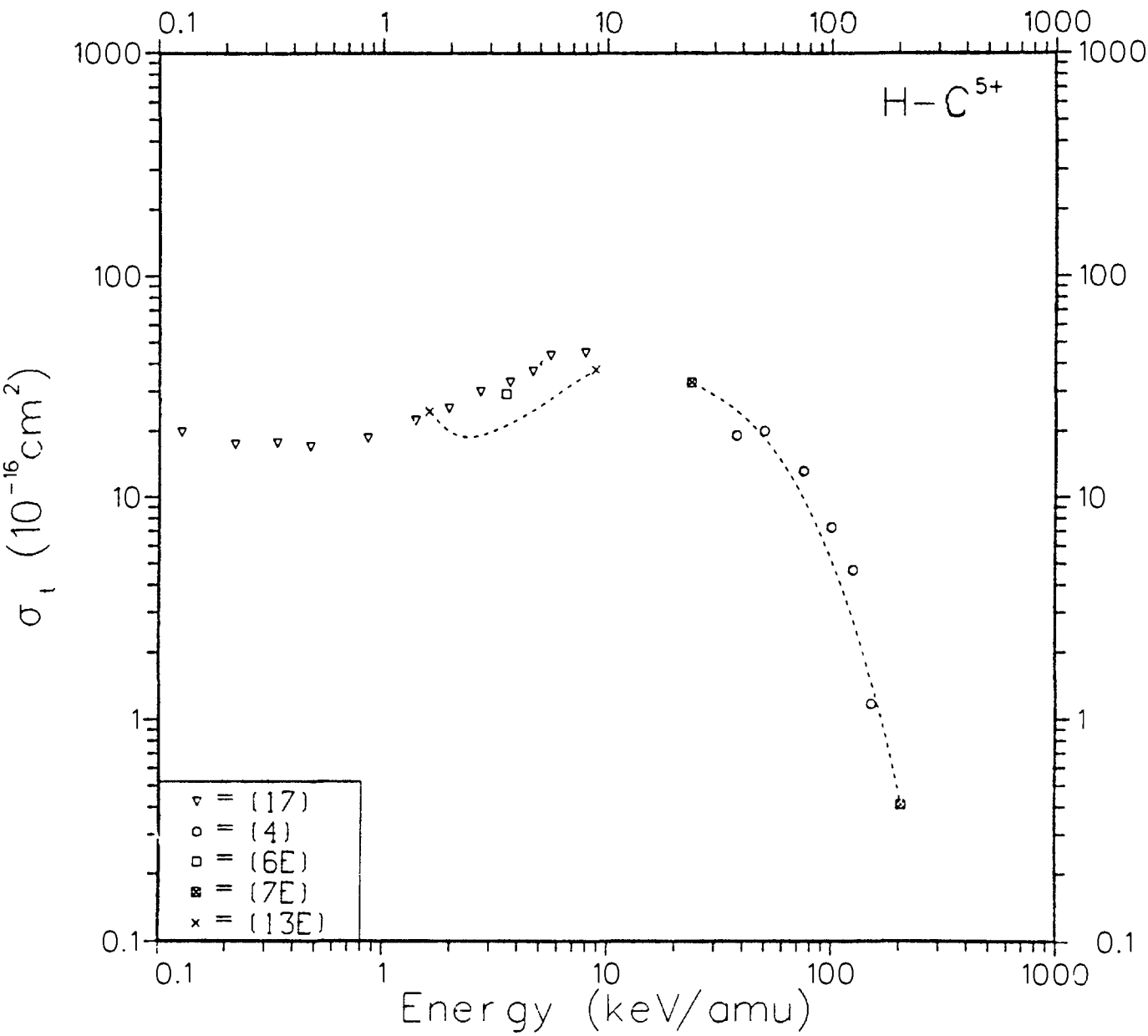
H – C5+
σt (10-16cm2)
Energy (keV/amu)
▽ = (17)
○ = (4)
□ = (6E)
⊠ = (7E)
× = (13E)
0.1
1
10
100
1000

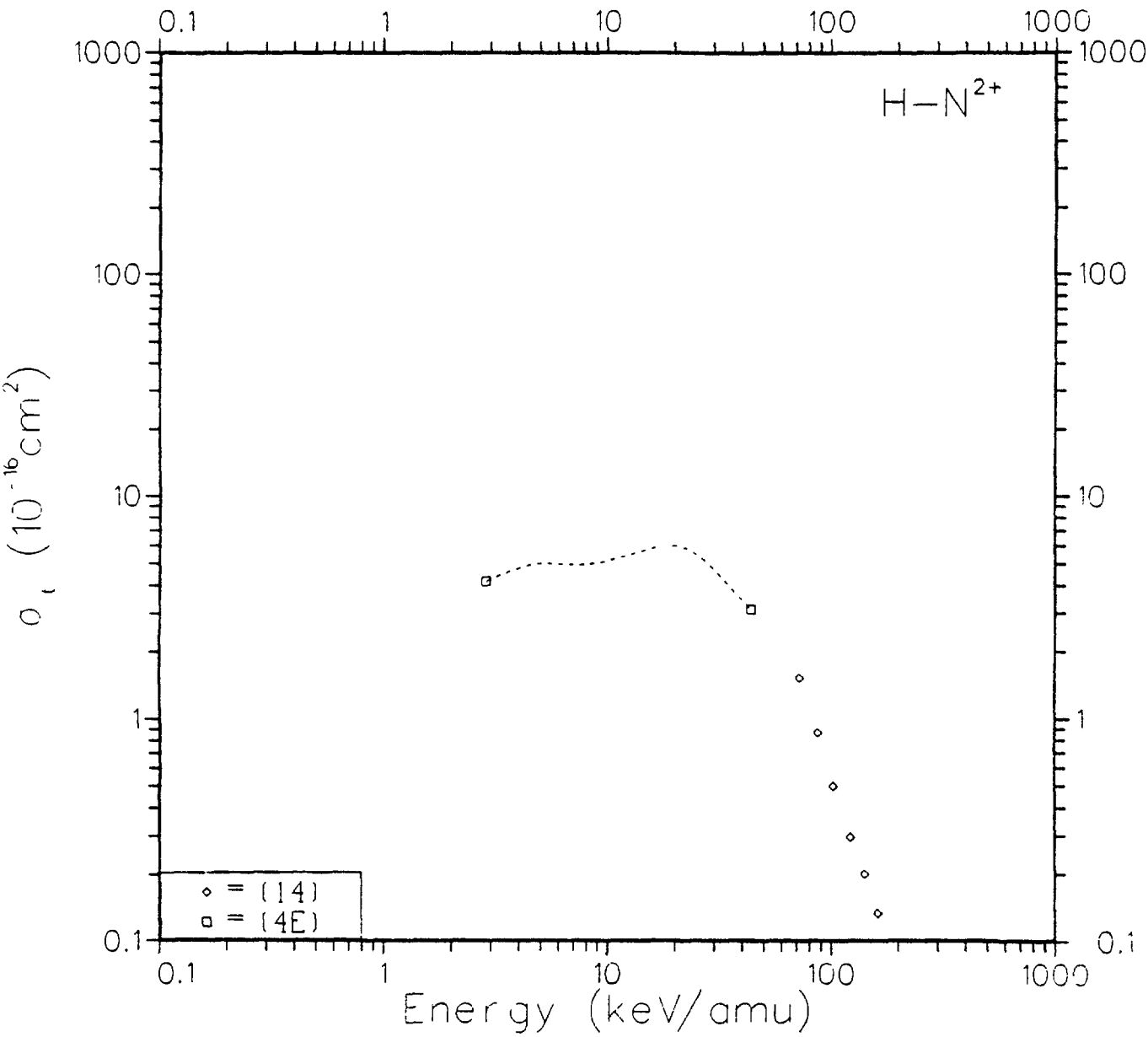
H—N2+
◇ = (14)
□ = (4E)
Energy (keV/amu)
σt (10-16cm2)
0.1
1
10
100
1000

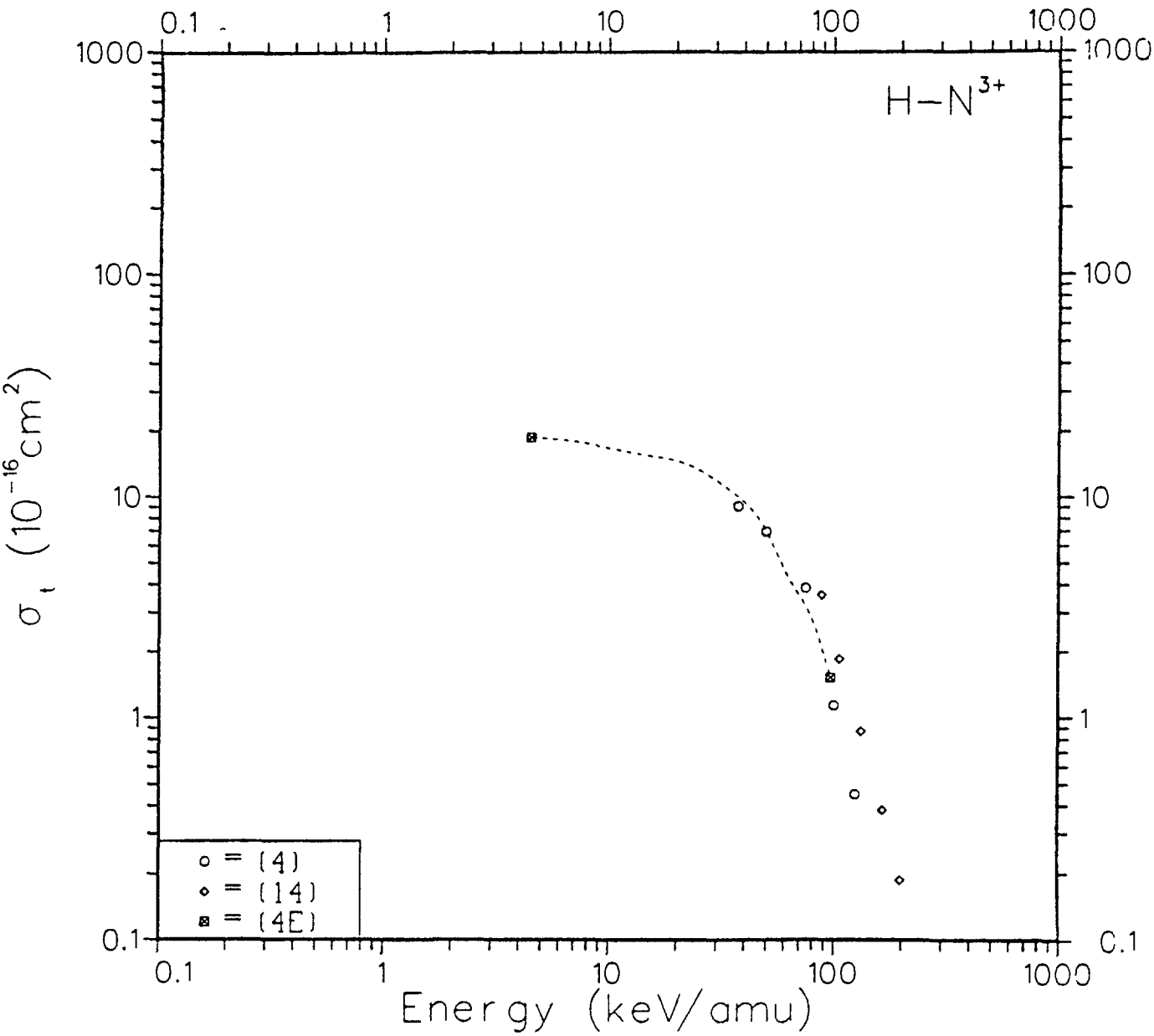
H−N3+
σt (10−16cm2)
Energy (keV/amu)
0.1
1
10
100
1000
o = (4)
◇ = (14)
⊠ = (4E)

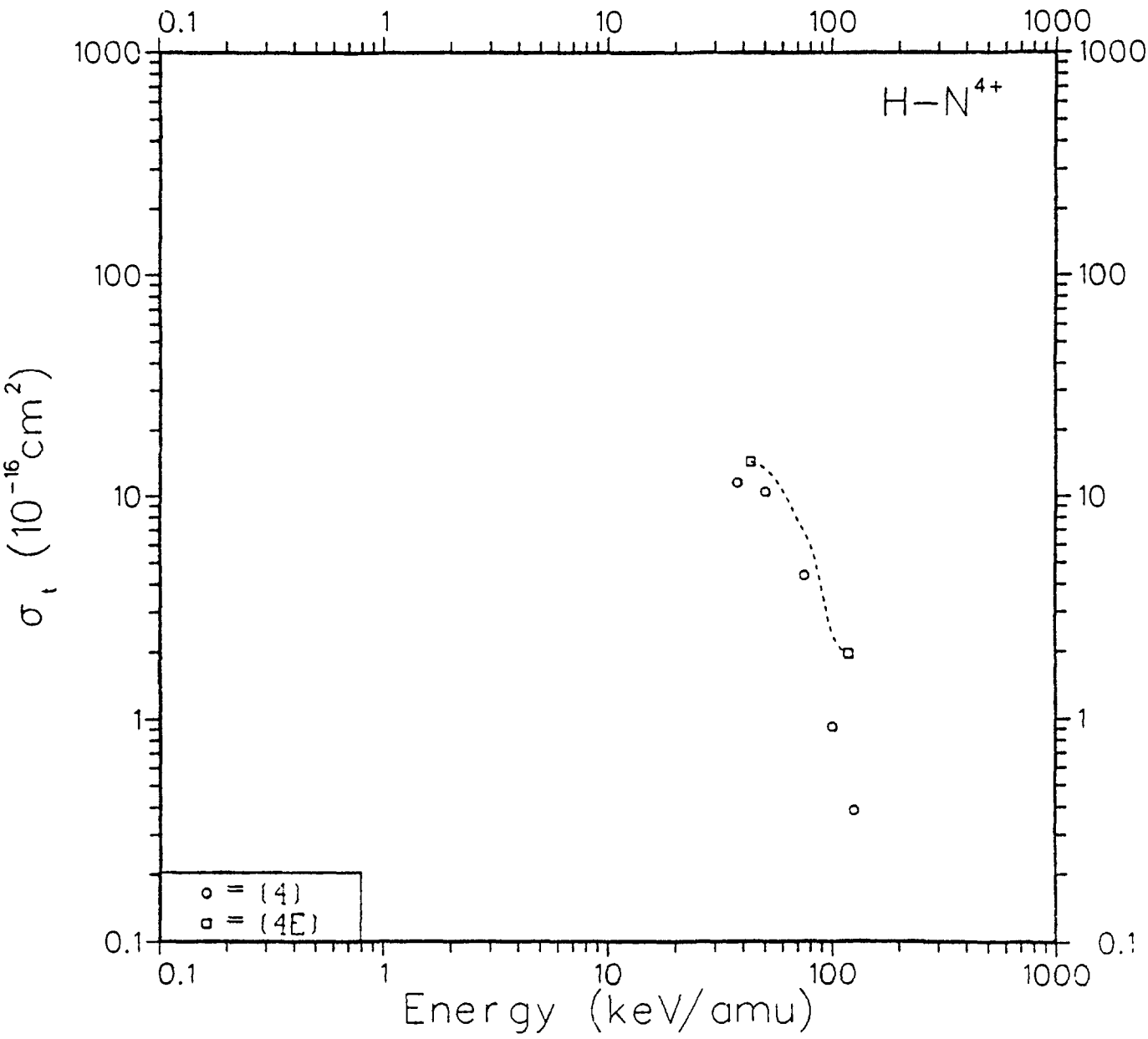
H−N4+
σt (10−16cm2)
Energy (keV/amu)
o = (4)
□ = (4E)
0.1
1
10
100
1000

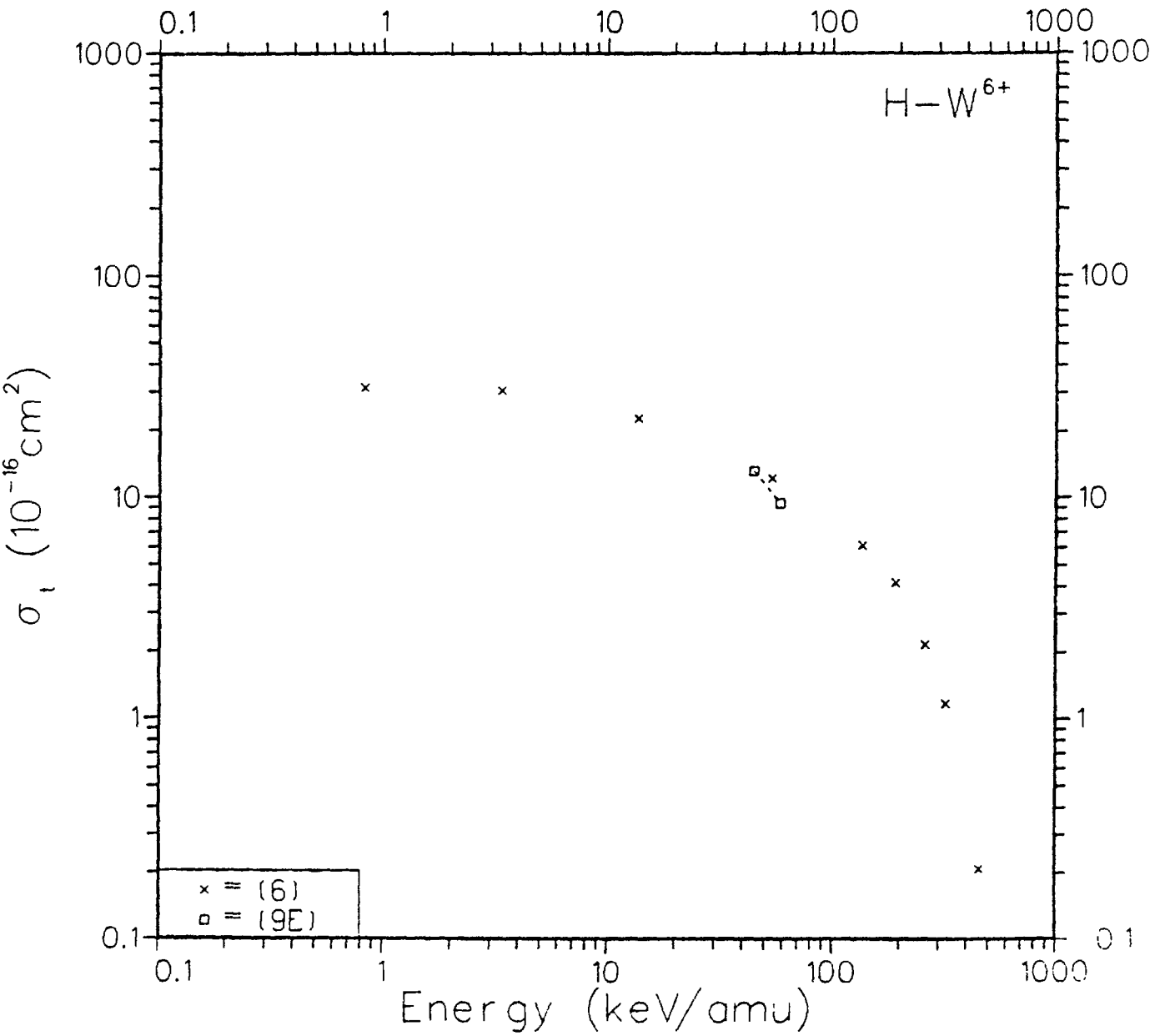
H−W6+
σt (10−16cm2)
Energy (keV/amu)
× = (6)
□ = (9E)
0.1
1
10
100
1000

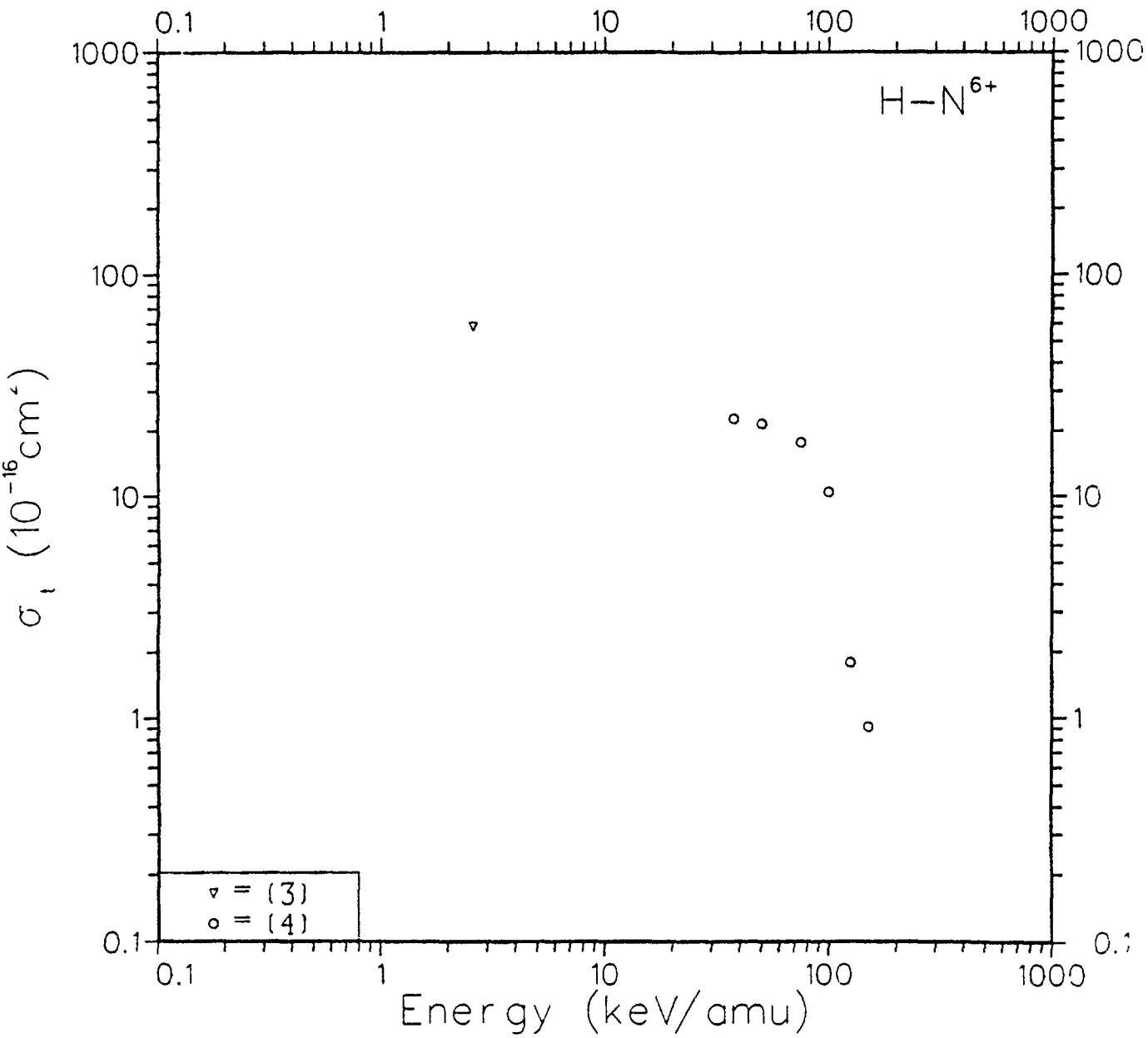
H—N6+
σt (10-16cm2)
Energy (keV/amu)
▽ = (3)
○ = (4)
0.1
1
10
100
1000

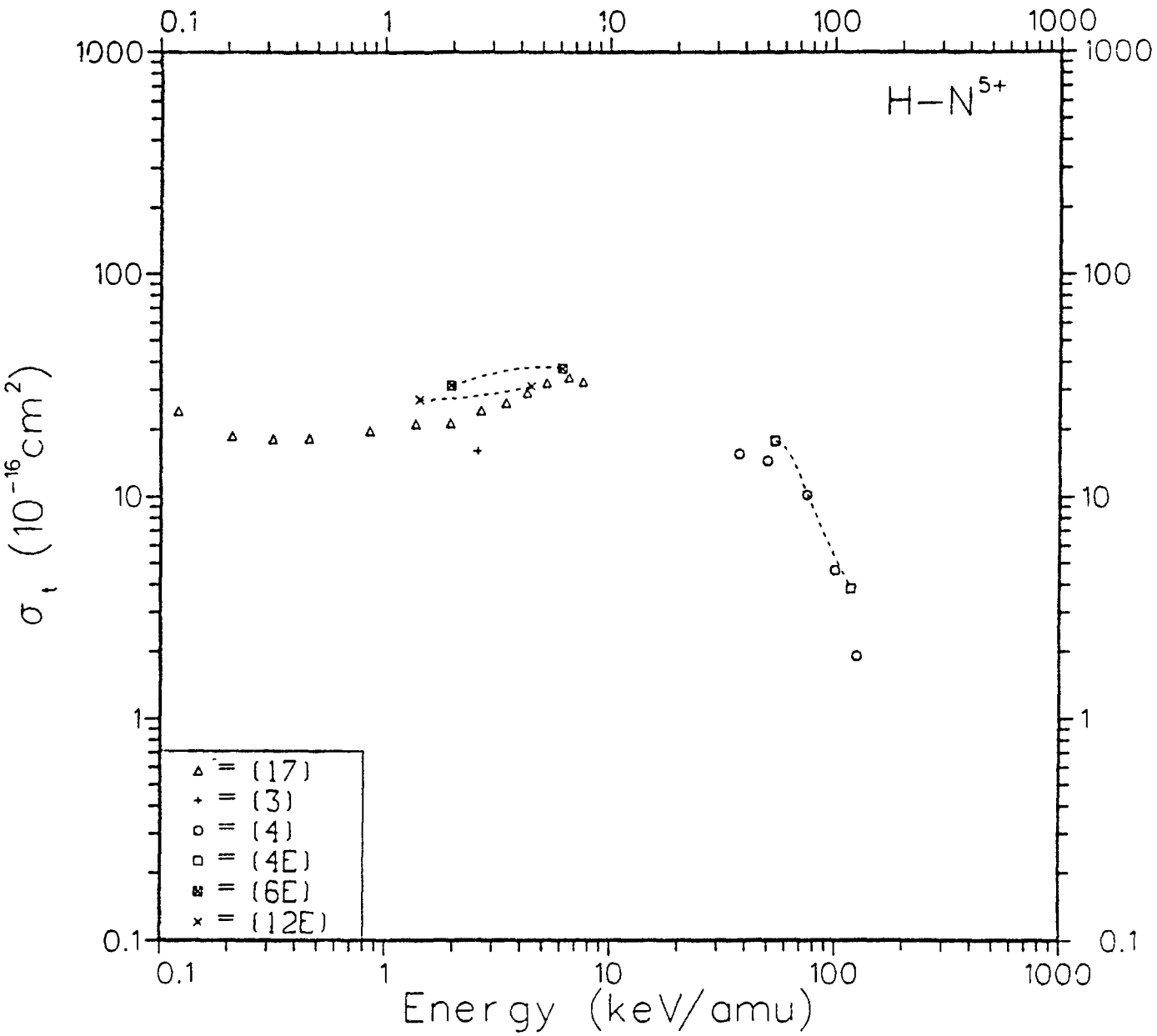
H—N5+
σt (10-16cm2)
Energy (keV/amu)
0.1
1
10
100
1000
Δ = (17)
+ = (3)
o = (4)
□ = (4E)
⊠ = (6E)
× = (12E)

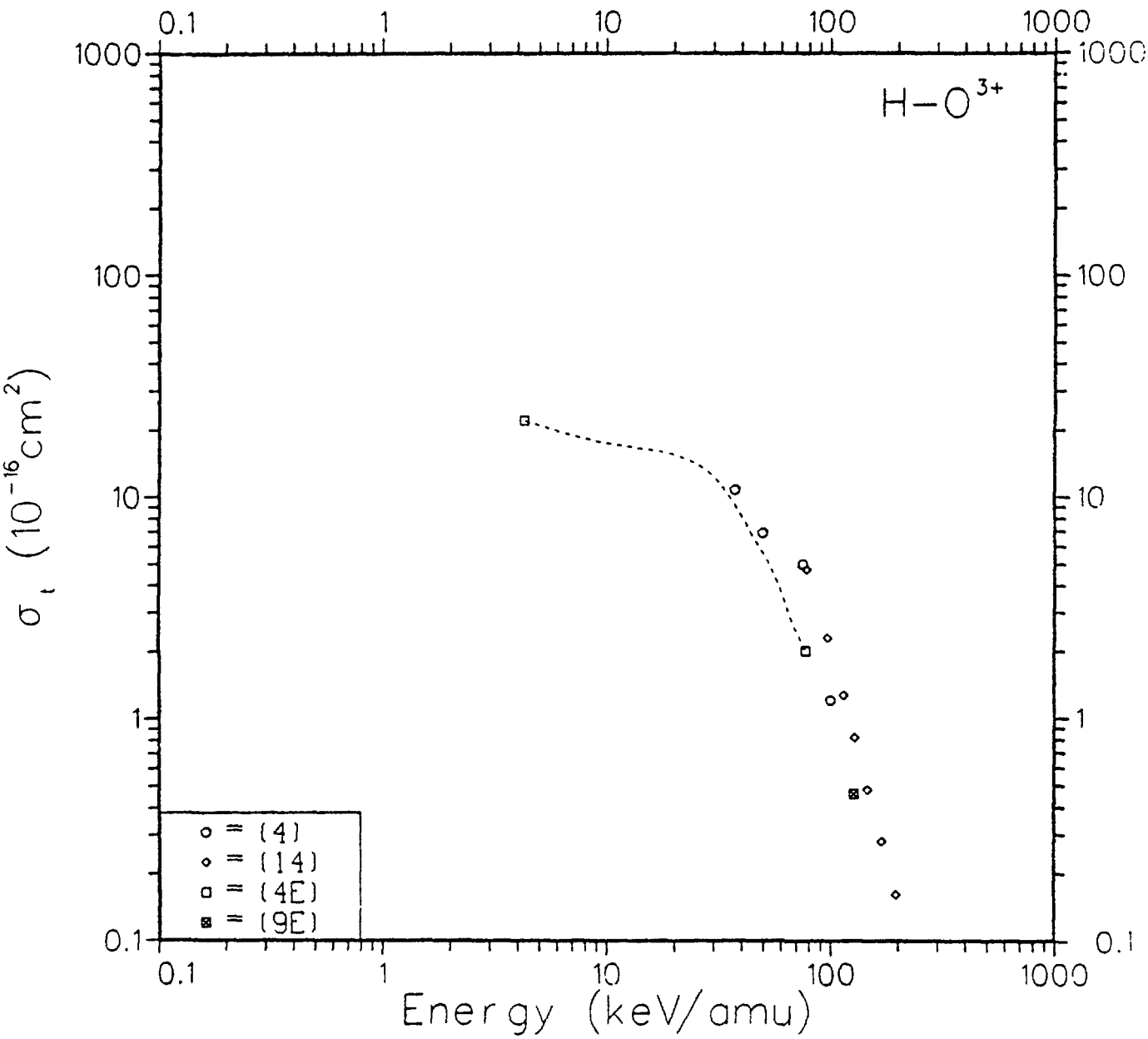
H−O 3+
σ t (10−16cm2)
Energy (keV/amu)
0.1
1
10
100
1000
o = (4)
◇ = (14)
□ = (4E)
▣ = (9E)

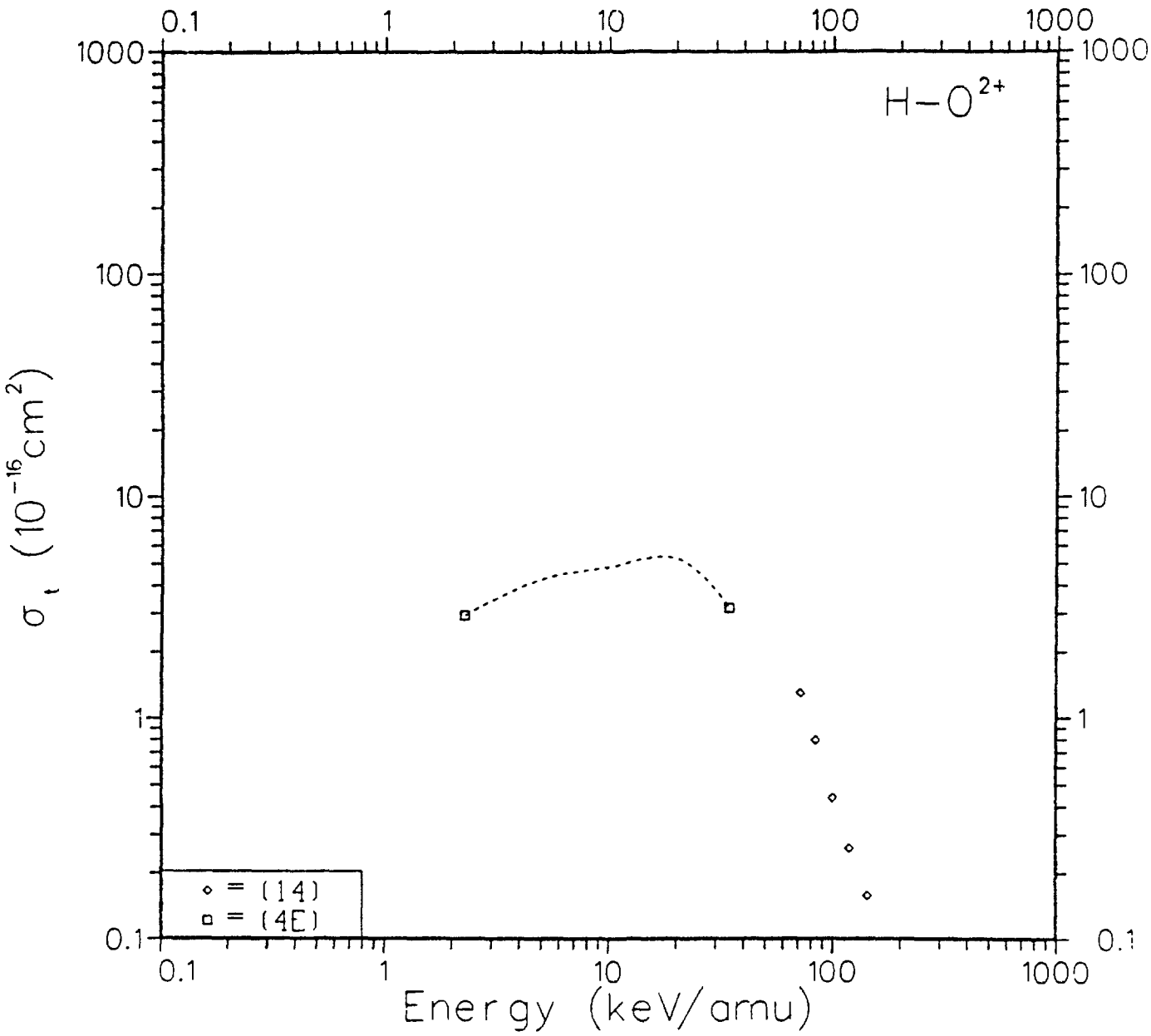
H−O2+
σt (10−16cm2)
Energy (keV/amu)
◇ = (14)
□ = (4E)
0.1
1
10
100
1000

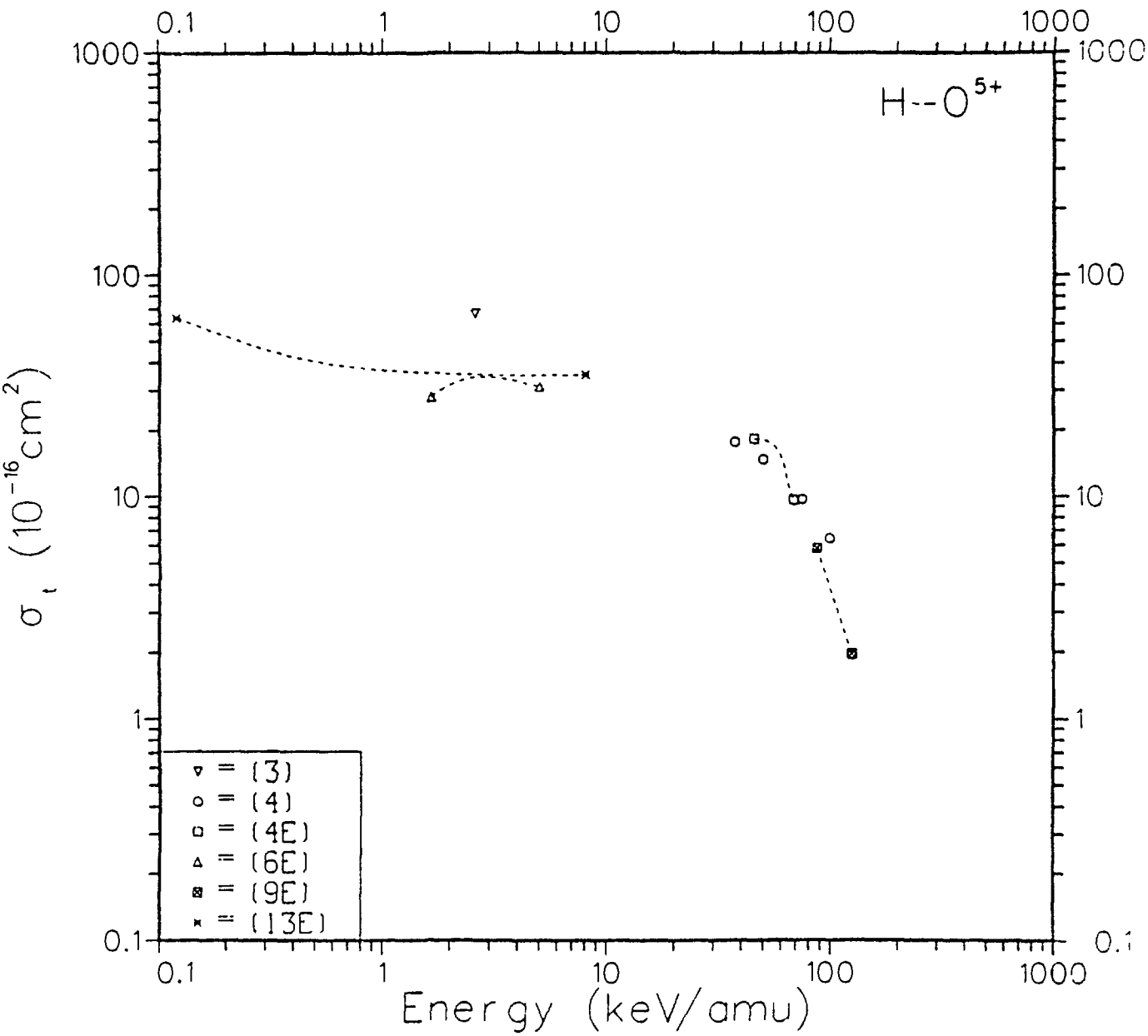
H--O5+
σt (10-16cm2)
Energy (keV/amu)
▽ = (3)
○ = (4)
□ = (4E)
△ = (6E)
⊠ = (9E)
× = (13E)
0.1
1
10
100
1000

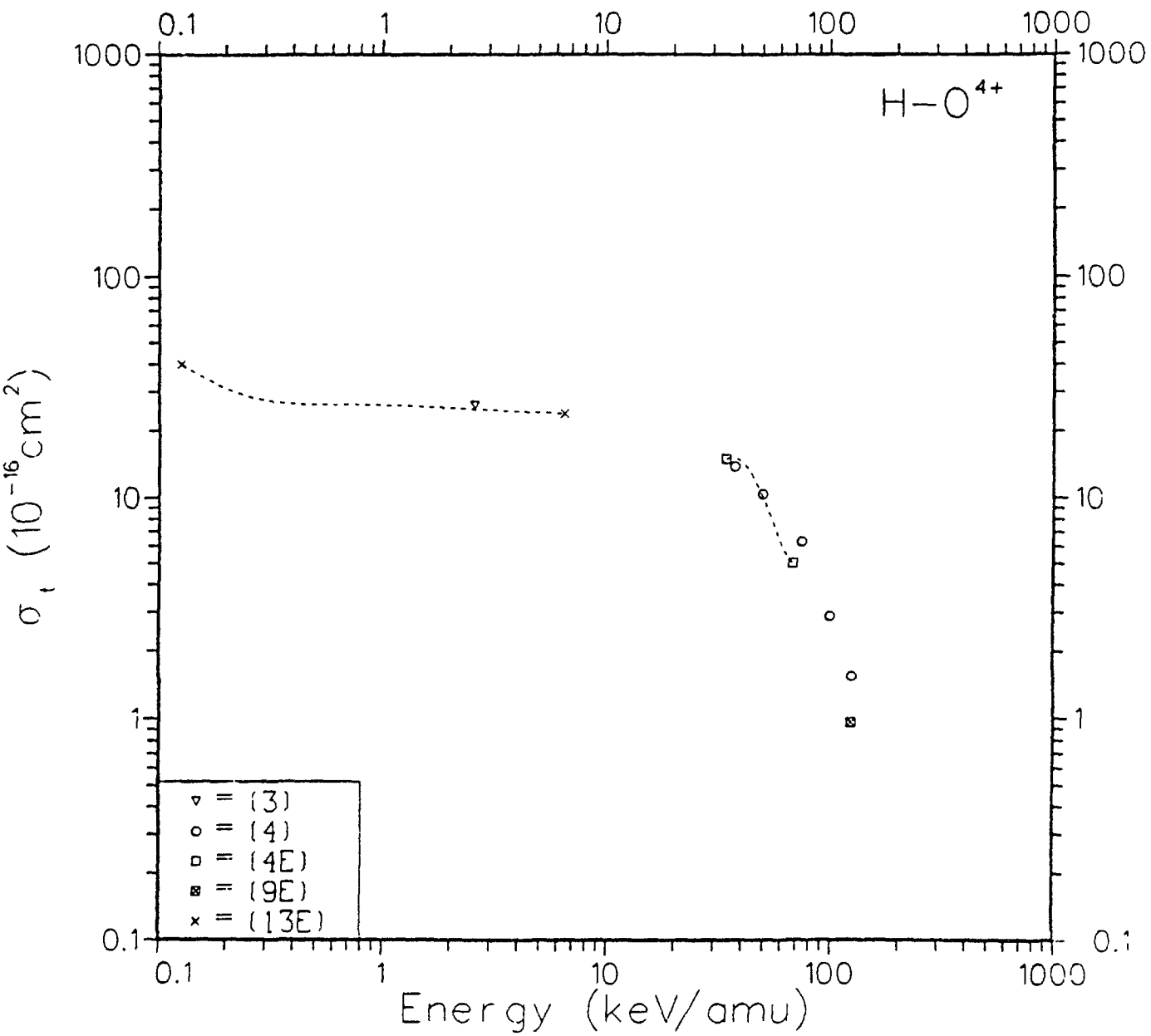
H−O4+
σt (10−16cm2)
Energy (keV/amu)
▽ = (3)
○ = (4)
□ = (4E)
⊠ = (9E)
× = (13E)
0.1
1
10
100
1000

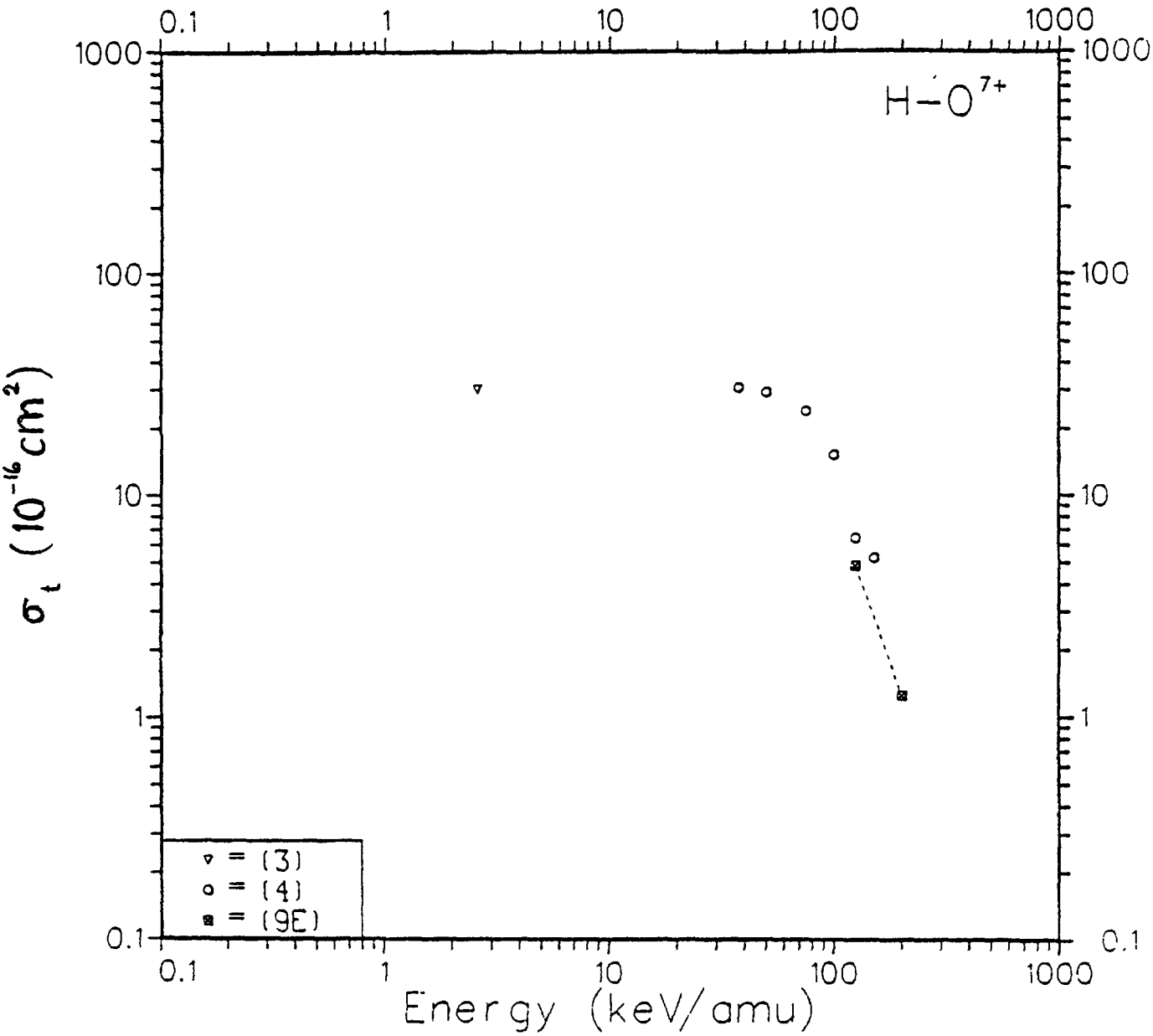
H−O7+
σt (10−16cm2)
Energy (keV/amu)
▽ = (3)
○ = (4)
▣ = (9E)
0.1
1
10
100
1000

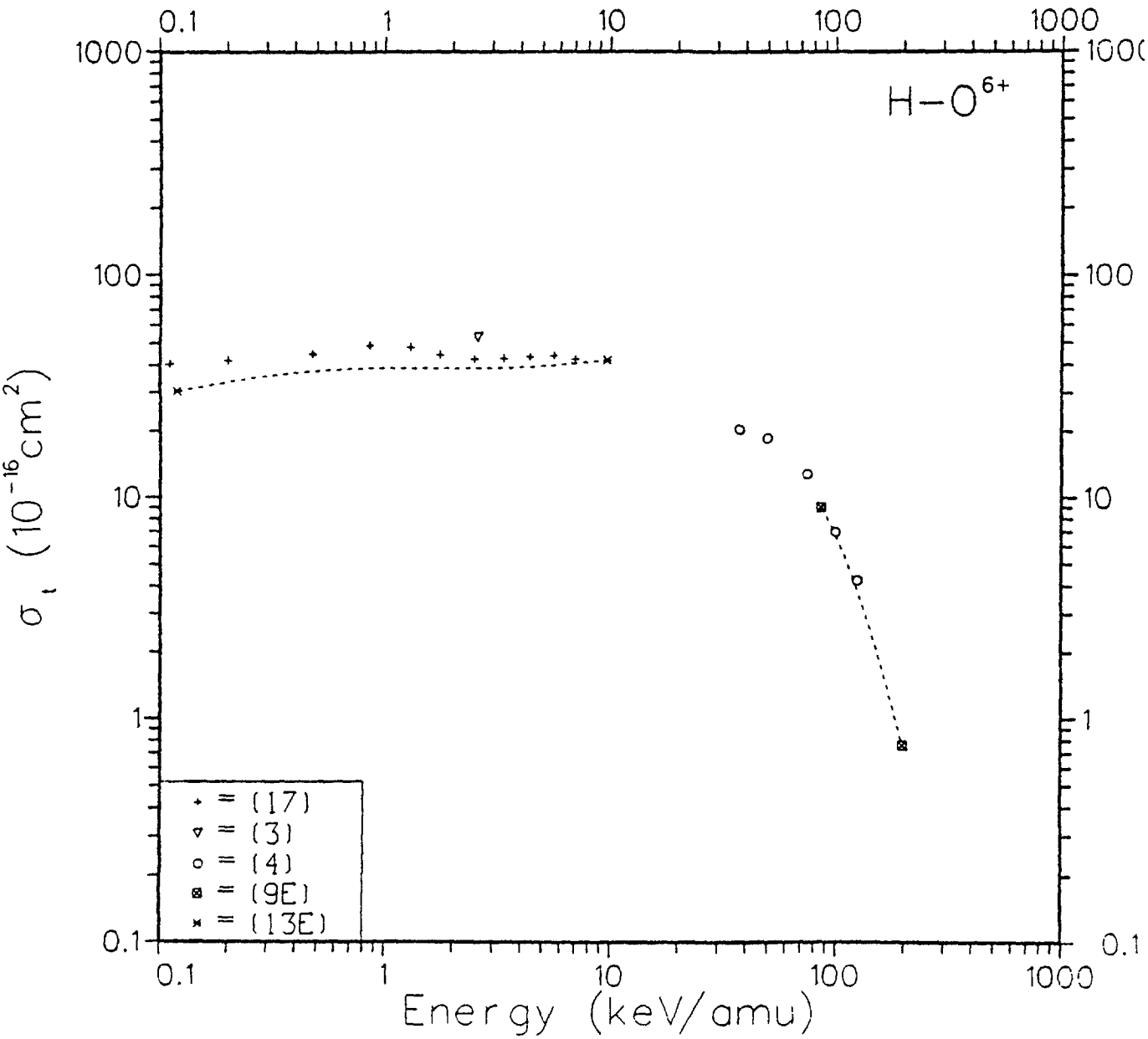
H−O6+
σt (10−16cm2)
Energy (keV/amu)
0.1
1
10
100
1000
+ = (17)
▽ = (3)
○ = (4)
⊠ = (9E)
× = (13E)

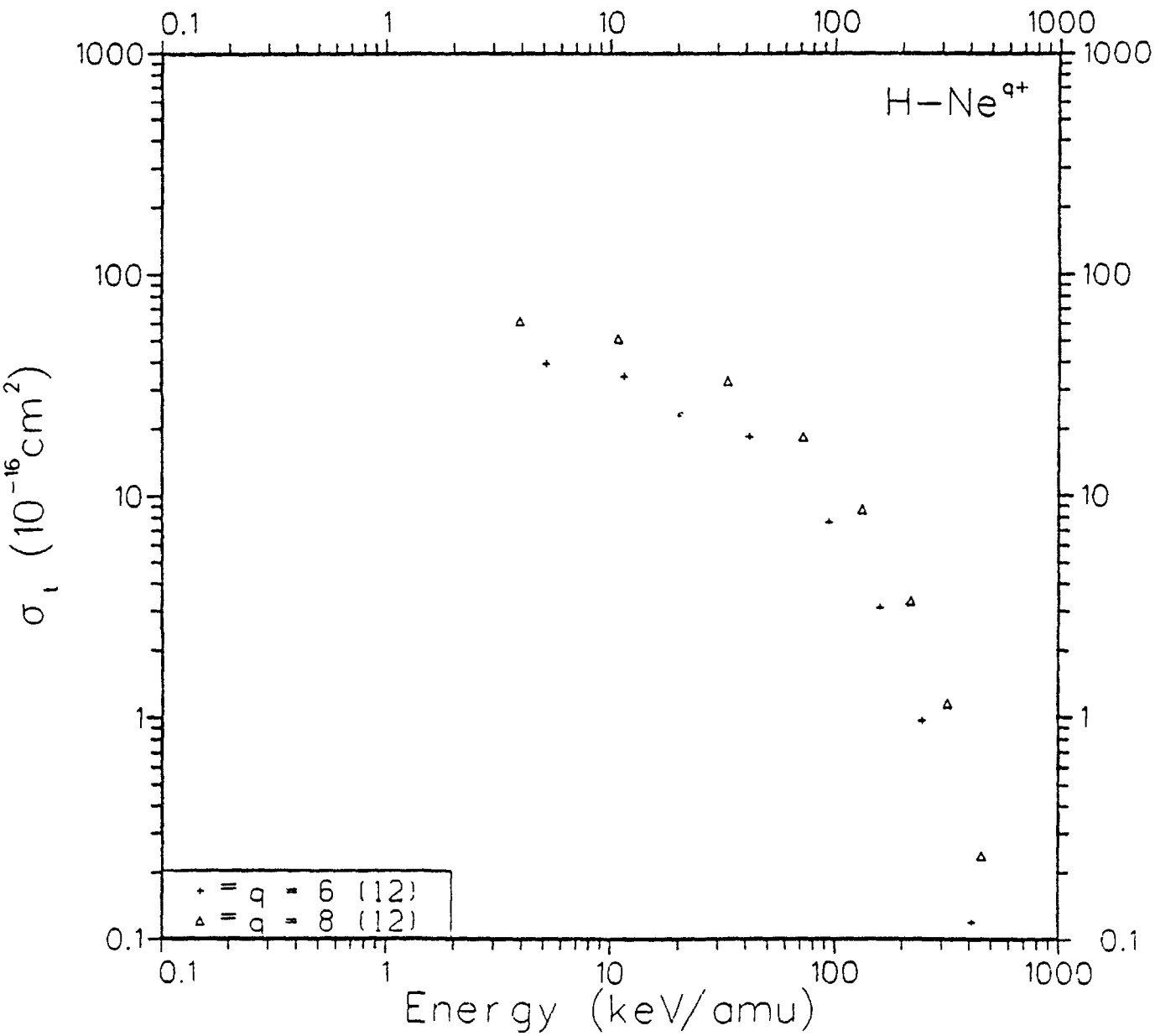
H−Ne^q+
σ_t (10^-16 cm^2)
Energy (keV/amu)
+ = q = 6 (12)
△ = q = 8 (12)
0.1
1
10
100
1000

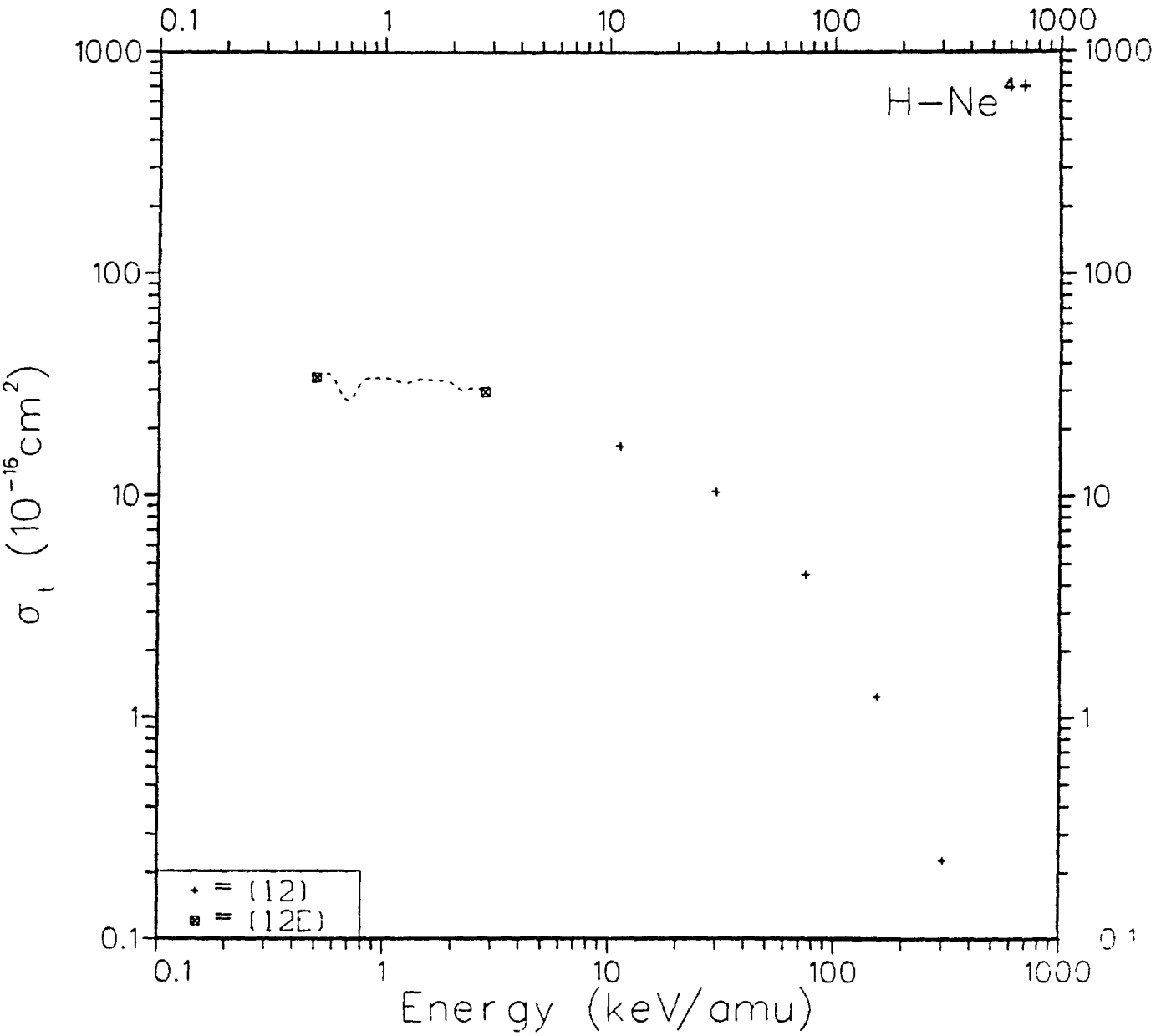
H–Ne4+
σt (10-16cm2)
Energy (keV/amu)
+ = (12)
⊠ = (12E)
0.1
1
10
100
1000

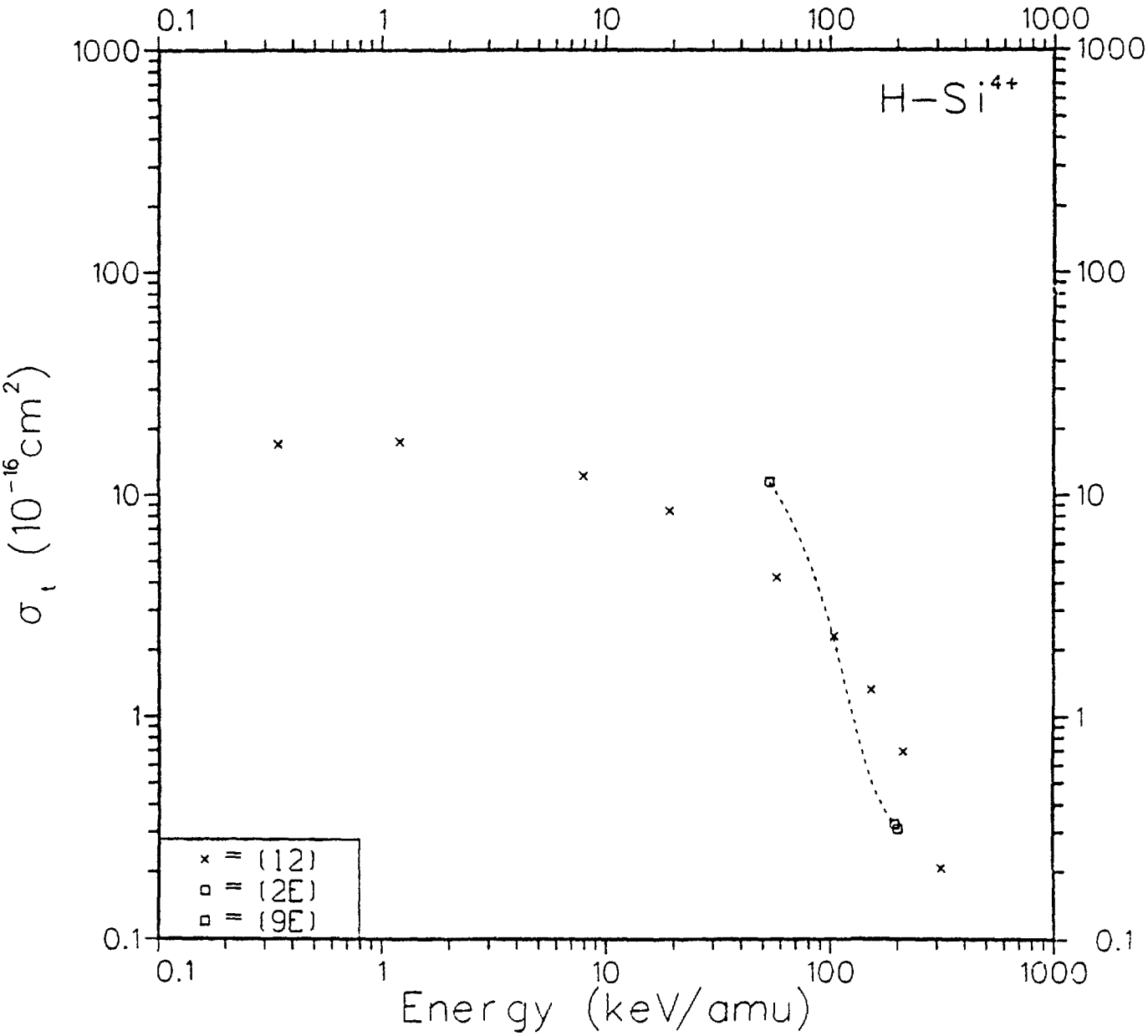
H–Si4+
× = (12)
□ = (2E)
□ = (9E)
σt (10-16cm2)
Energy (keV/amu)
0.1
1
10
100
1000

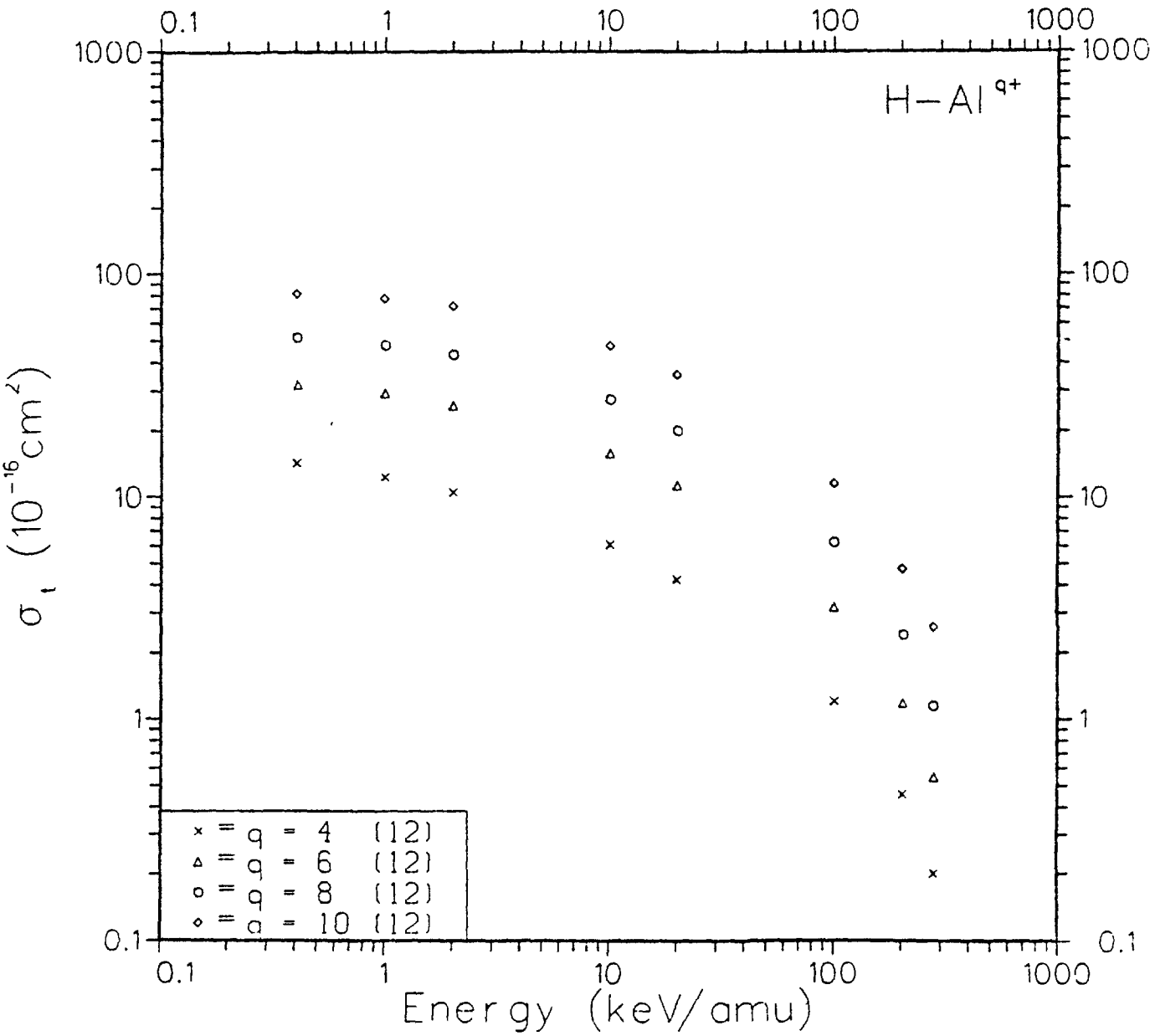
H–Al q+
σt (10-16cm2)
Energy (keV/amu)
0.1
1
10
100
1000
× = q = 4 (12)
△ = q = 6 (12)
○ = q = 8 (12)
◇ = q = 10 (12)

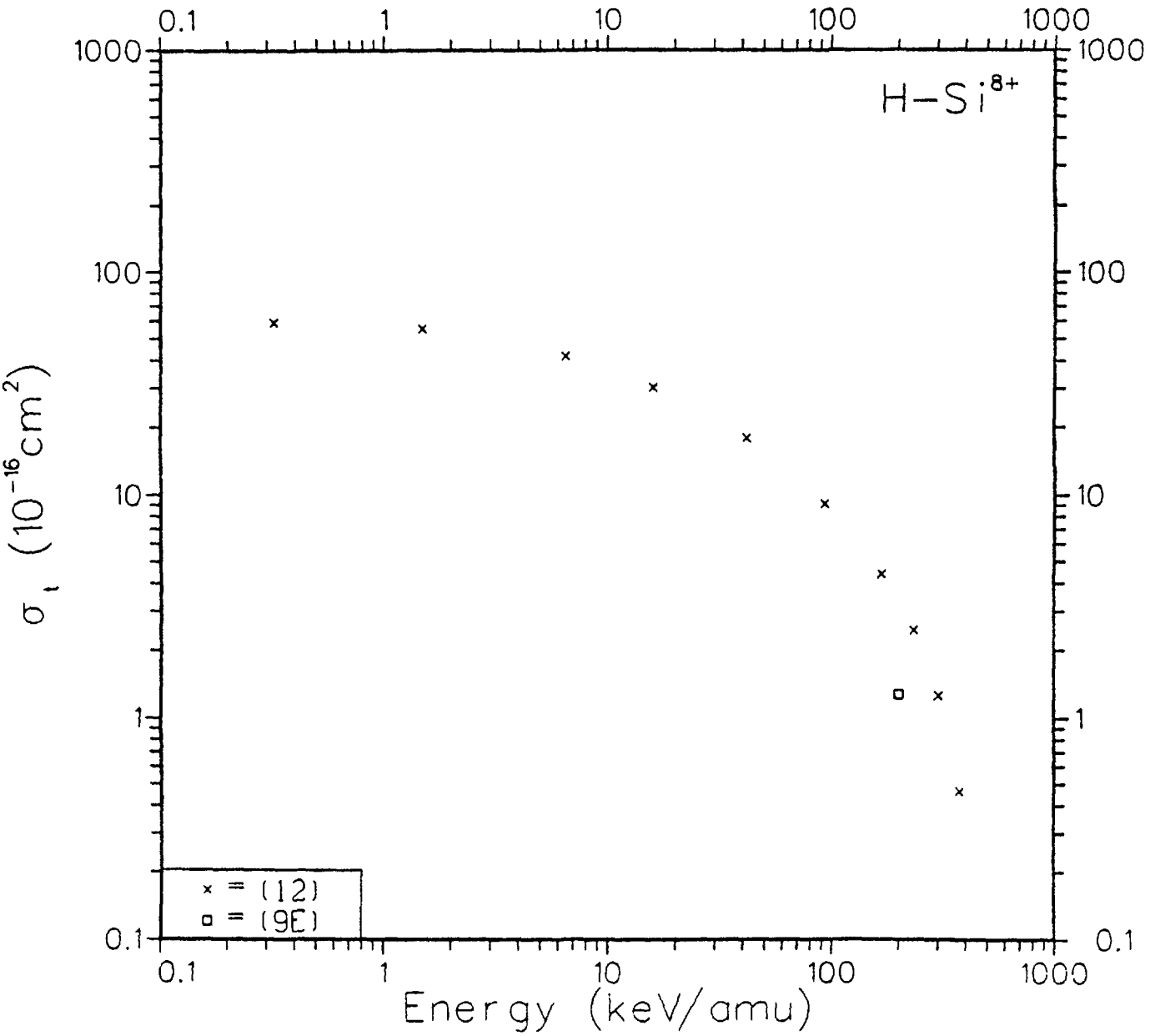
H–Si^{8+}
σ_t (10^{-16}cm^2)
Energy (keV/amu)
× = (12)
□ = (9E)
0.1
1
10
100
1000

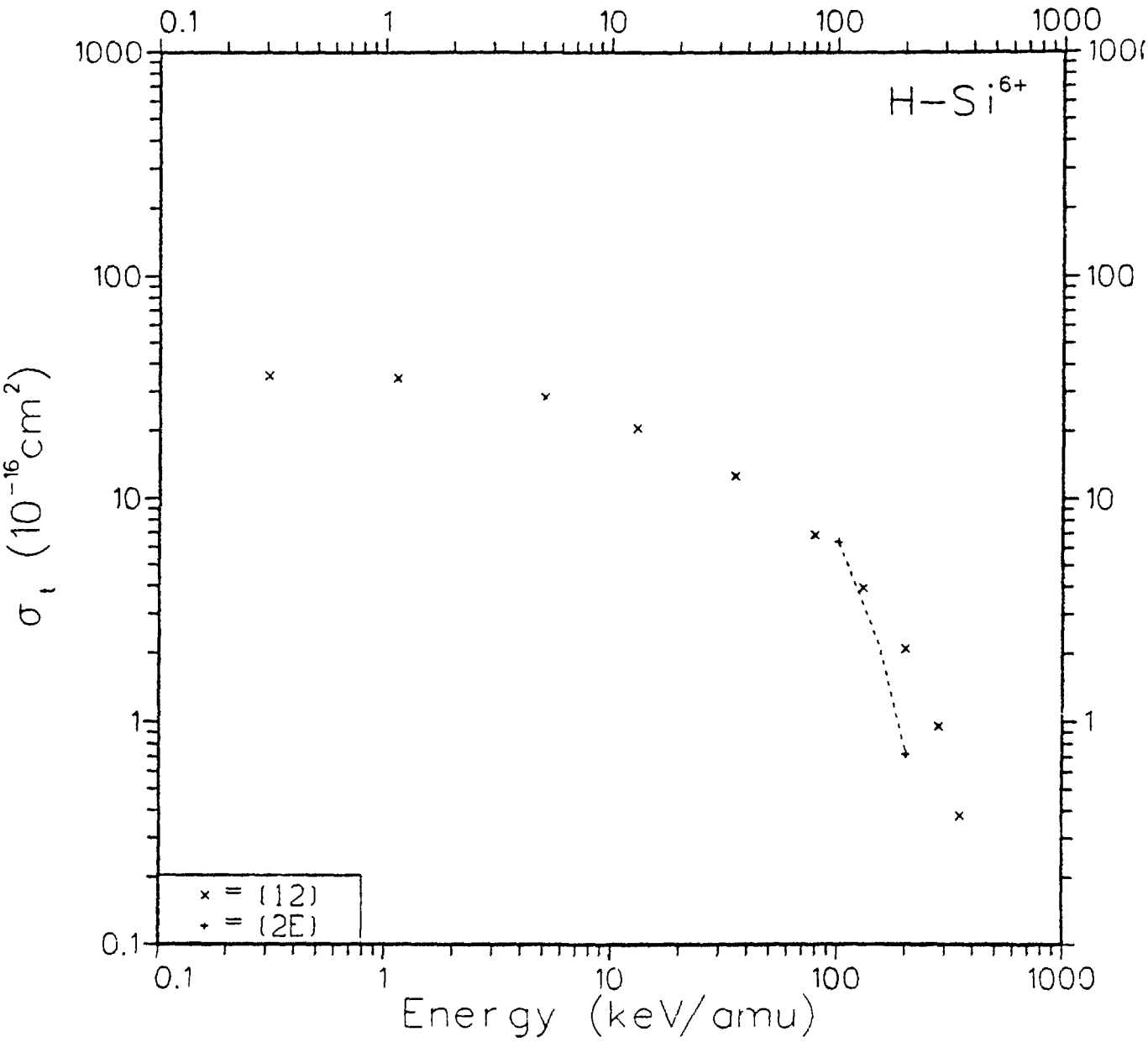
H−Si6+
σt (10−16cm2)
Energy (keV/amu)
× = (12)
+ = (2E)
0.1
1
10
100
1000

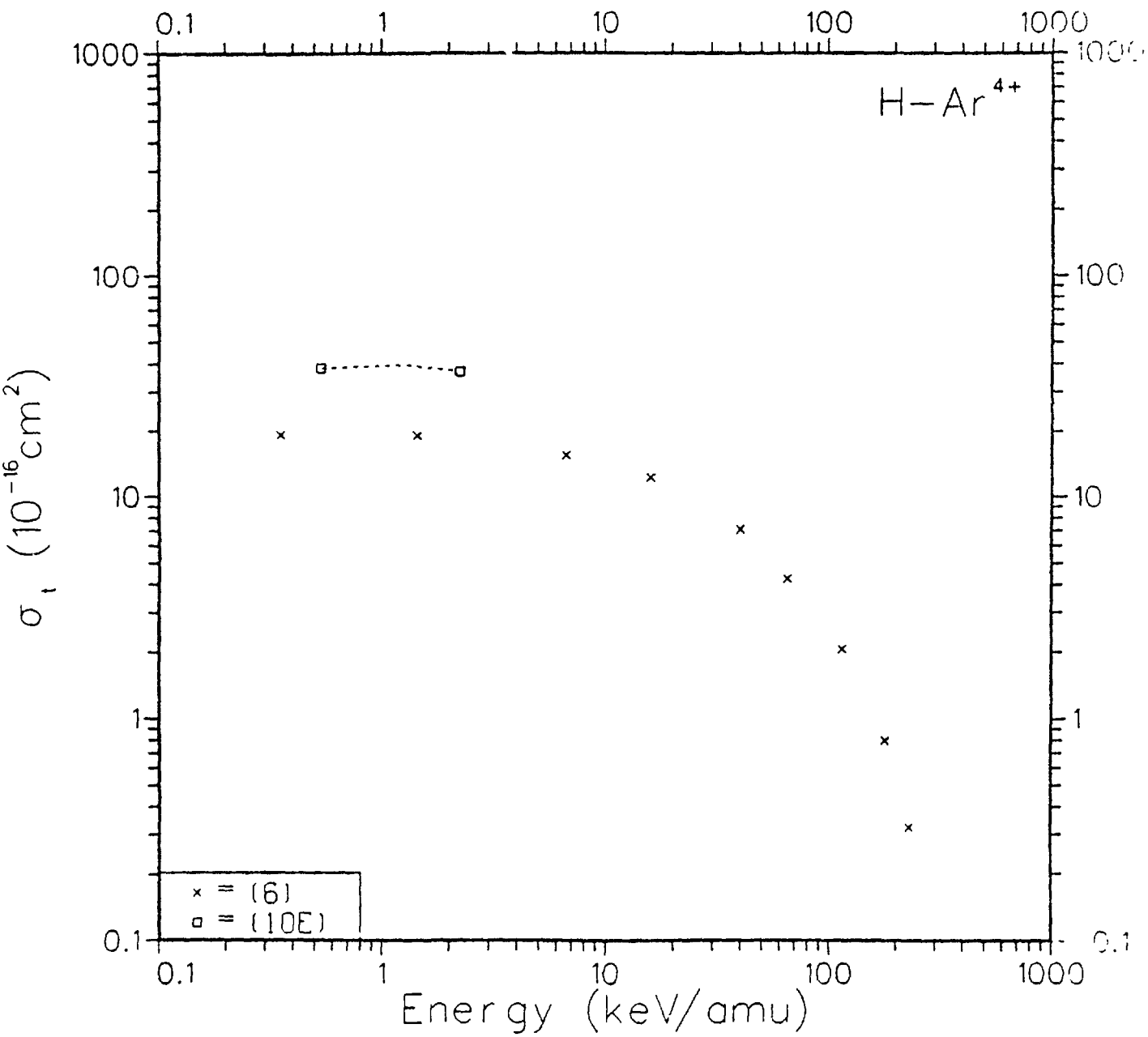
H−Ar4+
σt (10−16cm2)
Energy (keV/amu)
× = (6)
□ = (10E)
0.1
1
10
100
1000

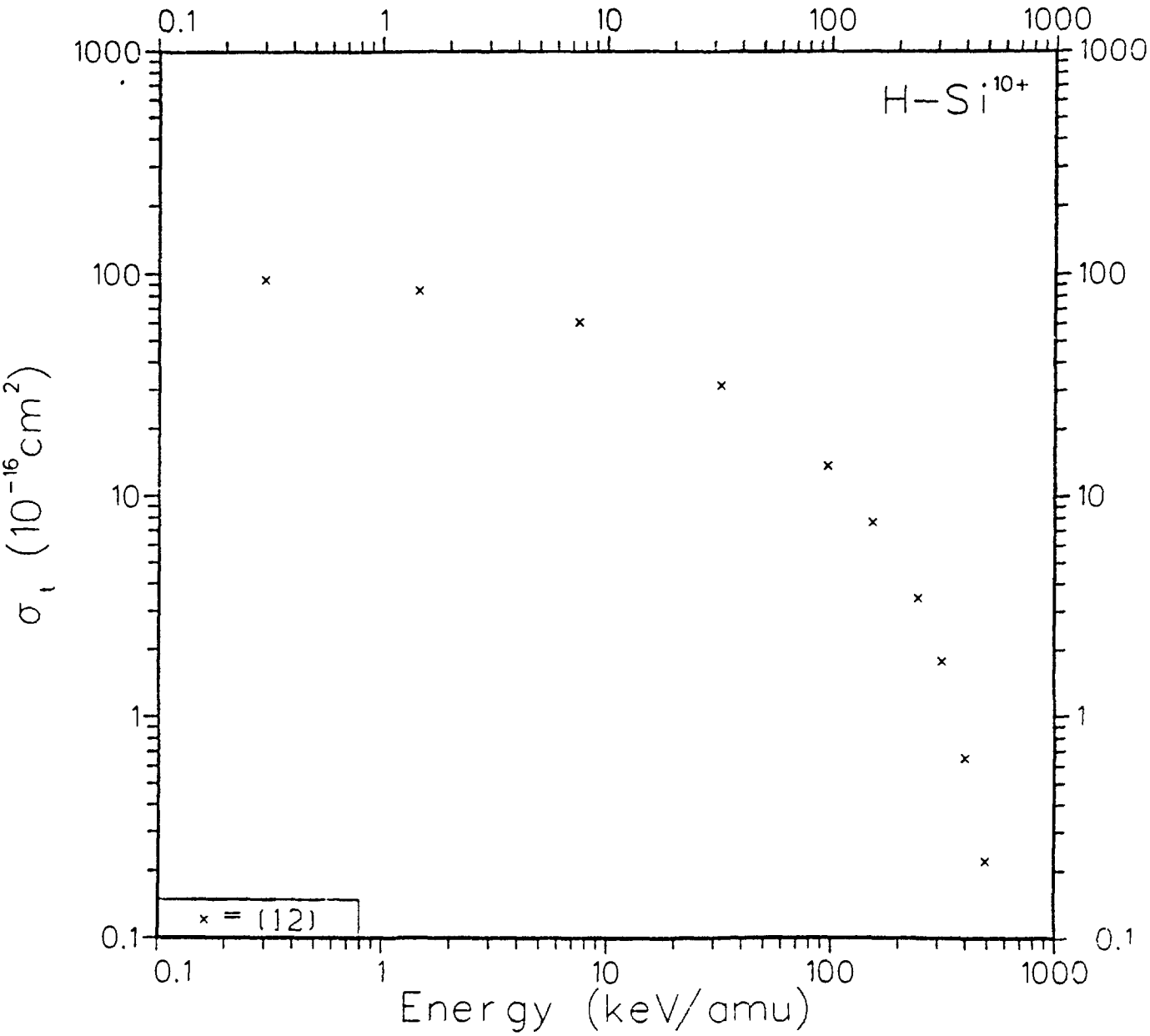
H—Si10+
σt (10-16cm2)
Energy (keV/amu)
× = (12)
0.1
1
10
100
1000

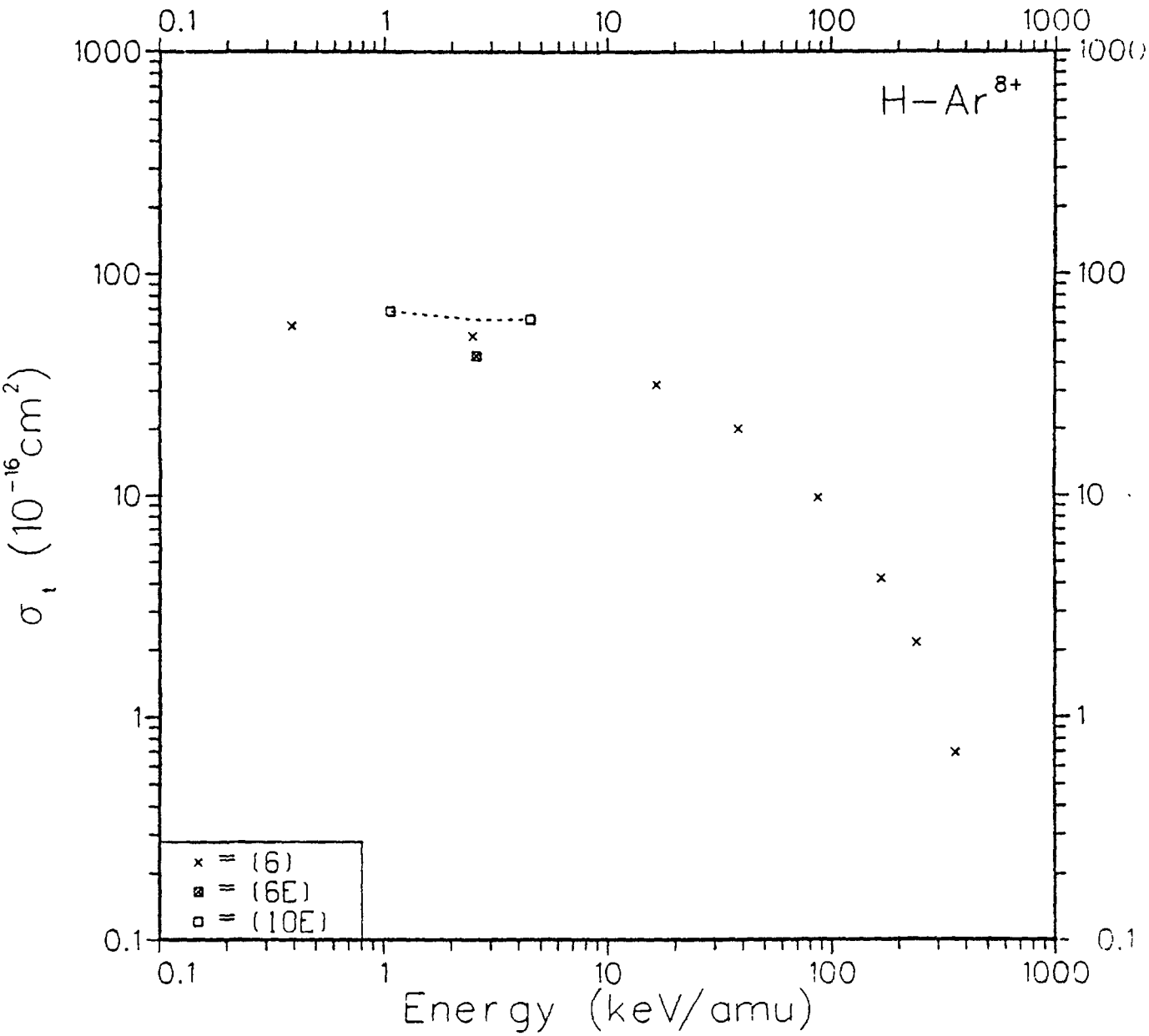
H–Ar^{8+}
σ_t (10^{-16}cm^2)
Energy (keV/amu)
× = (6)
▣ = (6E)
□ = (10E)
0.1
1
10
100
1000

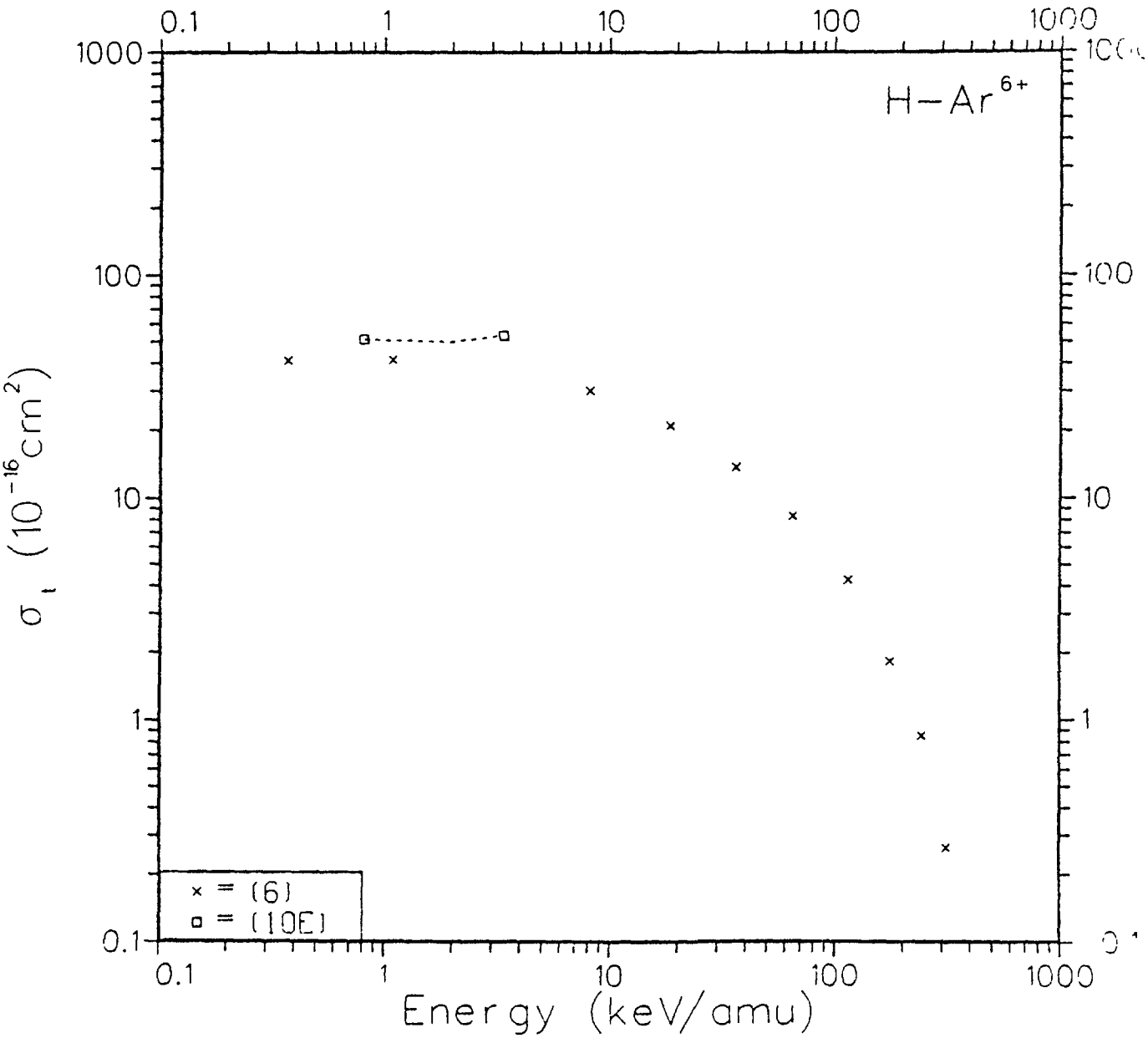
H−Ar 6+
σ t (10−16 cm2)
Energy (keV/amu)
× = (6)
□ = (10E)
0.1
1
10
100
1000

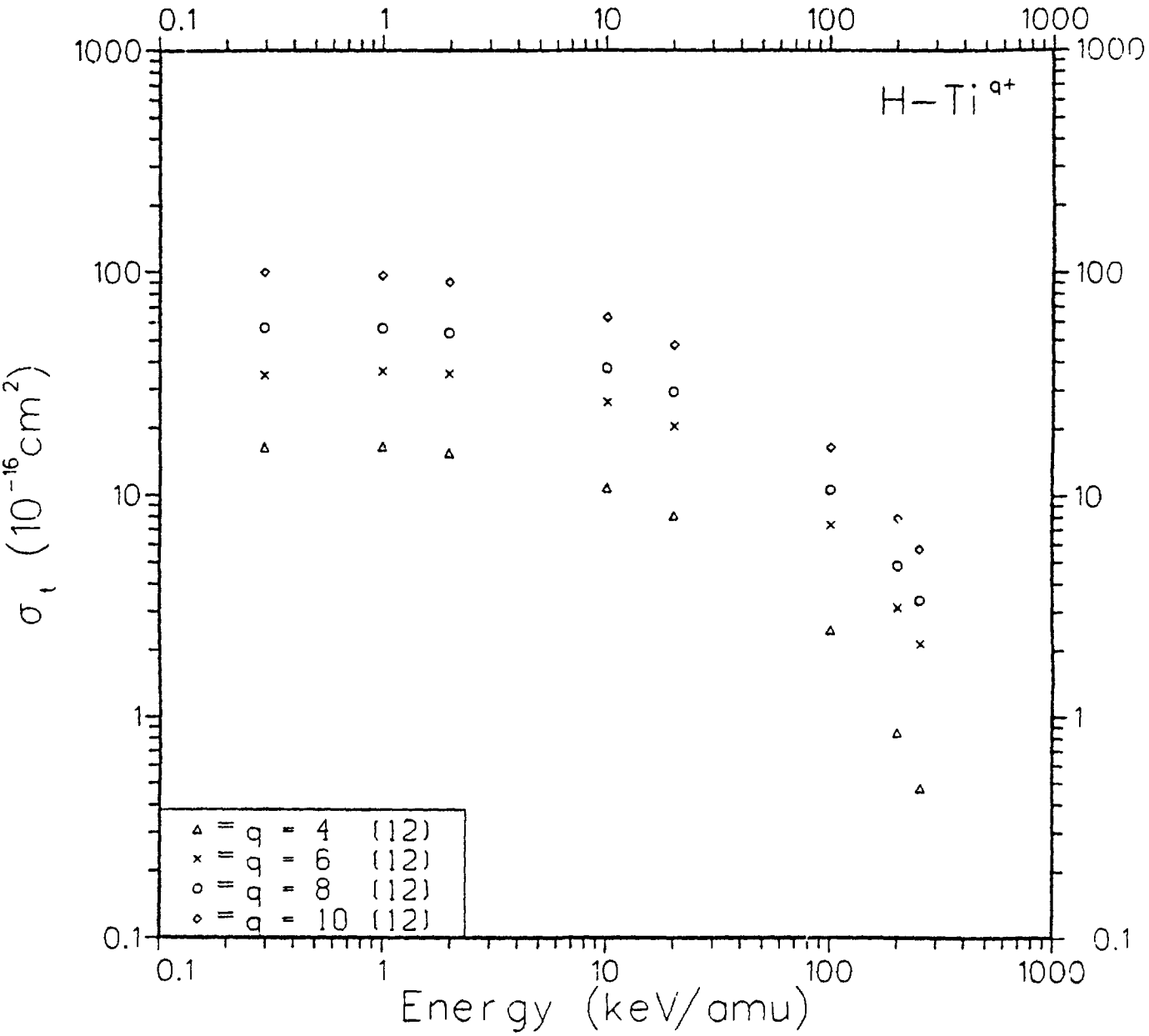
H—Ti q+
σt (10-16cm2)
Energy (keV/amu)
0.1
1
10
100
1000
△ = q = 4 (12)
× = q = 6 (12)
○ = q = 8 (12)
◇ = q = 10 (12)

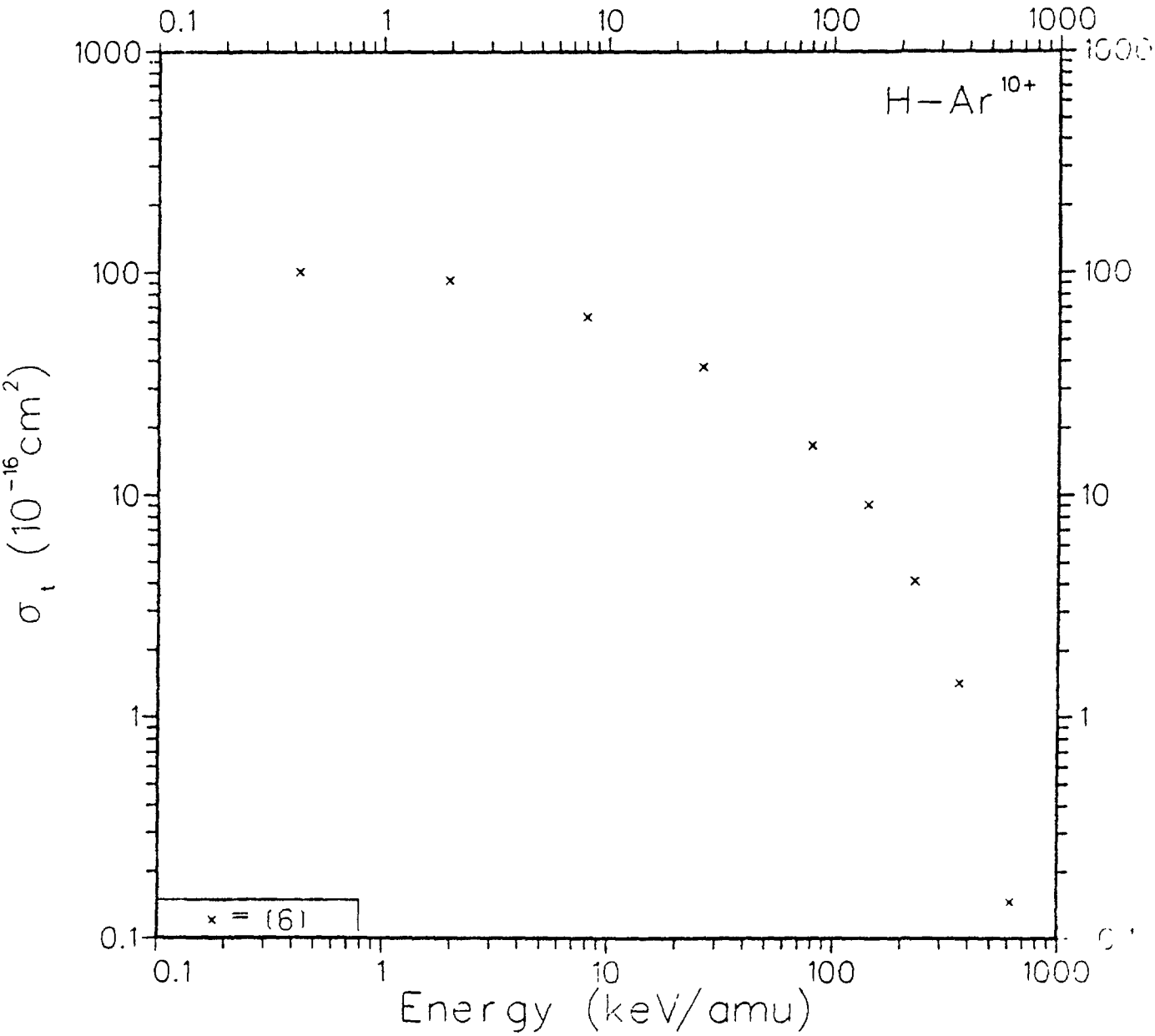
H−Ar 10+
× = (6)
σt (10−16cm2)
Energy (keV/amu)
0.1
1
10
100
1000

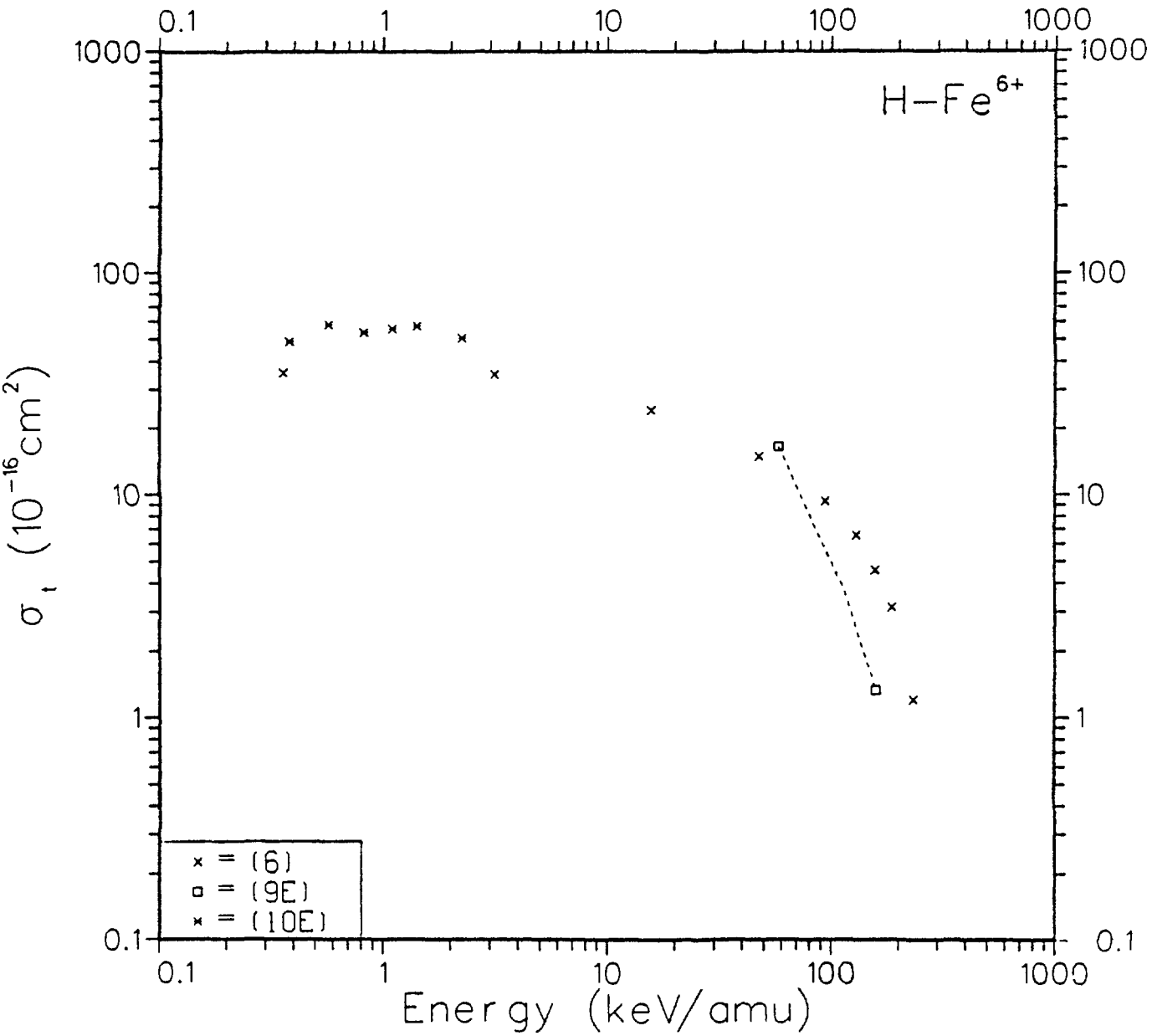
H–Fe6+
σt (10−16cm2)
Energy (keV/amu)
0.1
1
10
100
1000
× = (6)
□ = (9E)
× = (10E)

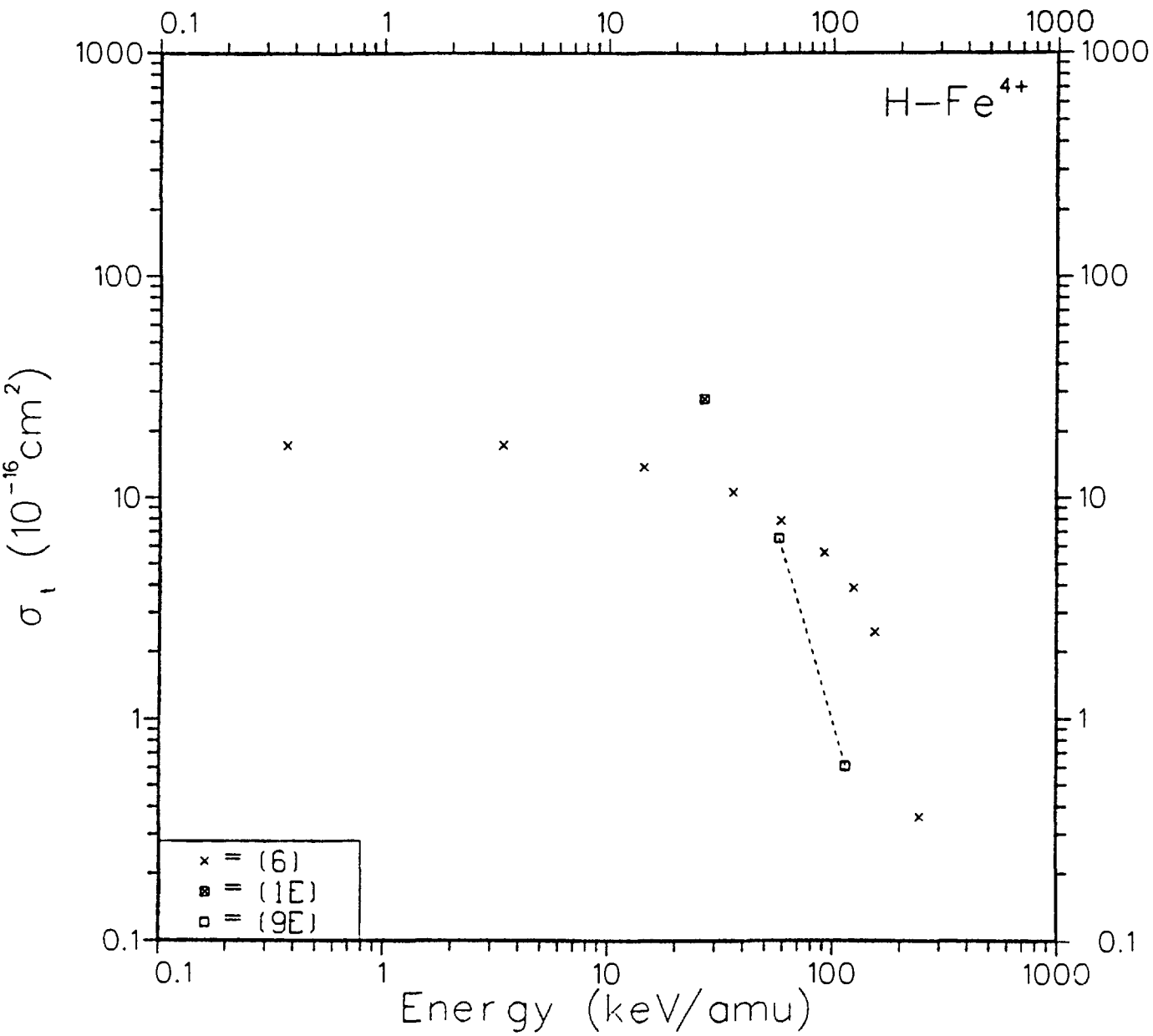
H–Fe4+
σt (10-16cm2)
Energy (keV/amu)
0.1
1
10
100
1000
× = (6)
⊠ = (1E)
□ = (9E)

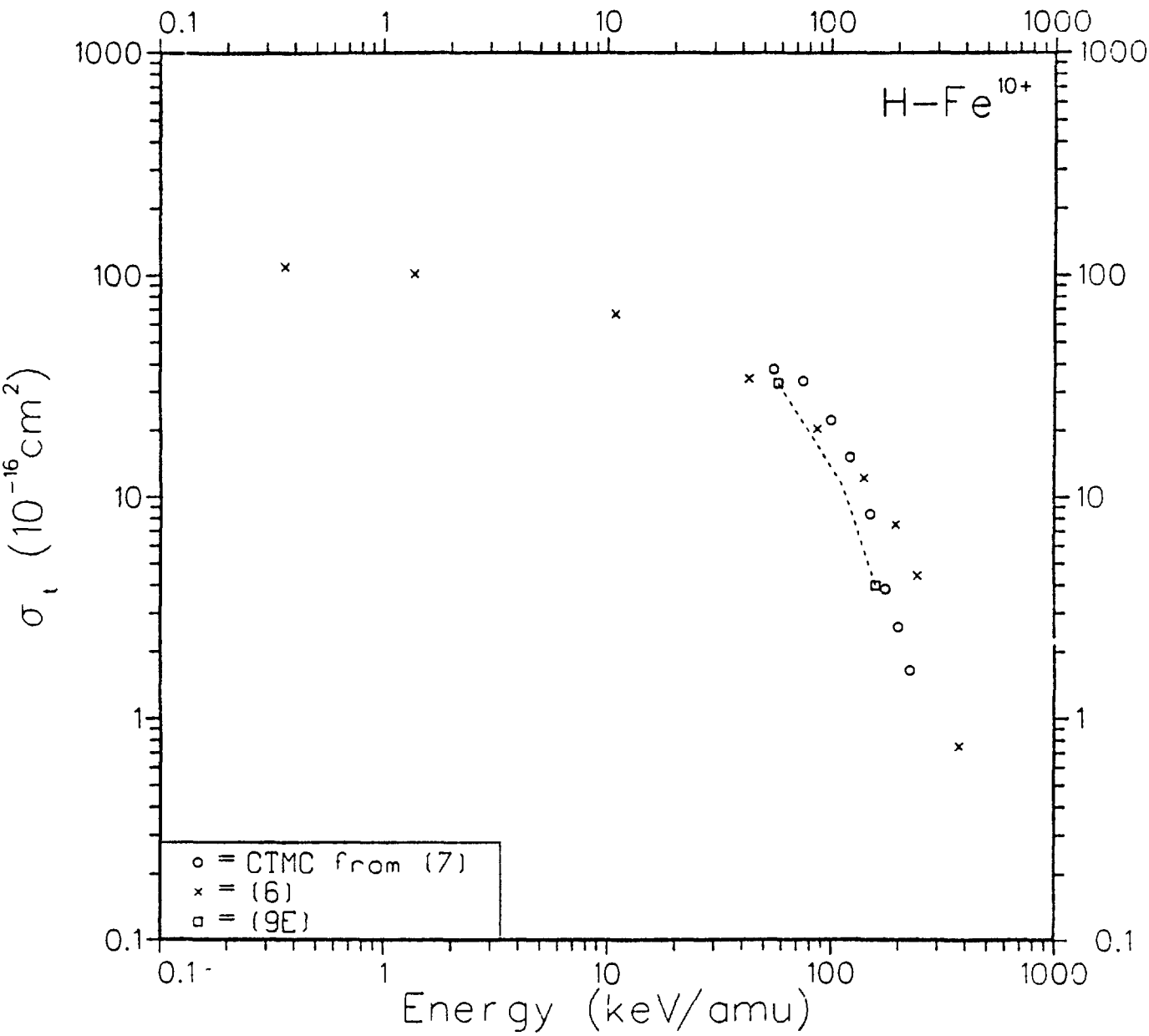
H−Fe10+
σt (10−16cm2)
Energy (keV/amu)
o = CTMC from (7)
x = (6)
□ = (9E)
0.1
1
10
100
1000

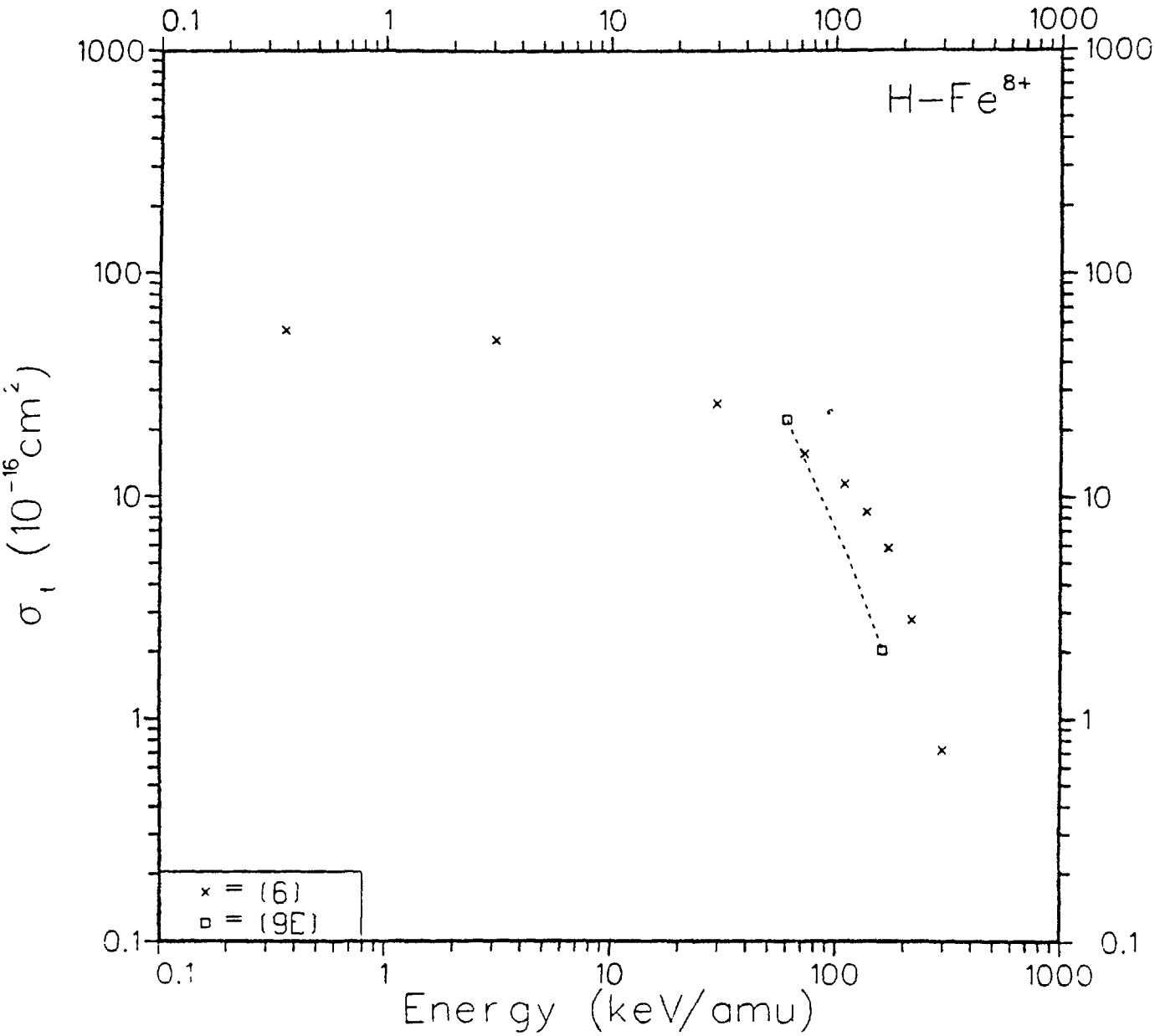
H–Fe8+
σt (10-16cm2)
Energy (keV/amu)
× = (6)
□ = (9E)
0.1
1
10
100
1000

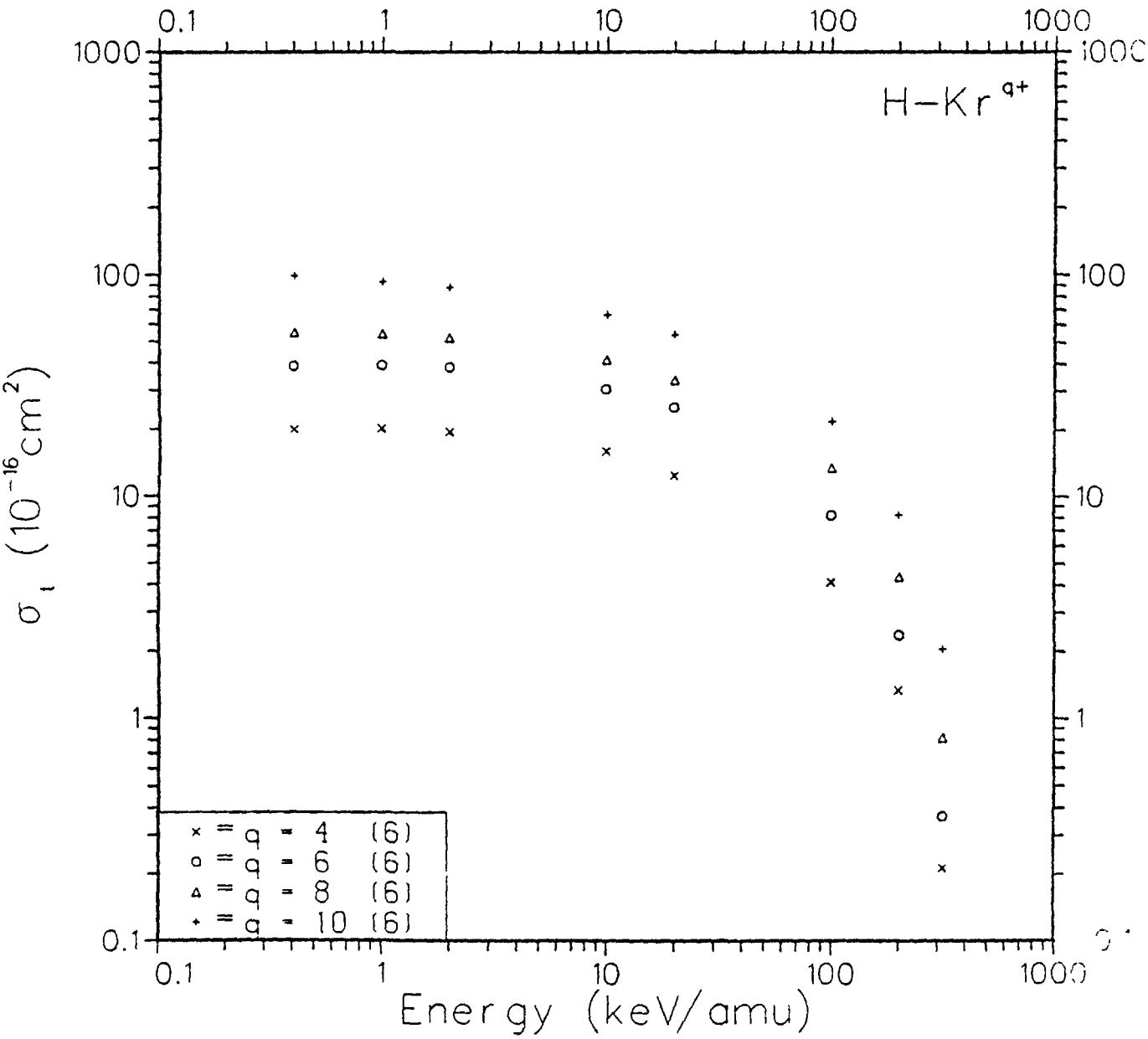
H−Kr q+
σt (10−16cm2)
Energy (keV/amu)
× = q = 4 (6)
o = q = 6 (6)
Δ = q = 8 (6)
+ = q = 10 (6)
0.1
1
10
100
1000

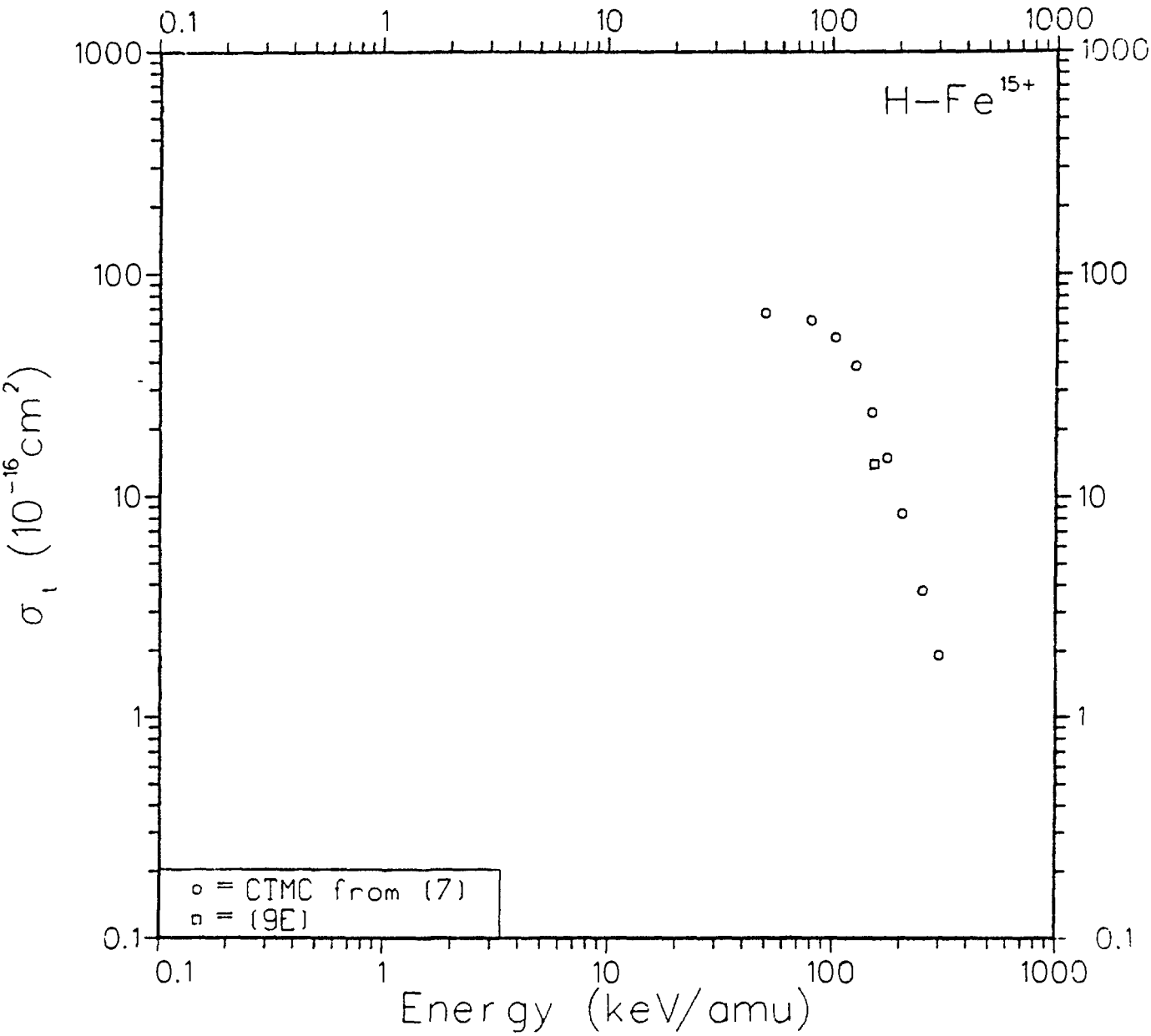
H–Fe15+
σt (10-16cm2)
Energy (keV/amu)
o = CTMC from (7)
□ = (9E)
0.1
1
10
100
1000

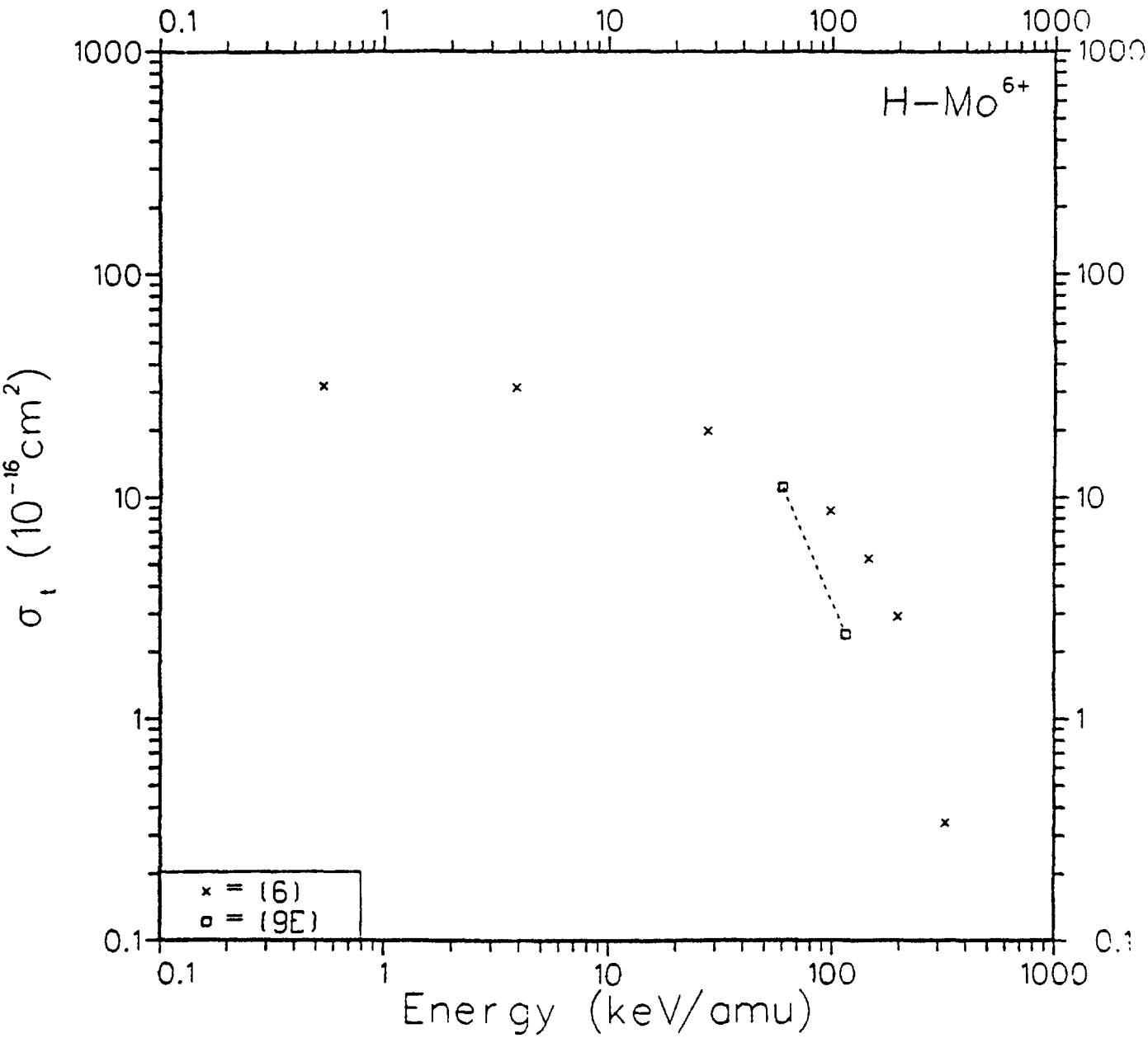
H−Mo6+
σt (10−16cm2)
Energy (keV/amu)
× = (6)
□ = (9E)
0.1
1
10
100
1000

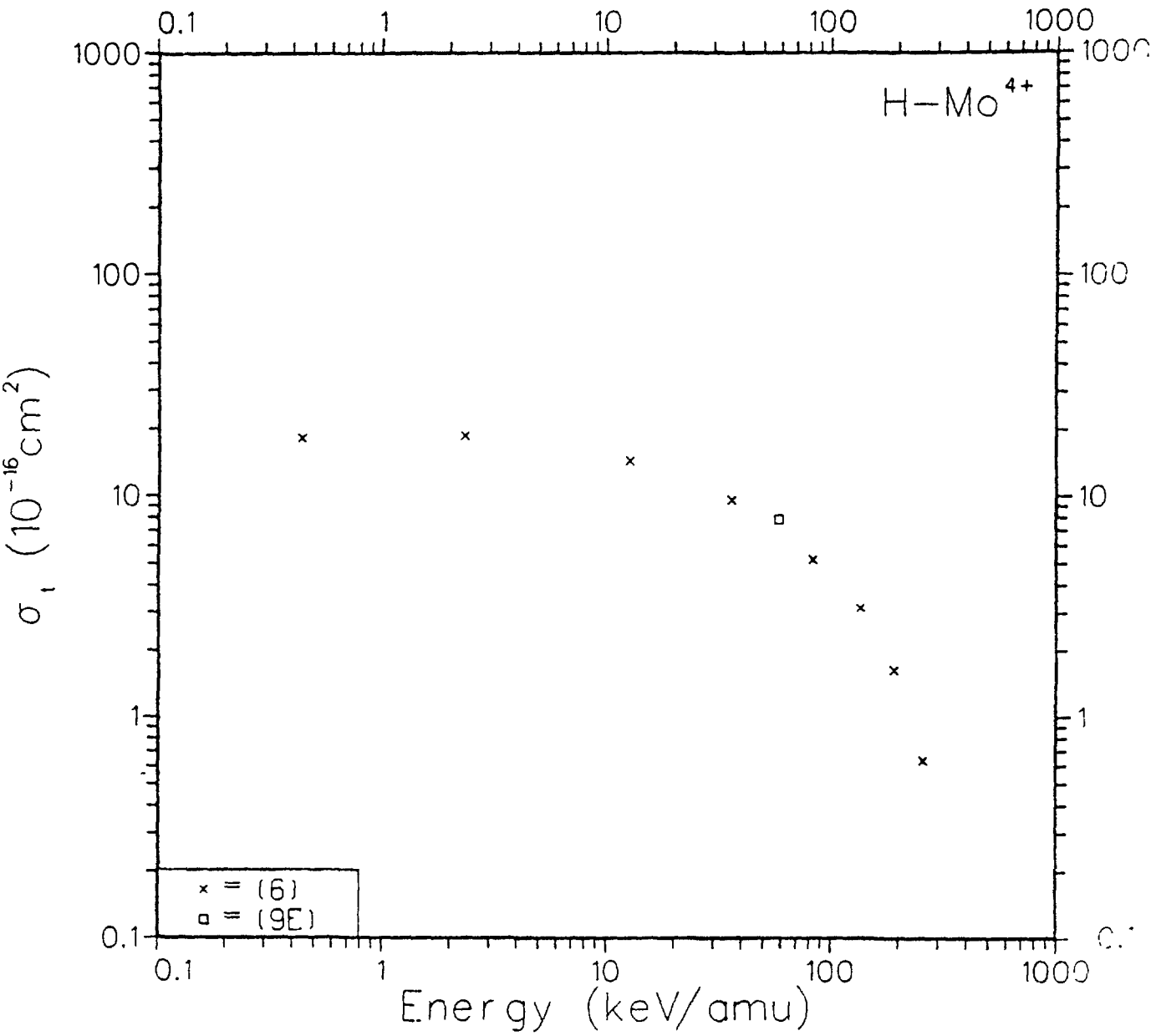
H−Mo^{4+}
σ_t (10^{-16}cm^2)
Energy (keV/amu)
× = (6)
□ = (9E)
0.1
1
10
100
1000

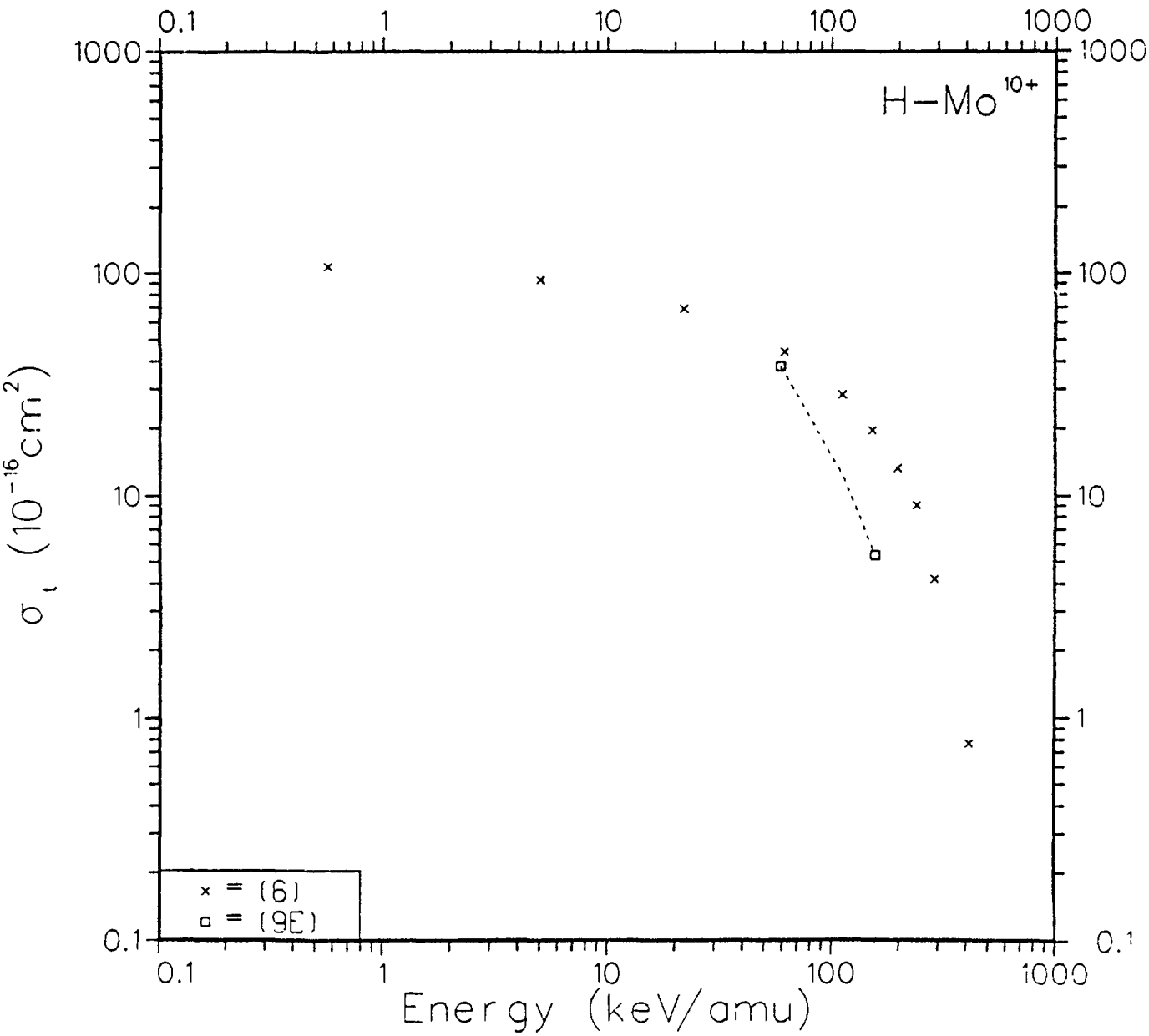
H−Mo 10+
σ t (10-16cm2)
Energy (keV/amu)
× = (6)
□ = (9E)
0.1
1
10
100
1000

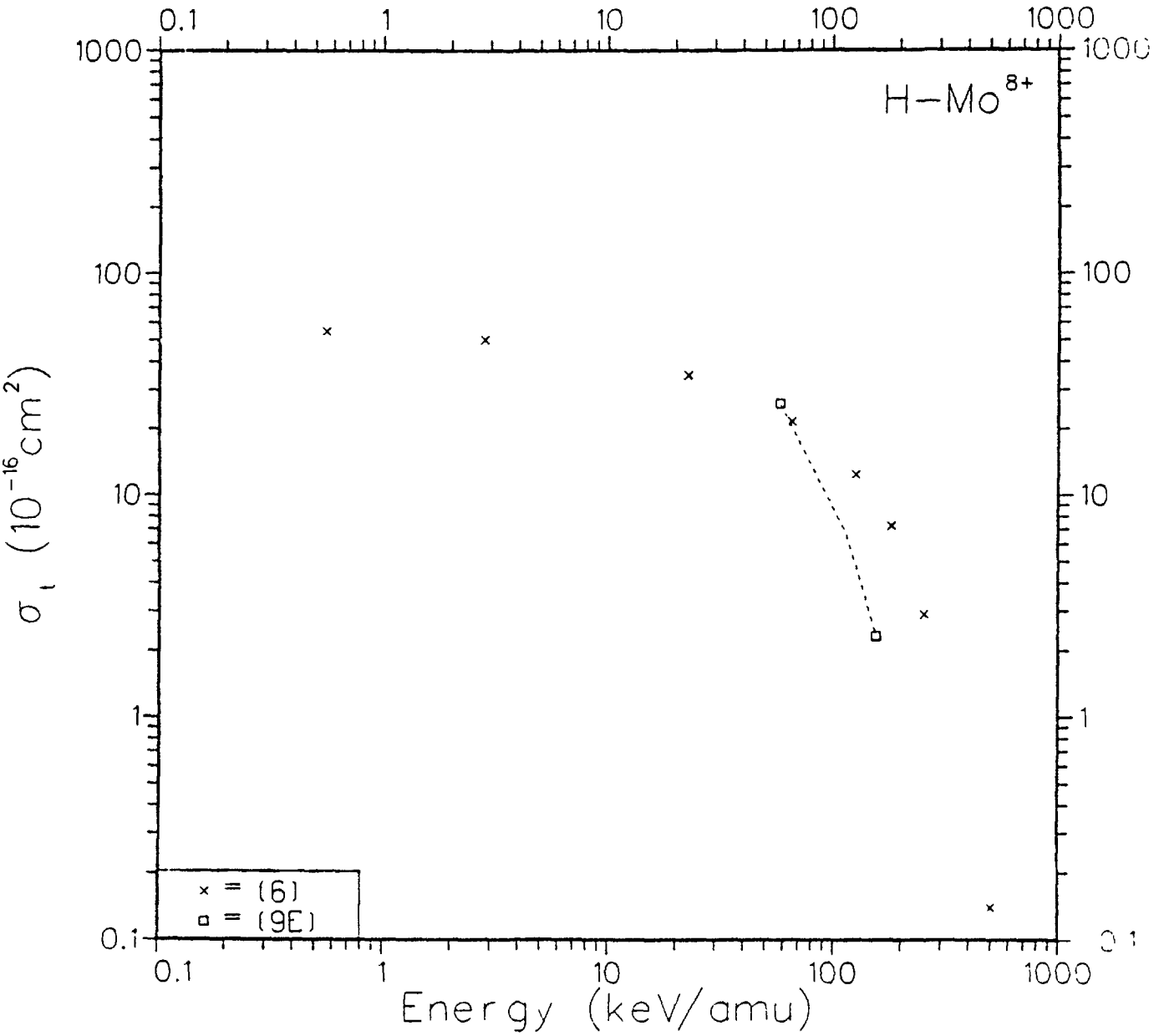
H−Mo8+
σt (10−16cm2)
Energy (keV/amu)
× = (6)
□ = (9E)
0.1
1
10
100
1000

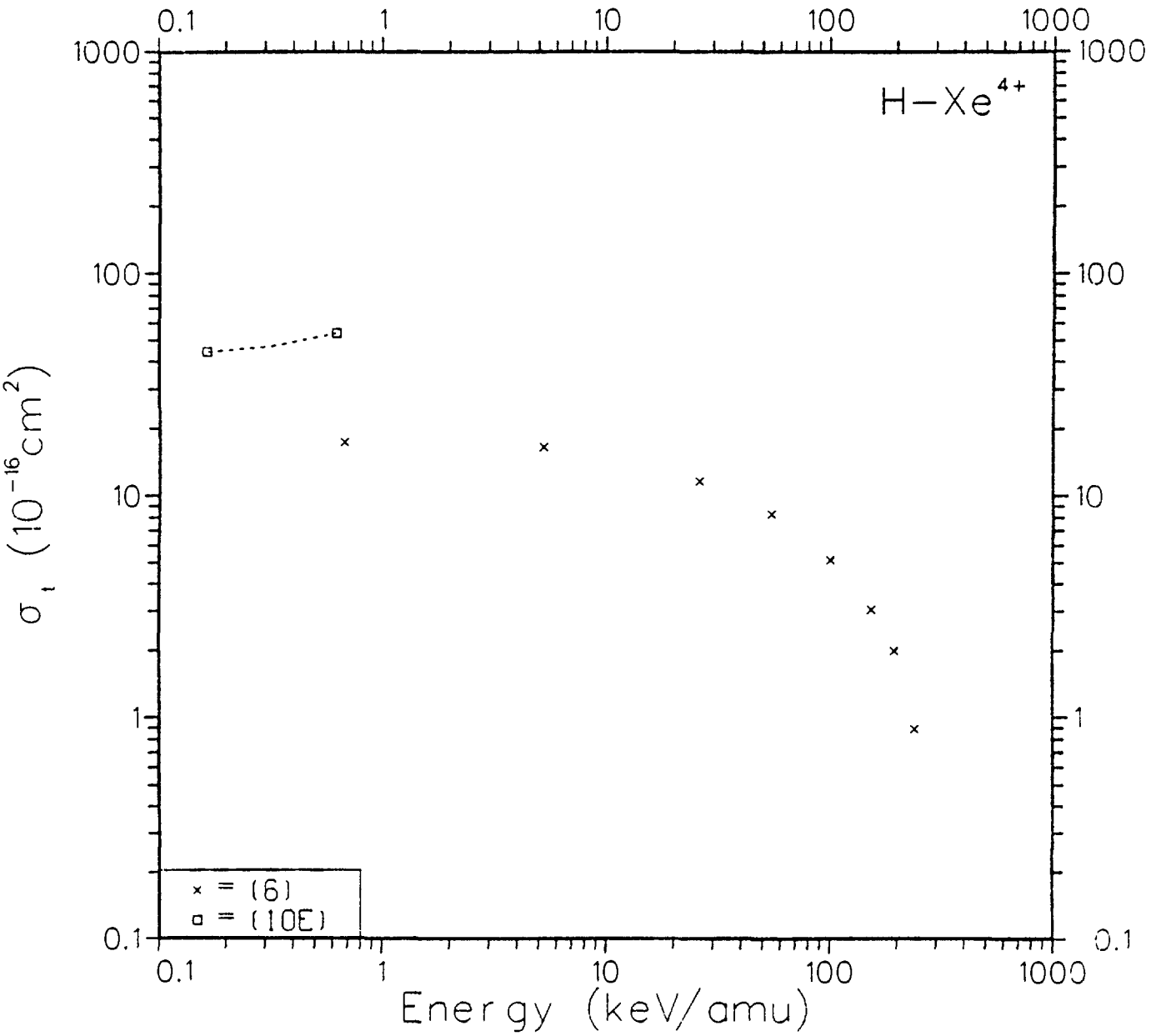
H−Xe4+
σt (10−16cm2)
Energy (keV/amu)
× = (6)
□ = (10E)
0.1
1
10
100
1000

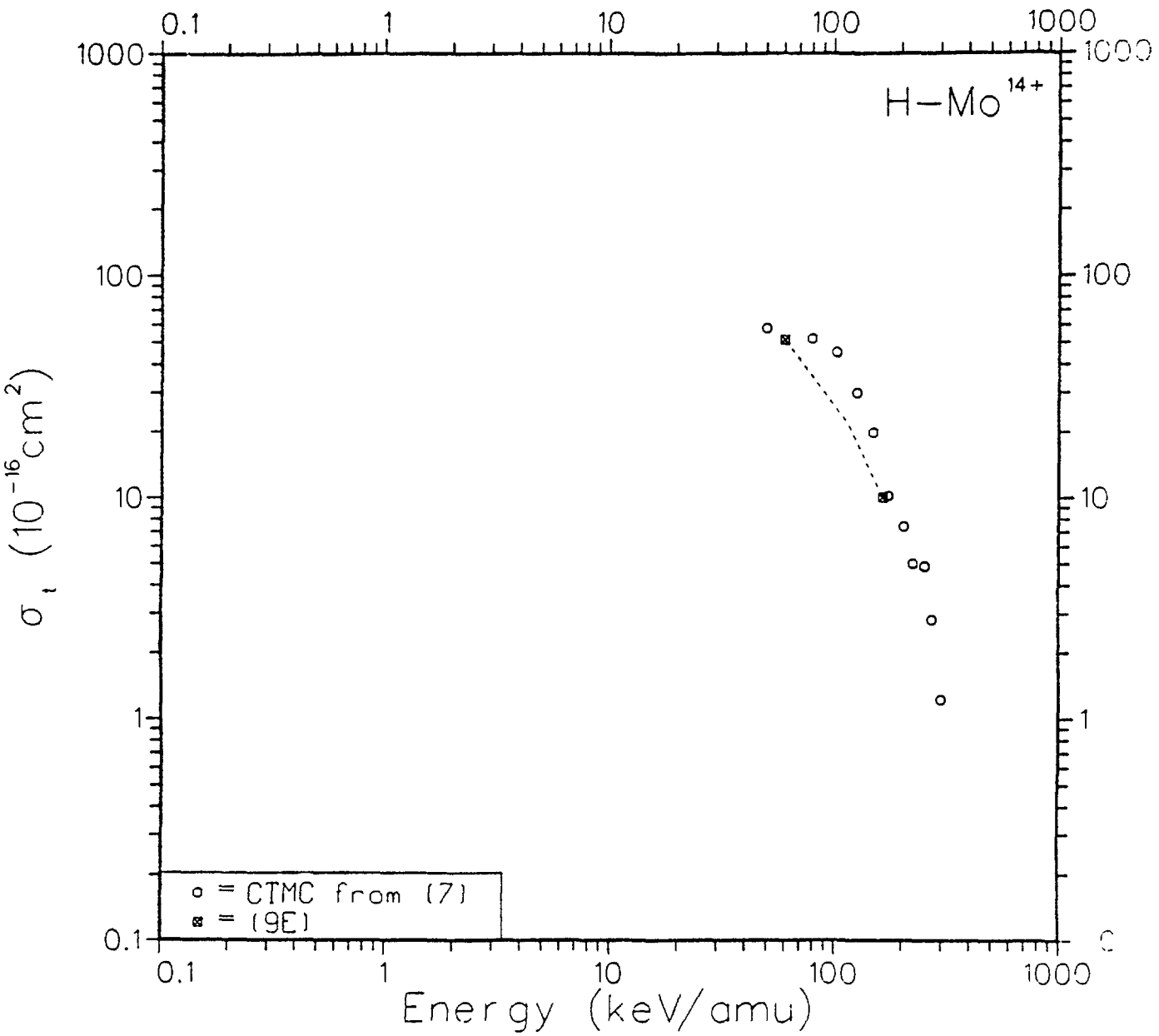
H−Mo 14+
σ t (10−16cm2)
Energy (keV/amu)
o = CTMC from (7)
⊠ = (9E)
0.1
1
10
100
1000

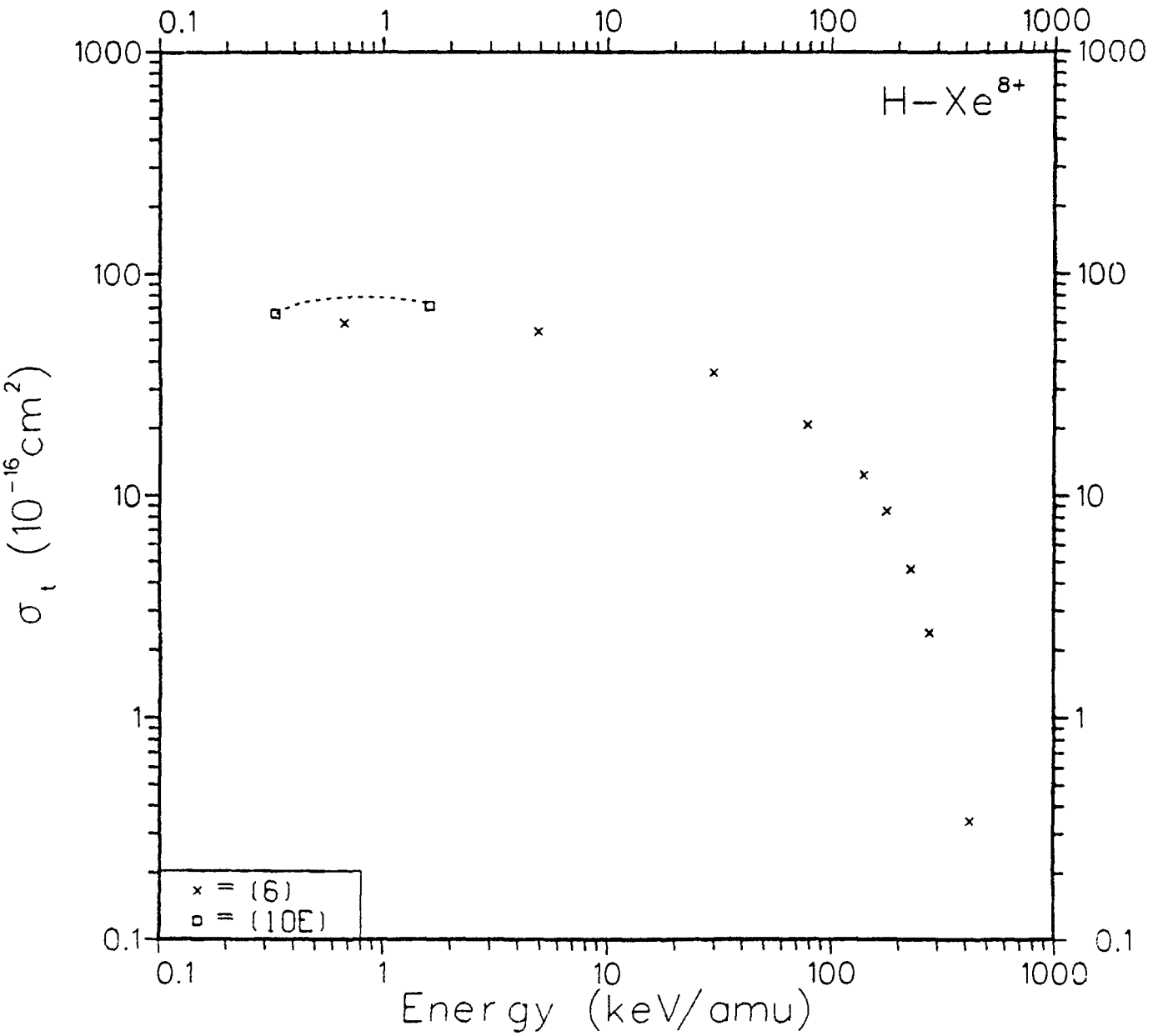
H−Xe8+
σt (10−16cm2)
Energy (keV/amu)
× = (6)
□ = (10E)
0.1
1
10
100
1000

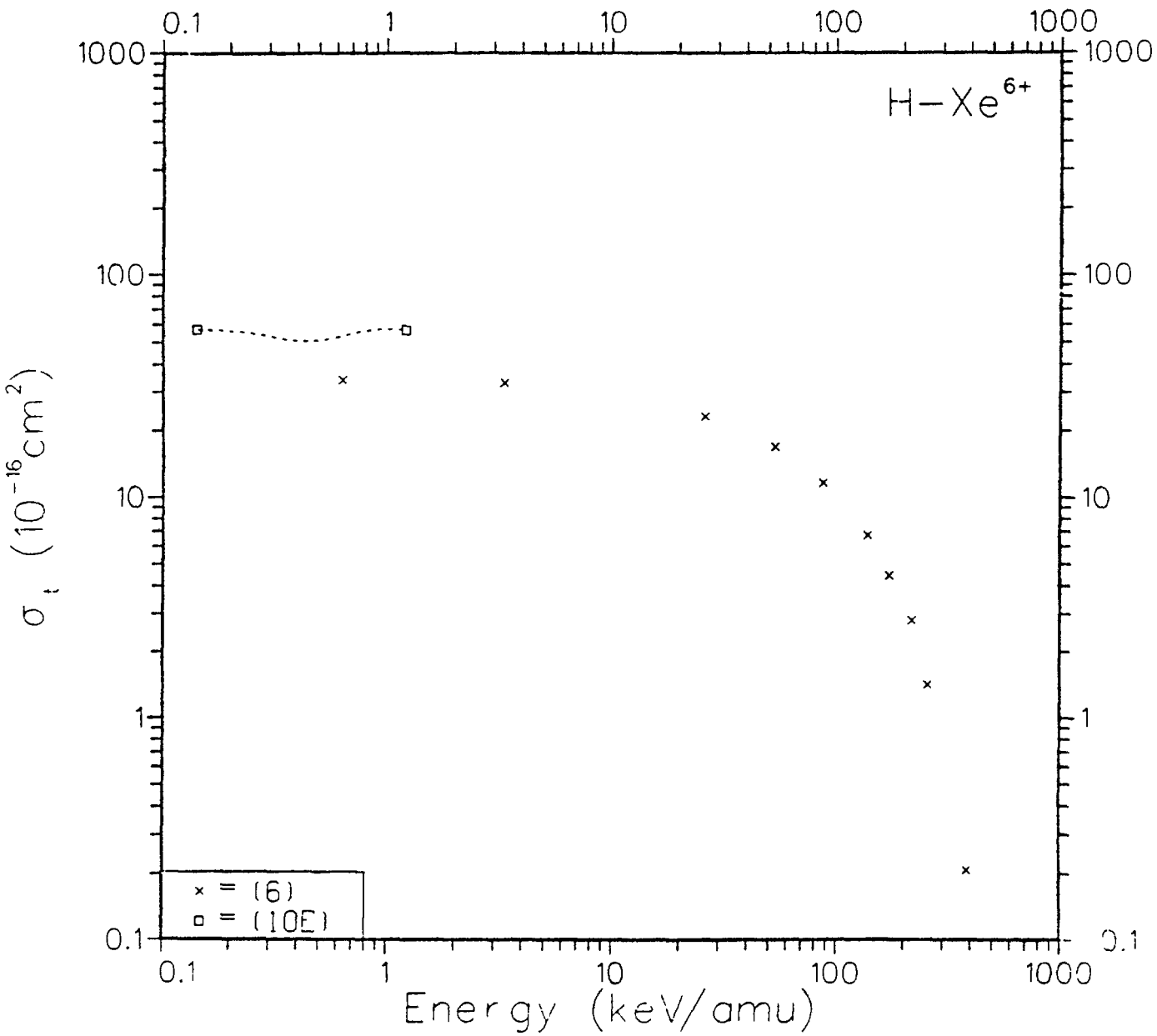
H−Xe6+
σt (10-16cm2)
Energy (keV/amu)
× = (6)
□ = (10E)
0.1
1
10
100
1000

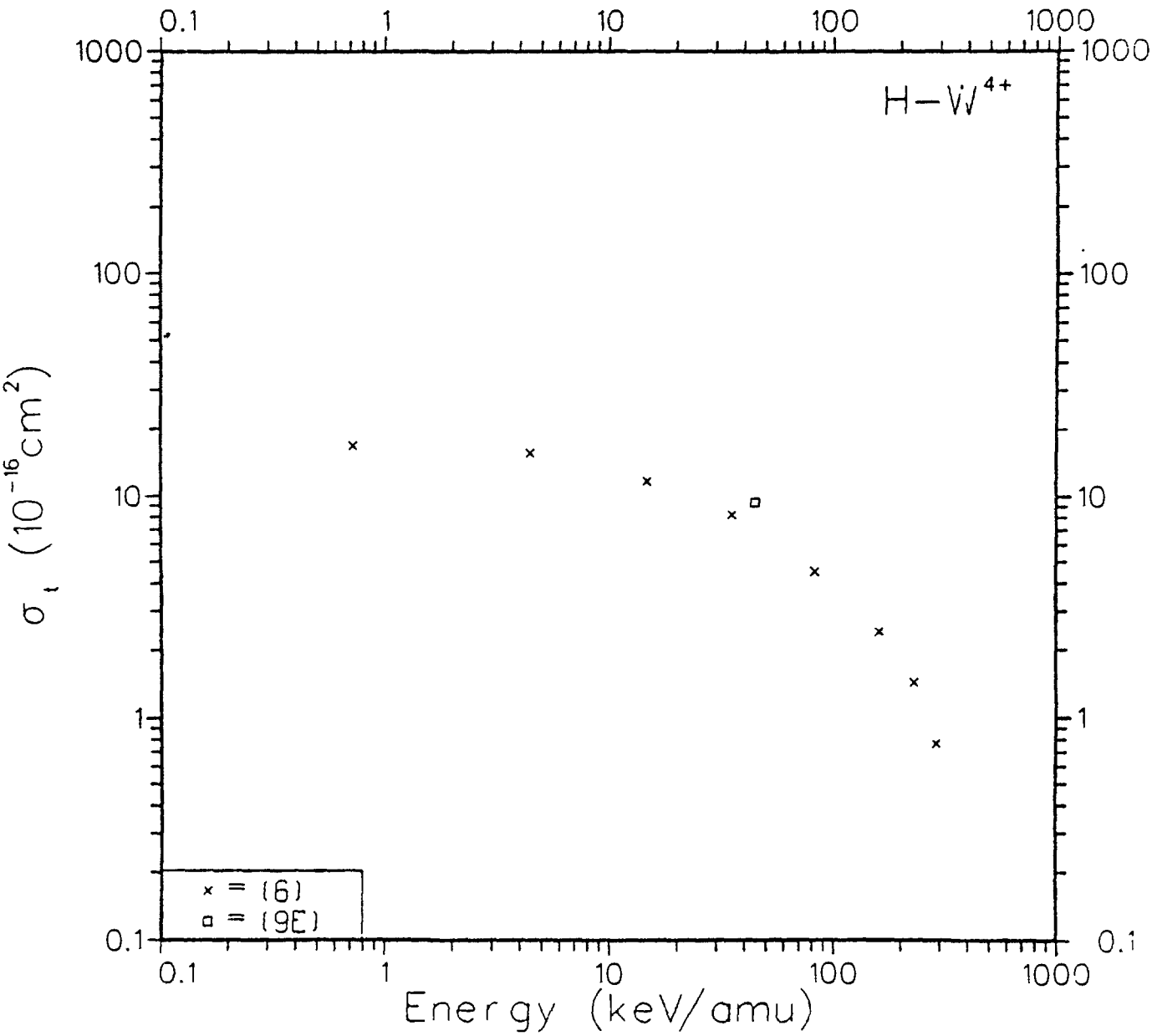
H—W^{4+}
σ_t (10^{-16}cm^2)
Energy (keV/amu)
× = (6)
□ = (9E)
0.1
1
10
100
1000

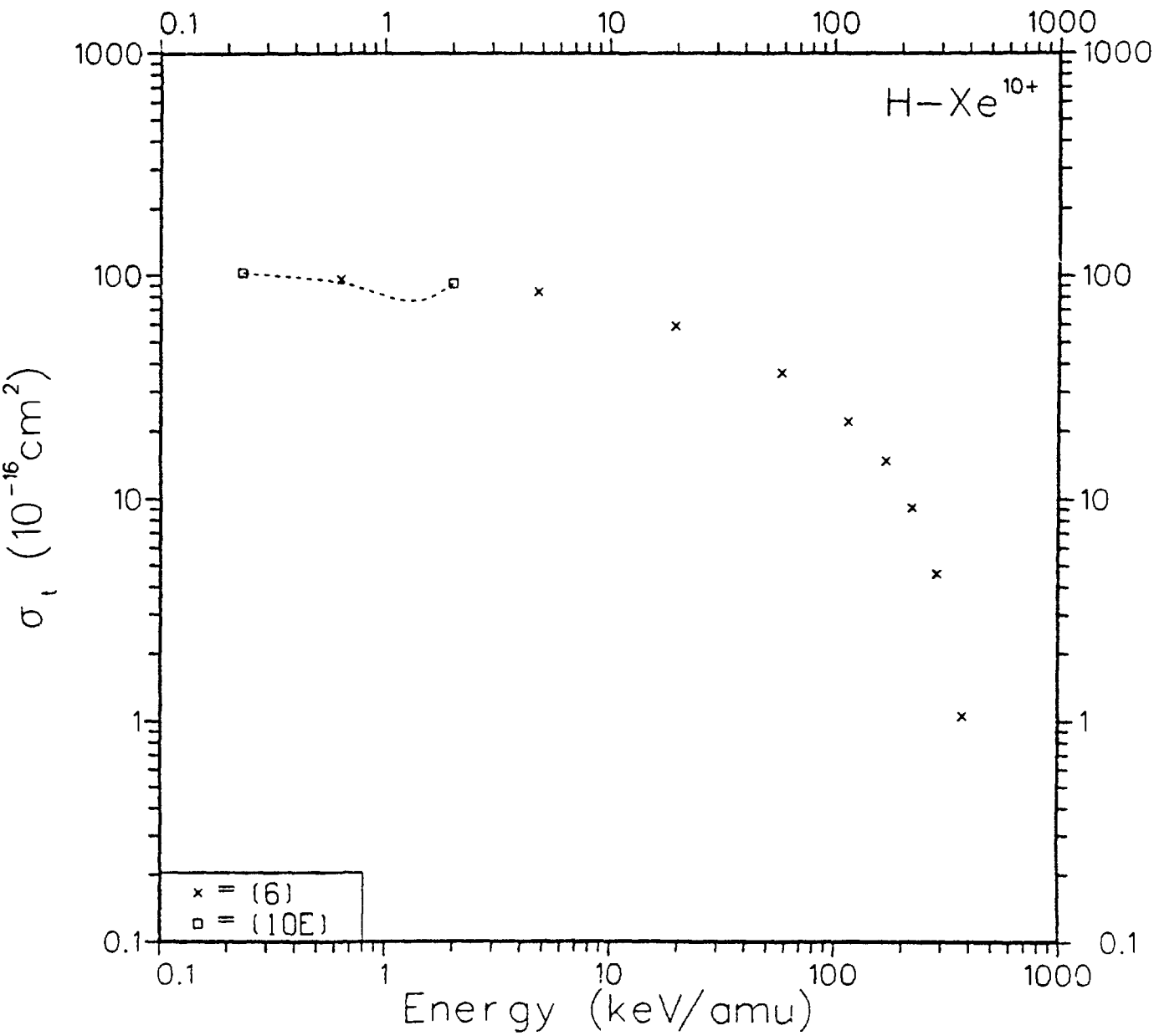
H−Xe10+
σt (10−16cm2)
Energy (keV/amu)
× = (6)
□ = (10E)
0.1
1
10
100
1000

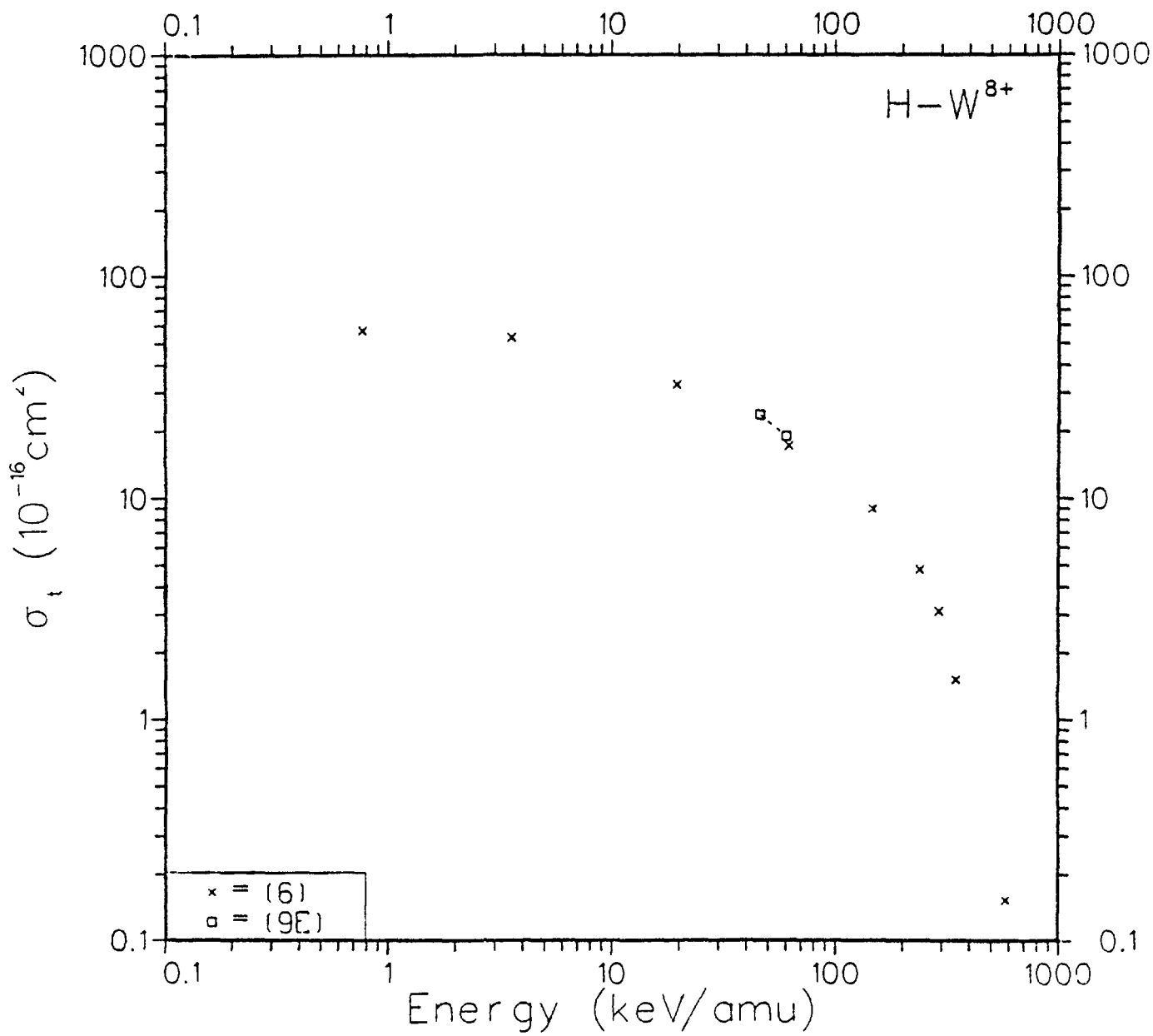
H−W8+
σt (10−16cm2)
Energy (keV/amu)
× = (6)
□ = (9E)
0.1
1
10
100
1000

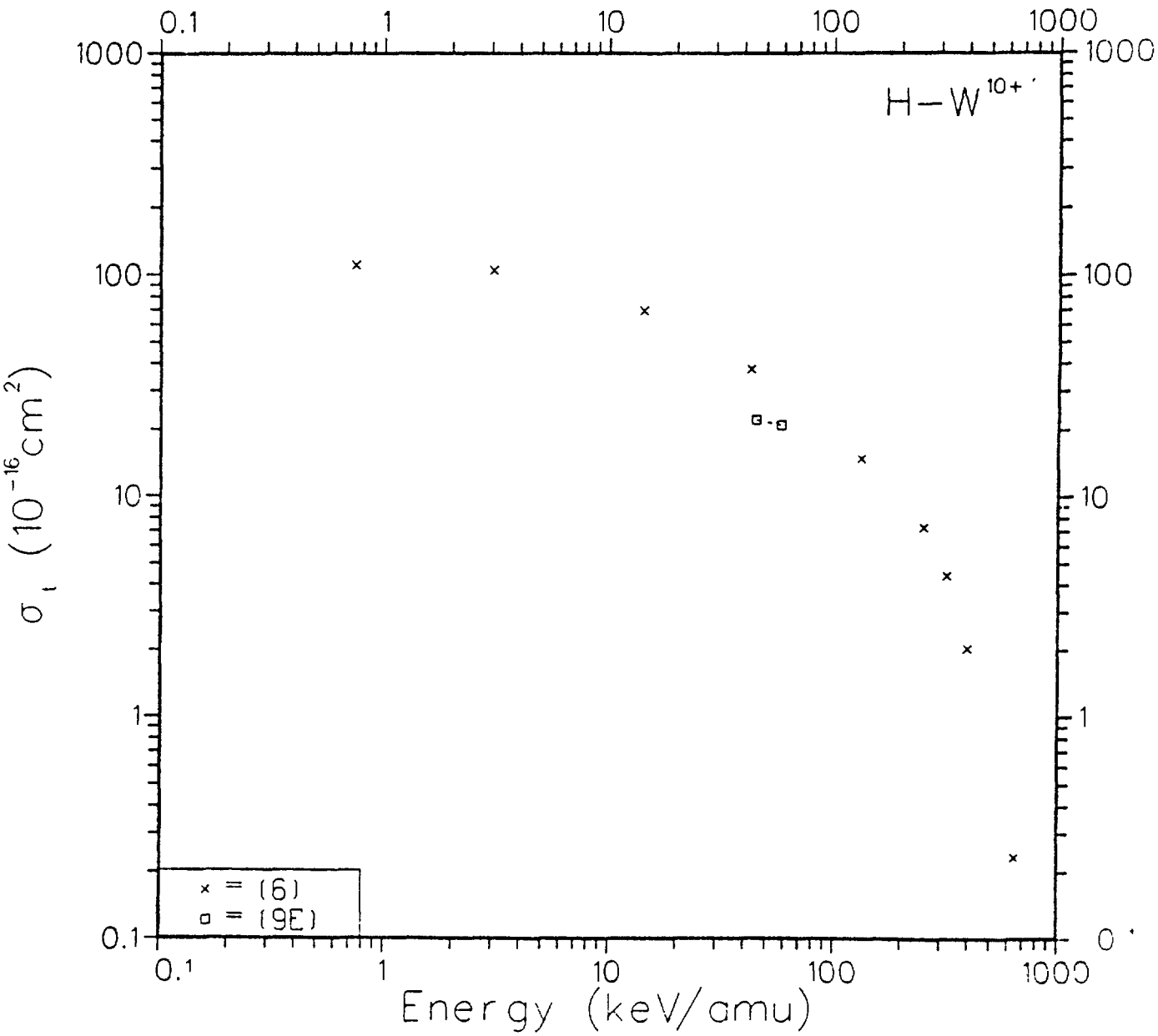
H−W10+
σt (10−16cm2)
Energy (keV/amu)
× = (6)
□ = (9E)
0.1
1
10
100
1000